DCU

*Library*
*Thesis*
*Copyright*
*Declaration*
*Form*

**Thesis Details:** This section to be completed in **BLOCK CAPITALS**

| | | | |
|---|---|---|---|
| **Author Surname** | BUCHANAN | **Author Firstname** | BARBARA. |
| **Title** | PREPARATION, CHARACTERISATION AND PROPERTIES OF RUTHENIUM COMPOUNDS | | |
| **Degree** | PHD | **Year** | 1989 |
| **Barcode** | 9 0 0 5 7 9 9 6 X | | |

This thesis is made available on the understanding that the reader will not publish in any form either the whole or any part of it without the written permission of the copyright holder.

The copyright of the thesis belongs to the author. Readers must sign their name to indicate that they accept these conditions, and give their permanent home address.

| | | | |
|---|---|---|---|
| **Reader Signature** | Claire Bergin | **Date** | 20/04/07 |
| **Reader Name** (print in block letters) | CLAIRE BERGIN. | | |
| **Permanent Address** (print in block letters) | 84 BEECHPARK ROAD, FOXROCK DUBLIN 18. | | |
| **ID Number** | 5331660. | | |
| **Other Dates accessed** | | | |

# PREPARATION, CHARACTERISATION AND PROPERTIES OF RUTHENIUM COMPOUNDS CONTAINING PYRIDYL-1,2,4-TRIAZOLES

by

Barbara E Buchanan BSc (Hons)

A Thesis presented to Dublin City University for the degree of Doctor in Philosophy

Supervisor Dr J G Vos

School of Chemical Sciences
Dublin City University

April 1989

To my parents

## ACKNOWLEDGEMENTS.

First and foremost I would like to acknowledge my supervisor Dr Han Vos for his continuous help, encouragement and advice during the course of this work

I would like to express my gratitude to Ronald Hage from the Gorleaus Laboratories in Leiden for solving the crystal structure of $[Ru(bpy)_2(3MePyrtr)](PF_6)\ 4H_2O$ during my stay in Leiden, and also for his help in the interpretation of some of the COSY n m r spectra I also wish to thank Jaap Haasnoot and Jan Reedijk for their help during my stay in The Netherlands

Many thanks to all my fellow postgrads for their friendship and assistance during these last few years In particular, I would like to acknowledge Andrew Kelly and Robert Forster for their help with the electrochemistry,

I wish to thank the technicians Teresa Mc Donald, Ita Kinehan, Mick Burke, Peig Ward and Maurice Burke for their help and advice during the experimental stage of this thesis

I would like to acknowledge Professor A Pratt and other members of staff for the use of the facilities of the chemistry department at Dublin City University

Many thanks to the following in Trinity College Dublin, the chemistry department for the use of the Time Correlated Single Photon Counting apparatus (TCSPC), Dr John Kelly for his useful discussions on the lifetime results, Dr Wilheim van der Putten and Dr Martin Murphy for showing me the use of the TCSPC apparatus, and special thanks to Martin Feeney for his continuous help during my work at TCD

Sincere thanks to Bernie Creaven, Dr Connor Long and Dr Alan Howie for their time and patience in solving the crystal structure of $[Ru(bpy)_2(3MePT)Cl]PF_6$

I wish to express my gratitude to the Department of Education for the maintenance grant which I received over the period of my research

For Dorothea, many thanks for her help with the secretarial work

Last but not least I wish to express my gratitude to my family for their support and encouragement and for "putting up" with me during the past few months of writing this thesis Sincere thanks to Tom Tynan for his assistance in the preparation of this manuscript

This thesis has not been submitted as an exercise for a degree at this or any other University Except as otherwise indicated, this work has been carried out by the author alone

Barbara E Buchanan

Barbara E Buchanan

## CONTENTS


| | | Page |
|---|---|---|
| CHAPTER 1 | General Introduction on $[Ru(bpy)_3]^{2+}$ | 1 |
| 1 1 | Application and Uses of Ruthenium | 2 |
| 1 2 | Photophysical Properties of $[Ru(bpy)_3]^{2+}$ | 4 |
| | References | 13 |
| CHAPTER 2 | Experimental. | 15 |
| 2 1 | Synthesis | 16 |
| 2 1 1 | Ligand Preparation | 16 |
| 2 1 2 | Preparation of Complexes of the Type Cis-$[Ru(bpy)_2(L\text{-}L')]^{n+}$ | 18 |
| 2 1 3 | Preparation of Complexes of the Type Cis-$[Ru(bpy)_2(L\text{-}L')Cl]PF_6$ | 22 |
| 2 1 4 | Preparation of Mononuclear and Dinuclear Complexes Containing Asymmetric Bridging Ligands | 23 |
| 2 2 | Instrumentation | 27 |
| 2 2 1 | Absorption and Emission Spectroscopy | 27 |
| 2 2 2 | $pK_a$ Measurement | 27 |
| 2 2 3 | Electrochemical Measurements | 27 |
| 2 2 4 | High Performance Liquid Chromatography (HPLC) | 28 |
| 2 2 5 | Semi-Preparative HPLC | 28 |
| 2 2 6 | Emission Quantum Yield Determination | 29 |
| 2 2 7 | Photochemistry Experimental | 29 |
| 2 2 8 | $^1H$ N m r Spectroscopy | 30 |
| 2 2 9 | X-Ray Crystallography | 30 |
| | (a) $[Ru(bpy)_2(3MePyrtr)](PF_6)\ 4H_2O$ | 30 |
| | (b) $[Ru(bpy)_2(3MePT)Cl]PF_6$ | 31 |

| | | |
|---|---|---|
| 2 2 10 | Time Correlated Single Photon Counting (TCSPC) Method of Lifetime Measurements | 32 |
| 2 2 10 1 | General Theory of TCSPC | 35 |
| 2 2 10 2 | Data Analysis | 36 |
| 2 2 10 3 | Evaluating the Success of the Fit | 37 |
| 2 2 10 4 | Standards for TCSPC | 38 |
| | References | 41 |

CHAPTER 3 Preparation, Characterisation and Photo-Physical Properties of Ruthenium Compounds Containing Chelating and Monodentate Asymmetric Pyridyltriazole ligands. 43

| | | |
|---|---|---|
| 3 0 | Introduction | 44 |

Section 1

Preparation and Characterisation of Cis-$[Ru(bpy)_2(L\text{-}L')]^{n+}$ Complexes Containing Asymmetric Bidentate Ligands 63

| | | |
|---|---|---|
| 3 1 1 | Preparation of Complexes of the type $[Ru(bpy)_2(L\text{-}L')]^{n+}$ | 64 |
| 3 1 2 | $^1H$ N m r Spectra | 69 |
| 3 1 3 | Crystal Structure of Bis(2,2'-bipyridine) Ruthenium-3-Methyl-5-(pyridin-2-yl)-1,2,4-triazole Hexafluorophosphate | 77 |
| 3 1 4 | Electronic Spectra and Redox Properties | 82 |
| 3 1 5 | Conclusion | 91 |

Section 2

Synthesis of Complexes Containing Monodentate Pyridyltriazole Ligands With a View to Preparing Intermediates Formed in Photochemical Reactions 93

| | | |
|---|---|---|
| 3 2 1 | Preparation of Complexes of the Type $[Ru(bpy)_2(L\text{-}L')Cl]^+$ | 94 |
| 3 2 2 | $^1H$ N m r Spectra of the Free Ligands | 98 |
| 3 2 3 | $^1H$ N m r Spectra of the Monodentate Coordinated Ligands | 99 |
| 3 2 4 | Crystal Structure of bis (2,2'bipyridine)-Chloro-Ruthenium-(3-Methyl-1-(pyridin-2-yl) -1,2,4(triazole) Hexafluorophosphate | 109 |
| 3 2 5 | Electronic Spectra and Redox Properties | 115 |
| 3 2 6 | Conclusion | 123 |

Section 3

Photolysis of Compounds Containing Chelating and Monodentate Pyridyl-Triazole Ligands 125

| | | |
|---|---|---|
| 3 3 1 | Introduction to Photolysis | 126 |
| 3 3 2 | Photolysis of a Model Compound $[Ru(bpy)_2(viz)_2]^{2+}$ | 127 |
| 3 3 2 1 | Photolysis of $[Ru(bpy)_2(PT)]^{2+}$ in Acetonitrile | 132 |
| 3 3 2 2 | Photolysis of $[Ru(bpy)_2(PT)]^{2+}$ in Acetonitrile-LiCl | 134 |
| 3 3 2 3 | Photolysis of $[Ru(bpy)_2(PT)]^{2+}$ in Methanol-LiCl | 137 |
| 3 3 2 4 | Photolysis of $[Ru(bpy)_2(4MePyrtr)]^{2+}$ in Acetonitrile | 143 |
| 3 3 2 5 | Photolysis of $[Ru(bpy)2(4MePyrtr)_]^{2+}$ in Acetonitrile-LiCl | 145 |
| 3 3 2 6 | Photochemical Stability of Compounds Containing the Chelating Ligands PT, 3BrPT, 3MePT, and 4MePyrtr | 149 |
| 3 3 3 | Photolysis of Compounds Containing Monodentate Coordinated Pyridyltriazole Ligands | 150 |
| 3 3 3 1 | Photolysis of $[Ru(bpy)_2(PT)Cl]^+$ in Acetonitrile | 150 |

| | | |
|---|---|---|
| 3 3 3 2 | Photolysis of $[Ru(bpy)_2(PT)Cl]^+$ in Acetonitrile-LiCl | 152 |
| 3 2 4 | Conclusion | 156 |
| | References | 158 |

| | | |
|---|---|---|
| CHAPTER 4 | Acid-Base Chemistry of Ruthenium Compounds Containing Pyridyl-1,2,4-triazoles. | 164 |
| 4 0 | Introduction | 164 |
| 4 1 | Acid-Base Chemistry of the Free Ligands | 174 |
| 4 2 | Acid-Base Chemistry of Ruthenium Compounds in the Ground State | 178 |
| 4 3 | Excited State Properties Including Lifetime and Quantum Yield Measurements | 184 |
| 4 4 | Conclusion | 196 |
| | References | 198 |

| | | |
|---|---|---|
| CHAPTER 5 | Synthesis and Characterisation of Mono-nuclear and Dinuclear Compounds Containing Asymmetric Potential Bridging Ligands. | 201 |
| 5 0 | Introduction | 202 |
| 5 1 | Preparation of Mononuclear and Dinuclear Compounds containing Asymmetric Potential Bridging Ligands | 215 |
| 5 1 1 | Preparation of Mononuclear Compounds | 215 |
| 5 1 2 | Preparation of Dinuclear Compounds | 220 |
| 5 2 | $^1H$ N m r Spectra | 222 |
| 5 2 1 | $^1H$ N m r Spectra of the Free Ligands | 222 |
| 5 2 2 | $^1H$ N m r Spectra of Mononuclear Compounds Containing 1,3-Bis(pyridin-2-yl) -1,2,4-triazole | 224 |
| 5 2 3 | $^1H$ N m r Spectra of Mononuclear Compounds Containing 1,3-Bis(pyridin-2-yl) -1,2,4-triazole | 230 |

| | | |
|---|---|---|
| 5 2 4 | $^1$H N m r Spectra of Dınuclear Compounds Contaınıng 1,3-Bıs(pyrıdın-2-yl) -1,2,4-trıazole | 233 |
| 5 3 | Electronıc Spectra and Electrochemıstry | 242 |
| 5 3 1 | Mononuclear Complexes Contaınıng 1,3-Bıs -(pyrıdın-2-yl)-1,2,4-trıazole | 242 |
| 5 3 2 | Mononuclear Complexes Contaınıng 1,3-Bıs -(pyrıdın-2-yl)-1,2,4-trıazole | 248 |
| 5 3 3 | Dınuclear Complexes Contaınıng 1,3-Bıs -(pyrıdın-2-yl)-1,2,4-trıazole | 252 |
| 5 4 | Conclusıon | 261 |
| | References | 264 |
| CHAPTER 6 | CONCLUSION | 268 |
| 6 0 | Conclusıon | 269 |
| APPENDIX | | |
| | Tables of Crystal Structure Data | 273 |
| | Lıst of Publıcatıons | 276 |

# PREPARATION, CHARACTERISATION AND PROPERTIES OF RUTHENIUM COMPOUNDS CONTAINING PYRIDYL-1,2,4-TRIAZOLES

BARBARA BUCHANAN

The synthesis and characterisation of ruthenium compounds of the type $[Ru(bpy)_2(L\text{-}L')]^{n+}$, where L-L' are a series of chelating pyridyltriazole ligands, are reported For 3-(pyridin-2-yl)-1,2,4-triazole, $^1H$ n m r and HPLC studies show that two isomers have been formed in the ratio 1 1 upon coordination to a $Ru(bpy)_2$ moiety These isomers have been separated using semi-preparative HPLC techniques Isomer 1 and isomer 2 were characterised using spectrophotometry, electrochemistry and $^1H$ n m r The $pK_a$ values of the isomers are different ($pK_a$ of isomer 1 = 5 95, $pK_a$ of isomer 2 is 4 07) The information obtained on the isomers suggests that in isomer 1 coordination to ruthenium is via the pyridine ring and the $N^{4'}$ nitrogen of the triazole ring, while isomer 2 is coordinated via the pyridine ring and $N^{2'}$ nitrogen of the triazole ring For $[Ru(bpy)_2(3MePyrtr)]PF_6$, where 3MePyrtr = 3-methyl-5-(pyridin-2-yl)-1,2,4-triazole two coordination mode are also possible However, $^1H$ n m r reveals the presence of one isomer only, indicating that the methyl group provides steric hindrance for coordination The X-ray crystal structure of this compound shows that coordination of the ligand takes place via the $N^{1'}$ atom of the triazole ring

The possibility of forming monovalent species of the type $[Ru(bpy)_2(L\text{-}L')Cl]^+$ where L-L' takes up monodentate coordination, was studied with a view to preparing monodenate intermediates analogous to those which are formed during the photolysis of the complex containing the chelating ligand Correlation spectroscopy n m r of the thermally produced monodentate complexes suggests that coordination takes place via the triazole ring, $N^{4'}$ for PT, 3BrPT and 3MePT and $N^{1'}$ for 4MePyrtr The x-ray crystal structure of $[Ru(bpy)_2(3MePT)Cl]^+$ confirms the $N^{4'}$ coordination mode It seems unlikely that the coordination mode for the photochemically produced monodentate-chloro species is the same, as this would probably mean irreversible ligand loss

Investigations into the formation of mononuclear and dinuclear complexes containing asymmetric bridging ligands were carried out using the ligands 1,3-bis(pyridin-2-yl)-1,2,4-triazole (bptn) and 3,5-bis(pyridin-2-yl)-1,2,4-triazole (Hbpt) For bptn only, the formation of the mononuclear complex was possible, suggesting that steric limitations of the ligand prevent the formation of the dinuclear complex Both mono- and di- nuclear complexes were formed containing $bpt^-$ The complexes were characterised using correlation spectroscopy, spectrophotometry and electrochemistry

# CHAPTER 1

## General Introduction on $[Ru(bpy)_3]^{2+}$

## 1 1 Applications and Uses of Ruthenium.

Ruthenium is a rare metal with a natural abundance in the earths crust of ca $10^{-3}$ p p m [1] It is a second row transition metal occurring in group VIIIA of the periodic table, under iron and above osmium, has seven stable isotopes and the electronic configuration $[Kr](4d)^7(5s)^1$

The principle use of ruthenium is for hardening alloys with palladium and platinum Alloys with platinum (12% ruthenium) find applications as electrical contacts, and both platinum and palladium alloys are used for jewellry and fountain pen nibs [1] More recently, labelled compounds containing ruthenium isotopes are reported to have a number of potential applications in nuclear medicine [2] For example, the radioactive isotope ruthenium-97 was recognised as a potential radionuclide (radioactive isotope) for nuclear medicine by Subramanian et al [3] in 1970

The usefulness of radiolabelled ruthenium (III) chloride as a potential subcutaneous tumour localising agent was investigated by Tanaba and Yamamoto in 1975 [4] Their results showed that the cancer cells were stained more intensely with "ruthenium red" than normal cells, indicating a possible preferential uptake of ruthenium [2]

One of the most spectacular advances in synthetic organic chemistry in recent years is the synthesis of enantiomer pure molecules via chiral catalysts [5-8] To date much of this work has been carried out by Noyori et al [5-7] in Japan using new mononuclear Ru(II) complexes containing axially dissymmetric (R)- or (S)-2,2'-bis(diphenylphosphino)-1,1'-binaphthyl [(R)- or (S)-BINAP] and its derivatives These complexes exhibit very high catalytic activity and enantioselectivity in the

hydrogenation of a wide range of substrates including enamides and α-amino ketones [7] These catalysts are also recovered from reactions in high yields

Ruthenium compounds can be stable in nine different oxidation states [Ru(0) to Ru(VIII)] Most of the current research involves the oxidation states (III) and (II) The chemistry of these two oxidation states is both interesting and diverse Ruthenium (III) shows an extensive co-ordination chemistry, forming many stable cationic, neutral and anionic monomeric species [8, 9] The photochemistry and photophysics of Ru(II) species have been studied extensively over the past few decades and continues to expand, and in particular that of $[Ru(bpy)_3]^{2+}$, where bpy = 2,2'-bipyridine [1, 8-10] Carbonyl and organometallic chemistry of Ru(II) is also developing very rapidly

$[Ru(bpy)_3]^{2+}$ was first prepared in 1936 [11] and since its use as a sensitiser was first proposed in 1971 by Demas and Adamson [12], $[Ru(bpy)_3]^{2+}$ has been the subject of extensive investigations [8-10, 13, 14] The compound $[Ru(bpy)_3]^{2+}$ possesses a unique combination of photo-chemistry, electrochemistry and chemical stability To date, a vast number of compounds containing ruthenium have been prepared [1, 8] The Ru(II)-polypyridine type complexes find their most extensive and interesting applications as [15],

(I) Photoluminescent compounds

(II) Excited stated reactants in electron and energy transfer processes

(III) Excited state products in electron transfer chemiluminescence and electrochemiluminescence

$Ru^{2+}$ is a $d^6$ system and the polypyridyl ligands such as 2,2'-bipyridine (bpy), 4,4'-dimethyl-2,2'-bipyridine ($Me_2$bpy), and 1,10-phenanthroline (phen), etc , are visually colourless molecules, possessing $\sigma$ donor orbitals localised on the nitrogen atoms and the $\pi$ and $\pi^*$ acceptor orbitals more or less delocalised on aromatic rings For the $d^6$ configuration a number of complexes of $Ru^{2+}$ and $Os^{2+}$ do luminesce [16, 17] Moreover, the significance of $d^6$ emitters is enhanced by the availability of two distinct energy level schemes [18]

(1)a localised "d-d" type emitter in which the ligands are a small perturbation upon the metal levels

(2)an emitter in which delocalised levels characteristic of the ligand or with mixed d-$\pi$ character emit

## 1 2 Photophysical Properties of $[Ru(bpy)_3]^{2+}$

The photophysical properties of $[Ru(bpy)_3]^{2+}$ may be explained with the aid of Figure 1 1 The absorption spectrum of $[Ru(bpy)_3]^{2+}$ exhibits an intense ($\epsilon$~14,600 $dm^3$ $mol^{-1}$ $cm^{-1}$) absorption band at 452 nm (1) assigned to a metal-to-ligand charge transfer (MLCT) transition [9], which is singlet in character Intersystem crossing (ISC) occurs (2) from the singlet state to four closely spaced $^3$MLCT states [19] The efficiency with which the lower $^3$MLCT states are populated following direct absorption into the higher singlet state is known to be ~1 [20]

The cation emits strongly at 298 K, with a broad structureless orange-yellow emission (3) occurring at 610 nm in water [21] At 77 K, in glassy solution the emission spectrum is well resolved into the different vibrational components with the maximum emission wavelength found at

580 nm Deactivation from the $^3$MLCT state to the ground-state may also occur via non-radiative decay (4) If the energy difference, $\Delta E$, between the $^3$MLCT state and the d-d level is small then thermal population of the d-d level may also occur (5), followed by thermal or photochemical deactivation to ground state (6)

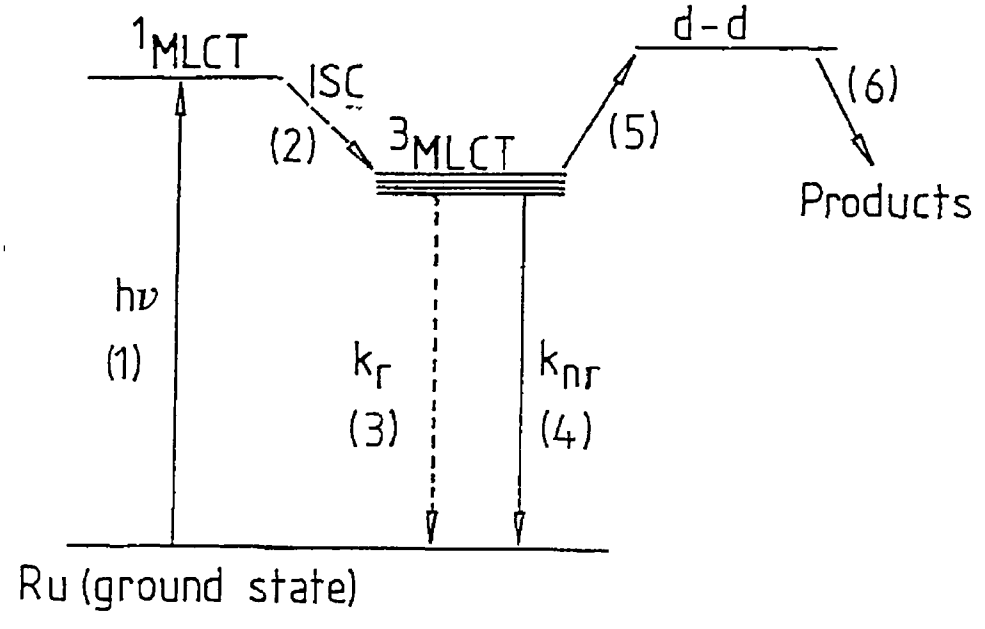


Figure 1 1 Representation of the excited state properties of $[Ru(bpy)_3]^{2+}$

Figure 1 1 may be summarised by the following scheme

$$\text{Ground State} \xrightarrow{h\upsilon} {}^1\text{MLCT} \qquad (1)$$

$$^1\text{MLCT} \xrightarrow{ISC} {}^3\text{MLCT} \qquad (2)$$

$$^3\text{MLCT} \xrightarrow{K_r} \text{Ground State} + h\upsilon \text{ (Emission)} \qquad (3)$$

$^3MLCT$ ---($K_{nr}$)---> Ground State + Heat (4)

$^3MLCT$ <---> dd (5)

dd ---> Ground State or Photochemistry (6)

$[Ru(bpy)_3]^{2+}$ is a very stable species in solution at room temperature and has a relatively long lived $^3MLCT$ state of 620 ns in degassed water [9] An important advantage of MLCT excited states is the presence of two distinct redox sites, i e an oxidising site on the metal and a reductive site on the ligands

$[Ru(bpy)_3]^{2+}$ is one of the few transition metal complexes that luminesces strongly in solution at room temperature and also exhibits a powerful photosensitisation capacity for electron- and energy- transfer processes These properties have resulted in the species being considered in the role of photocatalysts for the visible-light photo-induced decomposition of water into di-hydrogen and di-oxygen As water is transparent to visible and near uv light ($\lambda > 185$ nm) the addition of a sensitizer, such as, $[Ru(bpy)_3]^{2+}$ is necessary so that excitation energy/solar energy can be transmitted to the aqueous medium in order to generate $H_2$ and $O_2$

The photodissociation of water can be considered in terms of two half cell reactions

$$H_2O + e^- \text{ -------> } OH^- + 1/2\ H_2 \quad (7)$$

$$H_2O \text{ -------> } 2H^+ + 1/2\ O_2 + 2e^- \quad (8)$$

Thus generation of a molecule of hydrogen or oxygen involves multi-electron transfer ($2e^-$ for $H_2$ and $4e^-$ for $O_2$) Redox potentials for the above processes are 0 0 V for (7) and 1 23 V for (8) (versus Normal Hydrogen Electrode) at pH = 0 Therefore, the redox properties of $[Ru(bpy)_3]^{2+}$ must be > 1 23 V for oxidation to $[Ru(bpy)_3]^{3+}$, and < 0 00 V for reduction to $[Ru(bpy)_3]^{+}$ From Figure 1 2, which shows the structure of $[Ru(bpy)_3]^{2+}$ along with the ground state redox properties in acetonitrile, it is evident that $[Ru(bpy)_3]^{2+}$ complies with this criteria

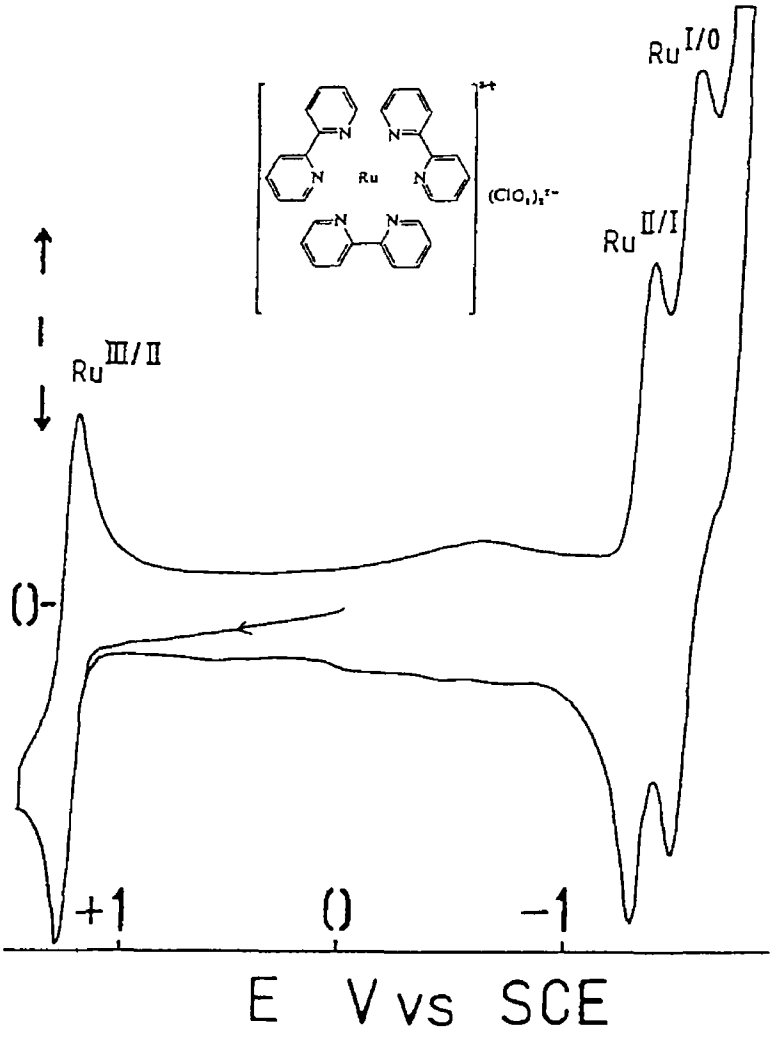


Figure 1 2 Structure and cyclic voltammogram of the oxidation and reduction potentials of $[Ru(bpy)_3]^{2+}$ in acetonitrile/0 1 M $NEt_4ClO_4$

Figure 1 3 shows the free energy diagram for the deactivation of the luminescent excited state of $[Ru(bpy)_3]^{2+}$ to the ground state via $[Ru(bpy)_3]^{+}$ and $[Ru(bpy)_3]^{3+}$ Comparing the redox potentials for the ground state and the excited state in Figure 1 3, it follows that $[Ru(bpy)_3]^{2+}$ is a better reductant and also a better oxidant in its excited state [9, 22]

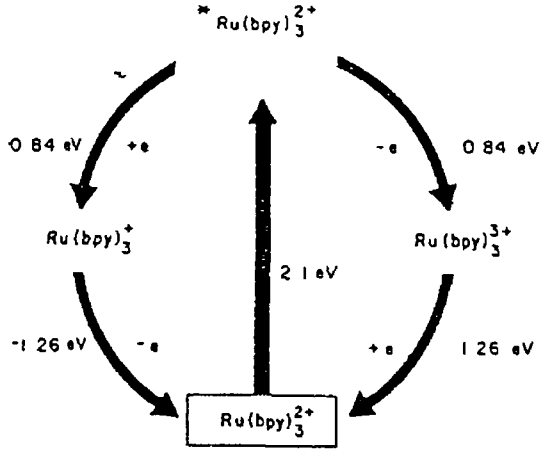


Figure 1 3 Free energy diagram for the deactivation of the luminescent excited state of $[Ru(bpy)_3]^{2+}$ to the ground state via $[Ru(bpy)_3]^{+}$ or $[Ru(bpy)_3]^{3+}$

Several redox schemes can be envisaged involving some of the ground and excited states in Figure 1 3 to achieve one or more of the above processes

(a) Photoreduction of water either with $[Ru(bpy)_3]^{+}$, or with a suitable acceptor relay reduced in an oxidative quenching step

$$2A^{-} + 2H_2O \xrightarrow{cat} 2A + 2OH^{-} + 2H_2O \qquad (9)$$

$A^{-}$ = $[Ru(bpy)_3]^{+}$, or other reduced acceptors such as $Eu^{3+}$ (Europium) or $MV^{+}$ (methyl viologen)

(b) Photooxidation of water either with $[Ru(bpy)_3]^{3+}$ or with some suitable oxidised donor produced in a reductive quenching step

$$4D^+ + 2H_2O \xrightarrow{cat} 4D + 4H^+ + O_2 \qquad (10)$$

The ideal system in which $H_2$ and $O_2$ can be obtained simultaneously has been achieved by Kalyanasundaram and Gratzel [17] and a schematic diagram of this system is presented in Figure 1 4 Low yields of $H_2$ and $O_2$ have been produced upon visible-light irradiation of $[Ru(bpy)_3]^{2+}$, $[MV]^+$, colloidal $RuO_2$, colloidal platinum and water

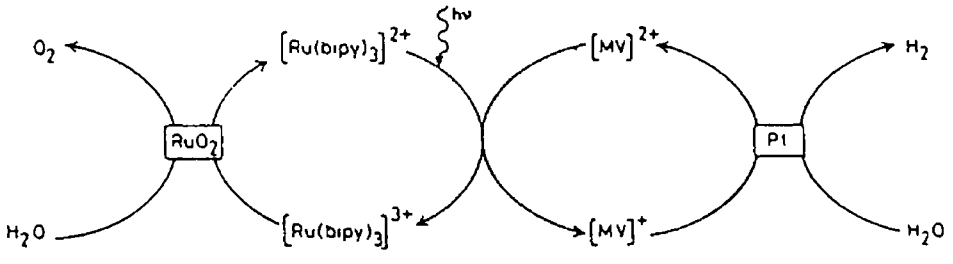


Figure 1 4 Simultaneous catalytic photodecomposition of water to $H_2$ and $O_2$

In general, systems for the light induced $H_2$ evolution from water have a sensitiser such as $[Ru(bpy)_3]^{2+}$, an electron acceptor relay (capable of carrying out reaction (3)), an electron donor to regenerate the sensitiser from its oxidised state and a redox catalyst (see Figure 1 4) Similarly, systems for light induced $O_2$ evolution from water invariably utilise an acceptor which decomposes/ disproportionates upon photoreduction and a redox catalyst to facilitate $[Ru(bpy)_3]^{3+}$ oxidation of water (see Figure 1 4) Multi-electron processes such as shown in equations

(9) and (10) are grossly inefficient in the absence of redox catalysts [9] Further information on photoinduced water splitting reactions may be found in references [1, 8]

The excited state of Ru(II) polypyridine complexes may be changed gradually or "tuned" by judicious choice and combination of the ligands In the majority of Ru(II)-polypyridine complexes the lowest luminescent excited state is a $^3$MLCT (or a cluster of $^3$MLCT levels) For systematic use of these complexes in luminescence and chemiluminescence experiments and in energy transfer processes it is important to have a series of complexes covering a broad range of excited state energies This can be done by,

(I) Changing the type of ligand involved in the formation of the MLCT excited state

(II) Controlling the amount of negative charge on the metal by changing the nature of the ligand

(III) Changing the solvent interaction

The parameters to be taken into consideration are the reduction potential of the free ligand, the $\sigma$ donor ability of the ligand (which is related to the $pK_a$ of the free ligand), the $\pi$ donor and acceptor properties of the ligand and solvent parameters which govern the complex-solvent interactions (dielectric constant)

Large changes in the excited state energy can be obtained by changing the ligand involved in the MLCT transition while substitution on the ligand aromatic rings offers the opportunity to carry out a fine tuning Therefore,

structural variation of ligands is expected to give rise to variations in the photochemical and photophysical properties of $[Ru(L\text{-}L)_3]^{2+}$ complexes, as well as the photoredox ability

One of the features about $[Ru(bpy)_3]^{2+}$ is that it is surrounded by three symmetrical bidentate ligands A wide variety of complexes of the type $[Ru(L\text{-}L)_n(L'\text{-}L')_{3-n}]^{m+}$ (n = 0-3, m = 2), where L-L and L'-L' are different symmetrical chelating ligands, have been synthesised [23-31] Complexes of the type $[Ru(bpy)_n(L\text{-}L')_{3-n}]^{m+}$ ( n = 0-3, m = 1, 2) have also been synthesised where L-L' is an asymmetric chelating ligand [1, 8, 32-34] Our interest lies in the replacement of one of the pyridine rings of $[Ru(bpy)_3]^{2+}$ with a five membered 1,2,4-triazole ring Variations of this pyridyl-1,2,4-triazole ligand include the introduction of a methyl substituent at different sites on the triazole ring, and modification of the pyridyl-triazole bond This work includes the preparation of compounds containing chelating and monodentate pyridyl-triazole ligands, and the investigation of the electronic, electrochemical and photophysical properties of the series of compounds containing pyridyl-1,2,4-triazole ligands (Chapter 3) The crystal structure of $[Ru(bpy)_2(3MePyrtr)]^{+}$ where 3MePyrtr is 3-methyl-5-(pyridin-2-yl)-1,2,4-triazole has been determined and is presented in Chapter 3 Compounds containing monodentate pyridyl-triazole ligands have also been prepared in an attempt to prepare intermediates analogos to those formed in the photochemical reactions of the chelating ligand The crystal structure of $[Ru(bpy)_2(3MePT)Cl](PF_6)$ there 3MePT is 3-methyl-1-(pyridin- 2-yl)-1,2,4-triazole is also presented in Chapter 3

The acid-base properties of $[Ru(bpy)_2(HPyrtr)]^{2+}$ (isomers 1 and 2) and $[Ru(bpy)_2(H3MePyrtr)]^{2+}$ are investigated and the

excited state lifetimes and quantum yields of these cations have been measured in both acidic and basic solutions (Chapter 4) The work concludes with the preparation of mononuclear compounds and the attempted preparation of dinuclear compounds containing asymmetric potentially bridging ligands (Chapter 5)

References.


1 E A Seddon and K R Seddon, "The Chemistry of Ruthenium", Monograph 19, Elsevier 1984, and refs therein

2 S L Waters, Coord. Chem. Rev., 1983, 52, 171

3 G Subramanian, J G McAffee, and J K Poggenburg, J. Nuc. Med., 1970, 11, 365A

4 M Tanabe and G Yamamoto, Acta Med. Okayama, 1975, 29, 43

5 T Ohta, H Takaya, and R Noyori, Inorg Chem., 1988, 27, 566

6 H Takaya, T Ohta, N Sayo, H Kumobayashi, S Akutagawa, S Inoue, I Kasahara, and R Noyori, J Am. Chem. Soc., 1987, 109, 1596

7 (a) B R James, R S McMillan, R H Morris, and D K W Wang, Adv. Chem. Ser., 1978, 167, 122 (b) U Matteoli, G Menchi, P Ferdiani, M Bianchi, and F Piacenti, J. Organomet. Chem., 1985, 285, 281

8 A Juris, V Balzani, F Barigelletti, S Campagna, P Belser, and A von Zelewsky, Coord. Chem Rev., 1988, 84, 85, and refs therein

9 K Kalyanasundaram, Coord. Chem. Rev., 1982, 46, 159

10 K R Seddon, Coord. Chem. Rev., 1982, 41, 79

11 F Burstall, J. Chem. Soc., 1936, 173

12 J N Demas and A W Adamson, J. Am. Chem. Soc., 1971, 93, 1800

13 S J Milder, J S Gold, and D S Kliger, J. Phys. Chem , 1986, 90, 548, and refs therein

14 J Ferguson and E Krausz, Inorg. Chem., 1986, 25, 3335

15 R J Crutchley and A B P Lever, Inorg. Chem., 1982, 21, 2276

16 J E Hillis and M K De Armond, Chem. Phys. Lett., 1971, 325, 10

17 K Kalyanasundaram and M Gratzel, Angew. Chem., Internat. Ed. Engl., 1979, 18, 781

18 M K De Armond, Acc. Chem. Res., 1974, 7, 309

19 E M Kober and T J Meyer, Inorg. Chem., 1984, 23, 3877, and refs therein

20 J N Demas and D G Taylor, Inorg. Chem., 1979, 18, 3177

21 F E Lytle and D M Hercules, J. Am. Chem. Soc., 1969, 91, 253

22 N Sutin and C Creutz, J. Am. Chem. Soc., Adv. Chem. Ser., 1978, 168, 1

23 W J Dressick, B L Hauenstein Jr , T B Gilbert,J N Demas, and B A DeGraff, J. Phys. Chem., 1984, 88, 3337

24 D Conrad, G H Allen, D P Rillema, and T J Meyer, Inorg. Chem., 22, 1614

25 V Skarda, M J Cook, A P Lewis, G S G McAuliffe, A J Thompson, and D J Robins, J. Chem. Soc., Perkin Trans. 2, 1984, 1309

26 P C Alford, M J Cook, A P Lewis, G S G McAuliffe, V Skarda, A J Thompson, J L Glasper, and D J Robins, J. Chem. Soc., Perkin Trans. 2, 1985, 705

27 A Juris, V Balzani, P Belser, and A von Zelewsky, Helv. Chim Acta, 1981, 64, 2175

28 G H Allen, R P White, D P Rillema, and T J Meyer, J. Am. Chem. Soc., 1984, 106, 2613

29 J N Demas, E W Harris, and R P McBride, J. Am. Chem. Soc., 1977, 99, 3547

30 J I Cline, W J Dressick, J N Demas, and B A DeGraff, J. Phys. Chem., 1985, 89, 94

31 D M Klassen, Chem. Phys. Lett., 1982, 93, 383

32 L J Fitzpatrick and H A Goodwin, Inorg. Chim. Acta, 1982, 61, 229

33 P J Steel, F Lahousse, D Lerner, and C Marzin, Inorg. Chem., 1983, 22, 1488

34 C T Lin, W Boettcher, M Chou, C Creutz, and N Sutin, J. Am. Chem. Soc., 1976, 98, 6536

# Chapter 2

## Experimental

## 2 1 Synthesis.

### 2 1 1 Ligand Preparation.

The following five ligands were kindly donated by R Hage from Leiden University and were prepared using literature methods

**(1) 3-(Pyridin-2-yl)-1H-1,2,4-triazole (HPyrtr)**
M P 158-160°C (lit [1] 164-165°C) $^{1}H$ N m r , [$(CD_3)_2SO$], 14 62 (s, N-H), 8 70 (1H, d, $H^6$), 8 27 (1H, s, $H^{5'}$), 8 09 (1H, d, $H^3$), 7 98 (1H, t, $H^4$) and 7 51 (1H, t, $H^5$) $^{13}C$, ($CDCl_3$), 154 8 ($C^{3'}$), 151 8 ($C^{5'}$), 146 6 ($C^2$), 137 8 ($C^4$), 125 0 ($C^5$) and 121 9 ($C^3$) p p m

**(2) 4-Methyl-3-(pyridin-2-yl)-4H-1,2,4-triazole (4MePyrtr)**
M P 96-99°C (lit [2] 104-105°C) $^{1}H$ N m r , [$(CD_3)_2SO$], 8 66 (1H, d, $H^6$), 8 62 (1H, S, $H^5$), 8 11 (1H, d, $H^3$), 7 95 (1H, t, $H^4$), 7 47 (1H, t, $H^5$) and 3 99 (1H, s, $CH_3$) $^{13}C$ ($CDCl_3$), 33 4 ($CH_3$), 122 8 ($C^3$), 124 2 ($C^5$), 137 4 ($C^4$), 147 2 ($C^5$), 147 5 ($C^2$), 149 0 ($C^6$) and 151 1 ($C^3$) p p m

**(3) 3-Methyl-5-(pyridin-2-yl)-1H-1,2,4-triazole(H3MePyrtr)**
M P 163-165°C (lit [3] 165-166°C) $^{1}H$ N m r , [$(CD_3)_2SO$] 14 2 (s, N-H), 8 83 (1 H, d, $H^6$), 8 02 (1 H, d, $H^3$), 7 90 (1 H, t, $H^4$), 7 43 (1 H, t, $H^5$) and 2 36 (3 H, s, $CH_3$) $^{13}C$,($CDCl_3$),13 0 ($CH_3$), 121 6 ($C^3$), 124 3 ($C^5$), 137 3 ($C^4$), 147 5 ($C^2$), 149 2 ($C^6$), 156 5 ($C^{3'}$), and 158 5($C^{5'}$) p p m

**(4) 1-Methyl-3-(pyridin-2-yl)-1,2,4-triazole (1MePyrtr)**
M P 51-54°C (lit [4] 47-48°C) $^{1}H$ N m r , [$(CD_3)_2SO$] 8 66 (1H, d, $H^6$), 8 61 (1H, s, $H^5$), 8 16 (1H, d, $H^3$), 7 91 (1H, t, $H^4$), 7 43 (1H, t, $H^5$) and 3 97 (3H, s, $CH_3$) $^{13}C$, ($CDCl_3$) 36 1 ($CH_3$), 121 4 ($C^3$), 123 8 ($C^4$), 136 9 ($C^4$), 145 8($C^{5'}$), 149 5, ($C^6$), 149 7 ($C^2$), and 161 2($C^{3'}$) p p m

**(5) 3,5-Bis(pyridin-2-yl)-1,2,4-triazole (bpt)**

Prepared according to literature methods, [5] M P 178-180°C (lit [5]) $^{1}H$ N m r , [$(CD_3)_2SO$] 8 67 (2H, d, $H^6$), 8 15 (2H, d, $H^3$), 8 00 (2H, t, $H^4$), 7 52 (2H, t, $H^5$) $^{13}C$ ($CDCl_3$) 158 9 ($C^{3'}$), 149 7 ($C^6$), 147 7 ($C^2$), 137 4 ($C^4$), 124 6 ($C^5$) and 122 1 ($C^3$) p p m

The following set of ligands were prepared using the Ullman Condensation reaction [6] This reaction involves the synthesis of biaryls by copper-induced coupling of aryl halides The purpose of this reactions is to vary the nature of the pyridyltriazole bond, that is, to form a C-N bond

**(6) 1-(Pyridin-2-yl)-1,2,4-triazole (PT)**

A mixture of 1,2,4-triazole (3 35g, 0 05 mole), 2-bromo-pyridine (11 25g, 0 05 mole), anhydrous potassium carbonate (7g), and copper(II) oxide (0 25g) in pyridine (10$cm^3$) was heated under reflux for 24 hours The cooled mixture was extracted three times with chloroform (40$cm^3$) The solvents were removed from the combined filtrates, and the residues thus obtained were absorbed on alumina and eluted with chloroform MP 90-93°C (lit [6] 92-94°C) $^{1}H$ N m r , [$(CD_3)_2SO$] 9 37 (1H, s, $H^{3'}$), 8 53 (1H, d, $H^6$), 8 30 (1H, s, $H^{5'}$), 8 06 (1H,t,$H^4$), 7 86 (1H, d, $H^3$) and 7 47 (1H, s, $H^5$) $^{13}C$, 112 9 ($C^3$), 123 6 ($C^5$), 140 2 ($C^{5'}$), 148 7 ($C^6$), 153 0 ($C^{3'}$) p p m

**(7) 3-Bromo-1-(pyridin-2-yl)-1,2,4-triazole (3BrPT)**

3-Bromo-1,2,4-triazole was prepared as described in the literature [7] This was mixed with 2-bromo-pyridine under the reaction conditions described above M P 107 5-108 5°C $^{1}H$ N m r , [$(CD_3)_2SO$] 9 21 (1H, s, $H^{3'}$), 8 54(1H, d, $H^6$), 8 16 (1H, t, $H^4$), 7 90 (1H, d, $H^3$), and 7 55 (1H, q, $H^5$) p p m $^{13}C$ ($CDCl_3$) 112 8 ($C^3$), 124 0 ($C^5$), 140 2 ($C^{5'}$), 143 8 ($C^{3'}$), 148 5 ($C^6$)

**(8) 3-Methyl-1-(pyridine-2-yl)-1,2,4-triazole. (3MePT)**

3-Methyl-1,2,4-triazole was prepared according to literature [7] and treated with 2-bromo-pyridine as above. MP.86-87°C. $^{1}H$ N.m.r., [$(CD_3)_2SO$]: 2.21 (3H, s, $CH_3$), 8.89 (1H, s, $H^{5'}$), 8.29 (1H, d, $H^6$), 7.83 (1H, d, $H^3$), 7.67 (1H, t, $H^4$), 7.21 (1H, q, $H^5$) p.p.m..

**(9) 1-(Pyridin-2-yl) pyrazole. (PNP)**

Pyrazole was mixed with 2-bromo-pyridine and treated as above. M.P. 38-40°C (lit. [6] 38-40°C). $^{1}H$ N.m.r., [$(CD_3)_2SO$]: 8.60 (1H, d, $H^{3'}$), 8.44 (1H, d, $H^6$), 7.8 - 7.90 (3H, m, $H^3$, $H^4$, $H^{5'}$), 7.30 (1H, m, $H^5$), 6.54 (1H, s, $H^{4'}$). $^{13}C$; $CDCl_3$ 108.1 ($C^{4'}$), 119.3 ($C^3$), 121.8 ($C^5$), 126.9 ($C^4$), 139.3 ($C^{5'}$), 142.1 ($C^{3'}$), 148.2 ($C^6$) and 150.8 ($C^2$) p.p.m.

**(10) 1,3-Bis(pyridin-2-yl)-1,2,4-triazole. (bptn)**

3-(pyridin-2-yl)-1H-1,2,4-triazole and 2-bromo-pyridine were mixed together under the reaction conditions described above. M.P. 128-131°C. $^{1}H$ N.m.r., [$(CD_3)_2SO$]: (see Figure 5.4 Chapter 5 for structure) 9.48 (1H, s, $H^5$), 8.70 (1H, d, $H^6$, A), 8.57 (1H, d, $H^6$, B), 7.46 - 7.54 (m, $H^5$, s), 7.92 - 8.01 (m, $H^4$,s) and 8.08 - 8.19 (m, $H^3$,). $^{13}C$; 153.8 ($C^3$), 143.13 ($C^5$), 148.83 ($C^2$, A and B), 122.11 ($C^3$, A), 113.0 ($C^3$, B), 137.23 ($C^4$, A), 140.24 ($C^4$, B), 124.58 ($C^5$, A), 123.74 ($C^5$,B), 149.82 ($C^6$, A), 140.74 ($C^6$, B). Ring A is the pyridine ring which is bound via the carbon atom of the triazole while ring B is bound to the triazole via the nitrogen atom of the triazole ring.

### 2.1.2 Preparation of Complexes of the Type Cis-[$Ru(bpy)_2(L\text{-}L')]^{n+}$.

(L-L') = HPyrtr, H3MePyrtr, 1MePyrtr, 4MePyrtr, PNP, PT, 3BrPT, 3MePT: n = 2. (L-L') = $Pyrtr^-$ and 3MePyrtr: n = 1. Hydrated ruthenium trichloride was obtained as a loan from

Johnson Matthey and used without further purification The complex cis-$[Ru(bpy)_2Cl_2]$ $2H_2O$ was prepared as described in the literature [8] All other reactants were reagent grade and used as received

**$[Ru(bpy)_2(HPyrtr)](PF6)_2$ (1)**

The cis-complex $[Ru(bpy)_2Cl_2]$ $2H_2O$ (520 mg, 1 mmol) was heated under reflux in water-methanol (50 50 $cm^3$) in the presence of an excess of 3-(pyridin-2-yl)-1H-1,2,4-triazole ligand (343 mg, 1 2 mmol) for 4 hours In order to ensure complete protonation of the bound ligand, 1-2 drops concentrated hydrochloric acid were added during heating The solvent was removed by rotary evaporation and the remaining residue was dissolved in water (5 $cm^3$) and added dropwise to an aqueous solution of $NH_4PF_6$ The resulting precipitate was collected by filtration and purified by column chromatography, using neutral alumina with ethanol as eluent Further purification was carried out by recrystallisation from acidic (2M HCl) mixtures of acetone-water [9] Yield 680 mg (80%) Found C, 38 0, H, 2 9, N, 13 1, $C_{27}H_{22}F_{12}N_8P_2Ru$ requires C, 38 2, H, 2 6, N, 13 9% Two isomers were obtained and were separated using semi preparative HPLC

**$[Ru(bpy)_2(Pyrtr)]PF_6$ $3H_2O$ (2)**

This compound was prepared as for (1) but no concentrated hydrochloric acid was added during the reflux and 1M NaOH (2 $cm^3$) was added to the recrystallisation mixture Yield 577 mg (68%) Found C, 42 3, H, 3 1, N, 14 8 $C_{27}H_{27}F_6N_8O_3PRu$ requires C, 42 8, H, 3 6, N, 14 8%

**$[Ru(bpy)_2(H3MePyrtr)](PF_6)_2$ $H_2O$ (3)**

This compound was prepared as for (1) Yield 828 mg (94%) Found C, 38 5, H, 3 1, N, 12 6, $C_{28}H_{26}F_{12}N_8OP_2Ru$ requires C, 38 2, H, 3 1, N, 12 7% $^1H$ N m r , $[CD_3)_2SO]$ Pyridyltriazole ligand, 2 40 ($CH_3$), 8 24 ($H^3$), 8 08 ($H^4$),

7 41 ($H^5$), 7 63 ($H^6$) Bipyridyl ligands, 8 53-8 62 ($H^3$), 7 95-8 03 ($H^4$), 7 31-7 38 ($H^5$), 7 57-7 73 ($H^6$) p p m

**[Ru(bpy)$_2$(3MePyrtr)]PF$_6$ 4H$_2$O (4)**

This compound was prepared as for (2) Yield 583 mg (70%) Found C, 42 7, H, 3 3, N, 14 4, $C_{28}H_{31}F_6N_8O_4PRu$ requires C, 42 6, H, 3 9, N, 14 2% $^1$H N m r, [$(CD_3)_2SO$] Pyridyltriazole ligand, 2 20 ($CH_3$), 8 02 ($H^3$), 7 99 ($H^4$), 7 23 ($H^5$), 7 67 ($H^6$) Bipyridyl ligands, 8 68-8 79 ($H^3$), 8 06-8 09 ($H^4$), 7 40-7 60 ($H^5$), 7 81-7 93 ($H^6$) p p m

**[Ru(bpy)$_2$(1MePyrtr)](PF$_6$)$_2$ (5)**

This compound was prepared as for (2) except no NaOH was added to the recrystallisation mixture Yield 634mg (72%) Found C, 38 4, H, 2 8, N, 12 7, $C_{28}H_{26}F_{12}N_8OP_2Ru$ requires C, 38 1, H, 3 0, N, 12 7% $^1$H N m r, [$(CD_3)_2SO$] Pyridyltriazole ligands, 3 97 ($CH_3$), 8 73 ($H^{5'}$), 8 36 ($H^3$), 8 10 ($H^4$), 7 46 ($H^5$), 7 58 ($H^6$) Bipyridyl ligands, 8 79-8 84 ($H^3$), 8 11-8 17 ($H^4$), 7 50-7 55 ($H^5$), 7 74-7 87 ($H^6$) p p m

**[Ru(bpy)$_2$(4MePyrtr)](PF$_6$)$_2$ (6)**

This compound was prepared as for (5) Yield 800 mg (70%) Found C, 38 7, H, 2 8, N, 12 5, $C_{28}H_{24}F_{12}N_8P_2Ru$ requires C, 39 0, H, 2 8, N, 13 0% $^1$H N m r, [$(CD_3)_2SO$] Pyridyltriazole ligand, 4 19 ($CH_3$) 8 88 ($H^{5'}$), 8 43 ($H^3$), 8 09 ($H^4$), 7 44 ($H^5$), 7 65 ($H^6$) Bipyridyl ligands, 8 72-8 85 ($H^3$), 8 12-8 20 ($H^4$), 7 51-7 58 ($H^5$), 7 76-7 83 ($H^6$) p p m

**[Ru(bpy)$_2$(PNP)](PF$_6$)$_2$ (7)**

This compound was prepared as for (5) Yield 800 mg (95%) Found C, 39 6 H, 2 7 N, 11 7 $C_{28}H_{23}F_{12}N_7P_2Ru$ requires C, 39 6, H, 2 7, N, 11 6% $^1$H N m r, [$(CD_3)_2SO$] Pyridyltriazole ligand, 9 35 ($H^{3'}$) 6 94 ($H^4$), 8 45 ($H^5$), 8 45 ($H^3$), 8 20 ($H^4$), 7 40 ($H^5$), 7 91 ($H^6$), Bipyridyl ligands, 8 75-8 85 ($H^3$), 8 13-8 25 ($H^4$), 7 50-7 62 ($H^5$), 7 70-7 86 ($H^6$) p p m

**$[Ru(bpy)_2(PT)](PF_6)_2$ (8)**

This compound was prepared as for (5) Yield 708 mg (85%) Found C, 37 8, H, 2 3, N, 13 1% $C_{27}H_{22}F_{12}N_8P_2Ru$ requires C, 38 7, H, 2 6, N, 13 4% $^1H$ N m r , $[(CD_3)_2SO]$ Pyridyltriazole ligand, 9 99 ($H^{3'}$), 8 39 ($H^{5'}$), 8 59 ($H^3$), 8 19 ($H^4$), 7 53 ($H^5$), 7 97 ($H^6$) Bipyridyl ligands 8 75- 8 85 ($H^3$), 8 20-8 30 ($H^4$), 7 55-7 65 ($H^5$), 8 05-8 20 ($H^6$) p p m

**$[Ru(bpy)_2(3BrPT)](PF_6)_2$ (9)**

This compound was prepared as for (5) Yield 780 mg (84%) Found C, 34 8, H, 2 2, N, 12 0, Br, 7 8 $C_{27}H_{22}BrF_{12}N_8P_2Ru$ requires C, 35 1, H, 2 5, N, 12 1, Br, 7 6% $^1H$ N m r , $[(CD_3)_2SO]$ Pyridyltriazole ligand, 10 18 ($H^{5'}$), 8 52 ($H^3$), 8 31 ($H^4$), 7 48 ($H^5$), 7 71 ($H^6$) Bipyridyl ligands, 8 77-8 86 ($H^3$), 8 09-8 34 ($H^4$), 7 50-7 63 ($H^5$), 7 65-8 09 ($H^6$) p p m

**$[Ru(bpy)_2(3MePT)](PF_6)_2$ (10)**

This compound was prepared as for (5) Yield 750 mg (87%) Found C, 39 0, H, 2 8, N, 13 2, $C_{28}H_{24}F_{12}N_8P_2Ru$ requires C, 38 9, H, 2 8, N, 13 0% $^1H$ N m r , $[(CD_3)_2SO]$ Pyridyltriazole ligand, 1 81 ($CH_3$), 10 05 ($H^{5'}$), 8 62 ($H^3$), 8 31 ($H^4$), 7 51 ($H^5$), 7 79 ($H^6$), Bipyridyl ligands, 8 85-8 89 ($H^3$), 8 20-8 38 ($H^4$), 7 57-7 66 ($H^5$), 7 90-8 24 ($H_6$) p p m

### 2 1 3 Preparation of Complexes of the Type *Cis*-$[Ru(bpy)_2(L\text{-}L')Cl]PF_6$.

(L-L') = PT, 3BrPT, 3MePT, 4MePyrtr

**$[Ru(bpy)_2(PT)Cl](PF_6)$ (11)**

The cis-complex $[Ru(bpy)_2Cl_2]$ $2H_2O$ (520 mg, 1 mmol) was heated under reflux in ethanol $H_2O$ (63 30 $cm^3$) Small aliquots of 1-(pyridin-2-yl)-1H-1,2,4-triazole dissolved in ethanol were added over a period of 10 minutes. The

mixture was refluxed for a further 20 minutes The solvent was removed on the rotary evaporator, and the remaining residue was dissolved in 5 $cm^3$ of methanol-diethyl ether (3 1) Purification took place by column chromatography using neutral alumina and methanol-ether (3 1) containing 1% acetone as eluent The dark red fraction later found to be the monodentate species eluted first, the orange fraction of the bidentate species was removed with methanol Fraction 1 was precipitated by addition to aqueous $NH_4PF_6$, filtered and dried overnigth under vacuum Yield 396 mg (52%) Found C, 43 8, H, 3 0, N, 14 6, Cl, 4 7, $C_{27}H_{22}ClF_6N_8PRu$ requires C, 43 8, H, 3 0, N, 15 1, Cl, 4 8% $^1H$ N m r , $[(CD_3)_2SO]$ Pyridyltriazole ligand, 8 02 ($H^{3'}$), 9 62 ($H^{5'}$), 8 66 ($H^3$), 8 15 ($H^4$), 8 03 ($H^5$), 10 03 ($H^6$) Bipyridine ligands, 8 48 8 86 ($H^3$), 7 84-8 15 ($H^4$), 7 27-7 66 ($H^5$), 7 80-8 69 ($H^6$) p p m

**$[Ru(bpy)_2(3BrPT)Cl](PF_6)$ (12)**

This compound was prepared as for (11) using (270 mg, 1 2 mmol) of 3-bromo-1-(pyridin-2-yl)-1H-1,2,4-triazole Yield 311 mg (38%) Found C, 39 5, H, 2 6, N, 13 4, Br, 9 7, Cl, 4 3% $C_{27}H_{21}BrClF_6N_8PRu$ requires C, 39 6, H, 2 6, N, 13 7, Br, 8 7, Cl, 3 6% $^1H$ N m r , $[(CD_3)_2SO]$ Pyridyltriazole ligand, 10 36 ($H^{5'}$), 8 60 ($H^3$), 8 17 ($H^4$), 7 90 ($H^5$), 10 06 ($H^6$) Bipyridine ligands, 8 48-9 10 ($H^3$), 7 81-7 98 ($H^4$), 7 25-7 80 ($H^5$), 7 80-8 26 ($H^6$)

**$[Ru(bpy)_2(3MePT)Cl](PF_6)$ (13)**

This compound was prepared as for (11) using (192 mg, 1 2 mmol) of 3-methyl-1-(pyridin-2-y,)-1H-1,2,4-triazole Yield 347 mg (46%) $^1H$ N m r , $[(CD_3)_2SO]$ Pyridyltriazole ligand, 1 20 ($CH_3$), 9 07 ($H^{5'}$), 8 66 ($H^3$), 7 90 ($H^4$), 8 18 ($H^5$), 10 12 ($H^6$) Bipyridine ligands, 8 58-8 73 ($H^3$), 7 92-8 18 ($H^4$), 7 28-7 70 ($H^5$), 7 78-8 90 ($H^6$) p p m

**[Ru(bpy)$_2$(4MePyrtr)Cl](PF$_6$) H$_2$O (14)**

The complex cis-[Ru(bpy)$_2$Cl$_2$] 2H$_2$O (520 mg, 1 mmol) was heated under reflux in acetone-ethanol (50 50 cm$^3$) The ligand 4-methyl-1-(pyridin-2-yl)-1,2,4-triazole (190 mg, 1 2 mmol) was dissolved in acetone (5 cm$^3$) and added to the reaction mixture over a period of 10 minutes and heated under reflux for 35 min The solvent was removed by rotary evaporation and the remaining residue dissolved in methanol-diethylether (3 1) and purified using alumina and methanol-diethylether (3 1) containing 1% acetone as eluent A dark red fraction later found to be the monodentate species eluted first and the solvent was removed by rotary evaporation, the residue dissolved in 5 cm$^3$ water and precipitated by addition to aqueous $NH_4PF_6$ Yield 527 mg (80%) Found C, 43 3, H, 3 2, N, 14 1, Cl, 4 4, $C_{28}H_{26}ClF_6N_8OPRu$ requires C, 43 5, H, 3 1, N, 14 5, Cl, 4 6% $^1$H N m r , [(CD$_3$)$_2$SO] Pyridyltriazole ligand, 4 39 ($CH_3$), 9 2 ($H^{3'}$), 8 83 ($H^3$), 7 31 ($H^4$), 8 09 ($H^5$), 10 05 ($H^6$) Bipyridine ligands, 8 52-8 86 ($H^3$), 8 03-8 28 ($H^4$), 7 45-7 68 ($H^5$), 7 79-8 01 ($H^6$) p p m

## 2 1 4 Preparation of Mononuclear and Dinuclear Ruthenium Complexes Containing Asymmetric Bridging Ligands.

Monomeric complexes of the type [Ru(L-L)$_2$(L'-L'')]$^{n+}$ (n = 1 or 2) were prepared along with the dimeric analogues [(L-L)$_2$Ru(L'-L")Ru(L-L)$_2$]$^{n+}$ (n = 3 or 4), where L'-L'' = 1,3-bis(pyridin-2-y)-1,2,4-triazole (bptn) or 3,5-bis(Pyridin-2-yl)-1,2,4-triazole (Hbpt) L-L = 2,2'bipyridine (bpy), 4,4'-dimethyl-2,2'bipyridine (Me$_2$bpy) or 1,10-phenthroline (phen) [Ru(Me$_2$bpy)$_2$Cl$_2$] 2H$_2$O and [Ru(phen)$_2$Cl$_2$] 2H$_2$O were prepared according to literature methods [8]

**[Ru(bpy)$_2$(bptn)](PF$_6$)$_2$ (15)**

[Ru(bpy)$_2$Cl$_2$] 2H$_2$O (520 mg, 1 mmol) was refluxed in ethanol/water (60 30 cm$^3$) in the presence of bptn (268 mg, 1 2 mmol) for 6h After solvent evaporation the residue was dissolved in a minimum amount of ethanol and purified by column chromatography using neutral alumina and ethanol as eluent Yield 1 6g (90%) Found C, 41 5, H, 2 9, N, 13 1% $C_{32}H_{25}F_{12}N_9P_2Ru$ requires C, 41 5, H, 2 7, N, 13 6%

**[Ru(Me$_2$bpy)$_2$(bptn)](PF$_6$)$_2$ 2H$_2$O (16)**

This compound was prepared as for (15) using [Ru(Me$_2$bpy)$_2$Cl$_2$] 2H$_2$O (575 mg, 1 mmol) and bptn (268 mg, 1 2 mmol) Yield 1 57g (89%) Found C, 42 5, H, 3 7, N, 11 8% $C_{36}H_{39}F_{12}N_9O_2P_2Ru$ requires C, 42 4, H, 3 4, N, 12 3%

**[Ru(phen)$_2$(bptn)]PF$_6$ (17)**

This compound was prepared as for (15) using [Ru(phen)$_2$Cl$_2$] 2H$_2$O (567 mg, 1 mmol) and bptn (268 mg, 1 2 mmol) Yield 1 39g (81%) Found C, 44 4, H, 2 6, N, 12 5% $C_{36}H_{25}F_{12}N_9P_2Ru$ requires C, 44 4, H, 2 5, N, 12 9%

**[Ru(bpy)$_2$(bpt)]PF$_6$ H$_2$O (18)**

This compound was prepared as for [5] Yield 1 19 g (70%) $^1$H N m r , [(CD$_3$)$_2$SO] Bpt$^-$ ligand, ruthenium-bound pyridine ring, 8 44 (H$^3$), 8 23 (H$^4$), 7 41 (H$^5$), 7 66 (H$^6$) Free pyridine ring of bpt, 7 20 (H$^3$), 7 90 - 8 20 (H$^4$), 7 27 (H$^5$), 8 23 (H$^6$) Bipyridine ligands, 8 70-8 85 (H$^3$), 7 90 - 8 20 (H$^4$), 7 40 - 7 60 (H$^5$), 7 90 - 8 20 (H$^6$)

**[Ru(Me$_2$bpy)$_2$(bpt)]PF$_6$ (19)**

The cis-complex [Ru(Me$_2$bpy)$_2$Cl$_2$] 2H$_2$O (575 mg, 1 mmol) was periodically added to a boiling mixture of Hbpt (267 mg, 1 2 mmol) in 60 cm$^3$ ethanol/water (2 1) for 6 h The hot solution was filtered and the filtrate evaporated to dryness, after which the residue was dissolved in a minimum

amount of ethanol This solution was purified by column chromatography using neutral alumina and ethanol as eluent Further purification took place using Sephadex C25 and 0 1M NaCl as eluent (to remove any traces of the dimer which may have formed) The purified mixture was evaporated to dryness after which the compound was extracted from the NaCl residue by addition of ethanol The NaCl was removed by filtration, and then the filtrate was precipitated by adding an excess of aqueous $NH_4PF_6$ to the solution After filtration the compound was recrystallised from water/ acetone (1 1) Yield 1 13 g (78%) Found C, 49 6, H, 3 7, N, 14 0% $C_{36}H_{32}F_6N_9PRu$ requires C, 51 6, H, 3 8, N, 15 0%

**$[(Ru(Me_2bpy)_2)_2(bpt)](PF_6)_3$ (20)**

The ligand Hbpt (110 mg, 1mmol) was added over a period of 10 minutes to a boiling mixture of cis-$[Ru(Me_2bpy)_2Cl_2]$ $2H_2O$ (630 mg, 2 2 mmol) in 100 $cm^3$ ethanol/water (2 1) for 8 h The hot solution was filtered and evaporated to dryness, after which the residue was dissolved in a minimum amount of ethanol The liquid residue was purified by column chromatography using neutral alumina and ethanol as eluent After solvent evaporation the liquid residue was added dropwise to an aqueous solution of $NH_4PF_6$ to yield the desired precipitate Further purification took place by recrystallisation from water/acetone (1 1) Yield 455 mg (24%) Found C, 39 8, H, 3 3, N, 9 8% $C_{60}H_{56}F^1{}_8N_{13}P_3Ru_2$ requires C, 45 1, H, 3 5, N, 11 4%

**$[Ru(phen)_2(bpt)]PF_6$ $H_2O$ (21)**

This compound was prepared as for (18) using cis-$[Ru(phen)_2Cl_2]$ $2H_2O$ (567 mg, 1 mmol) of and Hbpt (267 mg, 1 2 mmol) Yield 306 mg (77%) Found C, 51 0, H, 3 0, N, 14 7% $C_{36}H_{26}F_6N_9OPRu$ requires C, 51 0, H, 3 0, N, 14 8%

**[(Ru(phen)$_2$)$_2$(bpt)](PF$_6$)$_3$ (22)**

This compound was prepared as for (20) using Hbpt (110 mg, 1 mmol) and [Ru(phen)$_2$Cl$_2$] 2H$_2$O (635 mg, 2 2 mmol) Yield 368 mg (22%) Found C, 46 5, H, 3 0, N, 11 7% $C_{60}H_{48}f_{12}N_{13}P_3Ru_2$ requires C, 46 7, H, 2 7, N, 11 2%

**[(bpy)$_2$Ru(bpt)Ru(Me$_2$bpy)$_2$](PF$_6$)$_3$ 4H$_2$O (23)**

The monomer [Ru(bpy)$_2$(bpt)]PF$_6$ H$_2$O (18) (926 mg, 1 mmol) was heated under refluxed with [Ru(Me$_2$bpy)$_2$Cl$_2$] 2H$_2$O (690 mg, 1 2 mmol) in ethanol-water (120 60 cm$^3$) for 8 h The hot solution was filtered and evaporated to dryness, after which the residue was dissolved in a small amount of ethanol This liquid residue was purified by column chromatography using neutral alumina and ethanol as eluent After evaporation of ethanol the compound was precipitated in aqueous NH$_4$PF$_6$ Further purification took place by recrystallisation from acetone-water (1 1) Yield 1 41 g (85%) Found C, 41 6, H, 3 18, N, 11 2% $C_{56}H_{62}F_{18}N_{13}O_4P_3Ru_2$ requires C, 41 7, H, 3 4, N, 11 3%

**[(bpy)$_2$Ru(bpt)Ru(phen)$_2$](PF$_6$)$_3$ (24)**

This compound was prepared as for (23) using [Ru(bpy)$_2$(bpt)]PF$_6$ (18) (926 mg, 1 mmol) and [Ru(phen)$_2$Cl$_2$] 2H$_2$O (680 mg, 1 2 mmol) Yield 726 mg (40%) Found C, 39 9, H, 2 68, N, 11 7% $C_{56}H_{40}F_{18}N_{13}P_3Ru_2$ requires C,43 9, H,2 61, N,11 9%

**[(phen)$_2$Ru(bpt)Ru(Me$_2$bpy)$_2$](PF$_6$)$_3$ 2H$_2$O (25)**

This compound was prepared as for (23) using [Ru(phen)$_2$(bpt)]PF$_6$ 2H$_2$O (18) (846 mg, 1 mmol) and [Ru(Me$_2$bpy)$_2$Cl$_2$] 2H$_2$O (690 mg, 1 2 mmol) Yield 1 20 g (70%) Found C, 44 7, H, 3 27, N, 10,9 % $C_{60}H_{56}F_{18}N_{13}O_2PRu_2$ requires C,44 3, H, 3 2, N, 11 2%

## 2 2 Instrumentation

### 2 2 1 Absorption and Emission Spectra

Uv/vis spectra were obtained using either a Hewlett Packard 8452A Diode Array Spectrometer or a Shimadzu UV24 detector Absorption co-efficients are accurate to 5% Emission spectra were obtained on a Perkin-Elmer LS-5 luminescence spectrometer equipped with a red sensitive Hamamatsu R 928 photomultiplier tube An emission slit width of 10 nm was used at room temperature and 2 5 nm at 77 K and the results obtained were not corrected for photomultiplier response

### 2 2 2 $pK_a$ Measurement

Sample measurements were carried out in a Britton-Robinson (BR) buffer (0 04M boric acid, 0 04 M acetic acid, and 0 04M phosphoric acid) The pH of the solutions was adjusted using 2 M NaOH Luminescence titrations were carried out using an appropriate isosbestic point as the excitation wavelength To facilitate dissolution of samples in aqueous solutions the dichloride salt was used to determine $pK_a$ values

### 2 2 3 Electrochemical Measurements

(1) Electrochemical measurements were carried out with an EG&G Par 174A polarographic analyzer and an EG&G Par 175 universal programmer A saturated calomel electrode (SCE) was used as the reference electrode Measurements were carried out in dried spectroscopic grade $CH_3CN$ and with 0 1 mol $dm^{-3}$ $NEt_4ClO_4$ as a supporting electrolyte Both glassy carbon and platinum electrodes were used as working electrodes The scan rate used was 100 mV/sec

(2) Differential Pulse Voltametry (DPV)

DPV was carried out using a Metrohm 626 Polarecord A saturated potassium calomel electrode was used as reference electrode Platinum electrodes were used as working electrodes The scan rate used was 5 mV/sec

2 2 4 High Performance Liquid Chromatography (HPLC)

HPLC was carried out using a Waters 990 Photodiode array HPLC system in conjunction with a NEC APC III computer, a Waters pump model 6000 Å, a 20$\mu$l injector loop and a $\mu$-Partisil SCX radial PAK cartridge, with detection at 280nm The chromatography was carried out using acetonitrile water (80 20), containing either 0 08 M $LiClO_4$ or 0 02 M $HClO_4$ as a mobile phase The flow rate used was 2 0-3 0 ml/min

2 2 5 Semi-Preparative HPLC

Semi-preparative HPLC was carried out using an Applied Chromatography Services pump (model RR/066) and detector (model 750/11 uv/vis), a 1 ml injection loop and a Magnum 9 Partisil cation exchange column (10 mm / 25 cm) The mobile phase was acetonitrile-water (80 20) containing 0 078 M $LiClO_4$, the flow rate used was 5 2 ml/min

2 2 6 Emission Quantum Yield Determination

A comparative technique using the fluorescent standard $[Ru(bpy)_3]^{2+}$ was chosen This method is based on the fact that if two substances, a sample and a standard are studied in the same apparatus, and using the same incident light intensity, the quantum yield of the sample is related to

that of the standard as follows

$$Q_{sam} = \frac{F_{sam}}{A_{sam}} X \frac{F_{std}}{A_{std}} X \frac{P}{P} X Q_{std} \qquad (1)$$

Where Q values are quantum yields, F values are the areas under the fluorescent spectra, A values are the absorbances of the samples at the respective excitation wavelengths and the P value is the relative photon yield of the radiation source at the excitation wavelength

For each measurement the instrument settings remained fixed at the optimum setting with excitation slit width 10 nm and emission slit width 5 nm The spectra were not corrected for photomultiplier response As samples and standard emit in the same region it is assumed that correction factors are similar for both The quantum yield for $[Ru(bpy)_3]^{2+}$ in deaerated water is 0 042 Each sample was degassed with nitrogen before use The area under each spectrum was measured using a Spectrophysics SP4270 integrator

2 2 7 Photochemistry Experimental

Photochemical experiments were carried out using a high pressure 250 W mercury lamp The sample was placed in a cuvette (path length 1 $cm^3$) The light was focussed onto the sample cell by means of two glass lenses, the glass lenses also prevented any ultra-violet light from reaching the sample A transparent water bath was places infront of the sample cell to prevent sample degradation by heating

2 2 8 $^1$H N.m.r. Measurements

Proton n m r spectra were obtained either on a JEOL JNM-FX 200-MHz or on a Bruker 300-MHz spectrometer Measurements

were carried out in acetone-$d_6$ unless otherwise indicated The peak positions are relative to TMS For the COSY experiments 256 FID's of eight scans each, consisting of 1K data points, were accumulated After digital filtering (sine-bell squared), the FID was zero filled to 512 W in the F1 dimension Acquisition parameters were F1 = $\pm$ 500 Hz, F2 = 1000 Hz and t1/2 = 0 001 sec the recycle delay was 1 5 s N m r measurements were carried out in Leiden University, Leiden, The Netherlands

2 2 9 X-Ray-Crystallography

(a) $[Ru(bpy)_2(3MePyrtr)](PF_6)\ 4H_2O$

**X-Ray Data Collection**

A red octahedrally-shaped crystal (dimensions 0 5x0 3x0 3 mm) of bis(2,2'-bipyridine)ruthenium-3-methyl-5-(pyridin -2-yl)-1,2,4-triazole hexafluoro phosphate tetra hydrate, $[Ru(C_8H_7N_4)(C_{10}H_8N_2)_2]PF_6\ 4H_2O$ was selected to determine the molecular structure The diffraction data were collected at room temperature on an Enraf-Nonius CAD-4 automatic four circle diffractometer with graphite monochromated MoK$\alpha$ radiation ($\lambda$= 0 71073 Å) To measure any deterioration of the crystal the intensity data were checked every 90 minutes using selected intensity standards The data were corrected for Lorentz and polarisation effects No correction for absorption has been applied Atomic scattering factors for neutral atoms were taken from the literature [10] Details of crystal data and intensity collection are given in Chapter 3 Table 3 4

**Solution and refinement of the Structure**

The structure was solved in space group P $3_121$ Using

standard Patterson techniques the position of the ruthenium atom was obtained The positions of the P, F, O, N, and C atoms were found using Fourier synthesis and successive cycles of least-squares refinement, based on 4288 unique reflections (with $1>2\sigma(I)$) The function minimised was $[w(|Fo|-|Fc|)2]$ with $w=1/\sigma 2F$ All non-hydrogen atoms were given individual anisotropic thermal parameters in the refinement A difference fourier map yielded the positions of all hydrogen atoms, except for those of two water molecules The phosphorus atoms are located at special positions, ((x,x,o) and (o,x,1/6)) on a two fold axis Reliability indices $R = [||F_o|-|F_c||]/|F_o|$ and $R_w = [w(|F_o|-|F_c|)^2/w|F_o|^2]^{1/2}$ have the values 0 036 and 0 049 respectively

(b) $\underline{[Ru(bpy)_2(3MePT)Cl](PF_6)}$

X-Ray Data Collection

The crystal structure of bis(2,2'-bipyridine)-chloro-ruthenium-cis-3-methyl-1-(pyridin-2-yl)-1,2,4-triazole hexafluorophosphate has been determined The diffraction data were collected at room temperature on a Nicolet P3/R3 Diffractometer with graphite monochromated MoK$\alpha$ radiation ($\lambda$= 0 71069Å) Intensity data were collected for 4465 intensities averaging over equivalent reflections and rejecting systematic absences (those values with intensity < 3 standard deviation) reduces this to 3648 Intensities were corrected for Lorentz and polarisation effects and converted to structure amplitudes Details of crystal data and intensity collection are given in Chapter 3 Table 3 11

Approximate unit cell parameters were obtained from oscillation and Weissenberg photographs taken about the needle axis of a single crystal Atomic scattering factors were taken from literature [10]

**Solution and Refinement of The Structure**

The structure was solved in space group P The position of the ruthenium atom was obtained using a program called MULTAN [11] The positions of the C, N and Cl atoms were found using MULTAN and the structure was refined using successive weighted fourier transforms, a program called SHELX [12] The ruthenium atom was set anisotropic followed by the C, N and Cl atoms The $PF_6$ anion cannot be refined due to disorder Due to program limitations the positions of the hydrogen atoms could not be located

2 2 10 Time Correlated Single Photon Counting (TCSPC) Method of Determining Lifetime Measurements.

Lifetime measurements were carried out in Trinity College Dublin (TCD) using the technique of Time Correlated Single Photon Counting (TCSPC) [13] A schematic diagram of the apparatus is shown in Figure 2 1 The Applied Photophysics (AP) apparatus used consisted of

(1) AP gated nanosecond flashlamp housing with glass flashlamp was used as the excitation source Nitrogen was used as the filler gas at a pressure 200 mbar The excitation wavelength was 354 nm The lamp profile was taken using a milk/water scatter solution

(2) Start Photomultiplier (START PM) - Type 1P28

(3) AP model 435 gated lamp control unit (used to provide high voltage source across the lamp's electrodes and to provide the heating and pulse supply for the thyraton (EEV F2530)

(4) AP high radiance monochromator blazed at 500 nm

(5) Sample Compartment containing a cut off filter which ensured that only light with a wavelength longer than 600 nm was detected All samples were degassed with argon before measurement

(6) AP model 906 cooled PM housing containing a red sensitive Philips XP2233B PM tube (STOP PM)

(7) Ortec model 437A constant fraction descriminators used in the constant fraction mode (two modules one used on the START and one on the STOP channels used to provide logic pulses to the TAC and to discriminate against non-photon events)

(8) Ortec model 425A variable nanosecond delay (used to delay signals and to provide timing calibrations)

(9) An Ortec model 457 time-to-amplitude converter (TAC)

(10) Canberra Series 30 multichannel analyser (MCA) operated in the pulse-height-analysis (PHA) mode

(11) Apple II microcomputer - data was transferred via a RS232C interface to the Apple II and after suitable manipulation was stored on floppy disc

(12) DEC-2060 computer - due to the limited memory of the Apple II, it was not suitable for processing the data so data was transferred from the Apple to TCD's mainframe DEC-2060 using another RS232C interface Deconvolution analysis and high resolution plotting were performed on the mainframe using SINGLE FOR and DOUBLE FOR programmes written in FORTRAN [13]

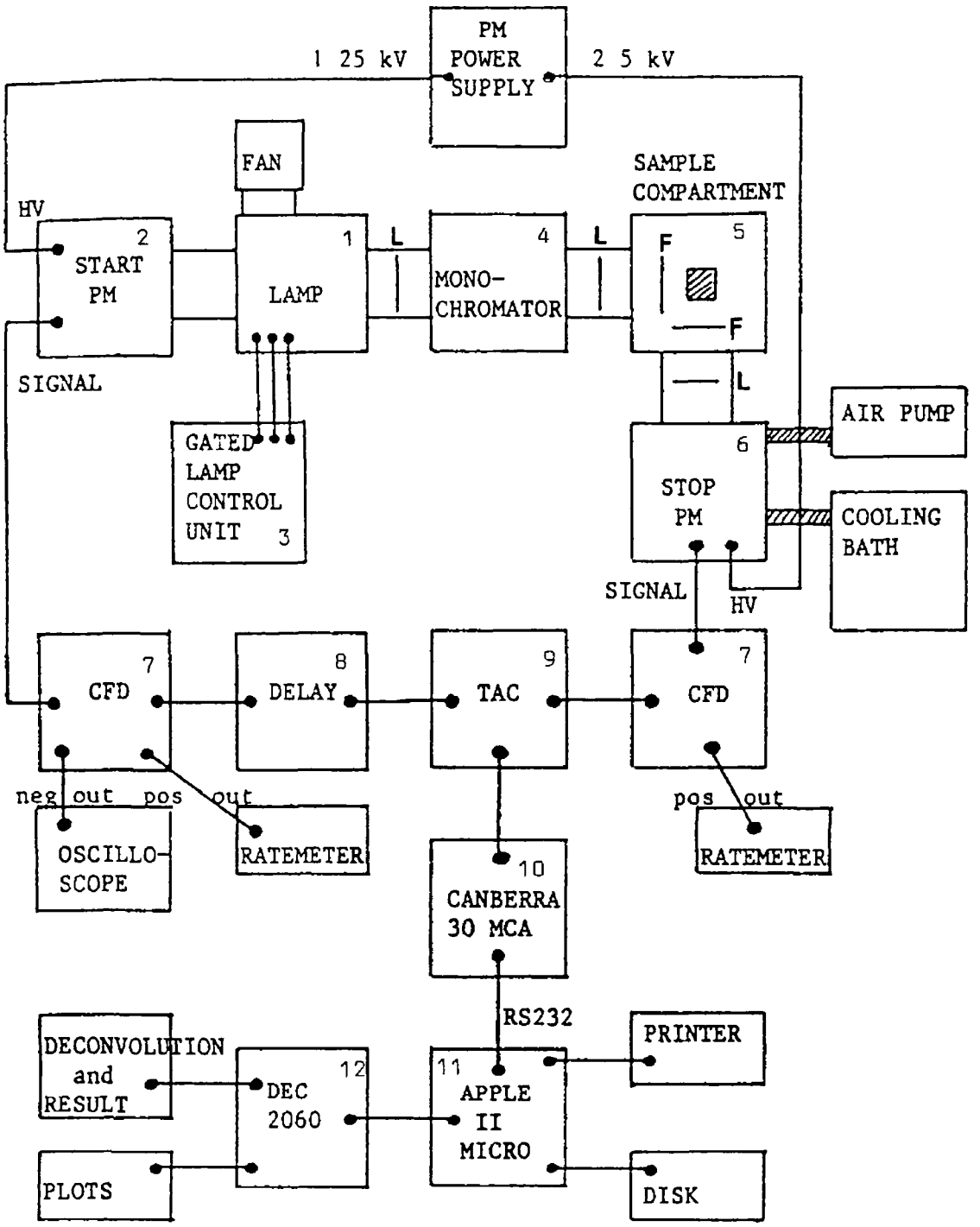


Figure 2 1 Schematic representation of the TCD TCSPC apparatus Lenses are denoted by "L" and filters by "F "

### 2 2 10 1 General Theory of TCSPC

When the flash lamp pulses (usually in the range 10-200 KHz), the pulse of radiation is detected by the START PM which sends a signal to the start channel of the TAC This initiates the charging of a capacitor Light from the source also passes through a monochromator or filters and excites the sample, which subsequently fluoresces An aperture has been adjusted so that at most one photon is detected at the high gain PM, the STOP PM for each exciting event The signal resulting from this photon stops the charging ramp in the TAC, which puts out a pulse, the amplitude of which is proportional to the charge in the capacitor, and hence the time difference between the START and STOP pulses Repetitive lamp pulsing and photon collection results eventually in a histogram of counts being retained in the memory of the MCA This is a direct analogue of the fluorescence decay function, that is, the experimentally observed decay

### 2 2 10 2 Data Analysis

In order to obtain the true fluorescence decay profile of the sample, two experimental decay profiles are measured (a) that of the scattered excitation function distorted by the measuring system and (b) that of the sample fluorescence, also distorted by the measuring system Various factors cause this instrumental distortion These include the fact that the pulse is not instantaneous (i e not a delta pulse) the time resolution of the STOP PM the delay and distortion of signals passing along coaxial cables and through various electronic devices Therefore the experimentally observed decay I(t) is a convolution of the true decay G(t) and the measured excitation function P(t)

$$I(t) = G(t) \otimes P(t)$$

(where $\otimes$ is the convolution operator) [17] G(t) can thus be determined by deconvoluting the experimentally observed decay I(t) and the excitation profile P(t) This expression only holds if both the observed decay and the observed excitation function have the same distortion function

The deconvolution technique available in TCD was the non-linear least squares iterative convolution A comparison of the various techniques are described in detail by McKinnon et al [15] and O'Connor et al [16] Both groups show that the iterative convolution method is the most successful and reliable of the deconvolution methods tested In this procedure the emission is assumed to follow an exponential of the type

$$G(t) = \Sigma a_1 e^{-t/\tau_1}$$

where $a_1$ is the pre-exponential factor which is a function of the spectral response of the detector, the concentration, emission and absorbtion properties of each component i in the sample, and $\tau_1$ is the fluorescent lifetime of each component i in the sample

The programmes SINGLE FOR and DOUBLE FOR use the Marquardt alogrithm [17] and many of the routines described in Bevington [18] The basic procedure for use of these programmes is as follows

Initial guesses are suggested for each $a_1$ and $\tau_1$, and these are used to create a calculated decay G'(t) This is then convoluted with the measured excitation function, E(t), to yield a calculated distorted decay function D'(t) This distorted decay function, D'(t), is then compared with the experimentally observed decay function, D(t), and the sum

of squares of the residuals, $\chi^2$, between them is determined Small changes are then made to $a_1$ and $T_1$, either singly or together, and the process repeated and a new $\chi^2$ evaluated When the difference in $\chi^2$ between D(t) and D'(t) reaches an acceptable level, or when the difference between the latest $\chi^2$ and the previous $\chi^2$ is less than a pre-set level, then the search routine terminates and the values of $a_1$ and $\tau_1$ are output

2 2 10 3 **Evaluating the Success of the Fit**

After deconvolution the success of the fit obtained must be evaluated This is carried out by doing several tests

(1) Graphical comparison of observed and calculated curves As this comparison is a subjective one, it may display differences if the fit is poor However if the fit "looks good" small discrepancies or small non-random oscillations may not show up

(2) $\chi^2$ The ideal value for $\chi^2$ is one Values above one indicate a poor fit and values below one indicate bad statistics Since acceptable values of $\chi^2$ sometimes obtained are symptomatic of poor fits, it is usual to inspect a plot of weighted residuals

(3) Plot of the weighted residuals Residuals from successful fits should be randomly distributed about zero for a good fit

(4) The auto-correlation function For a successful fit values obtained should be randomly scattered about zero

(5) Durbin-Watson Parameter DW This parameter has been suggested to be more sensitive than $\chi^2$ at spotting non-

random variations in the residuals Values of DW greater than 1 65 and 1 75 are indicative of a good fit for single and double exponential fits respectively Details of these parameters and functions can be found in an article by by O'Connor et al [16], and books by Demas [19] and Bevington [18]

### 2 2 10 4 Standards For TCSPC

Before sample measurements were carried out on the system it was necessary to check the accuracy of the TCSPC apparatus, using standard compounds of known decay characteristics The ideal standard should have a lifetime similar to that of the sample under investigation In our case standards acceptable should have a lifetime in the 10-150 ns region Although many standards have been published in the literature [16, 20, 21], many are unsuitable for our purposes for some or all of the following reasons

(1) Their fluorescent lifetime is too low (2-3 ns) to be measured accurately by the TCSPC apparatus

(2) They absorb at wavelengths where the nitrogen lamps spectral output is weak

(3) They emit at wavelengths similar to that of the strongest nitrogen emission

(4) They are difficult to obtain in pure form Both anthracene and 1-cyclonaphthalene would be suitable standards Their lifetimes are about 5 ns and 19 ns depending on the solvent However, anthracene is difficult to purify and 1-cyclonaphthalene emits at 345 nm, very close to the emission wavelength of the nitrogen lamp

Therefore, quinine sulphate and $[Ru(bpy)_3]^{2+}$ were chosen as standards Quinine sulphate is not an ideal standard, as in recent years, it has been suggested that it follows a double exponential decay that is strongly dependant on temperature and emission wavelength [22] The value obtained on the TCD apparatus for a single exponential decay of quinine sulphate in degassed 0 1 N $H_2SO_4$ was 20 5 ns, this agrees well with literature values [20, 21] A double exponential decay was also analysed and a better fit was obtained than for the single exponential decay analysis The lifetimes obtained were 14 ns and 25 ns in a ratio 1 1 The lifetime obtained for $[Ru(bpy)_3]^{2+}$ in degassed water was 575 ns, again in good agreement with literature values

Another method of checking the accuracy of the TCSPC apparatus involved determining the quenching rate constant $K_q$, both by lifetime measurements and fluorescent measurements For each experiment 100 $cm^3$ of a $10^{-4}$ M aqueous solution of $[Ru(bpy)_3]^{2+}$ was prepared The quenching agent, methyl viologen ($MV^{2+}$), was added to the ruthenium solution in aliquots An emission spectrum and lifetime measurement were performed after each addition Samples were not degassed prior to measurement

Stern-Volmer analysis is required to determine $K_q$ This involves plotting $I_o/I$ or $\tau_o/\tau$ against the concentration of $[MV^{2+}]$ $I_o$ and $\tau_o$ are the emission intensity and the lifetime of the unquenched species respectively while $I_o$ and $\tau_o$ are the emission intensity and lifetime of the quenched species respectively The quenching constant is obtained from the graph using the following equation

$$K_q = \frac{\text{slope}}{I_o \text{ or } \tau_o} \qquad (2)$$

For the lifetime experiment the results obtained show that

the lifetime of $^{*}[Ru(bpy)_3]^{2+}$ decays exponentially with increasing $[MV^{2+}]$ Hence, the Stern-Volmer plot is linear for low concentrations of $[MV^{2+}]$, that is concentrations up to 3 5 mM After this concentration a double exponential analysis is required This effect has also been observed by Kalyanasundaram [23] in his lifetime quenching studies using chloride ions as the quenching agent With increasing $Cl^-$ concentration, the MLCT state decays rapidly and a bis substitutional product is formed In our case, perhaps the TCSPC apparatus is more sensitive than the fluorimeter and a substitutional product which may have been formed is observed as the second lifetime Further investigations into this behaviour are required

References.


1 M Uda, G Hisazumi, W Sato, and S Kubota, Chem. Pharm. Bull., 1976, 24 3103

2 S Kubota, M Uda, and M Ohtsuku, Chem. Pharm. Bull., 1971, 19, 2331

3 R Hage, R Prins, J G Haasnoot, J Reedijk, and J G Vos, J. Chem. Soc., Dalton Trans., 1987, 1389

4 S Kubota, M Uda, and T Wakagasa, J. Heteroycl. Chem., 1975, 12, 855

5 J F Geldard and F J Lions, J. Org. Chem., (1965), 30, 318

6 A K Misbahul and J P Polya, J. Chem. Soc. (C), 1970, 85

7 (a)R G Jones and C Ainsworth, J. Am. Chem. Soc., 1955, 77, 1538 (b) C Ainsworth and R G Jones, J. Am. Chem Soc , 1953, 75, 4915

8 B P Sullivan, D J Salmon, and T J Meyer, Inorg. Chem., 1978, 17, 3334 (a) D F Mahony and J K Beattie, Inorg. Chem., 1973, 12, 2561

9 R Hage, A H Dijkhuis, J G Haasnoot, R Prins, J Reedijk, B E Buchanan, and J G Vos, Inorg. Chem., 1988, 27, 2185

10 International Tables for X-Ray Cryatallography (1962), Volume IV, Kynoch Press, Birmingham

11 Computer Program developed by T Debaerdemaeker, G Germaen, P Main, C Tate, and M M Noolfson, March 1987

12 G M Sheldrick, SHELX86 Program for Crystal Sturcture Determination, University of Gottingen, Federal Rep Germany, 1986

13 M Murphy, Thesis 1984, Trinity College Dublin

14 D V O'Connor and D Phillips, "Time Correlated Single Photon Counting" 1984, Academic Press, London

15 A E Mc Kinnon, A G Szabo, and D R Miller, J. Phys. Chem., 1977, 81, 1564

16 D V O'Connor, W R Ware, and J C Andre, J. Phys. Chem., 1979, 10, 1331

17 D W Marquardt, J. Soc. Ind. App. Math., 1963, 11, 431

18 P R Bevington, "Data Reduction and Error analysis for the Physical Sciences" 1969, McGraw-Hill, New-York

19 J N Demas, "Excited State Lifetime Measurements" 1983, Academic Press, New-York

20 R A Lampert, L A Chewter, D Phillips, D V O'Connor, A J Roberts, and S R Meech, Anal. Chem., 1983, 55, 66

21 D M Rayner, A E Mc Kinnon, G Szabo, and P A Hackett, Can. J. Chem., 1976, 54, 3246

22 D V O'Connor, S R Meech, and D Phillips, Chem. Phys. Lett., 1982, 88, 22

23 K Kalyanasundaram, J. Phys. Chem., 1986, 90, 2285

# CHAPTER 3

## Properties of Ruthenium Compounds Containing Chelating or Monodentate Asymmetric Pyridyltriazole Ligands

## 3 0 Introduction.

Our interest in ruthenium (II) compounds of the type $[Ru(bpy)_2(L\text{-}L')]^{2+}$, where L-L' is an asymmetric bidentate ligand, has arisen from the investigations of the unique photochemical and photophysical properties of $[Ru(bpy)_3]^{2+}$ [1-5] (see Chapter 1) In the literature, most of the research in the ruthenium field has been concerned with the formation of ruthenium complexes that contain symmetrical bidentate aromatic nitrogen donor ligands, with particular emphasis on $[Ru(bpy)_3]^{2+}$ [1-16] In recent years there has been increasing interest in mixed ligand complexes of the type $[Ru(L\text{-}L)_n(L'\text{-}L')_{3-n}]^{2+}$ [1, 3, 7, 9, 11, 17-29] (where n = 0, 1, 2 or 3, and L-L and L'-L' both different symmetrical bidentate ligands) Our work involves replacing a bipyridine ligand with a pyridyltriazole ligand with the aim of investigating the photochemical and photophysical properties of the compounds synthesised

By varying the nature of the bidentate ligands, the influence of the ligand structure on the electronic and electrochemical properties of the Ru(II) complex may be investigated Systematic variations of the ligands may lead to a detailed understanding of the effects of the ligand in the complex and hence, by proper choice of ligands certain desired properties such as luminescence, lifetimes and redox properties of the complex may be obtained The electronic, redox and excited state properties of the complex will in general be affected by the $\sigma$ and $\pi$ properties of the ligand The lowest energy absorption maxima of compounds of the type $[Ru(bpy)_2(L\text{-}L')]^{2+}$ have been assigned to MLCT bands The position of this band in $[Ru(bpy)_2(L\text{-}L')]^{2+}$ complexes can be taken as a measure for the $\pi$ acceptor capacity of the ligand [21] However, the $\sigma$ donor properties of the ligands also influences the band position

The effect of successively replacing a bipyridine ligand of $[Ru(bpy)_3]^{2+}$ with a phenanthroline (phen) ligand has been investigated by Crosby et al [7] to form complexes of the type $[Ru(bpy)_n(phen)_{3-n}]^{2+}$, (phen = 1,10-phenthroline, n = 0, 1, 2, or 3) The Ru(II) complexes exhibit a progressive shift to higher energy in the absorption and emission spectra on the replacement of a bpy ligand with a phen ligand As both the absorption and emission spectra of these complexes yield single peak MLCT bands, it has been suggested that the coupling between the two dissimilar ligands was strong [7] Luminescence decay data provided no evidence for multiple emission at 77K, and the observed spectral properties of the mixed ligand complexes represented an average or combination of the properties of $[Ru(bpy)_3]^{2+}$ and $[Ru(phen)_3]^{2+}$ Similarly, the properties of complexes of the type $[Ru(bpy)_n(Me_2bpy)_{3-n}]^{2+}$ also represent an average of the spectral, electrochemical and lifetime results of $[Ru(bpy)_3]^{2+}$ and $[Ru(Me_2bpy)_3]^{2+}$ [19] Other mixed ligand systems that follow this behaviour include $[Ru(bpy)_n(DMCH)_{3-n}]^{2+}$ where DMCH is 5,8-dimethyl-dibenzo-1,10-phenanthroline [20], $[Ru(bpy)_2(DAF)]^{2+}$ where DAF is 4,5-diazafluorene [6], and $[Ru(bpy)_n(taphen)_{3-n}]^{2+}$ where taphen is dipyrido-pyridazine [13] (see Figure 3 1 for ligand structures)

Meyer et al [17] have investigated the photophysical and photochemical properties of the series of tris-chelate complexes $[Ru(bpy)_n(bpyz)_{3-n}]^{2+}$ [14, 17], $[Ru(bpy)_n(bpym)_{3-n}]^{2+}$ [17] and $[Ru(bpym)_n(bpyz)_{3-n}]^{2+}$ [17] where bpyz = 2,2'-bipyrazine and bpym = 2,2'-bipyrimidine (see Figure 3 1) For the mixed-chelates containing different chromophoric ligands, no evidence was obtained for multiple emissions either from emission or lifetime measurements [17]

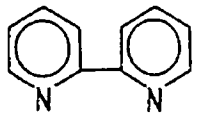

2,2'-bipyridine

(bpy)

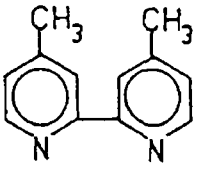

4,4'-dimethyl-2,2'-bipyridine

($Me_2$bpy)

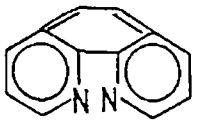

1,10-phenanthroline

(phen)

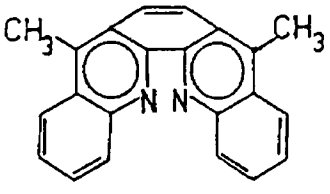

5,8-dimethyl-dibenzo-

1,10-phenanthroline

(DMCH)

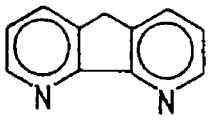

4,5-diazafluorene

(DAF)

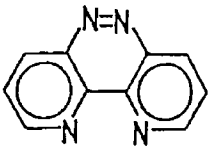

dipyrido-pyridazine

(taphene)

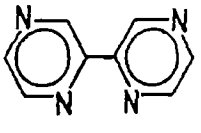

Bipyrazine

(bpyz)

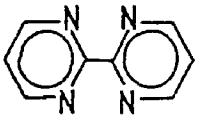

Bipyrimidine

(bpym)

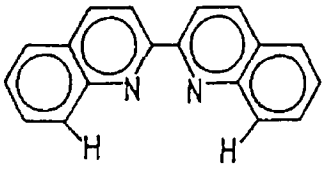

biquinoline

(biq)

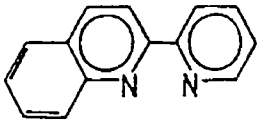

2,(2-pyridyl)quinoline

(pq)

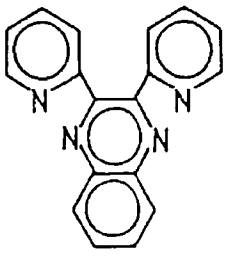

2,3-bis(2-pyridyl)quinoxaline

(BL)

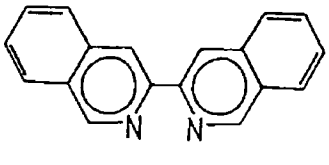

iso-biquinoline

(ibiq)

Figure 3 1 Structure and abbreviations of ligands cited in text

From trends in the emission maxima and electrochemical measurements it has been concluded, that in the mixed chelates the lowest lying emitting charge transfer states are based on Ru(III)(bpz) or Ru(III)(bpym) chromophores From electrochemical measurements, the relative ordering of the $\pi^*$ levels in the free and complexed chelates is $\pi^*$(bpyz) < $\pi^*$(bpym) < $\pi^*$(bpy) The lower $\pi^*$ energy levels for the bpyz and bpym ligands lead to changes in the ground and excited state redox potentials as a consequence of changes in electronic structure [28]

In contrast to the type of system where individual ligand identity is lost, the series of compounds $[Ru(bpy)_3(biq)_{3-n}]^{2+}$ (biq = 2,2'-biquinoline and n = 1 or 2) were investigated [24, 29], where the mixed ligand complexes retain the independent charge-transfer transitions of both ligands in the visible region of the absorption spectra Some complexes for which this behaviour has been observed are listed in Table 3 1 The intensities of the bands are weighted in accordance to the proportion of ligand present in the species This behaviour is also observed for the $[Ru(phen)_n(biq)_{3-n}]^{2+}$ (n = 1 or 2) series of mixed-ligand complexes studied [24]

Examination of the reduction potentials of the free ligands shows that the biq ligand is most easily reduced while bpy is the hardest to reduce [29] This indicate that the $\pi^*$ level in the complexes containing biq will be at lower energy than in pure bpy or phen ligands Hence the absorption maximum of $[Ru(phen)_3]^{2+}$ is found at higher energy than that of $[Ru(biq)_3]^{2+}$ and is found at slightly higher energy than that of $[Ru(bpy)_3]^{2+}$ (see Table 3 1) However, dual emission is not observed for the mixed ligand compounds in Table 3 1

Table 3.1 Absorption Bands of Several Complexes where Two MLCT bands are Observed in the Absorption spectrum [a]

| Compound | Absorption Maxima $\lambda_{max}$ nm (log$\epsilon$) | | ref |
|---|---|---|---|
| $[Ru(bpy)_3]^{2+}$ | - - | 453(4 14) | 10 |
| $[Ru(bpy)_2(biq)]^{2+}$ | 527(3 91) | 440(3 83) | 30 |
| $[Ru(bpy)(biq)_2]^{2+}$ | 546(3 86) | 480(3 70) | 30 |
| $[Ru(biq)_3]^{2+}$ | 524(3 95) | - - | 30 |
| $[Ru(phen)_3]^{2+}$ | - - | 445(4 30) | 31 |
| $[Ru(phen)_2(biq)]^{2+}$ | 523(3 97) | 439(3 98) | 24 |
| $[Ru(phen)(biq)_2]^{2+}$ | 551(3 93) | 478(3 81) | 24 |
| $[Ru(bpy)_2(pq)]^{2+}$ | 476sh | 452(4 02) | 24 |
| $[Ru(bpy)(pq)_2]^{2+}$ | 480(4 04) | 455sh | 24 |
| $[Ru(pq)_3]^{2+}$ | 488 - | - - | 9 |
| $[Ru(phen)_2(pq)]^{2+}$ | 476sh | 442(4 11) | 24 |
| $[Ru(phen)(pq)_2]^{2+}$ | 480sh | 453(4 07) | 24 |

[a] measured in methanol at room temperature

A slight variation of the biq ligand yields 2-(2-pyridyl) quinoline (pq) (Figure 3 1) From comparison of the tris complexes $[Ru(bpy)_3]^{2+}$ ($\lambda_{max}$ = 454 nm), $[Ru(pq)_3]^{2+}$ ($\lambda_{max}$ = 485 nm) and $[Ru(biq)_3]^{2+}$ ($\lambda_{max}$ = 523 nm), it is apparent that the benzo substituent on the 2,2'-bipyridine produces a red shift in energy of the lowest lying triplet state and the red shift for the biq complex is greater than that for the pq complex [30] Independent charge-transfer transitions, that can be ascribed to individual ligands, are observed in the absorption spectra of the series of compounds $[Ru(bpy)_n(pq)_{3-n}]^{2+}$ [24] and $[Ru(phen)_n(pq)_{3-n}]^{2+}$ [35] The room temperature emission spectra of the mixed ligand complexes of $[Ru(bpy)_n(pq)_{3-n}]^{2+}$ are all quite similar to that of $[Ru(pq)_3]^{2+}$ suggesting that mixing of the ligand emitting states occurs and both the initial excited states of pq and bpy rapidly convert to the emitting state of pq alone Similarly, for the $[Ru(phen)_n(pq)_{3-n}]^{2+}$ [33] system, results suggest that energy transfer occurs from the absorption state associated with phenanthroline to the emitting state associated with pyridylquinoline These results suggest that even in the presence of interligand energy transfer independent MLCT bands are observed in the absorption spectra of the mixed ligand compounds [8, 9]

Recently, Rillema et al [34] investigated the series of compounds $[Ru(bpy)_n(BL)_{3-n}]^{n+}$, where BL is 2,3-bis(2-pyridyl)quinoxaline The absorption spectra obtained for these compounds show a distinction between the MLCT transition involving two different ligands, with the $d\pi \dashrightarrow \pi^*(BL)$ transitions occurring at lower energy than the $d\pi \dashrightarrow \pi^*(bpy)$ transitions The absorption maxima for the $[Ru(bpy)_n(BL)_{3-n}]^{n+}$ series are 451 nm (4 14) for n = 0, 517 nm (3 92) and 426 nm (3 93) for n = 1, 512 nm (3 98) and 462 nm (3 91) for n = 2, and 499 nm (4 14) for n = 3 (log $\epsilon$ values follow in parenthesis) The electrochemical data

indicate that the complexes $[Ru(bpy)_n(BL)_{3-n}]^{2+}$ containing BL are poor reductants relative to $[Ru(bpy)_3]^{2+}$ due to the low energy $\pi^*$ orbitals of BL but are good oxidants due to enhanced $d\pi(Ru) \dashrightarrow \pi^*(BL)$ interaction The emission maxima for the series $[Ru(bpy)_n(BL)_{3-n}]^{n+}$ are found at 714, 734 and 760 nm for n = 0, 1 and 2 respectively compared to 610 nm for $[Ru(bpy)_3]^{2+}$ [10] Both the reduction potentials and emission spectra suggest that emission is from the $\pi^*$ (BL) ligand The successive replacement of BL with a bpy ligand also results in a decrease in lifetime of the complexes [34]

Another example of a system exhibiting multiple MLCT transitions in the absorption spectrum is the $[Ru(bpy)_2(1\text{-}biq)]^{2+}$ system, where 1-biq = 2,2'-biisoquinoline, studied by Balzani et al [14] However, the mixed ligand complexes exhibit only one emission band which is practically the same as that of $[Ru(bpy)_3]^{2+}$ This suggests that the emitting states of the mixed ligand complexes are essentially Ru $\dashrightarrow$ bpy CT in nature The spectroscopic results show that in the mixed ligand complexes the coupling between excited states involving bpy and excited states involving 1-biq are too weak to effect the energy levels in a substantial way but strong enough to allow fast radiationless deactivation of the upper excited states to the lowest one The reduction potentials of free bpy and 1-biq are almost equal (-2 22 and -2 20 V vs S C E respectively [29]) The first reduction potential of $[Ru(bpy)_3]^{2+}$, which is known to correspond to the reduction of one bpy ligand, is less negative than that of $[Ru(1\text{-}biq)_3]^{2+}$ [14] This indicates that for the coordinated ligands the $\pi^*$ levels of bpy lie at lower energy than that of 1-biq and hence the 1-biq ligand is not involved in the energy states that are responsible for the reduction and emission process

Another variation on the $[Ru(bpy)_3]^{2+}$ complex is to replace one of the pyridyl groups in 2,2'-bipyridine with a suitable five membered heterocyclic ring such as imidazole, thiazole, pyrazole or triazole Haga [11, 25] has investigated the biimidazole ($biimH_2$) and bibenzimidazole ($bibzimH_2$) complexes of $Ru(bpy)_2$ The spectral and electrochemical data show a dependence on the $\sigma$ donor property of $biimH_2$ and $bibzimH_2$ Both the $[Ru(bpy)_2(biimH_2)]^{2+}$ and $[Ru(bpy)_2(bibzimH_2)]^{2+}$ complexes absorb and emit at lower energies than $[Ru(bpy)_3]^{2+}$ indicating that the $biimH_2$ and $bibzimH_2$ ligands are stronger $\pi$ donors than bpy A stronger $\pi$ donor increases the electron density on the metal, resulting in a decrease of the MLCT band energies The deprotonated forms of the coordinated ligands are suggested to have a stronger $\pi$ donor capacity than the protonated forms, as deprotonation results in a shift to lower energy of the MCLT absorption bands The emission spectra of these compounds exhibit only one band, reduction and emission are suggested to involve bpy orbitals The emission lifetimes are shorter than that of $*[Ru(bpy)_3]^{2+}$

From the brief discussion above it can be concluded that variation of the nature of the ligand will induce changes in the electronic and electrochemical properties of the complex, and also in the excited state properties Even if the substituted ligand plays no active role in these properties its $\pi$ acceptor/$\pi$ donor properties will have an effect on the $d\pi$ level of ruthenium by either destabilizing or stabilizing it Ligands which do not take part in the absorption, emission and electrochemical processes are called spectator ligands An example would be the $biimH_2$ and $bibzimH_2$ ligands discussed above The luminactive ligand, the ligand that actively takes part in these processes, would be the bpy ligand in the complexes $[Ru(bpy)_2(biimH_2]^{2+}$ and $[Ru(bpy)_2(bibzimH_2]^{2+}$

The discussion up until now has been concerned with the variation of symmetric chelating ligands to change the properties of the complex It is only relatively recently that studies on ruthenium complexes have extended to ligands which are substantially different from bipyridine A number of complexes of the type $[Ru(bpy)_2(L\text{-}L')]^{2+}$ have been prepared where L-L' is a bidentate nitrogen-donor ligand containing two chemically different coordination sites For ligand structures and abbreviations discussed in this text see Figure 3 2 The effects of the nature of the asymmetric bidentate ligand on the spectral, electrochemical and photophysical properties of the complexes have been examined [1, 3, 10, 21, 22, 23, 25, 27, 35]

Haga, along with the investigations of the $[Ru(bpy)_2(biimH_2)]^{2+}$ and $[Ru(bpy)_2(bibzimH_2]^{2+}$ cations has studied the properties of complexes of the type $[Ru(bpy)_2(L\text{-}L')]^{2+}$ where L-L' is the asymmetric ligand 2-(2-pyridyl)benz-imidazole (PbzimH) or 2-(2-pyridyl)imidazole (PimH) [11] The absorption and emission data for these complexes are listed in Table 3 2 The formation of $[Ru(bpy)_2(PbzimH)]^{2+}$ and $[Ru(bpy)_2(PimH)]^{2+}$ is the equivalent of replacing one of the pyridine rings of $[Ru(bpy)_3]^{2+}$ by a benzimidazole and imidazole grouping respectively In comparison with the compounds $[Ru(bpy)_2(biimH_2)]^{2+}$ and $[Ru(bpy)_2(bibzimH_2]^{2+}$ the compounds containing the asymmetric ligands PimH and PbzimH absorb at slightly higher energies Both complexes exhibit lower energy absorption bands than $[Ru(bpy)_3]^{2+}$ indicating that these ligands are weaker $\pi$ acceptors than bpy The emission spectra of compounds containing PimH, PbzimH, $biimH_2$, $bibzimH_2$ and $imH_2$ exhibit only one band, closely resembling that of $[Ru(bpy)_3]^{2+}$ [16, 38]

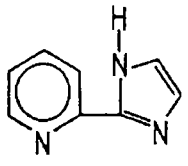

2-(2-Pyridyl)imidazole

(PimH)

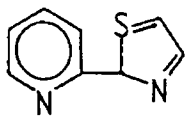

2-(2-pyridyl)thiazole

(Pth)

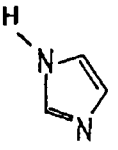

pyrazole

(pz)

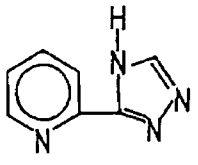

2-(2-pyridyl-1,2,4-triazole

(Pytrz)

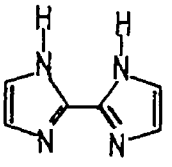

biimidazole

($biimH_2$)

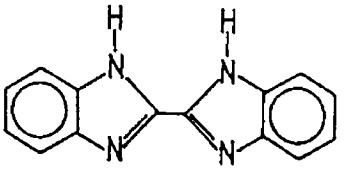

bibenzimidazole

($bibzimH_2$)

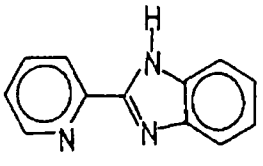

2-(2-pyridyl)benzimidazole

(PbzimH)

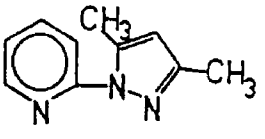

1-(2-pyridyl)-3,5-dimethyl-pyrazole

($Me_2PNP$)

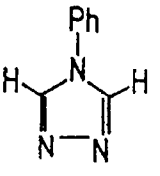

4-phenyl-1,2,4-triazole

(Phtrz)

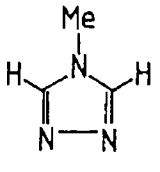

4-Methyl-1,2,4-triazole

(Metrz)

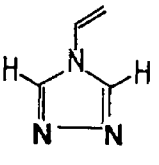

4-Allyl-1,2,4-triazole

(Altrz)

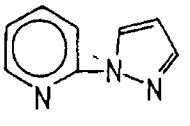

1-(2-pyridyl)-pyrazole

(PNP)

Figure 3 2 Structure and abbreviations of ligands cited in text

Table 3.2 Absorption and emission maxima for selected compounds

| Compound | Absorption $\lambda_{max}$ (nm) | Emission $\lambda_{max}$ (nm) | ref |
|---|---|---|---|
| $[Ru(bpy)_3]^{2+}$,a | 453 | 610 | 10 |
| $[Ru(bpy)_2(bibzimH_2)]^{2+}$,a | 473 | 656 | 24 |
| $[Ru(bpy)(bibzimH_2)_2]^{2+}$,a | 463 | 640 | 24 |
| $[Ru(bpy)_2(PimH)]^{2+}$,a | 460 | 633 | 24 |
| $[Ru(bpy)_2(PbzimH)]^{2+}$,a | 458 | 630 | 24 |
| $[Ru(Pythz)_3]^{2+}$,b | 462 | 590 | 22 |
| $[Ru(bpy)(Pythz)_2]^{2+}$,b | 458 | 597 | 22 |
| $[Ru(bpy)_2(Pythz)]^{2+}$,b | 452 | 598 | 22 |
| $[Ru(Me_2PNP)_3]^{2+}$,a | 382 | - | 10 |
| $[Ru(bpy)(Me_2PNP)_2]^{2+}$,a | 435 | 604 | 10 |
| $[Ru(bpy)_2(Me_2PNP)]^{2+}$,a | 450 | 602 | 10 |
| $[Ru(bpy)_2(phtrz)_2]^{2+}$,c | 468 | 645 | 36 |
| $[Ru(bpy)_2(Metrz)_2]^{2+}$,c | 473 | 660 | 36 |
| $[Ru(bpy)_2(Htrz)_2]^{2+}$,c | 470 | 660 | 36 |
| $[Ru(bpy)_2(trz)_2]$,d | 544 | - | 36 |
| $[Ru(bpy)_2(Hpz)_2]^{2+}$,c | 470 | 627[a] | 37 |
| $[Ru(bpy)_2(pz)_2]$,d | 581 | - | 37 |

[a] measured in acetonitrile [b] measured in ethanol/water [c] measured in acetone [d] measured in DMF

The first two reduction potentials for each compound are

due to stepwise reductions at the bpy ligands The metal based oxidation potentials of these complexes are observed at lower potential than that of $[Ru(bpy)_3]^{2+}$ while the oxidation potentials of the deprotonated forms are considerably lower Again, these results suggest that bpy is the luminactive ligand while imidazole and benzimidazole ligands act as spectator ligands The emission properties and redox potentials of complexes containing imidazole of benzimidazole ligands can therefore be tuned by the deprotonation of the coordinated ligands [25]

The emission lifetimes of the complexes $[Ru(bpy)_2(PimH)]^{2+}$ and $[Ru(bpy)_2(PbzimH)]^{2+}$ are shorter than $[Ru(bpy)_3]^{2+}$ but longer than those of the corresponding imidazole complexes $[Ru(bpy)_2(biimH_2]^{2+}$ and $[Ru(bpy)_2(bibzimH_2)]^{2+}$ discussed previously, indicating that the emission lifetimes decrease with increasing number of imidazole of benzimidazole rings in the ligands Haga has suggested that this decrease may be attributed to a rapid deactivation of the excited states, in which the excitation energy may be vibrationally dissipated to the solvent medium through the N-H bond of the imidazole or benzimidazole ligand [11]

The replacement of a pyridine ring with a thiazole ring is not expected to yield much change in the properties of the complex as thiazole is closely akin to pyridine in its aromaticity and general chemistry [36] Fitzpatrick and Goodwin [22] prepared three complexes $[Ru(L\text{-}L')_3]^{2+}$, $[Ru(bpy)(L\text{-}L')_2]^{2+}$ and $[Ru(bpy)_2(L\text{-}L')]^{2+}$ so as to examine the effect of successive replacement of 2,2'-bipyridine by (L-L') = 2-(2-pyridyl)-thiazole For these compounds, the absorption maxima decreases only slightly to lower energies as the number of coordinated thiazole molecules increases, this is probably associated with a slightly greater $\pi$-acceptor capacity of the thiazole ring The spectral and electrochemical properties of complexes containing

2-(2-pyridyl)-pyrazole show that this ligand has reduced $\pi$-acceptor capacity compared with 2-(2-pyridyl)thiazole [22]

Steel et al [10] have investigated the absorption and emission properties of compounds $[Ru(bpy)_n(Me_2PNP)_{3-n}]^{2+}$ where $Me_2PNP$ = 1-(2-pyridyl)-3,5-dimethyl pyrazole The results obtained, in Table 3 2, show that as the number of $Me_2PNP$ ligands increases the energy of the MLCT absorption band increases and the absorption maximum of the complex $[Ru(Me_2PNP)_3]^{2+}$ is at very high energy 382 nm The emission maxima for $[Ru(bpy)_2(Me_2PNP)]^{2+}$ and $[Ru(bpy)(Me_2PNP)_2]^{2+}$ are found at similar energies but slightly higher than that of $[Ru(bpy)_3]^{2+}$ The complex $[Ru(Me_2PNP)_3]^{2+}$ has no emission at room temperature This suggests that the $Me_2PNP$ ligand acts as a spectator ligand and the MLCT band observed is a $d\pi(Ru) \dashrightarrow \pi^*(bpy)$ transition

The first examples of ruthenium triazole complexes were reported in 1983 by Vos et al [36] Examples of such ligands are 1,2,4-triazole (Htrz), 4-phenyl-1,2,4-triazole (Phtrz), 4-methyl-1,2,4-triazole (Metrz) and 4-allyl-1,2,4-triazole (Altrz) The $\pi$ acceptor capabilities of these monodentate coordination ligands have been assessed The absorption and emission maxima of these compounds are presented in Table 3 2 The position of the lowest $d\pi(Ru) \dashrightarrow \pi^*(bpy)$ CT absorption in the cationic triazole complexes is very close to that observed in the corresponding pyrazole complex [37], but is found at lower energy than for the corresponding pyridine complex This suggests that in this type of complex, the 1,2,4 triazoles have similar $\pi$ acceptor capabilities to pyrazoles, but are weaker $\pi$ acceptors than pyridine The emission maxima for the triazole complexes are observed at lower energy than for $[Ru(bpy)_3]^{2+}$ The maximum for the Phtrz complex is

found at slightly higher energy than for the other compounds This suggests a somewhat more efficient back donation from the metal to the triazole ligand in this complex

Chapter 3 of this work reports the synthesis, characterisation and photochemical properties of cis-$[Ru(bpy)_2(L\text{-}L')]^{n+}$ (n = 1 or 2) complexes where L-L' is a series of pyridyl-1,2,4-triazoles, or 1-(pyridin-2-yl)-pyrazole The results obtained are compared with those reported for similar systems As discussed in Chapter 1 our aim is to study the photochemistry of the compounds prepared and to investigate the nature of possible intermediates This is of particular interest as in the investigations of the photochemical decomposition of $[Ru(bpy)_3]^{2+}$ intermediates containing monodentate ligands have been proposed [36, 40-44] The possibility of forming monovalent species analogous to monodentate bipyridyl and monodentate bipyrazine during the photolysis of ruthenium pyridyltriazole compounds and their possible isolation and characterisation may help us to increase our knowledge of the excited state properties of $[Ru(bpy)_3]^{2+}$ The photochemistry of $[Ru(bpy)_3]^{2+}$ has been investigated by a number of groups and a generally accepted model in which the photoinduced ligand loss is pictured to occur from an upper "dd" state, closely located to the $^3$MLCT excited state has been proposed by Kalyanasundaram [40] This "dd" state represents a major deactivation pathway for the $^3$MLCT state at room temperature (see Figure 1 1, Chapter 1) and has been used to explain the photolability of these type of compounds Our idea was that the introduction of an asymmetric bidentate ligand may facilitate monodentate coordination under photolysis conditions

Investigations of the photochemistry of $[Ru(bpy)_3]^{2+}$ in 0 1 M HCl at 95$^o$C by Van Houten and Watts [41], showed that

photolysis resulted in the disappearance of the absorption band at 450 nm and the appearance of a shoulder at 500 nm. Analysis of the photolysed solution by fluorescence spectroscopy clearly showed the presence of free protonated 2,2'-bipyridine, providing conclusive evidence for labilization of the bipyridine ligand. The authors suggest from the absorption at 500 nm in the uv spectrum and the appearance of uncomplexed ligand that at least two reactions occur: (1) displacement of one end of the bpy ligand by water or perhaps $Cl^-$, followed by protonation of the open end of bpy, and (2) subsequent reaction of the resulting complex leading to displacement of the bound end of the monodentate $Hbpy^+$ ligand and releasing free ligand into solution.

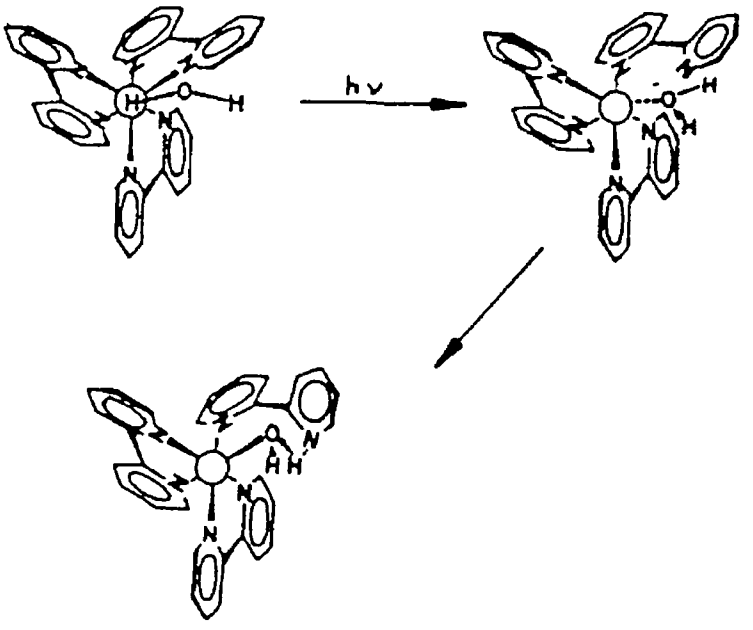


(1)

Investigations into the nature of the photoproduct obtained from photolysis of $[Ru(bpy)_3]^{2+}$ in 1M HCl were carried out by Van Houten and Watts [42]. By comparison with the photolysis of the corresponding iridium complex $[Ir(bpy)_3]^{2+}$ in 1M HCl where a monodentate bpy compound was isolated [43] it was observed that the ruthenium photolysis

showed similar characteristics From these results, van Houten and Watts suggested that the product being formed is $[Ru(bpy)_2(bpy)Cl]^+$ It was also suggested that the photoproduct formed on photolysis of $[Ru(bpy)_3]^{2+}$ is $[Ru(bpy)_2(bpy)OH]^+$ which converts to $[Ru(bpy)_2(bpy)H_2O]^{2+}$ by treatment with acid [43] The proposed intermediate for this reaction is shown in equation 1 However, no substantial evidence for this assumption was obtained

The photolysis of $[Ru(bpy)_3]^{2+}$ in chlorinated solvents such as $CH_2Cl_2$ was studied by Meyer and coworkers [45] and results showed that $[Ru(bpy)_2Cl_2]$ was formed as the final product The authors proposed that the mechanism for photolysis involved thermal activation population of the d-d excited state, leading to cleavage of an Ru-N bond, with formation of a five coordinated species In the absence of coordinating ions, chelate ring closure occurs with the reformation of $[Ru(bpy)_3]^{2+}$ [45] Upon photolysis in acetonitrile, the loss of a bpy ligand from the $[Ru(bpy)_3]Cl_2$ complex yields the formation of only one photoproduct $[Ru(bpy)_2(CH_3CN)Cl]^+$ [46]

Tachiyashiki et al [44] have studied the photolysis of the tris complex $[Ru(phen)_3]^{2+}$ in HCl solutions They found that the spectral changes upon photolysis were very similar to those obtained by van Houten and Watts for the photolysis of $[Ru(bpy)_3]^{2+}$ in HCl solutions [42] From this comparison, and from comparisons with thermal substitution reactions of $[M(bpy)_3]^{2+}$ (M = V, Ni and Fe) for which the reactions are widely accepted to proceed via a monodentate intermediate [47, 48] it was suggested that the photolysis of $[Ru(phen)_3]^{2+}$ proceeded through an intermediate containing a monodentate phen ligand Equation 2 was considered for the reaction mechanism

In this scheme a protonation (path (2)) of the nitrogen

atom of the monodentate phenanthroline ligand in the intermediate competes with a chelate ring closure of the ligand (path (1)) Thus with the increase in acid concentration, the ring closure is suppressed more efficiently In contrast with the $[Ru(bpy)_3]^{2+}$ system [41] where spectral evidence of monodentate formation was observed, there is no direct evidence that the phen monodentate intermediate exists However, the authors believe that the monodentate intermediate exists at least for a very short period of time

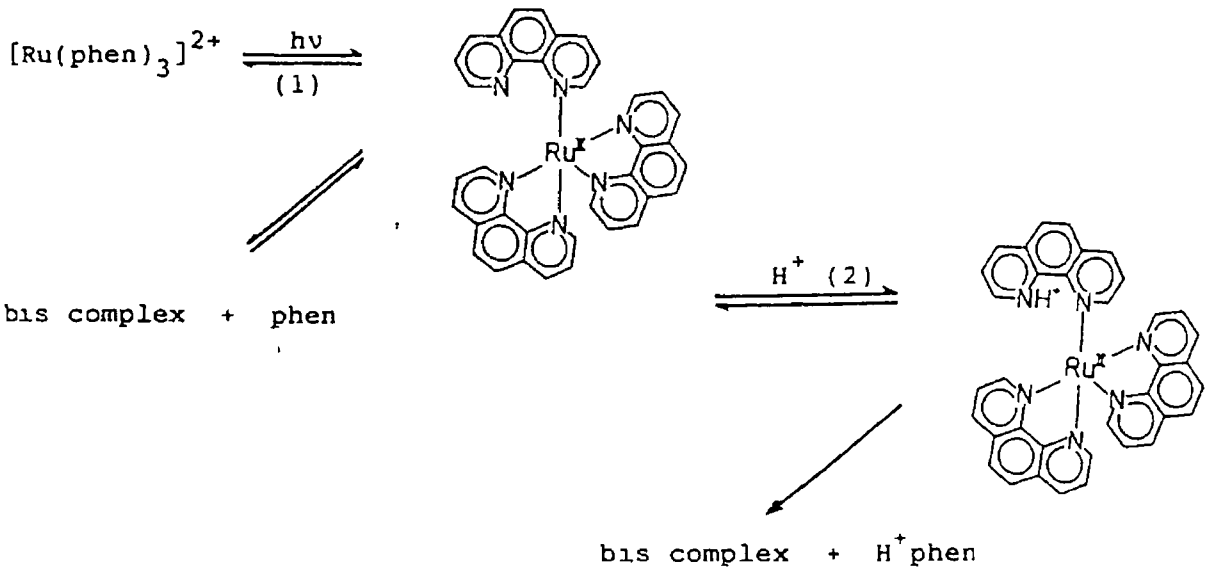


(2)

Extensive studies on various polypyridyl complexes in the presence of different coordinating ligands and solvents [36] have shown that photodecomposition occurs essentially in solvents that promote ion-pair formation $[Ru(L\text{-}L)_3]^{2+}[X^-]_2$ ($X = Cl^-$, $SCN^-$), and that the relative efficiency of ligand loss in tris complexes follows the order bpym > bpz > bpy The mechanism of photoanation of

$[Ru(bpz)_3]^{2+}$, by analogy to that of $[Ru(bpy)_3]^{2+}$, is believed to be dissociative, resulting in a five-coordinated intermediate with an end-bonded bipyrazine ligand [36] Complexes in non-aqueous solution associate with their counterions in ion-pairs Thus, as soon as the five-coordinate intermediate is formed, anation results from the $Cl^-$ associated in the ion-pair The only monodentate bipyridyl intermediate that has been isolated and seen spectroscopically is $[Ir(bpy)_2(bpy)Cl]^+$ [41, 49] The monodentate bipyridyl intermediate containing ruthenium is considered unstable, and it was suggested that in the case of $[Ru(bpz)_3]^{2+}$, the build up of monodentate bipyrazyl complex is not seen spectroscopically because of its rapid reformation to $[Ru(bpz)_3]^{2+}$ or conversion to $[Ru(bpz)_2(CH_3CN)Cl]^+$ [18]

Also the photoreactivity of ruthenium (II) complexes of the type $[Ru(bpy)_2(L)(L')]^{n+}$ where L and L' are any monodentate ligand, has been noted since the publication of a series of papers by Bosnich, Dwyer and co-workers [50] As expected, the photoreactions usually involve loss of the monodentate ligands according to reactions 3 and 4

$$[Ru(bpy)_2(L)(L')]^{n+} + S \text{ -------} \rightarrow [Ru(bpy)_2(L)S]^{m+} + L' \quad (3)$$

$$[Ru(bpy)_2(L)S]^{m+} + S \text{ -------} \rightarrow [Ru(bpy)_2S_2]^{q+} + L \quad (4)$$

Depending on the solvent dielectric constant, S may be a solvent molecule, a counter ion, added anions, or residual water in the solvent [49, 46, 48] These reactions have proven to be of some synthetic utility [49]

Chapter 3 has been divided into three sections, each deals with different aspects of compounds containing pyridyl-triazole ligands The first section looks at the effect of coordinating a series of chelating pyridyl-1,2,4-triazoles

to the $Ru(bpy)_2$ moiety The coordination modes for the ligands, except the HPyrtr ligand, have been determined by $^1H$ n m r spectroscopy The mode of coordination of $[Ru(bpy)_2(3MePyrtr)]^+$ is confirmed by the X-ray crystal crystallography The electronic and electrochemical properties of the compounds are examined and compared to $[Ru(bpy)_3]^{2+}$ In the last two sections of Chapter 3 the possibility of the formation, by thermal and photochemical means, of complexes containing pyridyltriazole ligands coordinated in a monodentate mode are investigated The coordination modes of the monodentate compounds produced thermally have been determined using $^1H$ n m r spectroscopy and the coordination mode of the compound $[Ru(bpy)_2(3MePT)Cl]PF_6$ is confirmed by X-ray crystal crystallography

# Chapter 3

## Section 1

## Preparation and Characterisation of $cis$-$[Ru(bpy)_2(L\text{-}L')]^+$ Complexes Containing Asymmetric Bidentate Ligands

3 1 1 Preparation of Complexes of the Type $[Ru(bpy)_2(L\text{-}L')]^{n+}$

The reaction of cis $[Ru(bpy)_2Cl_2]\ 2H_2O$ with equimolar amounts of L-L' yielded a series of compounds of the type cis-$[Ru(bpy)_2(L\text{-}L')]^{n+}$ (n = 1 or 2)

$$cis[Ru(bpy)_2Cl_2] \xrightarrow{L\text{-}L'} cis[Ru(bpy)_2(L\text{-}L')]^{n+}$$

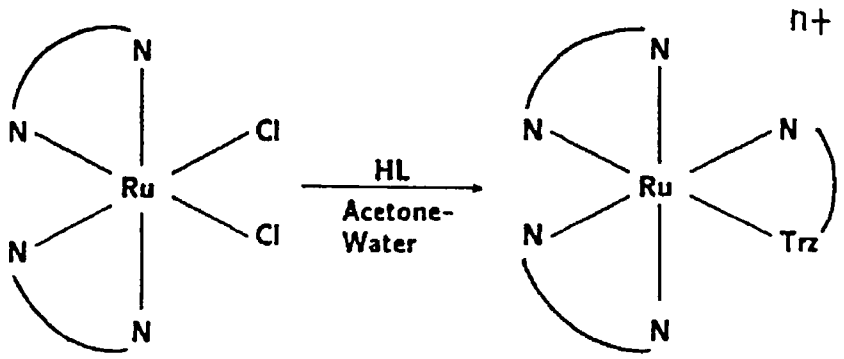


All compounds were isolated as bivalent cations with $PF_6$ counter ions For the ligands HPyrtr and H3MePyrtr deprotonation occurs easily, therefore, in order to ensure complete protonation the two complexes were recrystallised from acidic acetone/water mixtures The deprotonated complexes were isolated as monovalent cations with $PF_6^-$ counter ions All compounds prepared were analysed for their purity using the HPLC system described in Chapter 2

The structures and numbering scheme for the ligands are presented in Figure 3 3 For three of the chelating ligands HPyrtr, H3MePyrtr and 1MePyrtr, different coordination modes are possible (Figure 3 3) Coordination of ruthenium to the triazole ring may occur either via the $N^{2'}$ or $N^{4'}$ nitrogen atoms of the triazole ring

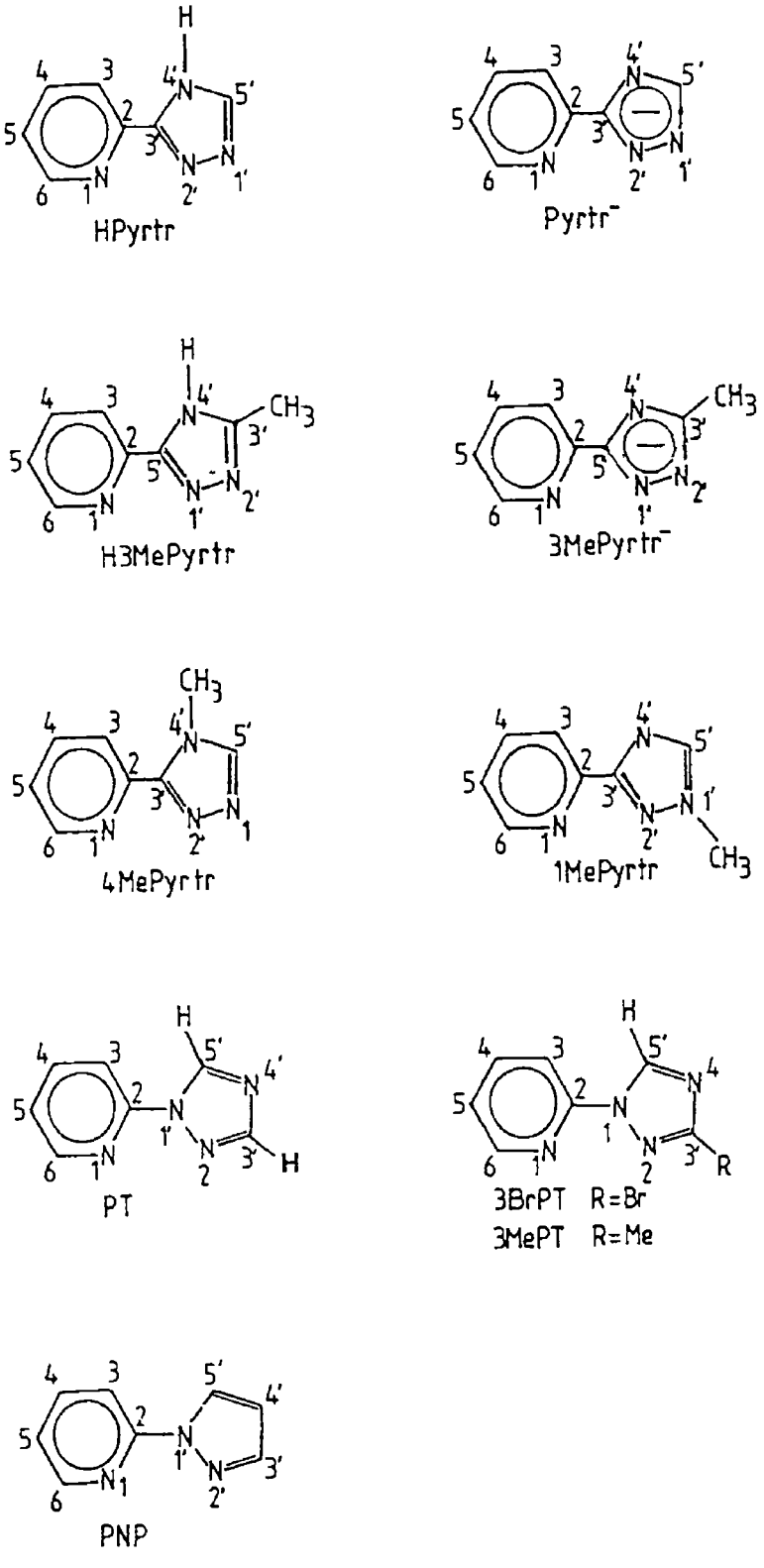


Figure 3 3 Structures and abbreviations of pyridyl-1,2,4-triazole ligands

The mode of coordination is anticipated to be affected by the position of the methyl substituent present on the ring The coordination mode may also have an effect on the electronic properties of the ligand (i e $\pi$-acceptor properties) because of the localised nature of the double bond in 1,2,4-triazoles As $[Ru(bpy)_2(HPyrtr)]^{2+}$ contains no methyl substituents on the triazole ring it is likely that there is an equal possibility of coordination via both sites The $^1H$ n m r spectrum of this compound indicates the presence of two isomers The HPLC system developed was capable of separating a mixture of the two isomers into two individual components Figure 3 4 (a) shows the separation of the two isomers of complex $[Ru(bpy)_2(HPyrtr)]^{2+}$ and with use of the diode array detection system, the corresponding uv/vis spectra of each isomer was obtained Deprotonation of the sample occurs when the sample is in the mobile phase, and this facilitates elution of the isomers since singly charged species elute before doubly charged species The uv/vis spectra of the deprotonated isomers are quite similar, so for this reason, the chromatogram presented in Figure 3 4 (a) was obtained using the acidic mobile phase acetonitrile water (80 20) containing 0 04 M $HClO_4$ The uv/vis spectra of the protonated isomers are less similar to each other than those of the deprotonated isomers

Adaptions of this procedure using semi-preparative HPLC led to the isolation of the individual isomers in milligram quantities

As $[Ru(bpy)_2(HPyrtr)]^{2+}$ is composed of two isomers, a $pK_a$ value is found for each one Isomer 2 and $[Ru(bpy)_2(H3MePyrtr)]^{2+}$ act as rather strong acids, the $pK_a$'s for each complex is 4 07 $\pm$ 0 2 and 4 85 $\pm$ 0 2, respectively, while the $pK_a$ for isomer 1 is 5 95 $\pm$ 0 2 The acid-base behaviour of these two complexes and their corresponding ligands will be discussed in more detail in Chapter 4

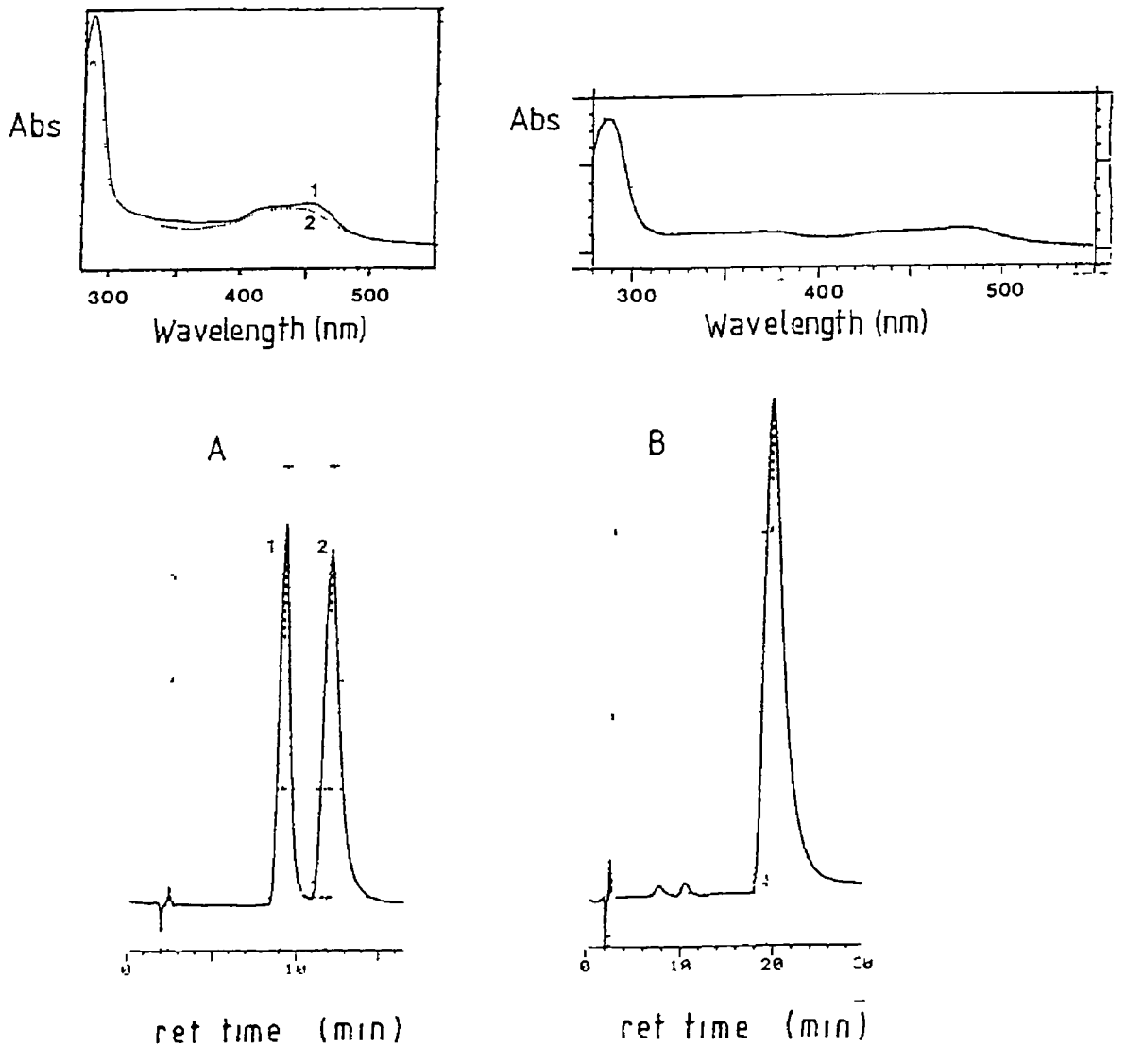


Figure 3 4 Chromatograms of the isomers of (a) $[Ru(bpy)_2(HPyrtr)]^{2+}$ in acetonitrile water (80 20) with 0 04 M $HClO_4$ (flow rate 3 5 ml/min) and (b) $[Ru(bpy)_2(3MePyrtr)]^{+}$ in acetonitrile water (80 20) with 0 08 M $LiClO_4$ (flow rate 2 0 ml/min) (see Chapter 2), both with the corresponding uv/vis spectra obtained using diode array techniques

For $[Ru(bpy)_2(H3MePyrtr)]^{2+}$ two coordination sites are also possible as the three nitrogens in the triazole ring are unsubstituted But as the methyl group is situated on the 3' carbon of the triazole ring it is anticipated that it will provide steric hindrance for coordination at the $N^{4'}$ atom and coordination via the $N^{1'}$ atom will be favoured Figure 3 4 (b) shows a chromatogram of this complex along with the uv/vis spectrum, the presence of one peak indicates that one isomer only has been formed The X-ray crystal structure of a salt of the comples has been determined which confirms that steric hindrance of the methyl group does take place and coordination of the triazole ring to ruthenium is via the $N^{1'}$ atom

Two coordination modes are also possible at the triazole ring $[Ru(bpy)_2(1MePyrtr)]^{2+}$ But, due to the presence of the methyl group at $N^{1'}$ position it is expected that coordination will occur at the $N^1$ of the pyridine ring and at the $N^{4'}$ of the triazole ring This is confirmed by $^1H$ n m r spectroscopy

For $[Ru(bpy)_2(4MePyrtr)]^{2+}$, only one coordination mode is possible for the triazole ring As the $N_{4'}$ position is substituted with a methyl group then coordination of the 4MePyrtr ligand must take place via the $N^1$ of the pyridine ring and the $N^{2'}$ of the triazole ring

For complexes where the pyridyltriazole bond is a C-N bond i e $[Ru(bpy)_2(PT)]^{2+}$, $[[Ru(bpy)_2(3BrPT)]^{2+}$, $[Ru(bpy)_2(3MePT)]^{2+}$ and $[Ru(bpy)_2(PNP)]^{2+}$, the formation of only one isomer is possible for bidentate coordination (see Figure 3 3)

Because of the presence of two bipyridyl ligands and one pyridyltriazole ligand in these complexes, neither uv-visible spectroscopy nor the electrochemical properties of

the complexes can be used to identify unambiguously in which manner the triazole ring is coordinated to the central ruthenium atom $^{1}H$ n m r spectroscopy has been the technique used [21] to ascertain the mode of coordination for these pyridyltriazole ligands

3 1 2 $^{1}H$ N.m.r. Spectra.

The resonances for the free and the coordinated ligands can be found in Chapter 2, Experimental The n m r spectra confirm cis-geometry for all complexes [32, 33]

For each pyridyltriazole ligand, coordination to ruthenium in a bidentate mode results in the $H^{6}$ protons of the pyridine ring to be shifted upfield, and the $H^{3}$ protons of the pyridine ring to be shifted downfield This is similar behaviour as that observed for other bivalent pyridyl-triazole complexes [21, 51] The resonances of the triazole protons/methyl substituents are also anticipated to be affected by the presence of the metal

For the ligands H3MePyrtr and 1MePyrtr (see Figure 3 3), the resonances of the methyl groups on the triazole rings are expected to be influenced by coordination mode of the ligand If a neighboring nitrogen atom is coordinated to ruthenium, these groups will be affected not only by a change in electron density but also by the presence of the shielding cone of a bipyridyl ring Comparison with literature data suggests that upon coordination through $N^{4'}$, the $CH_3$ group on the $C^{3'}$ position in 3Mepyrtr and the H group on the $C^{5'}$ position in 1MePyrtr are shielded In the case of coordination at $N^{1'}$ in 3MePyrtr the $C^{3'}$ methyl substituent should be found at lower field than that of the free ligand For 1MePyrtr coordination via $N^{2'}$ should result in a shift to higher field of the $CH_3$ resonance

while the H on the $C^{5'}$ position should be found at higher field than the free ligand This effect was clearly shown by Steel et al [10] for the complex $[Ru(bpy)_2(L\text{-}L')]^{2+}$ where L-L' = 3,5-dimethyl-1-(pyridin-2-yl)pyrazole Relative to the free ligand, a shift of -0 72 p p m was observed for the methyl group on the 3' position close to the coordinating $N^{2'}$, while the methyl group on the 5' position was shifted downfield by +0 26 p p m Taking the above into account and as the position of the $CH_3$ group of H3MePyrtr is shifted downfield by +0 04 p p m with respect to that of the free ligand to 2 4 p p m Therefore, it seams likely that the triazole ring in 3MePyrtr is bound through the $N^{2'}$ atom Similarly, as the resonance of the coordinated and free 1MePyrtr ligand are the same, it seams that in 1MePyrtr, ruthenium is bound via the $N^{4'}$ atom As expected, the triazole ring in 4MePyrtr is bound to ruthenium via the $N^{2'}$ atom

Deprotonation of $[Ru(bpy)_2(H3Mepyrtr)]^{2+}$ causes the methyl resonance to shift upfield to 2 20 p p m along with a slight shift upfield for the protons on the pyridyltriazole ligand These shifts can be attributed to an increase in electron density in the triazole ring [21]

The $^1H$ n m r spectra of $[Ru(bpy)_2(HPyrtr)]^{2+}$ confirm the presence of two isomers as seen with HPLC It is anticipated that the mode of coordination of each isomer may be distinguished by n m r spectra of the pure isomers The two modes of coordination are shown in Figure 3 5 (a) and (b) while Figure 3 6 presents the $^1H$ n m r spectra of the deprotonated forms of the two isomers The $^1H$ n m r data for the protonated and deprotonated forms of each isomer are listed in Table 3 3

Figure 3 5 Possible coordination modes for the two isomers of $[Ru(bpy)_2(HPyrtr)]^{2+}$

Coordination of the HPyrtr ligand to ruthenium results in a slight shift upfield for the $H^3$ protons of the pyridyltriazole ligands of both isomers There is a dramatic shift upfield for the $H^6$ protons of the protonated and deprotonated isomers indicating that these protons are in the shielding cone of a pyridine ring of a bipyridine ligand The $H^{5'}$ singlets also shift upfield suggesting that they are being shielded to some extent

The shift of the $H^{5'}$ singlet upon protonation and deprotonation may yield information about the coordination mode for each isomer Deprotonation of each isomer has a strong influence on the resonance of the $H^{5'}$ singlet and appreciable shifts in the bpy protons are also observed Upon deprotonation of $[Ru(bpy)_2(H3MePyrtr)]^{2+}$ similar shifts are observed The shift in the resonance positions, can be explained by the increased electron density in the triazole ring [36], which probably also effects the electron density in the pyridyl ring of the pyridyltriazole ligand

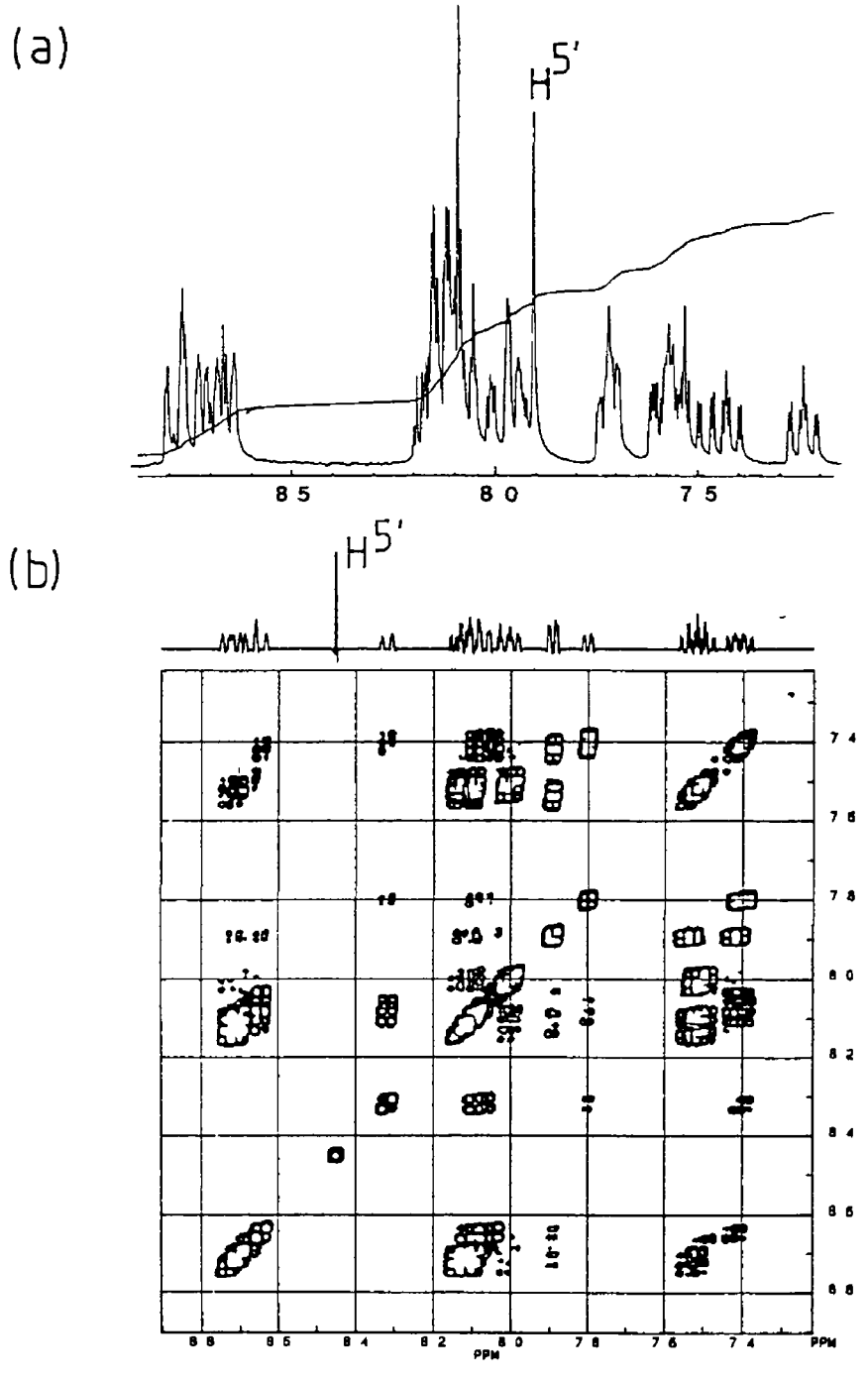


Figure 3 6 (a) $^{1}H$ n m r spectrum of isomer 1 of $[Ru(bpy)_2(Pyrtr)]^+$ (300 MHz) and (b) COSY n m r spectrum of isomer 2 of $[Ru(bpy)_2(Pyrtr)]^+$ (300 MHz) in $(CD_3)_2SO$

Table 3 3 Correlation Spectroscopy Data for the Protonated and Deprotonated forms of the two isomers of $[Ru(bpy)_2(HPyrtr)]^{2+}$ (Solvent acetone - $d^6$, 300 MHz) (ppm)

| Compound | | Pyridyl-Triazole Ligands | | | | | Bipyridine Ligands | | | |
|---|---|---|---|---|---|---|---|---|---|---|
| | | $H^{5'}$ | $H^3$ | $H^4$ | $H^5$ | $H^6$ | $H^3$ | $H^4$ | $H^5$ | $H^6$ |
| $[Ru(bpy)_2(HPyrtr)]^{2+}$ | (1a) | 8 78 | 8 45 | 8 17 | 7 54 | 7 89 | 8 73-8 89 | 8 10-8 17 | 7 47-7 67 | 8 02-8 33 |
| | (2a) | 8 68 | 8 46 | 8 17 | 7 48 | 7 93 | 8 72-8 82 | 8 13-8 17 | 8 47-8 59 | 8 01-8 20 |
| $[Ru(bpy)_2(Pyrtr)]^{+}$ | (1b) | 7 91 | 8 02 | 7 91 | 7 24 | 7 72 | 8 63-8 82 | 8 03-8 20 | 7 39-7 63 | 7 69-7 99 |
| | (2b) | 8 45 | 8 32 | 8 09 | 7 41 | 7 80 | 8 63-8 77 | 8 02-8 16 | 7 40-7 56 | 7 88-8 08 |

a = Protonated form of Isomers 1 and 2

b = Deprotonated form of Isomers 1 and 2

The difference between the singlet proton resonances for the isomers in the protonated form is 0 1 p p m (see Table 3 3) The resonance of isomer 1 is found at higher field than that of isomer 2 By comparison with the compounds containing 4MePyrtr and 1MePyrtr, information on the effect of the different coordination modes of the triazole ring ($N^{2'}$ or $N^{4'}$) on the resonance of the 5' proton can be examined (see Figure 3 7) For the complex $[Ru(bpy)_2(4MePyrtr)]^{2+}$, the 4MePyrtr ligand is bound to ruthenium via $N^{2'}$ and $H^{5'}$ is found at 8 88 p p m , while for $[Ru(bpy)_2(1MePyrtr)]^{2+}$, the 1MePyrtr ligand is bound via the $N^{4'}$ of the triazole ring and $H^{5'}$ is found at 8 73 p p m The difference between the two coordination modes being 0 15 p p m This suggests that for coordination via $N^{4'}$ of the triazole ring the $H^{5'}$ atom is shielded to a greater extent by a bpy group than the $H^{5'}$ atom if coordination takes place via $N^{2'}$ The resonance of the compound containing the 4MePyrtr ligand is found at slightly higher p p m than that containing the 1MePyrtr ligand This may suggest that isomer 1 may be bound to ruthenium via the $N^{2'}$ atom and isomer 2 may be bound via the $N^{4'}$ atom

For the deprotonated isomers on the other hand, quite a large difference exists between the singlet resonances (0 54 p p m ), this shift is observed in Figure 3 6 (a) and (b) The $H^{5'}$ of isomer 1 has the highest p p m value of 7 91 p p m while the $H^{5'}$ resonance for isomer 2 is found at 8 45 p p m This difference in p p m between the two isomers is important as it reflects the effect of coordination at different nitrogens in the triazole ring

With this in mind, our results obtained for the resonances of the $H^{5'}$ atoms for isomer 1 and isomer 2 suggests that the 5' proton of isomer 1 is shielded more than that of isomer 2 This suggests that coordination of the triazole

ring to ruthenium in isomer 1 may be via the $N^{4'}$ position, Figure 3 5 (a), and coordination mode of isomer 2 may be via the $N^{2'}$ site, Figure 3 5 (b)

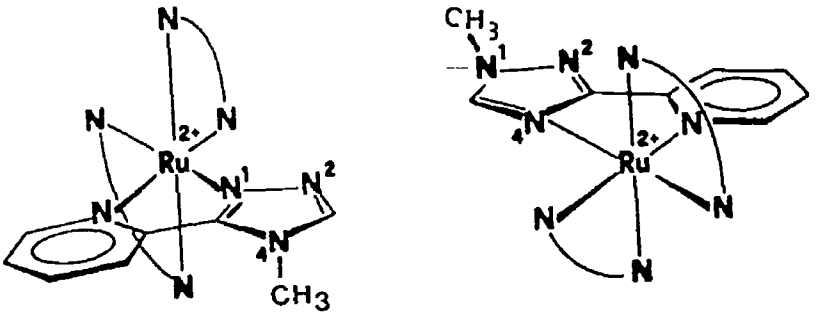


(a) (b)

Figure 3 7 Proposed structures of (a) $[Ru(bpy)_2(4MePyrtr)]^{2+}$ and (b) $[Ru(bpy)_2(1MePyrtr)]^{2+}$ showing the effect of coordination mode on the position of the $H^{5'}$ atom in relation to the bpy groups

The spectra of the protonated isomers are difficult to interpret because the 5' proton resonance will also depend on the location of N-H proton It is expected that uv/vis spectra, emission spectra, electrochemistry and $pK_a$ measurements will support the suggested coordinated modes for the two isomers

For the three ligands containing a C-N pyridyltriazole bond, only one isomer is possible for bidentate coordination The structures in Figure 3 3 shows that coordination to ruthenium is via the $N^1$ of the pyridine ring and the $N^{2'}$ of the triazole ring As expected, all the n m r spectra of these complexes indicate the presence of only one isomer In comparison with the free ligands, coordination to ruthenium results in the $H^{5'}$ and/or the $H^{3'}$ protons being shifted downfield The $^1H$ n m r spectra of

the free and chelating ligands PT, 3MePT, 3BrPT and 4MePyrtr are described in more detail in Section 2 of this chapter as a comparison with compounds containing these ligands in a monodentate coordinated mode

The assignment of the singlet resonances for the ligand PT is not straight forward From the $^{1}H$ n m r spectra of the free and bound ligand it is not possible to unambiguously assign which singlet resonances at 9 37 and 8 30 p p m are due to which proton, the $H^{3'}$ or $H^{5'}$ proton In order to ascertain which resonance belongs to which proton, it is necessary to compare n m r spectrum of the ligand PT with that of the ligand 1,3-bis(pyridin-2-yl)-1,2,4-triazole (bptn) (see Chapter 5 Figure 5 4 (a) for the structure) This ligand is similar to the ligand PT but has a pyridine ring substituent on the 3' carbon on the triazole ring The resonance for the remaining proton, $H^{5'}$, on the triazole ring is found at 9 48 p p m A singlet at 9 37 p p m is also observed in the $^{1}H$ n m r spectrum of PT, indicating that this resonance belongs to the $H^{5'}$ proton while that at 8 30 p p m belongs to the $H^{3'}$ proton The coordination of PT to $Ru(bpy)_2$ results in a shift upfield for the $H^{5'}$ proton due to the shielding effect of the bipyridyl ring while the resonance for the $H^{3'}$ proton remains relatively unchanged

The methyl resonances of $[Ru(bpy)_2(4MePyrtr)]^{2+}$ and $[Ru(bpy)_3(3MePT)]^{2+}$ are also affected by their position on the triazole ring with respect to the bpy groups The methyl substituent of $[Ru(bpy)_2(4Mepyrtr)]^{2+}$ shifts downfield by 0 20 p p m as it is not under the influence of the shielding effects of bpy groups The methyl substituent of the 3MePT compound, on the other hand shifts upfield by 0 04 p p m As this methyl group on the other hand may be lying adjacent to a pyridine ring of one of the bipyridyl ligands, this substituent is slightly shielded by

the aromatic ring and the signal shifted upfield

So, from this discussion, it is clear that $^{1}H$ n m r is a useful technique in determining the coordination modes for the pyridyl-1,2,4-triazoles Unfortunately, for the two isomers of $[Ru(bpy)_2(HPyrtr)]^{2+}$ it is not possible to unambiguously assign the coordination mode for each isomer

### 3 1 3 Crystal Structure of Bis(2,2'-bipyridine) Ruthenium-3-Methyl-5-(pyridin-2-yl)-1,2,4-triazole Hexafluorophosphate Tetrahydrate

A projection of the structure of $[Ru(bpy)_2(3MePyrtr)]^{+}$ as obtained from X-ray techniques is presented in Figure 3 8 For reasons of clarity, all P, F, O and H atoms have been omitted A summary of crystal data and collection intensities is presented in Table 3 4 while the relevant bond lengths and angles are listed in Table 3 5 The ruthenium atom is six-coordinated by one pyridyltriazole and two bipyridine molecules The ruthenium-nitrogen distances of 2 06-2 09 Å are in the normal range for this type of compound, although the Ru-N(51) (pyridine ring of the pyridyltriazole ligand) is somewhat longer than expected at 2 086 Å [52-58] The ruthenium-triazole distance for $[Ru(bpy)_2(Prtrz)_2]^{2+}$ (Prtrz = 4-propene-4H-1,2,4-triazole) are 2 095 and 2 083 Å [54], slightly longer than the value of 2 050 Å obtained for the Ru-N(trz) bond length in our structure The reason for our shorter bond length may be due to the negative charge on the triazole ring of $3MePyrtr^{-}$ making the triazole ring a better $\sigma$ donor

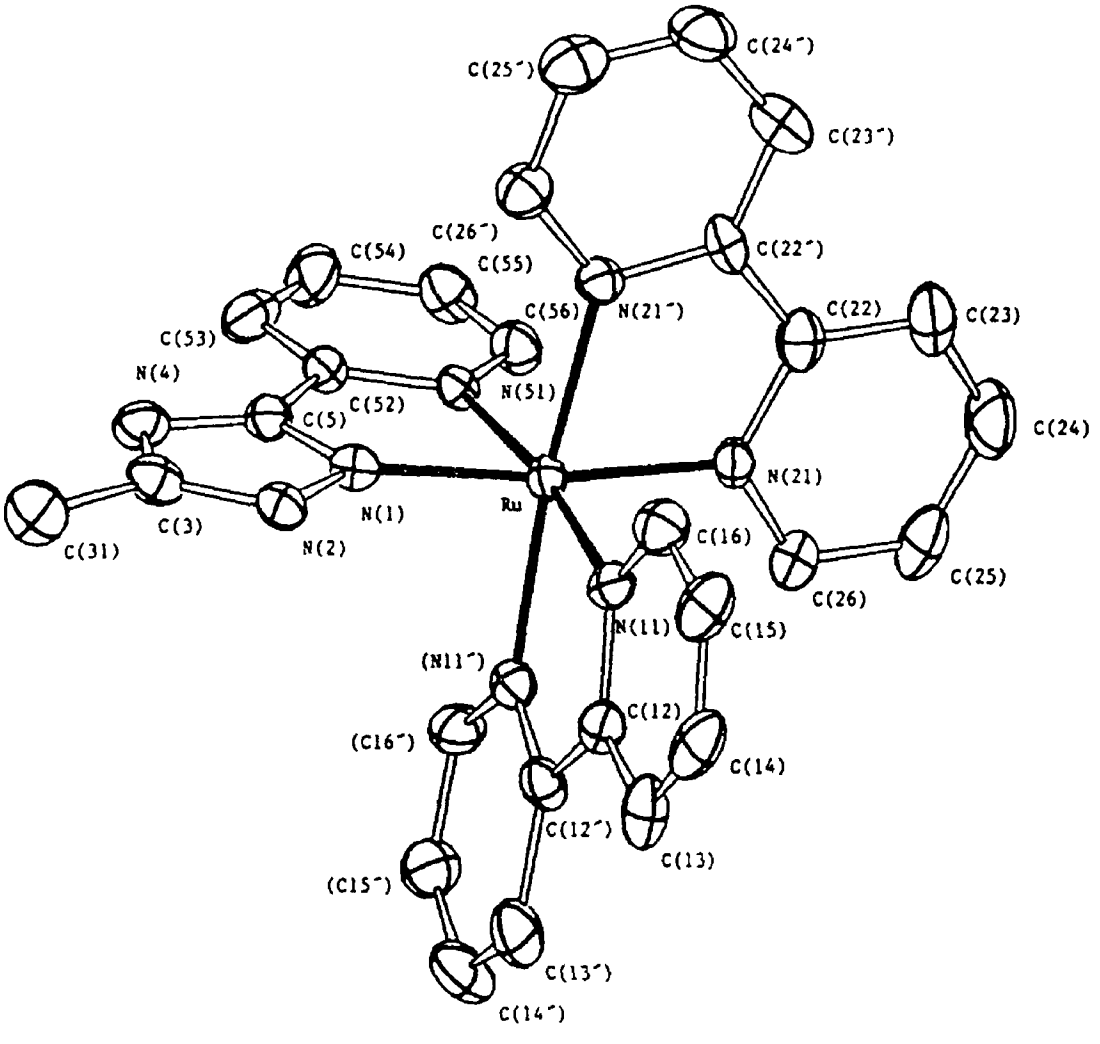


Figure 3 8 X-Ray crystal structure of the cation $[Ru(bpy)_2(3MePyrtr)]_+$ showing atom labeling

Table 3 4 Summary of Crystal Data and Collection of Intensities of Bis(2,2'-bipyridine)Ruthenium 3-Methyl-5-(pyridin-2-yl)-1,2,4-triazole Hexafluorophosphate Tetrahydrate

| | |
|---|---|
| Formula | $RuC_{28}H_{31}N_8PF_6O_4$ |
| $M_r$ | 789 64 |
| Space group | P $3_1$ 2 1 |
| $\alpha$ | 90° |
| ß | 90° |
| $\gamma$ | 120° |
| a=b, A | 13 760 (6) |
| c, Å | 30 503 (9) |
| V, $Å^3$ | 5003 |
| Z | 6 |
| $D_{obs}$ (by flotation), Mg $m^{-3}$ | 1 55 |
| $D_{calc}$ , Mg $m^{-3}$ | 1 57 |
| $\mu$ (MoK$\alpha$), $cm^{-1}$ | 5 84 |
| $\theta$ range, deg | 2-30 |
| data collection range | h,-19 to 19, k,0 to 19, l 0 to 43 |
| no of indep reflections | 7867 |
| no of sign refl (I>2$\sigma$(I)) | 4288 |
| $F_{000}$ | 2279 |
| R | 0 036 |
| $R_w$ | 0 049 |
| $R_{int}$ | 0 010 |

Table 3 5 Selected Bond Distances (A) ανδ Ανγλεσ (o) o Bis(2,2'-bipyridine)Ruthenium-3-Methyl-5-(pyridin 2 yl)-1,2,4-triazole Hexafluorophosphate Tetrahydrate

Bond distances (Å)

| | | | |
|---|---|---|---|
| Ru - N(1) | 2 050 (5) | C(3) - N(4) | 1 349 (8) |
| Ru - N(51) | 2 086 (4) | N(4) - C(5) | 1 334 (7) |
| Ru - N(11) | 2 055 (4) | C(5) - C(52) | 1 456 (8) |
| Ru - N(11') | 2 042 (5) | C(52) - N(51) | 1 357 (7) |
| Ru - N(21) | 2 060 (4) | N(51) - C(56) | 1 327 (7) |
| Ru - N(21') | 2 056 (4) | C(56) - C(55) | 1 417 (9) |
| N(1) - C(5) | 1 349 (7) | C(55) - C(54) | 1 36 (1) |
| N(1) - N(2) | 1 374 (6) | C(54) - C(53) | 1 367 (9) |
| N(2) - C(3) | 1 317 (7) | C(53) - C(52) | 1 357 (9) |
| C(3) - C(31) | 1 493 (8) | | |

Bond angles (deg)

| | | | |
|---|---|---|---|
| N(1) - Ru - N(51) | 78 0 (2) | C(12') - C(13') - H(13') | 129 5 (4) |
| N(1) - Ru - N(11) | 96 1 (2) | C(13') - C(14') - H(14') | 124 6 (5) |
| N(1) - Ru - N(21') | 96 5 (5) | C(14') - C(15') - H(15') | 118 9 (5) |
| N(1) - Ru - N(11') | 87 4 (2) | C(15') - C(16') - H(16') | 119 8 (5) |
| N(51) - Ru - N(11') | 95 0 (2) | C(22) - C(23) - H(23) | 128 2 (5) |
| N(51) - Ru - N(21) | 95 9 (2) | C(23) - C(24) - H(24) | 132 6 (5) |
| N(51) - Ru - N(21') | 90 9 (2) | C(24) - C(25) - H(25) | 118 7 (4) |
| N(11) - Ru - N(11') | 79 4 (2) | C(25) - C(26) - H(26) | 122 3 (4) |
| N(11) - Ru - N(21) | 90 5 (2) | C(22') - C(23') - H(23') | 125 7 (5) |
| N(11') - Ru - N(21) | 98 0 (2) | C(23') - C(24') - H(24') | 108 5 (4) |
| N(21) - Ru - N(21') | 78 7 (2) | C(24') - C(25') - H(25') | 129 6 (5) |
| | | C(25') - C(26') - H(26') | 116 2 (5) |

For our structure, the Ru-N bond lengths for the pyridyltriazole ligand are 2 086 Å for Ru-N(pyr) and 2 050 Å for Ru-N(trz) Recently, the crystal structure of $[Ru(bpy)_2(bpt)]^+$ [52] (see Chapter 5) has been determined [52], where $bpt^-$ is 3,5-bis-(pyridin-2-yl)-1,2,4,-triazole, which exhibits similar Ru-N(pyr) and Ru-N(trz) bond lengths to our structure The ruthenium-pyridine bond in $[Ru(bpy)_2(bpt)]^+$ is slightly longer than normal at 2 11 Å and has been explained by diminished $\pi$ backbonding in the system due to the negative charge on the $bpt^-$ ligand The ruthenium-triazole bond length is 2 03 Å The slightly longer bond length obtained for the ruthenium-pyridine bond in our structure may also be attributed to diminished $\pi$ backbonding activity in the $3MePyrtr^-$ ligand

The bite angles for the bpy ligands of 78 8 and 79 2° of the $bpt^-$ complex are very similar to those of 78 7 and 79 4° for the bpy ligands in our complex The pyridyl-triazole bite angles for both complexes are also very similar, 77 9° for the $bpt^-$ complex and 80 0° for the $3MePyrtr^-$ complex These angles are comparable to chelating angles observed normally for similar structures [52-58]

For $[Ru(bpy)_2(3MePyrtr)]^+$, four water molecules have been found near N(4') of the triazole ring These water molecules give rise to an extensive hydrogen-bonding network, intermolecular distances of about 2 8 Å are observed between the oxygen atoms (see Table I in the Appendix) One oxygen atom (O(1)) is located near N4 of the triazole ring and linked to O(3) O(3) is located near another oxygen atom (O(4)) and finally O(4) is linked with the last water molecule (O(2)), which is in its turn connected to N2 of the triazole ring of another $[Ru(bpy)_2(3MePyrtr)]PF_6$ group The $[Ru(bpy)_2(3MePyrtr)]PF_6$ groups in the lattice are all linked by these water

molecules This is quite interesting as this might suggest similar extended hydrogen bonding in "hydrogen-bonding" solvents, something which would effect the photophysical properties of the ruthenium compounds A similar phenomenon has been observed in the molecular structure of $[Ru(bpy)_2Cl_2]$ 3 $5H_2O$ where water molecules bridge the $Ru(bpy)_2Cl_2$ moieties via the chlorides [53]

3 1 4 Electronic Spectra and Redox Properties

The electronic and electrochemical properties of the complexes are listed in Table 3 6 As for other ruthenium compounds the absorption bands of lowest energy can be assigned to $d\pi$ ---> $\pi^*$ MLCT bands The position of these bands is determined by both $\sigma$ and $\pi$ effects of the ligands [59] which in turn may be affected by the presence of substituents on the triazole ring The bands below 300 nm have been assigned to bipyridine [25] and L-L' intraligand $\pi$ ---> $\pi^*$ transitions [2, 4] For the divalent cations where the pyridyltriazole bond is C-C in nature i e $[Ru(bpy)_2(HPyrtr)]^{2+}$ (isomers 1 and 2), $[Ru(bpy)_2(H3MePyrtr)]^{2+}$, $[Ru(bpy)_2(4MePyrtr)]^{2+}$ and $[Ru(bpy)_2(1MePyrtr)]^{2+}$ (Table 3 6) the lowest energy absorption band is found at slightly higher energy than the MLCT band of $[Ru(bpy)_3]^{2+}$ For the bivalent cations where the pyridyltriazole bond is a C-N bond i e $[Ru(bpy)_2(PT)]^{2+}$, $[Ru(bpy)_2(3BrPT)]^{2+}$, $[Ru(bpy)_2(3MePT)]^{2+}$ and $[Ru(bpy)_2(PNP)]^{2+}$ (Table 3 6) the MLCT bands are found at higher energies than compounds containing a C-C pyridyl-triazole bond and hence at higher energy than the MLCT band of $[Ru(bpy)_3]^{2+}$

The absorption, emission and electrochemical studies are expected to yield information leading to determination of structural differences in the $[Ru(bpy)_2(HPyrtr)]2^+$ isomers

Table 3 6 Electronic and Electrochemical Data for Complexes $[Ru(bpy)_2(L\text{-}L')]^{n+}$

| Compound | | Absorption [c] λ Max | (log ε) | Emission (nm) [d] 300K | 77K | Redox Potentials [e] $Ru^{III/II}$ | Ligand Based | | Ref |
|---|---|---|---|---|---|---|---|---|---|
| $[Ru(bpy)_2(HPyrtr)]^{2+}$ | (1a) | 452 | (4 05) | 615 | 590 | 1 20 | -1 47 | -1 72[f] | g |
| | (2a) | 444 | (4 11) | 625 | 575 | 1 10 | -1 49 | -1 73[f] | g |
| $[Ru(bpy)_2(Pyrtr)]^{+}$ | (1b) | 488 | (3 97) | 670 | 609 | 0 90 | -1 51 | -1 78[f] | g |
| | (2b) | 484 | (4 04) | 670 | 608 | 0 83 | -1 48 | -1 74[f] | g |
| $[Ru(bpy)_2(H3MePyrtr)]^{2+}$ | (3) | 444 | (4 03) | 600 | 587 | 1 20 | -1 55 | -1 81 | 21 |
| $[Ru(bpy)_2(3MePyrtr)]^{+}$ | (4) | 476 | (3 93) | 660 | 610 | 0 79 | -1 50 | -1 72 | 21 |
| $[Ru(bpy)_2(4MePyrtr)]^{2+}$ | (5) | 440 | (4 16) | 600 | 584 | 1 21 | -1 42 | -1 64 | 21 |
| $[Ru(bpy)_2(1MePyrtr)]^{2+}$ | (6) | 452 | (4 03) | 600 | 585 | 1 20 | -1 42 | -1 64 | 21 |
| $[Ru(bpy)_2(PT)]^{2+}$ | (7) | 420 | (4 03) | - | 560 | 1 35 | -1 42 | -1 63 | g |
| $[Ru(bpy)_2(3BrPT)]^{2+}$ | (8) | 420 | (4 06) | - | 553 | 1 42 | -1 35 | -1 59 | g |
| $[Ru(bpy)_2(3MePT)]^{2+}$ | (9) | 433 | (4 00) | 590 | 520 | 1 36 | -1 36 | -1 56 | g |
| $[Ru(bpy)_2(PNP)]^{2+}$ | (10) | 450 | (3 97) | 609 | 572 | 1 26 | -1 40 | -1 59 | g |
| $[Ru(bpy)_3]^{2+}$ | | 452 | (4 11) | 608 | 582 | 1 22 | -1 36 | -1 53 | 1 |

a Protonated b Deprotonated [c] Measured in $CH_3CN$ λmax in nm, ε in $dm^3mol^{-1}cm^{-1}$ [d] Spectra at room temperature in $CH_3CN$, at 77K in Ethanol, λmax in nm [e] Measured in $CH_3CN$ with 0 1M $NEt_4ClO_4$ volts vs s c e , n h e = s c e + 0 2415V [f] Reduction potentials at approximately -2 2V for isomers, measurements carried out in Leiden University [g] This work

The absorption spectra of the protonated and deprotonated forms of the two isomers are illustrated in Figures 3 9 and 3 10, while the emission low temperature are illustrated in Figure 3 11 From Figure 3 9, 3 10 and 3 11 and Table 3 6, it is observed that only slight differences exist between the absorption and emission maxima for the protonated and deprotonated forms of the two isomers The emission maxima at room temperature and at low temperature for isomer 1 are found at higher energy than those of isomer 2 This suggests that the $d\pi$ orbitals of ruthenium are stabilized in this instance, suggesting that this isomer of the ligand is a better $\pi$ acceptor This would suggest that isomer 1 would have the structure (a) in Figure 3 5, and as isomer 2 emits at lower energy indicating that the $d\pi$ orbitals of ruthenium are destabilized by the better $\sigma$ donor properties of the ligand in configuration (b) Figure 3 5

It is interesting that the only one oxidation potential is observed for the mixture of the isomers when the oxidation potentials of each isomer separately differ by 100 mV The potential of 1 20 V observed for the mixture is the same as that obtained for isomer 1 The oxidation potential for isomer 2 is 1 10 V, 100 mV lower than isomer 1 suggesting that the HPyrtr ligand in isomer 2 is a better $\sigma$ donor The structure in Figure 3 5 (b) is considered a better $\sigma$ donor than the structure in Figure 3 5 (a) because of the presence of a nitrogen adjacent to the coordinating nitrogen These results support the evidence obtained from the $^{1}H$ n m r spectra that suggests that isomer 2 may be coordinated to ruthenium via the $N^{2'}$ atom of the triazole ring, i e Figure 3 5 (b) and isomer 1 via the $N^{4'}$ atom of the triazole ring, Figure 3 5 (a)

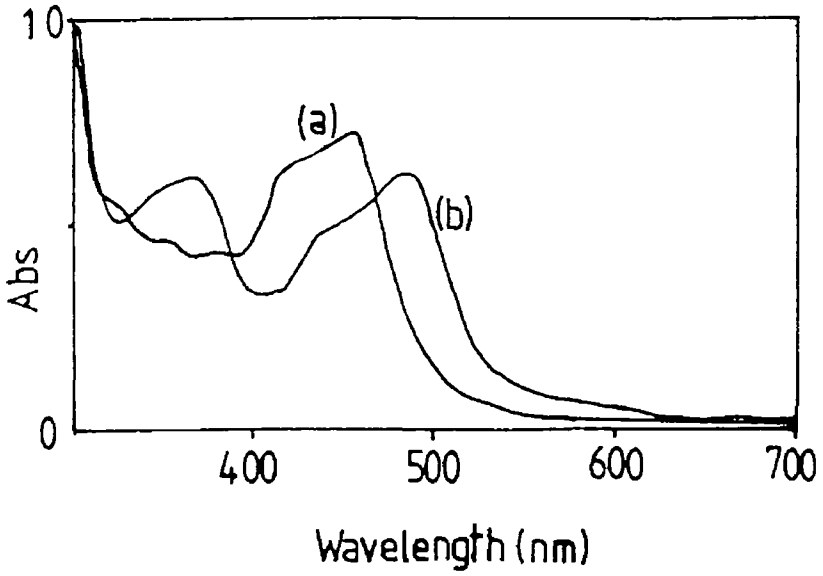


Figure 3 9 Absorption spectra in acetonitrile of (a) the protonated and (b) the deprotonated form of isomer 1 of $[Ru(bpy)_2(HPyrtr)]^{2+}$

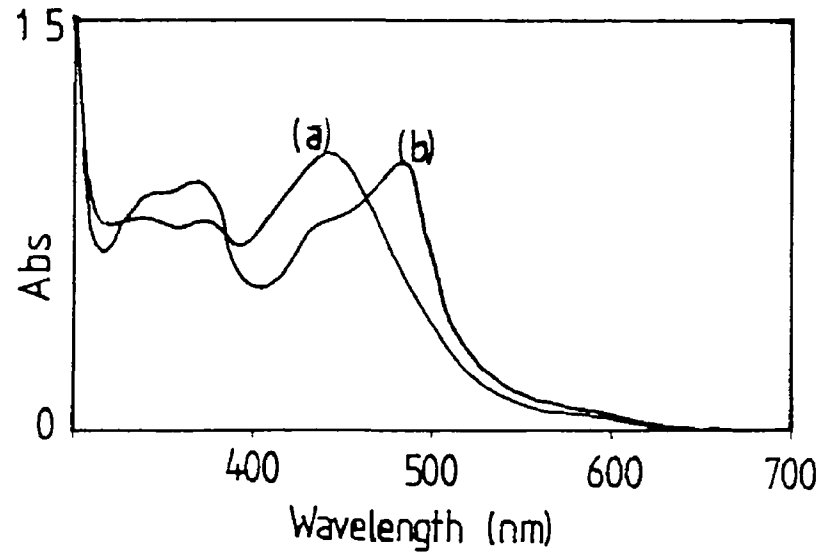


Figure 3 10 Absorption spectra in acetonitrile of (a) the protonated and (b) the deprotonated form of isomer 2 of $[Ru(bpy)_2(HPyrtr)]^{2+}$

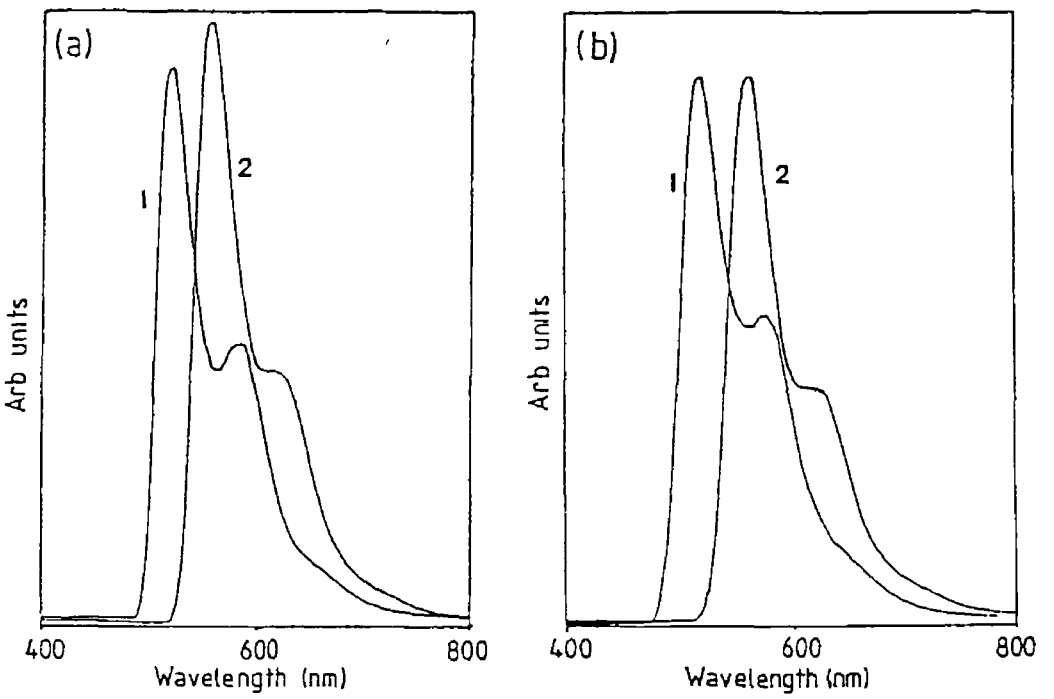


Figure 3 11 Emission spectra at low temperature in ethanol of the protonated (1) and deprotonated (2) form of (a) isomer 1 and (b) isomer 2 of $[Ru(bpy)_2(HPyrtr)]^{2+}$

The first two reversible reduction potentials for the isomers are the bpy based reductions while the irreversible potentials found at approximately -2 2 V vs s c e (measurements carried out in Leiden University) may be attributed to the reduction potentials of the pyridyltriazole ligands This indicates that the $\pi^*$ levels for the pyridyltriazole ligands are at higher energy than those of bipyridine and hence the pyridyltriazole ligands act as spectator ligands in the two isomers

Examination of the $pK_a$ results (see Chapter 4) where the $pK_a$ of isomer 1 is 5 95 ± 0 1, and the $pK_a$ of isomer 2 is 4 07 ± 0 1, suggests that as isomer 2 is more acidic hence a better $\sigma$ donor towards ruthenium A $pK_a$ of 4 87 is found for $[Ru(bpy)_2(H3MePyrtr)]^{2+}$, where the triazole ring of the 3MePyrtr ligand is coordinated to ruthenium via the $N^{2'}$ Allowing a slight increase in $pK_a$ for the methyl substituted pyridlytriazole, this $pK_a$ reasonably close to that of isomer 2 This suggests that isomer 2 may have the same coordination mode as that of $[Ru(bpy)_2(H3MePyrtr)]^{2+}$, that is via the $N^{2'}$ atom of the triazole ring and hence, isomer 1 is coordinated via $N^{4'}$ of the triazole ring On the basis of these results and in conjunction with the $^1H$ n m r results obtained, it is concluded that isomer 1 has structure (a) in Figure 3 5 and isomer 2 has structure (b) The proposed structures for the two isomers are shown in Figure 3 12

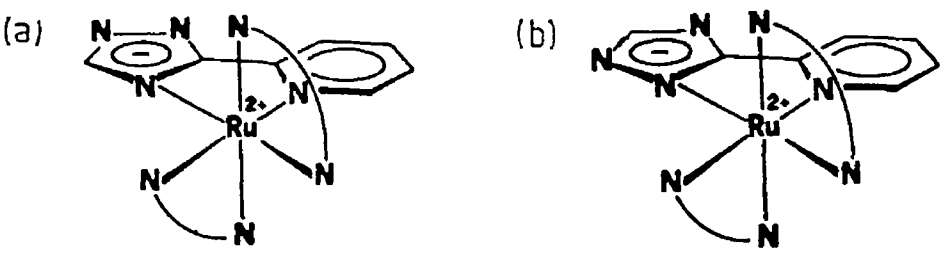


Isomer 1 Isomer 2

Figure 3 12 Proposed structures for the two isomers of $[Ru(bpy)_2(Pyrtr)]^+$

Deprotonation of $[Ru(bpy)_2(H3MePyrtr)]^{2+}$ and $[Ru(bpy)_2(HPyrtr)]^{2+}$ (isomers 1 and 2) to form the monovalent complexes $[Ru(bpy)_2(3MePyrtr)]^{+}$ and $[Ru(bpy)_2(Pyrtr)]^{+}$ is accompanied by a shift to lower energy for the MLCT band (i e to approx 475 nm) Similar behaviour has been observed for complexes of the type $[Ru(bpy)_2L_2]^{n+}$ [36] where L = 1,2,4-triazole or pyrazole The lowest energy absorption for the deprotonated neutral species $[Ru(bpy)_2(trz)_2]$ $H_2O$ shifts considerably to lower energy, with an absorption maximum similar to that of $[Ru(bpy)_2Cl_2]$ The shift to lower energy for the MLCT band for these complexes has been explained by the increase in the $\pi$-donor properties of the deprotonated ligands For the compounds $[Ru(bpy)_2(HPyrtr)]^{2+}$ and $[Ru(bpy)_2(Pyrtr)]^{+}$ the addition of a methyl substituent on the 3' carbon of the triazole produces very little effect in both the absorption and emission spectra On the other hand, in comparison with the deprotonated compound $[Ru(bpy)_2(Pyrtr)]^{+}$, the addition of a methyl substituent on any of the free nitrogens on the triazole ring to form either $[Ru(bpy)_2(1MePyrtr)]^{2+}$ or $[Ru(bpy)_2(4MePyrtr)]^{2+}$ will produce the same shift to higher energy as protonation of the $[Ru(bpy)_2(Pyrtr)]^{+}$ does (see Table 3 6) Similar behaviour has been observed with the neutral $[Ru(bpy)_2(trz)_2]$ on the addition of the methyl substituent to form $[Ru(bpy)_2(Metrz)_2](PF^6)_2$ $H_2O$ a shift to higher energy is observed (470 nm and 473 nm respectively) [36]

From Table 3 6, the reduction potentials indicate that all the pyridyltriazole ligands which contain a carbon-carbon linking bond, and the pyridylpyrazole ligand are less efficient $\pi$ acceptors than bipyridine This is also evident from the $Ru^{II/I}$ reduction potentials In general, these potentials become less negative with increasing $\pi$-acceptor abilities of the ligands [25] The redox potentials of all pyridyltriazole ligands (measurements

carried out in Leiden University) are more negative than that of bipyridine indicating that the ligand reductions are bipyridine based The electrochemical data of the complexes containing pyridyltriazoles with a carbon-nitrogen linking bond, compounds 7, 8 and 9 in Table 3 6, show that this type of ligand possibly has better $\pi$ acceptor properties than bpy as the oxidation potentials are higher than that of $[Ru(bpy)_3]^{2+}$, in particular that of $[Ru(bpy)_2(3BrPT)]^{2+}$ whose oxidation potential is 1 42 V The reduction potentials of these free ligands are found at less negative potentials than those of bpy However, the reduction potentials of these compounds are approximately the same as those obtained for $[Ru(bpy)_3]^{2+}$ suggesting that bpy is the active ligand and the pyridyltriazole ligand is the spectator All compounds emit in fluid at room temperature, with the exception of $[Ru(bpy)_2(PT)]^{2+}$ and $[Ru(bpy)_2(3BrPT)]^{2+}$ The electrochemical results indicate that the absorption and emission processes arise from the bipyridine ligands and not from the pyridyltriazole ligands

All compounds including $[Ru(bpy)_2(PT)]^{2+}$ and $[Ru(bpy)_2(3BrPT)]^{2+}$ emit at low temperature (77K) For all compounds, the emission bands sharpen and exhibit vibrational structure at 77 K It is well known that the intensity of emission depends, among other things, on the energy difference between the deactivating antibonding d-d orbital and the emitting $^3$MLCT state [4, 32, 52] In $[Ru(bpy)_3]^{2+}$ the energy of this d-d orbital is about 4000 $cm^{-1}$ higher than that of the $^3$MLCT band Therefore, thermal population of this level is possible at room temperature [82] Possible explanations for the absence of emission at room temperature for compounds $[Ru(bpy)_2(PT)]^{2+}$ and $[Ru(bpy)_2(3BrPT)]^{2+}$ are (1) the energy difference between the $^3$MLCT level and the d-d level is smaller Hence, the population of the d-d level at room

temperature would be more efficient and therefore emission weaker or (2) deactivating PT and 3BrPT ligand states are involved in the emission process As $[Ru(bpy)_2(3MePT)]^{2+}$ emits at room temperature and low temperature it is evident that the methyl substituent, an electron donating substituent on the triazole ring is required before the species emits at room temperature The $[Ru(bpy)_2(3MePT)]^{2+}$ compound is a weak emitter relative to compounds containing a C-C pyridyltriazole bond For the low temperature studies it was observed, by comparison of concentration with emission intensities, that the emission intensities of the three compounds varied in order of decreasing emission intensity, ($[Ru(bpy)_2(3MePT)]^{2+}$ > $[Ru(bpy)_2(PT)]^{2+}$ > $[Ru(bpy)_2(3BrPT)]^{2+}$)

The three compounds containing the PT type ligands, differ from the other compounds by the nature of the pyridyltriazole bond However, the pyridylpyrazole ligand in $[Ru(bpy)_2(PNP)]^{2+}$, see Table 3 6, contains a carbon nitrogen bond also As this compound emits at room temperature and at low temperature the presence of a C-N bond in the chelating ring cannot be the main reason for absence of emission at room temperature

For all compounds the emission intensities at low temperature are stronger than those at room temperature, because the d-d level is not as thermally accessible as it is at room temperature and hence $K_r$ becomes more pronounced (see Figure 1 1, Chapter 1) A shift to higher energy at 77 K compared to the energy at room temperature is observed for all species Deprotonation of complexes $[Ru(bpy)_2(HPyrtr)]^{2+}$ (isomers 1 and 2) and $[Ru(bpy)_2(H3MePyrtr)]^{2+}$ also has a strong effect on the emission spectra The shift of emission energy to lower energy upon deprotonation of the compounds $[Ru(bpy)_2(HPyrtr)]^{2+}$ and $[Ru(bpy)_2(H3MePyrtr)]^{2+}$ is consistent with the shift to lower energy

in the absorption spectra It is interesting that the compounds $[Ru(bpy)_2(Pyrtr)]^+$ (isomer 1 and 2) and $[Ru(bpy)_2(3MePyrtr)]^+$, containing deprotonated ligands do emit at room temperature This is unusual in the respect that most complexes of the type $[Ru(bpy)_2(L)X]^+$ have a rather weak emission [1]

3 1 5 Conclusion,

From the $^1H$ n m r spectra of these series of compounds containing pyridyltriazole ligands the coordination mode of the ligands to the $Ru(bpy)_2$ moiety were determined However, the analysis of the $^1H$ n m r spectra of the two protonated isomers of $[Ru(bpy)_2(HPyrtr)]^{2+}$ was inconclusive in respect to structural determination The $^1H$ n m r data of the deprotonated isomers along with studies of the electronic, electrochemical and acid-base properties of each isomer lead to the following structures being suggested For isomer 1 coordination to the pyridyl-triazole ligand is via $N^1$ of the pyridine ring and $N^{4'}$ of the triazole ligand For isomer 2 coordination takes place via the $N^1$ of the pyridine ring and $N^{2'}$ of the triazole ring $^1H$ n m r analysis of $[Ru(bpy)_2(3MePyrtr)]^+$ indicated that coordination of the pyridyltriazole ring takes place via the $N^{1'}$ atom, this was confirmed by crystal structure determination

The electronic and electrochemical data presented indicates that the pyridyl-1,2,4-triazoles with the possible exception of PT, 3BrPT and 3MePT are weaker $\pi$-acceptors than bpy The compounds $[Ru(bpy)_2(HPyrtr)]^{2+}$ (isomers 1 and 2), $[Ru(bpy)_2(H3MePyrtr)]^{2+}$, $[Ru(bpy)_2(4MePyrtr)]^{2+}$, $[Ru(bpy)_2(1MePyrtr)]^{2+}$ and $[Ru(bpy)_2(PNP)]^{2+}$ described have similar excited state properties as $[Ru(bpy)_3]^{2+}$ whereas the compounds containing the ligands PT, 3BrPT and 3MePT

are weaker emitters than $[Ru(bpy)_3]^{2+}$ For $[Ru(bpy)_2(PT)]^{2+}$ and $[Ru(bpy)_2(3BrPT)]^{2+}$ no emission was detected at room temperature As the corresponding compound containing pyridylpyrazole (PNP) emits, the presence of a pyridylpyrazole C-N bond cannot be the reason for this behaviour The strong emission observed for the deprotonated compounds, $[Ru(bpy)_2(Pyrtr)]^{+}$ (isomers 1 and 2) and $[Ru(bpy)_2(3MePyrtr)]^{+}$, is unusual as emission observed from ruthenium compounds of the type $[Ru(bpy)_2(L)X]^{+}$ where L is a monodentate ligand and X is a halide or $CN^{-}$ [1] are rather weak

The variation of the absorption and emission properties with the nature of L-L' is small and further investigations are required in order to differentiate between the electronic properties of the ligands

# Chapter 3

## Section 2

## Synthesis of Complexes Containing Monodentate Pyridyltriazole Ligands with a View to Preparing Intermediates formed in Photochemical Reactions

### 3 2 1 Preparation of Complexes of the Type $[Ru(bpy)_2(L\text{-}L')Cl]^+$

As already pointed out in the introduction, the purpose of these investigations is to prepare compounds which can be used as model compounds for intermediates proposed in the photochemical decomposition of ruthenium polypyridyl compounds Attempts have been made to prepare such compounds $[Ru(bpy)_2(L\text{-}L')Cl]^+$, in which L-L' a potentially bidentate ligand acts as a monodentate ligand, using thermal methods The approach was to utilize the well known stability of the compound $[Ru(bpy)_2(S)Cl]^+$ (S = solvent) in solvent mixtures containing little or no water This species is formed as in reaction (4)

$$[Ru(bpy)_2Cl_2] + S \text{ ----> } [Ru(bpy)_2(S)Cl]^+ + Cl^- \qquad (4)$$

This approach has also been used successfully in the preparation of compounds of the type $[Ru(bpy)_2(L)Cl]^+$, where L is a monodentate nitrogen donor such as pyridine or imidazole [1, 59]

Upon reflux in reaction mixtures free of water, reaction (5) will take place, in which the second chloride will remain bound to the metal center

$$[Ru(bpy)_2(S)Cl]^+ + L\text{-}L' \text{ ----> } [Ru(bpy)_2(L\text{-}L')Cl]^+ + S \qquad (5)$$

For the reactions carried out with the ligands PT, 3BrPT, 3MePT and 4MePyrtr, a high yield for the product containing the monodentate ligand may not be obtained as a by-product containing the chelating ligand may also be formed In the presence of water however, the chloride will be removed and is subsequently replaced by the second chelating ring of the pyridyltriazole ligand The bivalent compound containing the chelated ligand is obtained as the product

of reactions (6) and (7)

$$[Ru(bpy)_2(L\text{-}L')Cl]^+ + H_2O \text{ ----}> [Ru(bpy)_2(L\text{-}L')(H_2O)]^{2+} + Cl^- \quad (6)$$

$$[Ru(bpy)_2(L\text{-}L')(H_2O)]^{2+} \text{ ----}> [Ru(bpy)_2(L\text{-}L')]^{2+} + H_2O \quad (7)$$

Reactions of the cis-complex $[Ru(bpy)_2Cl_2]\ 2H_2O$ with equimolar amounts of L-L' in ethanol/water (where L-L' = PT, 3BrPT, or 3MePT) or ethanol/acetone (where L-L' = 4MePyrtr) for short reflux times of up to 30 mins yielded a series of monovalent cations (see reactions (4) and (5))

The reactions were followed by uv/vis spectroscopy and also by HPLC Figure 3 13 shows the progress of the reaction of $[Ru(bpy)_2Cl_2]$ with 4MePyrtr followed by uv/vis spectroscopy while Figure 3 14 shows a sample chromatogram taken two minutes after reflux commenced, with uv/vis spectra corresponding to $[[Ru(bpy)_2(4MePyrtr)Cl]^+$ (peak 1, absorption maximum 500 nm) Other compounds in this chromatogram include $[Ru(bpy)_2Cl_2]$ (peak 2, absorption maximum 530 nm), $[Ru(bpy)_2(CH_3CN)Cl]^+$ (peak 3, absorption maximum 475 nm) and $[Ru(bpy)_2(4MePyrtr)]^{2+}$ (peak 4, absorption maximum 420 nm), taken during the reaction From Figure 3 14, it is observed that the desired monodentate-chloride compound has been formed and also that the compound containing the chelating ligand (peak 4) is rapidly formed In our investigations it was found that, as expected, shorter reflux times did yield smaller amounts of compounds containing the bidentate ligands However, for very short reflux times rather large amounts of the starting material $[Ru(bpy)_2Cl_2]$ were obtained Compounds were purified using column chromatography Pure compounds containing the ligands PT, 3BrPT, 3MePT and 4MePyrtr in a monodentate coordination mode were obtained

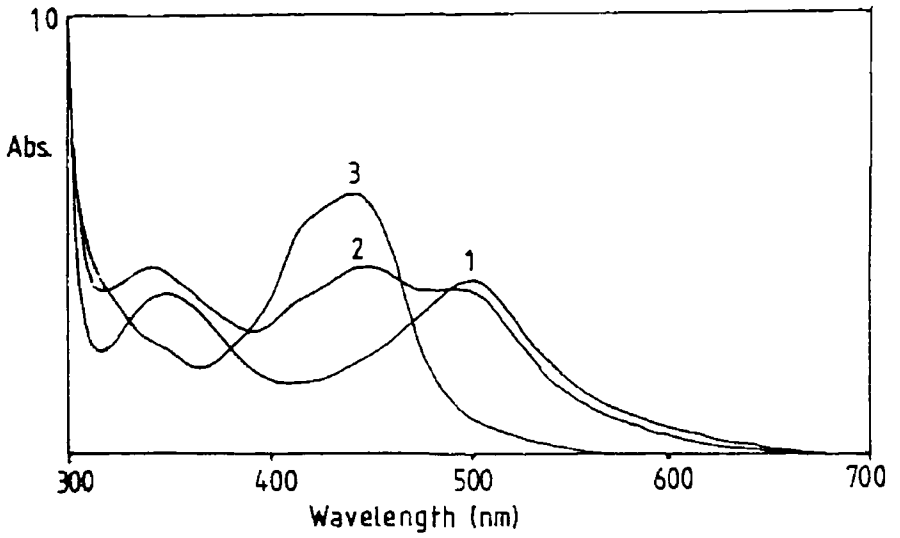


Figure 3 13 Reaction of $[Ru(bpy)_2Cl_2]$ with 4MePyrtr in ethanol acetone (70 30), 1 = at reflux, 2 = 2 min reflux and 3 = 25 min reflux

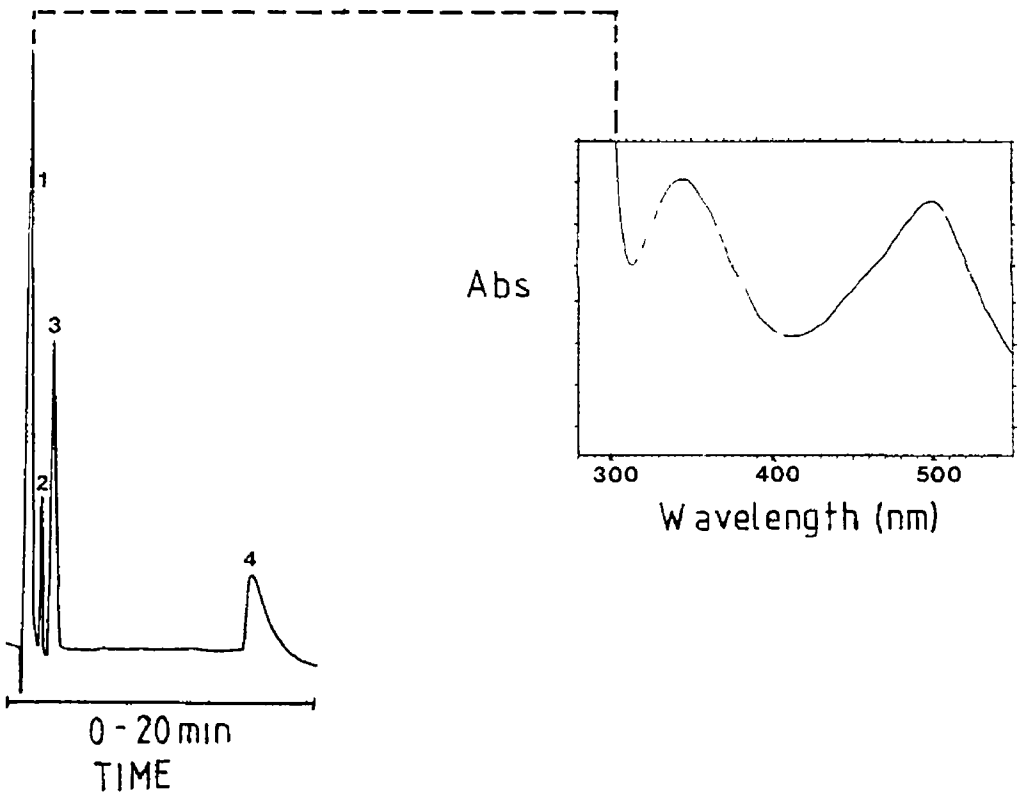


Figure 3 14 Sample chromatogram of the reaction of $[Ru(bpy)_2Cl_2]$ with 4MePyrtr in ethanol acetone (70 30) taken after 2 min reflux Flow rate 3 0 ml/min, detection wavelength 280 nm

Repeated attempts to prepare similar compounds with 1MePyrtr and PNP (see Figure 3 3 for ligand structures) always resulted in the formation of compounds containing the chelating ligands The presence of a methyl group in 1MePyrtr eliminates the possibility of coordination via the $N^{1'}$ nitrogen Monodentate coordination via the 2' nitrogen or the nitrogen on the pyridine ring is expected to result in conversion to the bidentate species Hence, coordination via the 4' nitrogen might be favoured for the ligand 1MePyrtr As monodentate coordination is not obtained for $[Ru(bpy)_2(1MePyrtr)Cl]^+$ then it might be possible that the coordination site for the ligand 4MePyrtr is via the 1' nitrogen

As the two nitrogens in PNP are in close proximity to one another, it is anticipated that the formation of any monodentate species would result in rapid ring closure to form the bivalent compound $[Ru(bpy)_2(PNP)]^{2+}$ As the monovalent species $[Ru(bpy)_2(PNP)Cl]^+$ was not observed it is therefore unlikely that monodentate coordination for L-L' = PT, 3BrPT and 3MePT would take place via the nitrogen on the pyridine ring or the $N^{2'}$ atom on the triazole ring

The results obtained for absorption and emission spectroscopy of the monovalent complexes prepared were ambiguous concerning the "ring" of coordination Proton n m r data for these monovalent complexes is expected to yield more definite information

The compounds obtained have been characterised using $^1H$ n m r spectroscopy to establish the nature of coordination of the L-L' ligands The results of these studies are reported below

3 2 2 $^{1}$H N.m.r spectra of the free Ligands

The resonances for the free ligands, PT, 3MePT, 3BrPT and 4MePyrtr are given in Table 3 7 The atom numbering scheme for the ligands is shown in Figure 3 3

As shown in Section 1 of this Chapter, it is possible to assign the $H^{3'}$ and $H^{5'}$ resonances for the free ligand PT by comparison with the $^{1}$H n m r data for the ligand bptn

Table 3.7 $^{1}$H N m r Resonances of the free ligands (p p m ) Solvent [$(CD_3)_2SO$] (200 MHz)

| Ligand | $CH_3$ | $H^{3'}$ | $H^{5'}$ | $H^3$ | $H^4$ | $H^5$ | $H^6$ |
|---|---|---|---|---|---|---|---|
| 4MePyrtr | 3 99 | - | 8 62 | 8 11 | 7 95 | 7 47 | 8 66 |
| PT | - | 8 30 | 9 37 | 7 86 | 8 06 | 7 47 | 8 53 |
| 3BrPT | - | - | 9 21 | 7 90 | 8 16 | 7 55 | 8 54 |
| 3MePT | 2 21 | - | 8 89 | 7 21 | 7 67 | 7 83 | 8 29 |
| bpy | - | - | - | 8 54 | 7 98 | 7 46 | 8 78 |

The resonance of the $H^{3'}$ proton of PT is found at higher field than the resonance of the $H^{5'}$ proton due to shielding effects of the pyridine ligand The proton n m r spectra of the ligands 3BrPT and 3MePT contain only one singlet The singlets for 3BrPT and 3MePT are found at 9 21 and 8 89 p p m respectively, at very similar values to that of the $H^{5'}$ proton of PT Therefore, it was concluded that the proton singlets of 3BrPT and 3MePT can be attributed to the presence of a $H^{5'}$ proton in the triazole ring This indicates that the bromo and methyl substituents are bound to the triazole ring via the 3' carbon atom as shown in Figure 3 3 The position of the methyl substituent on the triazole ring has been confirmed by the crystal structure of [$Ru(bpy)_2(3MePT)Cl](PF_6)$, which will be discussed later

on in the text

For the free ligands, the position of the $H^{5'}$ singlet of the triazole ring is affected by the nature of the methyl and bromo substituents In comparison with the $H^{5'}$ proton of the ligand PT, the presence of a bromo- group on the $H^{3'}$ position causes a slight shift upfield by 0 16 p p m whereas, the presence of a methyl group shifts the resonance upfield by 0 48 p p m The proton n m r data for 4MePyrtr show the $H^{5'}$ singlet at 8 62 p p m , and the methyl singlet at 3 99 p p m

### 3 2 3 $^{1}$H N m.r. Spectra of the Monodentate Coordinated Ligands.

The coordination mode of the monodentate coordinated ligands is by no means easily established As there are three nitrogens available for coordination, that is, one from the pyridine ring and two from the triazole ring, three different coordination isomers can be expected for the ligands 4MePyrtr, PT, 3BrPT and 3MePT The $^{1}$H n m r spectra of all monovalent species suggest the presence of one isomer only The proton n m r spectra confirm cis geometry for all monovalent complexes [32, 33, 60], and the $^{1}$H n m r data for the monovalent and bivalent complexes containing the ligands 4MePyrtr, PT, 3BrPT and 3MePT are listed in Table 3 8

The correlation-spectroscopy (COSY) n m r of $[Ru(bpy)_2(PT)Cl]^+$ (10 15 - 7 21 p p m ) in Figure 3 15 represents a typical n m r for the monovalent species studied The pyridyltriazole protons have been assigned as shown in Figure 3 15 The $H^{5'}$ and $H^{3'}$ singlets are assigned at 9 62 and 8 02 respectively, as no other coupling to these signals is observed

Table 3 8 Correlation spectroscopy data for monovalent and bivalent complexes containing the ligands 4MePyrtr, PT, 3BrPT and 3NePT (Solvent acetone -$d_6$, 300 MHz) (ppm)

| Compound | | Pyridine-triazole ligand | | | | | | Bipyridine ligands | | | |
|---|---|---|---|---|---|---|---|---|---|---|---|
| | | $H^{5'}$ | $H^{3'}$ | $H^3$ | $H^4$ | $H^5$ | $H^6$ | $H^3$ | $H^4$ | $H^5$ | $H^6$ |
| $[Ru(bpy)_2(4MePyrtr)Cl]^+$ | (11) | 4 39[a] | 9 20 | 8 83 | 8 09 | 7 31 | 10 05 | 8 52-8 86 | 8 03-8 28 | 7 45-7 68 | 7 79-8 01 |
| $[Ru(bpy)_2(PT)Cl]^+$ | (12) | 9 62 | 8 02 | 8 66 | 8 15 | 8 03 | 10 03 | 8 48-8 66 | 7 48-8 15 | 7 27-7 66 | 7 80-8 69 |
| $[Ru(bpy)_2(3BrPT)Cl]^+$ | (13) | 10 36 | - | 8 60 | 8 17 | 7 90 | 10 06 | 8 48-9 10 | 7 81-7 98 | 7 25-7 80 | 7 80-8 26 |
| $[Ru(bpy)_2(3MePT)Cl]^+$ | (14) | 9 07 | 1 20[b] | 8 66 | 8 18 | 7 90 | 10 12 | 8 58-8 73 | 7 92-8 18 | 7 28-7 70 | 7 78-8 90 |
| $[Ru(bpy)_2(4MePyrtr)]^{2+}$ | (5) | 4 19[a] | 8 88 | 8 43 | 8 09 | 7 44 | 7 65 | 8 72-8 85 | 8 12-8 20 | 7 51-7 58 | 7 76-7 83 |
| $[Ru(bpy)_2(PT)]^{2+}$ | (7) | 10 19 | 8 35 | 8 57 | 8 18 | 7 47 | 7 67 | 8 78-8 82 | 8 17-8 19 | 7 47-7 89 | 7 69-8 08 |
| $[Ru(bpy)_2(3BrPT)]^{2+}$ | (8) | 10 18 | - | 8 52 | 8 31 | 7 48 | 7 71 | 8 77-8 86 | 8 09-8 34 | 7 50-7 63 | 7 65-8 09 |
| $[Ru(bpy)_2(3MePT)]^{2+}$ | (9) | 10 05 | 1 81[b] | 8 62 | 8 31 | 7 51 | 7 79 | 8 85-8 89 | 8 20-8 38 | 7 57-7 66 | 7 90-8 24 |

a $CH_3$ group on the 4' Nitrogen on the triazole ring

b $CH_3$ group on 5' carbon on the triazole ring

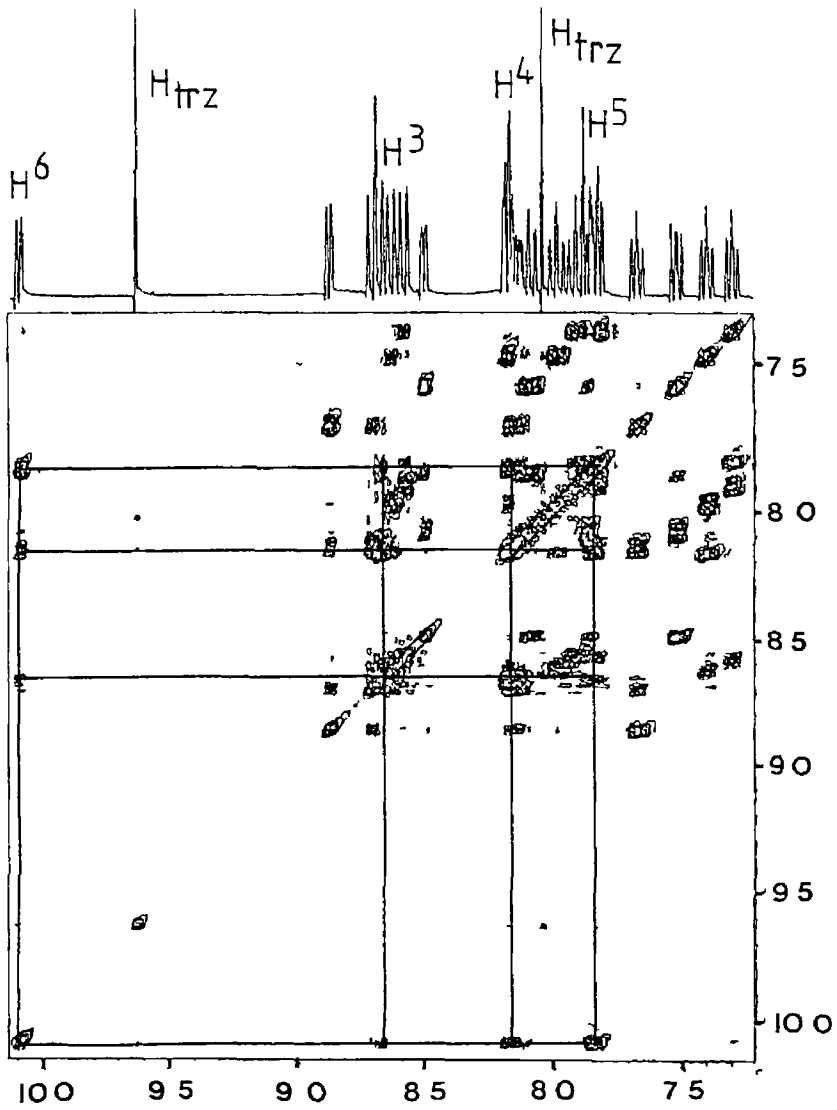


Figure 3 15 The correlation two -dimensional n m r spectrum of $[Ru(bpy)_2(PT)Cl]^+$ from 7 21 to 10 15 p p m , in $[(CD_3)_2SO]$ (300 MHz)

The n m r spectra of complexes of the type $[Ru(bpy)_2(L\text{-}L')Cl]^+$ where L-L' = PT, 3BrPT, 3MePT and 4MePyrtr are currently under investigation

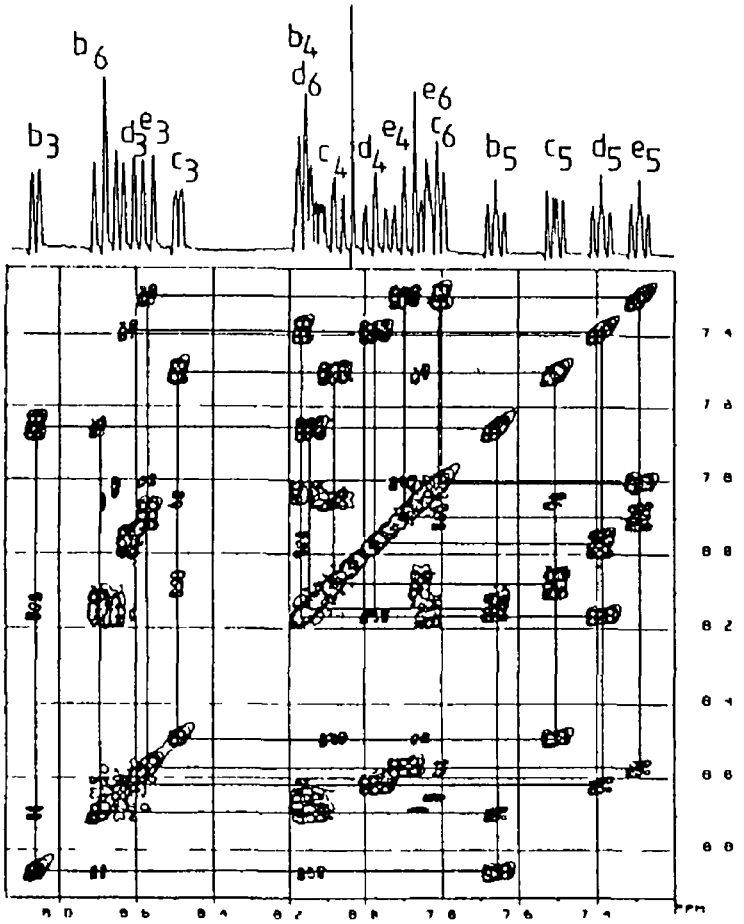


Figure 3 16 The correlation two-dimensional n m r spectra of $[Ru(bpy)_2(PT)Cl]^+$, 7 20 to 8 90 p p m in $[(CD_3)_2SO]$, (300 MHz)

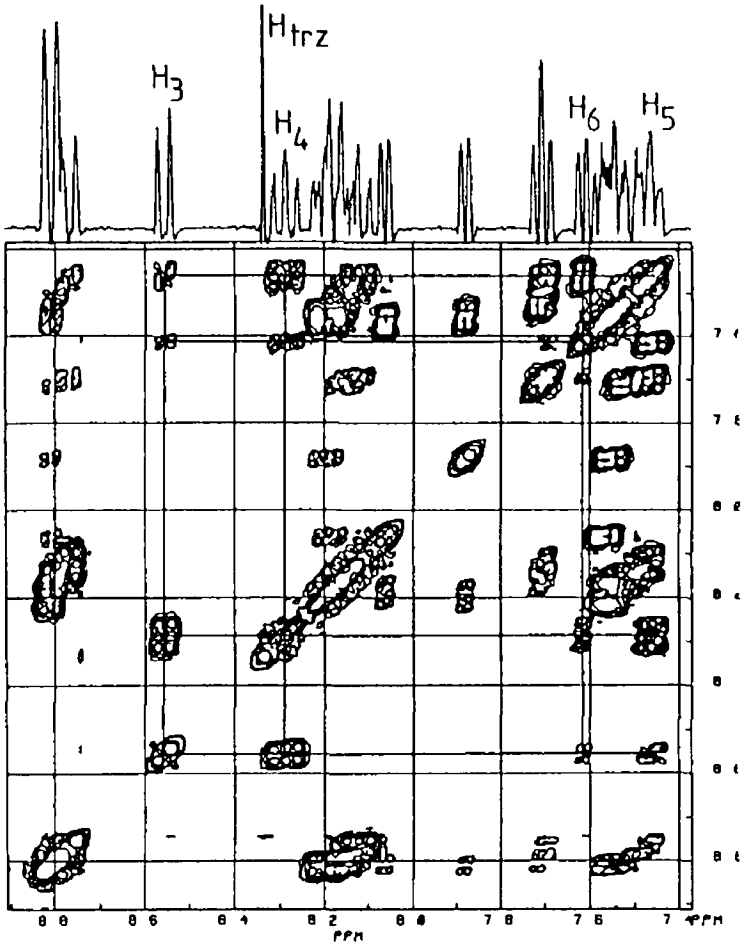


Figure 3 17 The correlation two-dimensional n m r spectra of $[Ru(bpy)_2(PT)]^{2+}$, 7 38 to 8 91 p p m in $[(CD_3)_2SO]$, (300 MHz)

Figure 3 16 shows an expansion of the COSY spectra of $[Ru(bpy)_2(PT)Cl]^+$ in the region 7 20 to 8 87 p p m , and Figure 3 17 shows the COSY n m r of $[Ru(bpy)_2(PT)]^{2+}$

One of the first noticeable features about the $^1H$ n m r data in Table 3 8 is that the $H^6$ doublets of the monovalent complexes appear at significantly lower field (in region 10 03 - 10 12 p p m ) than the $H^6$ doublets of the corresponding bidentate species (in the region 7 44 - 7 53 p p m ) A smaller shift downfield of the $H^3$ doublet of the pyridine rings is also observed This data is a clear indication that the pyridine rings of the pyridyltriazole ligand for the monovalent complexes are not in the same environment as those of the corresponding bivalent cations As the pyridine ring of the latter is bound to the metal center it is therefore likely that the large shift in the $H^6$ protons in the monodentate coordination of L-L' is due to the fact that coordination is via the triazole ring A probable explanation for this large shift downfield is that the $H^6$ proton of the rotating pyridine ring is not rigidly located above the plane of an aromatic ring and hence resonates at lower frequency than the $H^6$ protons observed in $[Ru(bpy)_3]^{2+}$ [61, 62] The x-ray crystal structure of $[Ru(bpy)_2(3MePT)Cl]^+$ shows that the plane of the pyridine ring of the pyridyltriazole ligand lies at an angle of 12 5° to the plane of the triazole ring (vide infra) At the same time, if this is true, then the positions in the n m r spectra of any protons present on the triazole ring should be quite similar to those in the analogous bivalent species, and the positions of the pyridine ring protons should be quite different to those in the analogous bivalent complex

The $H^{3'}$ and $H^{5'}$ protons of the triazole ring of the monovalent complex $[Ru(bpy)_2(PT)Cl]^+$ are both shifted upon coordination The $H^{5'}$ proton has shifted downfield by 0 25

p p m in comparison with the free ligand, while the $H^{3'}$ proton has shifted upfield by approximately the same amount The upfield shift of $H^{3'}$ is due to the magnetic anisotropic effect of a pyridine ring of a bpy ligand [63] For bidentate coordination of this ligand the $H^{5'}$ proton experiences a large shift downfield of 0 82 p p m , while the $H^{3'}$ proton experiences a smaller one 0 05 p p m

The $H^{5'}$ protons of the ligands 3MePT, 3BrPT and 4MePyrtr all appear at lower field upon monodentate coordination with respect to the resonances of the free ligands Coordination of the 3MePT ligand to ruthenium, either in bidentate or monodentate form results in a shift upfield of the methyl resonance Coordination of the 4MePyrtr ligand, on the other hand, results in a shift downfield of the methyl resonance The methyl group shift for the monovalent complex is further downfield than that for the bivalent complex As there are so many effects which determine the position of the proton resonances on the triazole ring, it is difficult to unambiguously decide what factors are causing the varying shifts in the triazole ring For example, the effects include, the inductive effects of the bromine substituent on the triazole ring, the presence of a chlorine atom bound to ruthenium, the magnetic anisotropic effect which includes the relative orientation of the bound ligand, and Van Der Waals interaction Thus, since several effects are operative, it is difficult to quantify relative shifts of the 3'and 4' methyl protons of the triazole rings The orientation of the ligand is particularly important when analysing the monovalent spectra, as the ligand is not as rigid as it is when it is acting as a chelating ligand

Figure 3 16 represents the COSY n m r of $[Ru(bpy)_2(PT)Cl]^+$ in the region 7 2 - 8 87 p p m From this expansion it is possible to assign every proton of the bipyridine ligands

As can be seen from Figure 3 18 all bipyridyl protons are in different environments so sixteen different signals are observed The assignments made are shown in Table 3 9

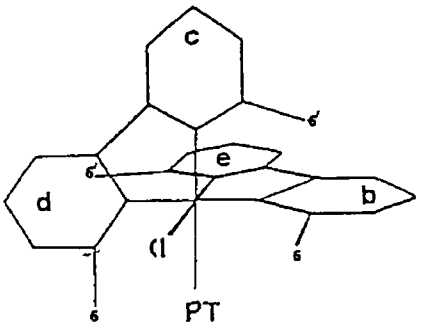


Figure 3 18 Representation of a bis-bipyridyl octrahedral complex

Now as can be seen from Figure 3 18 the $H^{6'}$ protons lie above a pyridine ring of the adjacent ligand while the $H^{6}$ protons do not, it should be possible to distinguish which $H^{6}$ proton lies above the chlorine atom and which lies over the triazole ring These two $H^{6'}$ protons will be shielded in comparison to the $H^{6}$ protons and hence the two doublets are observed at higher field than the other protons The $^{1}H$ n m r data for the pyridine rings of $[Ru(bpy)_2(PT)Cl]^{+}$ are presented in Table 3 9

Table 3 9 COSY n m r data for the $Ru(bpy)_2$ - moiety in the complex $[Ru(bpy)_2(PT)Cl]^{+}$ (p p m )

| | $H^3$ | $H^4$ | $H^5$ | $H^6$ |
|---|---|---|---|---|
| Ring b | 8 86 | 8 15 | 7 66 | 8 69 |
| Ring c | 8 48 | 8 08 | 7 51 | 8 03 |
| Ring d | 8 64 | 7 96 | 7 39 | 8 15 |
| Ring e | 8 50 | 7 84 | 7 29 | 7 80 |

The $H^6$ proton which appears furthest downfield will be that which is under the influence of the inductive effect of the chlorine atom, this is attributed to ring b [60, 62] This doublet appears at 8 69 p p m , in comparison to the $H^6$ doublet of $[Ru(bpy)_3]^{2+}$ which is found at 8 07 p p m In order to determine the pyridine ring which ring b is attached to, it is necessary to compare the $H^6$ proton resonances with the n m r spectrum of $[Ru(bpy)_2Cl_2]$ [60] In this spectrum, the signal at 7 80 p p m has been assigned to the $H^6$ proton of a pyridine ring (ring e), which is attached to the pyridine ring that lies over the chlorine atom (ring b) Hence, ring b and e must constitute one bipyridyl group while ring c and d the other, see Figure 3 18 As the resonance of the $H^6$ proton of ring c is found at a similar value to that of the $H^6$ protons in $[Ru(bpy)_3]^{2+}$ [63], it was concluded that this ring lies over the pyridine ring of the pyridyltriazole ligand This indicates that the $H^6$ proton on ring d lies over the triazole ring of the pyridyltriazole ligand From these results, it is concluded that COSY techniques are very useful as it has allowed the assignment of all the protons in the molecule

For the complex, $[Ru(bpy)_2(PT)]^{2+}$, the assignments for the pyridyltriazole are shown in Figure 3 17 One of the singlet proton resonances, at 10 03 p p m , of the triazole ring does not appear on this diagram As coordination of the monodentate ligands takes place via the triazole ring, a closer look at the n m r spectra may yield more information on the site of coordination on the triazole ring In comparison with Figure 3 16, the obvious difference, as discussed before, is the position of the pyridine ring $H^6$ protons Those of the monodentate species occur at much lower field than those of the bidentate species, the difference being 2 36 p p m, the difference between the $H^5$ protons is 0 56 p p m , the $H^4$ protons is

0 05 p p m and lastly, the $H^3$ protons 0 09 p p m This suggests that monodentate coordination takes place at 4' nitrogen on the triazole ring If coordination was via the 2' nitrogen then such a large shift in the $H^6$ proton resonance would not be expected This shift of the $H^6$ protons to lower field indicates that the proton is not in the vicinity of any other ligands

From Figure 3 17 it is not possible to unambiguously assign all the protons of the bipyridyl ligands As the $H^6$ protons are sensitive to the nature of the ligand L-L', all of them exist in sufficiently different environments The frequencies for the $H^6$ protons are listed in Table 3 10 The $H^3$, $H^4$, and $H^5$ protons signals overlap with the proton signals in the same positions of other rings

Table 3.10 $^1H$ N m r resonances for the $H^6$ Protons of $[Ru(bpy)_2(PT)]^{2+}$ (p p m )

| | B | C | D | E |
|---|---|---|---|---|
| $H_6$ | 7 69 | 7 89 | 7 72 | 8 08 |

Assignments of the rings is more complicated than for the monodentate complex due to the absence of the chlorine atom These $H^6$ protons cannot be unambiguously assigned to a particular pyridine ring as the resonance values are too similar

Similar $^1H$ n m r behaviour is observed for the other two substituted ligands 3MePT and 3BrPT For the mono and bivalent cations containing the ligand 3MePT the shift in the $CH_3$ resonance is from 1 20 to 1 81 p p m i e 0 61 p p m downfield, and the shift of the $H^{5'}$ singlet is from 9 07 to 10 05, i e 0 98 p p m downfield As the shifts here are large, the coordination site for the monodentate

species must be close to the methyl group and the 5' proton on the triazole ring From this evidence, it is likely that monodentate coordination takes place via the 4' nitrogen on the triazole ring If coordination takes place via the 2' nitrogen, then such large shifts in the resonances of the $CH_3$ and $H^{5'}$ would not be expected Coordination via the 4' nitrogen on the triazole is confirmed by the x-ray crystal structure of $[Ru(bpy)_2(3MePT)Cl](PF_6)$ which will be discussed at a later stage

From the $^1H$ n m r data of $[Ru(bpy)_2(3BrPT)Cl]^+$ the $H^6$ doublet of the pyridyltriazole ligand has shifted from 7 48 in the chelating mode to 10 06 p p m This is accompanied by a shift downfield of the $H^{5'}$ proton of the triazole ring from 10 18 to 10 39 p p m For the ligands PT and 3MePT, a shift in the opposite direction is observed for the $H^{5'}$ proton A possible explanation for this behaviour may be that the inductive effect of the bromine substituent will cause the $H^{5'}$ proton to resonate at lower field [60]

The compounds $[Ru(bpy)_2(4MePyrtr)Cl]^+$ and $[Ru(bpy)_2(4MePyrtr)]^{2+}$ exhibit similar behaviour as the other three ligands Monodentate coordination is anticipated to be via the 1' nitrogen as there is a shift in the $H^{5'}$ proton resonance of 0 32 p p m , and a smaller shift in the methyl resonance 0 20 p p m , in comparison to the bidentate analogue In comparison with the free ligand, where the $H^{5'}$ proton is at 8 62 p p m , monodentate coordination is accompanied by a large shift downfield to 9 20 p p m while bidentate coordination causes a downfield shift to 8 88 p p m A large shift downfield to 10 05 p p m of the $H^6$ protons of the pyridine ring of 4MePyrtr is observed This is similar behaviour to that observed for the pyridine rings in PT, 3BrPT and 3MePT upon monodentate coordination and suggests that coordination of

the triazole ring to ruthenium is via $N^{1'}$ It is anticipated the if coordination is via $N^{2'}$ then this shift would not be as large As the inductive effect of ruthenium deshields ring protons and the $H^{5'}$ proton of the monovalent complex has a large shift downfield compared to that of the bivalent complex, it suggests that coordination of ruthenium to the triazole is closer to the 5' carbon Therefore monodentate coordination may take place via the 1' nitrogen atom

In conclusion, from the $^{1}H$ n m r evidence the pyridyltriazole ligands containing a carbon-nitrogen linking bond are likely to be coordinated via the $N^{4'}$ atom for the monodentate complex and the ligand 4MePyrtr is likely to be coordinated at the $N^{1'}$ atom These are interesting results, as it means that conversion from the monovalent complex to the bivalent complex involves loss of monodentate ligand, reorientation of the ligand in solution and subsequent coordination via the nitrogen of the pyridine ring and the $N^{2'}$ atom of the triazole ring One would expect monodentate coordination to be either via the nitrogen of the pyridine ring or 2' nitrogen of the triazole ring, and subsequent bidentate coordination as a result of the ligand swinging around to form the coordination bond

### 3 2 4 Crystal Structure of Bis(2,2'-bipyridine)chloro ruthenium-3-Methyl-1-(pyridin-2-yl)-1,2,4-triazole Hexafluorophosphate,

The structure of the cation in $[Ru(bpy)_2(3MePT)Cl](PF_6)$ is illustrated in Figure 3 19 A summary of the crystal data and collection intensities is presented in Table 3 11 The relevant bond lengths and angles are listed in Table 3 12

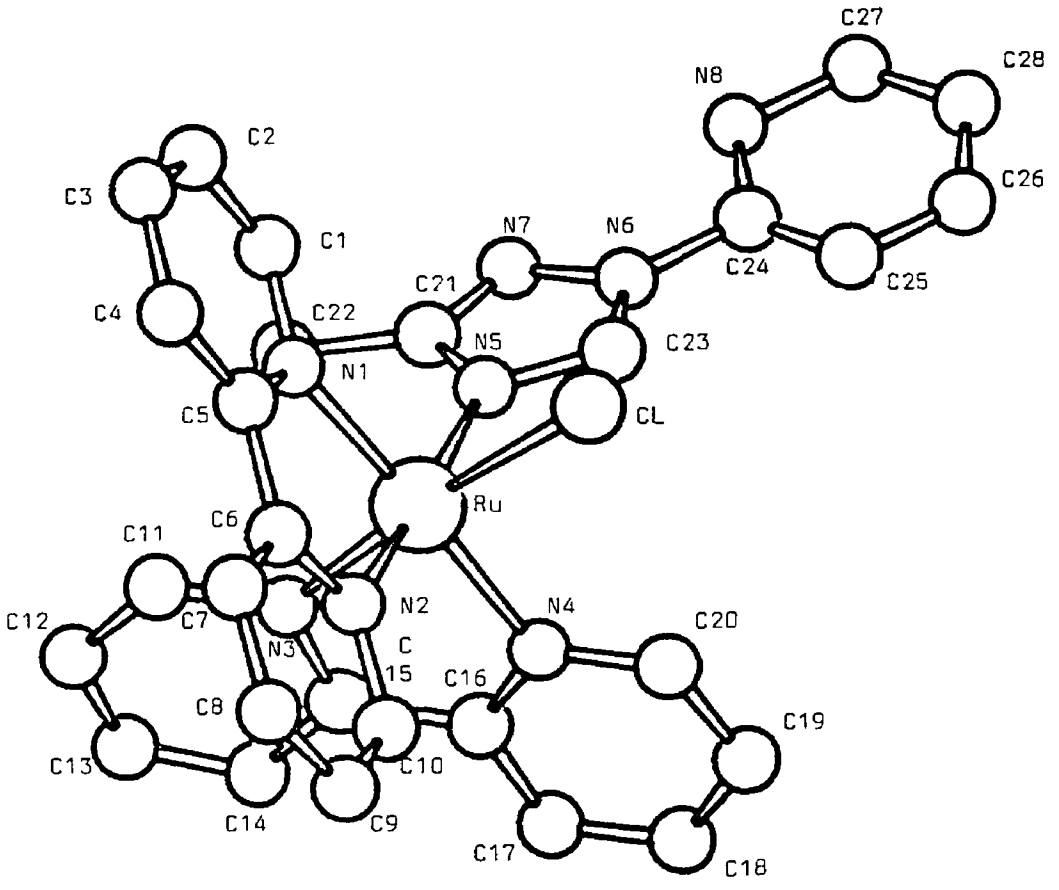


Figure 3 19 X-Ray crystal structure of the $[Ru(bpy)_2(3MePT)Cl]^+$ cation, showing the atom labelling

Table 3 11 Summary of Crystal Data and Collection Intensities of Bis(2,2'-bipyridine)chloro-ruthenium-3-methyl-1-(pyridin-2-yl)-1,2,4-triazole Hexafluorophosphate

| | |
|---|---|
| Formula | $RuC_{28}H_{24}N_8ClPF_6$ |
| Cell Type | Triclinic |
| Space Group | P |
| $M_r$ | 753.75 |
| $\alpha$ | 89 88° |
| $\beta$ | 117 22° |
| $\gamma$ | 111 08° |
| a, Å | 8.599(12) |
| b, Å | 13.503(16) |
| c, Å | 16.526(16) |
| V, $Å^3$ | 1561 37 |
| Dobs, (by flotation), Mg m-3 | 1.66 |
| Dcalc, Mg m-3 | 1.60 |
| $\mu$(MoK$\alpha$), cm-1 | 0.71069 Å |
| Data collection Range | h, 0 to 11: k,-17 to 17 |
| | l, -21 to 21 |
| $\theta$ range (o) | 0 - 50 |
| No. of Indep. Reflections | 4465 |
| No of Single Reflections | 3648 or 2252 |
| Fooo | 755.99 |
| R | 0.0750 |
| $R_w$ | 0.0750 |

Table 3 12

Selected Bond Distances (A) and angles (°) of cis-(5-Methyl-(1-pyridin2-yl)-1,2,4-triazole)bis(2,2-bipyridine)-chloro-ruthenium hexaflouorphosphate

Bond Distances.

| | |
|---|---|
| Ru - N(1) | 2 061(8) |
| Ru - N(2) | 2 029(8) |
| Ru - N(3) | 2 008(11) |
| Ru - N(4) | 2 057(8) |
| Ru - N(5) | 2 136(8) |
| Ru - C1 | 2 410(4) |

Pyridyltriazole ring

| | |
|---|---|
| N(5) - C(21) | 1 360(24) |
| N(5) - C(23) | 1 343(23) |
| C(21) - C(22) | 1 652(22) |
| C(21) - N(7) | 1 313(20) |
| C(23) - N(6) | 1 346(19) |
| N(6) - N(7) | 1 356(24) |
| N(6) - C(24) | 1 450(15) |
| C(24) - C(25) | 1 264(13) |
| C(24) - N(8) | 1 400(10) |
| C(25) - C(26) | 1 351(11) |
| C(26) - C(28) | 1 405(10) |
| C(27) - C(28) | 1 342(13) |
| C(27) - N(8) | 1 425(11) |

Bond Angles (A)

| | |
|---|---|
| N(1) - Ru - C1 | 86 6(3) |
| N(2) - Ru - C1 | 88 7(3) |
| N(3) - Ru - C1 | 173 7(3) |

| | | |
|---|---|---|
| N(4) - Ru - Cl | 94 | 8(2) |
| N(5) - Ru - Cl | 88 | 6(3) |
| N(1) - Ru - N(2) | 78 | 7(4) |
| N(1) - Ru - N(3) | 99 | 8(4) |
| N(1) - Ru - N(4) | 177 | 4(4) |
| N(1) - Ru - N(5) | 97 | 2(3) |
| N(2) - Ru - N(3) | 89 | 2(4) |
| N(2) - Ru - N(4) | 98 | 7(4) |
| N(2) - Ru - N(5) | 173 | 4(4) |
| N(3) - Ru - N(4) | 79 | 7(4) |
| N(3) - Ru - N(5) | 93 | 9(4) |
| N(4) - Ru - N(5) | 85 | 3(4) |

Pyridyltriazole ligand

| | | |
|---|---|---|
| C(21) - N(5) - Ru | 135 | 2(8) |
| C(23) - N(5) - Ru | 119 | 9(7) |
| C(21) - N(5) - C(23) | 104 | 8(9) |
| C(22) - C(21) - N(5) | 122 | 5(10) |
| C(22) - C(21) - N(7) | 124 | 1(11) |
| N(5) - C(21) - N(7) | 113 | 4(11) |
| C(21) - N(7) - N(6) | 103 | 3(9) |
| N(5) - C(23) - N(6) | 107 | 3(9) |
| C(23) - N(6) - N(7) | 111 | 2(9) |
| C(23) - N(6) - C(24) | 125 | 0(9) |
| N(7) - N(6) - C(24) | 123 | 7(9) |
| N(6) - C(24) - C(25) | 115 | 4(11) |
| N(6) - C(24) - N(8) | 115 | 8(11) |
| C(25) - C(24) - N(8) | 128 | 7(13) |
| C(24) - N(8) - C(27) | 113 | 4(13) |
| N(8) - C(27) - C(28) | 119 | 6(15) |
| C(27) - C(28) - C(26) | 119 | 9(15) |
| C(28) - C(26) - C(25) | 121 | 5(15) |
| C(26) - C(25) - C(24) | 116 | 5(14) |

The ruthenium atom is coordinated by two bipyridine molecules, one pyridyltriazole and one chlorine atom As can be seen from the structure in Figure 3 19 the site of coordination of the pyridyltriazole ligand is via the $N^{4'}$ atom of the triazole ring This is in agreement with the interpretation of the COSY n m r data The ruthenium - nitrogen bond distances of the bipyridyl ligands range from 2 03 to 2 06 Å, *avδ* agree well with the values obtained by Rillema et al for $[Ru(bpy)_3]^{2+}$ [55] The Ru-($N^5$) bond is rather long at 2 14 Å The Ru-N(triazole) bond length in the complex $[Ru(bpy)_2(3MePyrtr)]^+$ (see Section 3 13), where the pyridyltriazole ligand is coordinated via both the pyridine and the triazole ring is much shorter at 2 050 Å This increase in bond length may be attributed to the weak $\pi$ acceptor properties of the pyridyltriazole ligand The pyridyltriazole coordinated in a monodentate fashion is a weaker $\pi$ acceptor than that coordinated in a bidentate fashion and hence has a longer bond The Ru-N(trz) bond length in $[Ru(bpy)_2(bpt)]^+$ is 2 03 Å [52], considerably shorter than our value of 2 14 Å, again indicating that the chelating ligands are better $\pi$ acceptor ligands than the monodentate coordinated ligands

The bond length of the Ru-Cl bond, 2 41 Å, is similar to the bond distance of 2 43 Å obtained by Eggleston et al for $[Ru(bpy)_2Cl_2]$ [53]

The bite angles of the two bipyridine ligands are 78 7° and 79 6° which is in agreement with other bipyridine compounds [52, 55] The bond angles between the pyridine ring and the triazole ring of 3MePT, i e N(7)-N(6)-C(24) and N(6)-C(24)-N(8) are 123 and 115° respectively compared to the same pyridyltriazole angles of 122 and 117° obtained for the free pyridine ring and the coordinated triazole ring of $bpt^-$ in $[Ru(bpy)_2(bpt)]^+$ [52] The bond lengths and bond angles of the triazole ring are in good agreement

with those obtained in reference [64]

In the crystalline state, the plane of the pyridine ring in the pyridyltriazole ligand lies at an angle of 12 5° to the plane of the triazole ligand

3 2 5 Electronic Spectra and Redox Properties.

The electronic and electrochemical properties of the $[Ru(bpy)_2(L\text{-}L')Cl]^+$ complexes are listed in Table 3 13 As in similar Ru(II) compounds, the lowest energy absorption band has been assigned to $d\pi(Ru) \dashrightarrow \pi^*$ (ligand) transition [65] In comparison with $[Ru(bpy)_3]^{2+}$ the compounds containing monodentate ligands absorb at lower energy, but they absorb at higher energy than the neutral species $[Ru(bpy)_2Cl_2]\ 2H_2O$ [66, 67] This suggests that the energy of the absorption maximum decreases as the number of chlorine atoms coordinated to ruthenium increases This suggests that the $\pi$ donor ability of the chlorine ligand lowers the energy of the MLCT excited states by increasing the negative charge on the metal

In comparison with the lowest energy absorption maxima for the bivalent compounds containing the chelating ligands 4MePyrtr, PT, 3BrPT and 3MePT (Table 3 6), the absorption maxima for the compounds containing the monodentate ligands are found at much lower energy, see Table 3 13 The presence of the chlorine atom, along with the pyridyl-triazole coordinated in a monodentate mode stabilize the $d\pi$ orbitals of Ru(II) resulting in lower energy absorption maxima The ligand L-L' in its monodentate coordination form is not as good a $\pi$ acceptor as in its bidentate coordination form This is as expected as in the complexes $[Ru(bpy)_2(L\text{-}L')]^{2+}$, it is easier for the charge from the metal to delocalise over the chelating ligand

Table 3 13 Electronic and Electrochemical Data for Complexes $[Ru(bpy)_2(L\text{-}L')Cl]^+$

| Compound | Absorption[A] | Emission (nm)[B] | | Redox Potentials[C] | | |
|---|---|---|---|---|---|---|
| | $\lambda$ max(log$\epsilon$) | $\lambda$Max 300K | $\lambda$Max 77K | $Ru^{3+/2+}$ | Ligand Based | |
| $[Ru(bpy)_2(4MePyrtr)Cl]^+$ (11) | 508(3 96) | 710 | 655 | 0 66[E] | -1 34 | |
| $[Ru(bpy)_2(PT)Cl]^+$ (12) | 500(3 97) | 710 | 653 | 0 78 | -1 53 | |
| $[Ru(bpy)_2(3MePT)Cl]^+$ (13) | 502(3 97) | 680 | 658 | 0 79 | -1 45 | -1 57 |
| $[Ru(bpy)_2(3BrPT)Cl]^+$ (14) | 488(3 96) | - | 655 | 0 86 | -1 45 | -1 55 |
| $[Ru(bpy)_2Cl_2]$ [1] | 553(3 95)[D] | - | 705[D] | 0 32 | -1 67 | |
| $[Ru(bpy)_3]^{2+}$ [1] | 452(4 11) | 608 | 582 | 1 22 | -1 36 | -1 53 |

[A] measured in $CH_3CN$, max in (nm), E in $dm^3\ mol^{-1}\ cm^{-1}$

[B] Spectra at room temperature were measured in $CH_3CN$ at 77K in Ethanol [C] measured in $CH_3CN$ with 0 1M TEAP volts vs S C E, n h e = S C E + 0 2415V [D] measured in DMF

[E] measured in methanol/ethanol

From Figure 3 20 and Table 3 13 it is observed that little difference exists between the absorption and low temperature emission maxima for the compounds $[Ru(bpy)_2(4MePyrtr)Cl]^+$, $[Ru(bpy)_2(PT)Cl]^+$ and $[Ru(bpy)_2(3MePyrtr)Cl]^+$ The monovalent compound containing the 3BrPT ligand however, absorbs at slightly higher energy

By comparison with similar compounds containing ligands coordinated in a monodentate mode and a chlorine atom, the ring of coordination of our compounds may by deduced The $^1H$ n m r spectra of our compounds suggest that coordination takes place via the triazole ring The compound $[Ru(bpy)_2(Phtrz)Cl]^+$ where Phtrz = phenyl-triazole, coordinated to ruthenium via the triazole ring, has its absorption maximum in acetonitrile at 495 nm [68] The absorption maximum of the imidazole compound $[Ru(bpy)_2(mim)Cl]^+$ where mim = N-methyl-imidazole is at 512 nm in acetonitrile [69] Compounds where coordination occurs via the pyridine ring include $[Ru(bpy)_2(4,4'-bpy)Cl]^+$, $[Ru(bpy)_2(py)Cl]^+$ and $[Ru(bpy)_2(4vpy)Cl]^+$ where 4,4'-bpy = 4,4'-bipyridine, py = pyridine and 4vpy = 4-vinylpyridine The absorption maxima of these compounds are found at 490 nm in acetonitrile [70], 505 nm in dichloromethane [71] and 500 nm in acetonitrile [68] respectively As can be seen from these results quite a difference exists between the absorption maxima of the compounds containing the ligands 4,4'-bpy, py and 4vpy, where coordinated to ruthenium occurs via a pyridine ring A difference of only 17 nm exists between the compounds containing Phtrz and mim This indicates that the ring of coordination cannot be distinguished by the uv/vis spectra Therefore, no conclusive evidence concerning the ring of coordination of our pyridyltriazoles to ruthenium was obtained from the uv/vis spectra

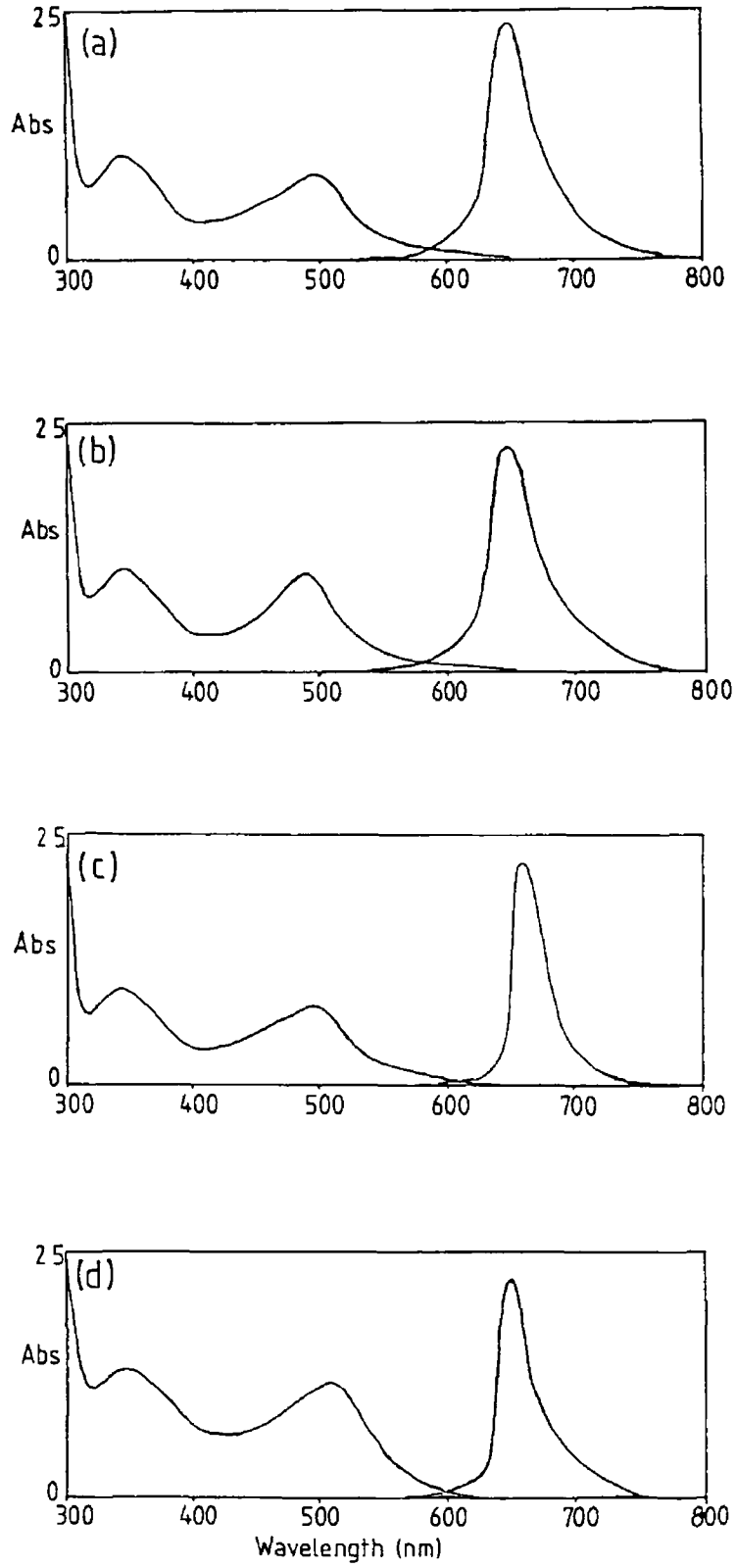


Figure 3 20 Absorption spectra in acetonitrile and low temperature emission spectra in ethanol of complexes of the type $[Ru(bpy)_2(L\text{-}L')Cl]^+$ where L-L' = (a) PT, (b) 3BrPT, (c) 3MePT and (d) 4MePyrtr

The presence of electron-donating methyl and electron-withdrawing bromine have no prominent effects on the absorption and emission properties of the complexes, however some differences do exist The compound $[Ru(bpy)_2(3BrPT)Cl]^+$ absorbs at slightly higher energy than the other monodentate compounds Neither $[Ru(bpy)_2(3BrPT)Cl]^+$ nor the bivalent compounds $[Ru(bpy)_2(3BrPT)]^{2+}$ and $[Ru(bpy)_2(PT)]^{2+}$ emit at room temperature This absence of emission may explained by the fact that more efficient population of the d-d level is possible at room temperature than at low temperature, or that deactivating 3BrPT or PT states are involved in the emission process The complexes containing the methyl substituted ligands are the stronger emitters, determined from a concentration point of view The compound $[Ru(bpy)_2(4MePyrtr)Cl]^+$ is a stronger emitter than $[Ru(bpy)_2(3MePT)Cl]^+$, (similar behaviour is observed for the chelating ligand analogues $[Ru(bpy)_2(4MePyrtr)]^{2+}$ and $[Ru(bpy)_2(3MePT)]^{2+}$)

All monovalent complexes are weaker emitters than their corresponding bivalent complexes All compounds containing monodentate pyridyltriazole ligands emit at low temperature, see Table 3 13

The presence of a chlorine atom bound to ruthenium in the compound containing a monodentate ligand is reflected in the oxidation potentials The oxidation potential of $[Ru(bpy)_2Cl_2]$ is found at 0 32 V (see Table 3 13) and that of $[Ru(bpy)_3]^{2+}$ is found at 1 22 V (see Table 3 6) The oxidation potentials of our compounds containing monodentate ligands and one chlorine atom bound to ruthenium are found approximately half way between those of $[Ru(bpy)_2Cl_2]$ and $[Ru(bpy)_3]^{2+}$

For the monovalent compounds containing 4,4'-bpy and PY the

oxidation potentials are 0 79 V [70] and 0 80 V [72] respectively The oxidation potential of the compound containing vinylimidazole is 0 67 V [73] These values suggest that the results obtained for the oxidation potentials may be more diagnostic in ascertaining the ring of coordination than the uv/vis results

In comparison with the bivalent compounds containing the chelating pyridyltriazole ligands, the oxidation potentials of the compounds containing the monodentate pyridyltriazole ligands are found at lower potential For many $[Ru(bpy)_2L_2]^{2+}$ compounds reported in literature, a linear relationship exists between the energy of the lowest MLCT band and $\Delta E_{1/2}$ [34, 74] $\Delta E_{1/2}$ is the difference between the $Ru^{II/III}$ oxidation potential, and the $Ru^{II/I}$ reduction potential These relationships also hold for the compounds reported here (see Table 3 14 and Figure 3 21) indicating emission from the same $^3$MLCT level as is observed for other ruthenium polypyridyl complexes [74, 75] Figure 3 21 also includes the bivalent complexes reported in Chapter 3 section 1, and other monovalent complexes found in the literature

Table 3 14 Absorption and emission energies as a function of $\Delta E_{1/2}$

| Compound | | $\Delta E_{1/2}$ (V)[c] | Absorption Energy (V) | Emission Energy (V) |
|---|---|---|---|---|
| $[Ru(bpy)_2(HPyrtr)]^{2}$ | (1a) | 2 67 | 2 74 | 2 11 |
| $[Ru(bpy)_2(HPyrtr)]^{2}$ | (2a) | 2 59 | 2 79 | 2 06 |
| $[Ru(bpy)_2(Pyrtr)]^{+}$ | (1b) | 2 41 | 2 54 | 2 09 |
| $[Ru(bpy)_2(Pyrtr)]^{+}$ | (2b) | 2 31 | 2 56 | 2 01 |
| $[Ru(bpy)_2(H3MePyrtr)]^{2}$ | (3) | 2 75 | 2 79 | 2 11 |
| $[Ru(bpy)_2(3MePyrtr)]^{2}$ | (4) | 2 29 | 2 60 | 2 03 |
| $[Ru(bpy)_2(4MePyrtr)]^{2}$ | (5) | 2 63 | 2 81 | 2 12 |
| $[Ru(bpy)_2(PT)]^{2+}$ | (7) | 2 77 | 2 95 | 2 21 |
| $[Ru(bpy)_2(3BrPT)]^{2+}$ | (8) | 2 77 | 2 95 | 2 24 |
| $[Ru(bpy)_2(3MePT)]^{2+}$ | (9) | 2 72 | 2 86 | 2 38 |
| $[Ru(bpy)_2(PNP)]^{2+}$ | (10) | 2 66 | 2 75 | 2 17 |
| $[Ru(bpy)_2(4MePyrtr)Cl]$ | (11) | 2 00 | 2 44 | 1 89 |
| $[Ru(bpy)_2(PT)Cl]^{+}$ | (12) | 2 23 | 2 48 | 1 89 |
| $[Ru(bpy)_2(3BrPT)Cl]$ | (13) | 2 24 | 2 54 | 1 89 |
| $[Ru(bpy)_2(3MePT)Cl]$ | (14) | 2 31 | 2 47 | 1 88 |
| $[Ru(bpy)_3]^{2}$ | (15) | 2 58 | 2 74 | 2 13 |
| $[Ru(bpy)_2(PY)Cl]^{+}$ | (16) | 2 27 | 2 45 | 1 88 |

a = Protonated forms of isomers 1 and 2 b = Deprotonated form is isomers 1 and 2

c $\Delta E_{1/2}$ = Oxidation potential minus the first reduction potential

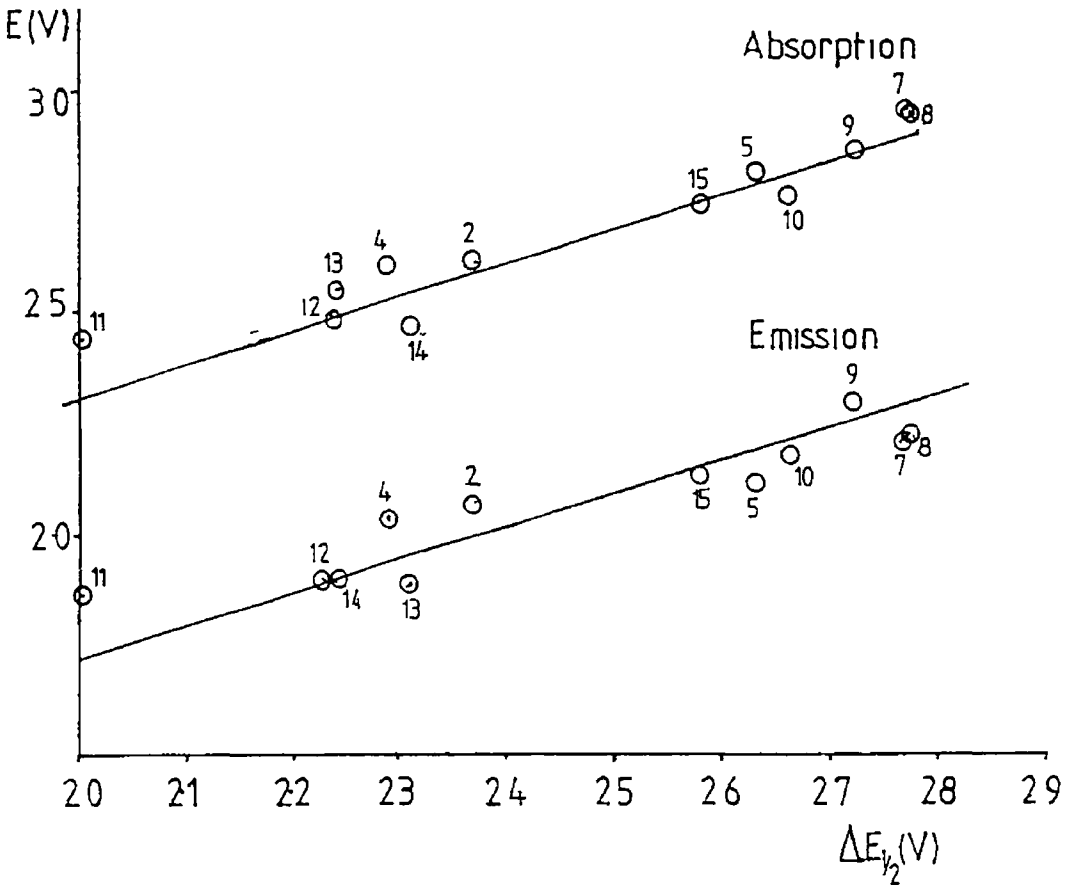


Figure 3 21 Plots of $\Delta E_{1/2}$ vs absorption (a) and emission (b) energies for compounds of the type $[Ru(bpy)_2(L\text{-}L')]^{n+}$ and $[Ru(bpy)_2(L\text{-}L')Cl]^{+}$, and $[Ru(bpy)_3]^{2+}$ Absorption spectra and values for $\Delta E_{1/2}$ were obtained at room temperature in acetonitrile Emission maxima were obtained at 77 K in ethanol

3 2 6 Conclusion.

The monovalent cations $[Ru(bpy)_2(4MePyrtr)Cl]^+$, $[Ru(bpy)_2(PT)Cl]^+$, $[Ru(bpy)_2(3BrPT)Cl]^+$ and $[Ru(bpy)_2(3MePT)Cl]^+$, containing monodentate coordinated pyridyl-1,2,4-triazole ligands have been prepared $^1H$ n m r spectra reveal that coordination of the ligands to the central metal atom is via the triazole ring However, the exact site of coordination could not be determined unambiguously from the n m r spectra The crystal structure of the compound $[Ru(bpy)_2(3MePT)Cl]^+$ confirmed that coordination is via the triazole ring and the site of coordination is through the $N^{4'}$ atom Due to the similarity between the n m r spectra of the compounds containing the PT and 3BrPT ligands it was concluded that the site of coordination for these ligands is also via the $N^{4'}$ of the triazole ring As the resonances of the protons in the pyridyltriazole ring of $[Ru(bpy)_2(4MePytr)Cl]^+$ exhibit similar behaviour to those of the other ligands it is suggested that the coordination mode of this ligand is via the $N^{1'}$ of the triazole ring To confirm this suggestion, x-ray crystal structure determination is required

Of the four monovalent compounds prepared, $[Ru(bpy)_2(4MePyrtr)Cl]^+$ has the lowest oxidation potential and absorbs at the lowest energy The compound $[Ru(bpy)_2(3BrPT)Cl]^+$, on the other hand has the highest oxidation potential and absorbs at the highest energy The absorption and oxidation potentials for $[Ru(bpy)_2(PT)Cl]^+$ and $[Ru(bpy)_2(3MePT)Cl]^+$ are very similar These results suggest that the pyridyltriazole ligand containing the bromo substituent is a stronger $\pi$ acceptor relative to 4MePyrtr, PT and 3MePT, while 4MePyrtr is the weakest $\pi$ acceptor The results also suggest that the pyridyltriazole ligand containing a carbon-carbon

connecting bond, i e 4MePyrtr is a weaker $\pi$ acceptor than the ligands which contain a carbon-nitrogen bond

The monovalent complexes are unstable in comparison with the bivalent analogues Decomposition of the monovalent complexes occurs in the presence of water A more detailed analysis of the photochemical stability of these complexes will be presented in the following section

# Chapter 3

## Section 3

## Photolysis of Compounds Containing Chelating and Monodentate Pyridyltriazole Ligands

3 3 1 Introduction to Photolysis.

As is observed in Section 2, monovalent complexes can be formed thermally from the reaction of $[Ru(bpy)_2Cl_2]$ with ligand (L-L'), by loss of a chlorine ion and replacement of that chlorine with a pyridyltriazole ligand, coordinated via the triazole ring Of particular interest would be, to see if similar monodentate species could be produced photochemically As only small quantities of monovalent species may be produced photochemically, conventional methods for synthetic and photochemical studies, using spectroscopic or electrochemical techniques would be of no use as these methods are not sensitive to small amounts of "impurities" Problems are also encountered in the photochemical studies of compounds of the type $[Ru(bpy)_2(L\text{-}L')]^{n+}$, where the simultaneous formation of more than one reaction product can hinder the spectroscopic study of the reaction

A technique which is ideally suited to investigate such complicated systems is High Performance Liquid Chromatography (HPLC) Only few applications of HPLC in ruthenium chemistry have been reported, these only dealing with $[Ru(bpy)_3]^{2+}$ type compounds [75-79] A literature search in the area of $[Ru(bpy)_2(L\text{-}L')]^{n+}$ compounds in connection with HPLC studies proved futile An HPLC system suitable for the separation of species with a different charge, and separation of species of similar charge was developed [80] The system developed consisted of an SCX cation exchange column similar to the one reported by O'Loughlin for the separation of different tris (bpy) compounds of different transition metals [77]

For the HPLC system developed, see Chapter 2 Experimental, all the singly charged species elute in general, before the doubly charged species The peaks of the doubly charged

cations are not as sharp as those of the singly charged species For the bivalent complexes a certain amount of tailing is observed This tailing may be reduced by increasing the flow rate and/or increasing the lithium perchlorate concentration in the mobile phase However, if the lithium salt concentration is increased problems occur as some of the peaks due to the $1^+$ species coalesce One method of increasing the elution time of the $2^+$ species without interfering with the elution time of the $1^+$ species was to increase the flow rate after all the $1^+$ species have eluted So, for example, a flow rate of 2 0 ml/min was maintained for 3 0 min, then the flow rate is changed to 4 0 ml/min over a two minute interval In this manner, shorter retention times and sharper peaks were obtained for the $2^+$ species This procedure was not necessary for many of the photolysed samples as the retention times of the doubly charged complexes were within 10-15 min

### 3 3 2 Photolysis of a Model Compound $[Ru(bpy)_2(viz)_2]^{2+}$

The photolysis of $[Ru(bpy)_2(viz)_2]^{2+}$ where viz = bisvinylimidazole, was investigated as a model system for the pyridyltriazole compounds and also to develop a suitable HPLC system to follow the photochemical reactions To examine the spectroscopic properties of photoproducts such as $[Ru(bpy)_2(L)Cl]^+$ and $[Ru(bpy)_2(L)(CH_3CN)]^{2+}$ (where L = viz or other N-donor ligands) which may be produced during photolysis, $[Ru(bpy)_2(viz)_2]^{2+}$ was photolysed in $CH_3CN$/0 01 M LiCl When the photolysis of the bis-(vinylimidazole) compound is followed by uv/vis spectroscopy, no isosbestic points are observed and a complicated reaction path is therefore expected This is confirmed by the HPLC results (Figure 3 22), which show the formation of at least five different species during the photolysis

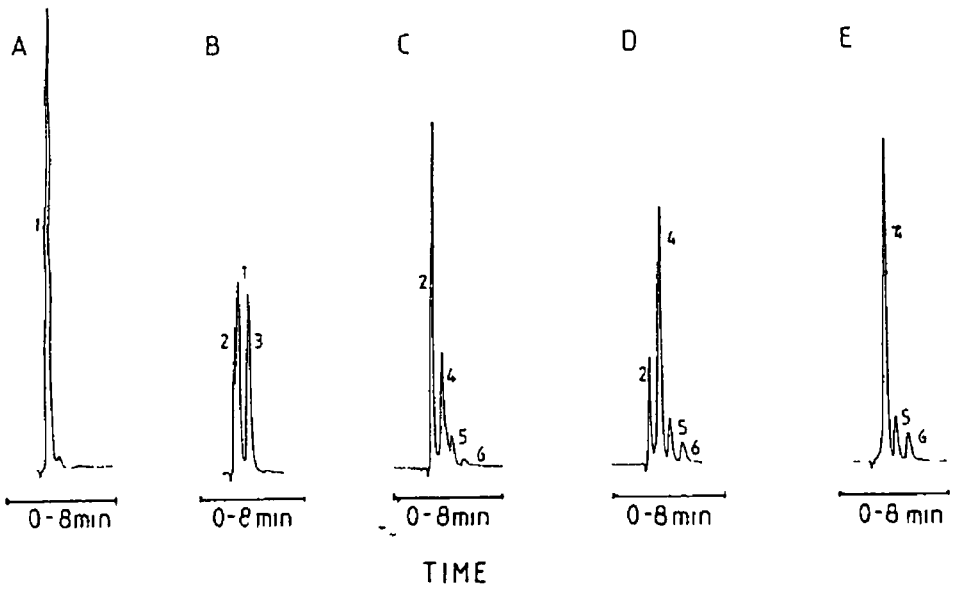


Figure 3 22 Chromatograms taken during the photolysis of $[Ru(bpy)_2(viz)_2](PF_6)_2$ in $CH_3CN$/0 01 M LiCl Irradiation times A, 0 sec , B, 20 sec , C, 130 sec , d, 350 sec , E, 1,200 sec Flow rate 1 5 ml/min Detection wavelength 280 nm

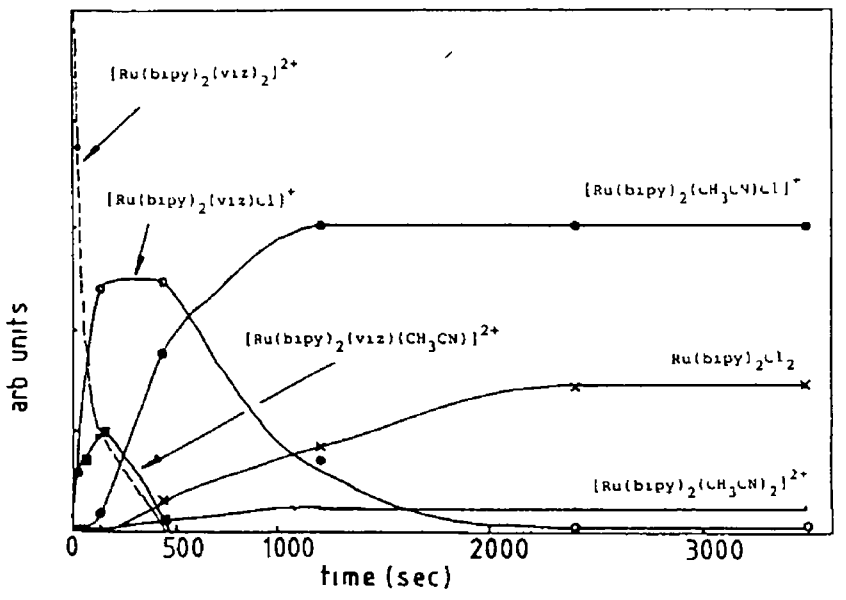


Figure 3 23 Diagramatic representation of product formation during the photolysis of $[Ru(bpy)_2(viz)_2](PF_6)_2$ in $CH_3CN$/0 01 M LiCl, as measured from peak area

The peaks were assigned using a photodiode array detector, comparison with literature values [36, 81], and also by injection of standards where possible

From the results obtained, it can be concluded that during the photolysis of $[Ru(bpy)_2(viz)_2]^{2+}$, the species $[Ru(bpy)_2(viz)Cl]^{2+}$, (retention time 2 87 min , absorption maxima 515 and 360 nm, peak 2), $[Ru(bpy)_2(viz)(CH_3CN)]^{+}$, (retention time 3 88 min , absorption maximum 455 nm, peak 3) and $[Ru(bpy)_2(CH_3CN)Cl]^{+}$ (retention time 3 60 min , absorption maxima 475 and 340 nm,peak 4) are formed The nature of the products was confirmed by comparison of the absorption spectra obtained with those of authentic samples [46] and by additional photochemical experiments of $[Ru(bpy)_2(viz)_2]^{2+}$ and $[Ru(bpy)_2(viz)Cl]^{+}$ in acetonitrile where the product $[Ru(bpy)_2(viz)(CH_3CN)]^{2+}$ appears to be formed [81] The chromatograms in Figure 3 22 suggest that during the first part of the photolysis $[Ru(bpy)_2(viz)Cl]^{+}$ and $[Ru(bpy)_2(viz)(CH_3CN)]^{2+}$ are formed in parallel as in reactions 8 and 9,

$$[Ru(bpy)_2(viz)_2]^{2+} \xrightarrow[h\nu]{CH_3CN} [Ru(bpy)_2(viz)(CH_3CN)]^{2+} + viz \quad (8)$$

$$[Ru(bpy)_2(viz)_2]^{2+} \xrightarrow[h\nu]{Cl^-} [Ru(bpy)_2(viz)Cl]^{+} + viz \quad (9)$$

Upon further photolysis $[Ru(bpy)_2(CH_3CN)Cl]^{+}$ (peak 4), is formed as the main product Figure 3 23 is a diagrammatic representation of product formation and shows that two minor products were obtained with retention times of 4 29 and 5 14 min (peaks 5 and 6) The nature of these products, that have their lowest absorption maxima at 495 and 445 nm respectively, is at present unknown However,

there is a possibility that during the photolysis, photoisomerisation may occur resulting in the formation of trans species This would involve cleavage of a ruthenium - pyridine bond (of a bipyridine ligand) and subsequent rearrangement to form a trans $Ru(bpy)_2$ complex

The presence of a small amount of water in the photolysis solvent may result in the formation of a quantity of trans-$[Ru(bpy)_2(H_2O)_2]^{2+}$ Substitution of one or more of the water molecules may occur upon injection into the mobile phase to yield trans-$[Ru(bpy)_2(H_2O)(CH_3CN)]^{2+}$ and/or trans-$[Ru(bpy)_2(CH_3CN)_2]^{2+}$ The most obvious difference between the cis- and trans- complexes concerns the energy of the absorption maxima The trans- complexes absorb at slightly lower energy that the cis- complexes The wavelengths of maximum absorbance of the trans species $[Ru(bpy)_2(CH_3CN)_2]^{2+}$, $[Ru(bpy)_2(H_2O)(CH_3CN)]^{2+}$ and $[Ru(bpy)_2(H_2O)_2]^{2+}$ are 440, 465, and 495 nm respectively, the former two are measured in acetonitrile and the latter in $CF_3COOH$ [82] The absorption maxima values for the corresponding cis compounds are 425, 445 and 480 nm Rapid ligand exchange of water for solvent is believed to occur [82] for $[Ru(bpy)_2(H_2O)(CH_3CN)]^{2+}$

In order to examine the possibility of trans- species being formed, trans-$[Ru(bpy)_2(H_2O)_2]^{2+}$ was prepared by photolysis of $[Ru(bpy)_2(CO_3)]$ in 1M $HClO_4$ [83] The product obtained was filtered and injected on the HPLC system where several peaks were obtained This suggests that either the photolysis product was impure or rapid degradation occurred The photolysis product was refluxed in the presence of acetonitrile in the hope of yielding the trans-$[Ru(bpy)_2(CH_3CN)_2]^{2+}$ product However, isolation of the product and analysis on the HPLC resulted in a multitude of peaks

From these results, it is not entirely clear what is happening concerning the formation of trans products but the possibility of formation during photolysis reactions must not be eliminated The peaks 5 and 6 which were obtained during the photolysis of $[Ru(bpy)_2(viz)_2]^{2+}$ in $CH_3CN/LiCl$ have their lowest absorption maxima at 495 and 445 nm respectively These absorption maxima correspond quite well with those obtained for trans-$[Ru(bpy)_2(H_2O)_2]^{2+}$ and trans-$[Ru(bpy)_2(CH_3CN)_2]^{2+}$ However, further experiments are required to establish the nature of these photolysis products

The results of the photolysis experiment of $[Ru(bpy)_2(viz)_2]^{2+}$ in $CH_3CN/LiCl$ clearly show that HPLC is ideally suited for such studies, as intermediates formed during the photolysis may be detected and their relative amounts quantified, whereas the detection of these species using spectroscopic techniques would be difficult

Compounds containing the chelating and monodentate ligands were photolysed in $CH_3CN$ and $CH_3CN/0$ 01 M LiCl The photolysis reactions were followed by uv/vis spectroscopy and HPLC The photolysis of complexes of the type $[Ru(bpy)_2(L\text{-}L')]^{2+}$ where L-L' = PT, 3BrPT, 3MePT and 4MePyrtr will be discussed first, followed by a discussion on the photolysis of their monovalent analogues As the reactions for the compounds containing PT type ligands are very similar, the results obtained for the complexes $[Ru(bpy)_2(PT)]^{2+}$ and $[Ru(bpy)_2(PT)Cl]^{+}$ are taken as representative samples for the PT type ligands The photolysis of these two compounds in both solvent systems will be discussed in detail followed by a general reaction scheme for the compounds containing the ligands 3BrPT and 3MePT The photolysis of the monovalent and bivalent species containing the ligand 4MePyrtr is also discussed in detail

3 3 2 1 Photolysis of $[Ru(bpy)_2(PT)]^{2+}$ in Acetonitrile

The uv/vis spectra of $[Ru(bpy)_2(PT)]^{2+}$ taken at different intervals during the photolysis in $CH_3CN$ are shown in Figure 3 24 Chromatograms taken at different intervals during the same photolysis are shown in Figure 3 25 From the uv/vis spectra an isosbestic point is observed in the initial stages of the reaction This was an indication that initially only one photoproduct is formed The chromatograms obtained clearly show that small amounts of other photoproducts which are undetected by uv/vis have been formed at this stage The formation of these products is observed at a later stage of the photolysis by uv/vis spectra as the isosbestic point shifts slightly, however, the exact nature of these products cannot be determined spectrophotometrically due to the small quantities formed

The major product which is formed at the completion of this photolysis is the bis-acetonitrile complex, $[Ru(bpy)_2(CH_3CN)_2]^{2+}$ (retention time 10 4 min , absorption maximum 425 nm , peak 4, Figure 3 25) The second major product, peak 1, is free ligand, this peak increased steadily with a corresponding increase in intensity of peak 4 The assignment of peak 1 was confirmed by injection of ligand standard Two other products were also formed, peaks 2 and 3 (retention times 2 97 and 6 44 min respectively) The uv/vis spectra of peak 2 absorption maximum = 475 nm, corresponds to the $[Ru(bpy)_2(CH_3CN)Cl]^{+}$ complex, injection of the acetonitrile-chloride standard confirmed this, however, the presence of chlorine ions in the solution is unaccounted for The absorption maximum for peak 3 is at 440 nm This is one of the products formed at the initial stage of the reaction, along with peak 4, the $[Ru(bpy)_2(CH_3CN)_2]^{2+}$ complex Peak 3 increases to its maximum intensity after 900 s, and subsequently decreases in intensity

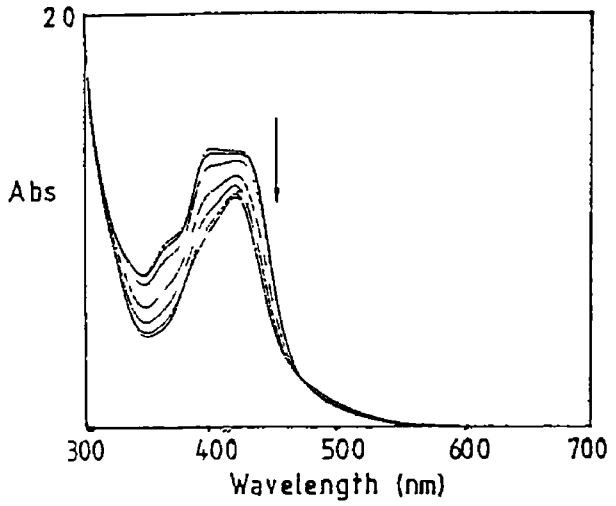


Figure 3 24 Uv/vis spectra of $[Ru(bpy)_2(PT)]^{2+}$ taken during a photolysis reaction in $CH_3CN$ with respect to time, T = 0 to T = 9,480 sec

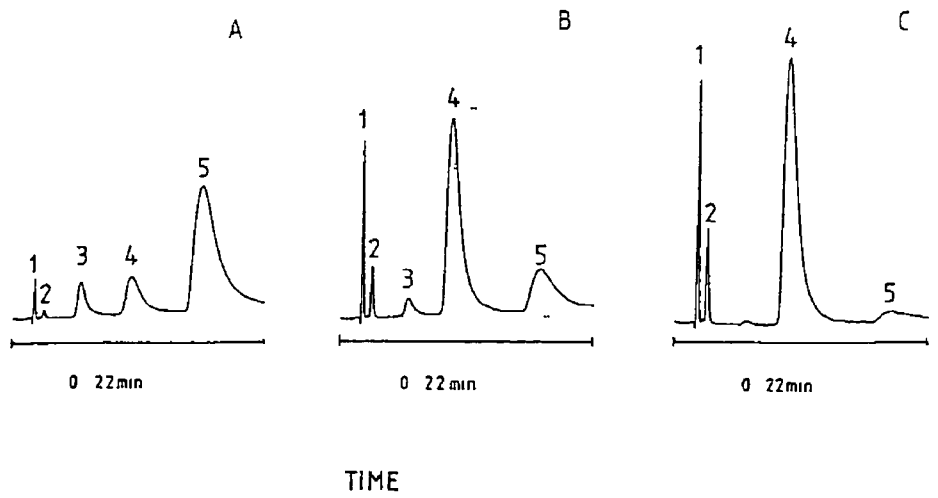


Figure 3 25 Chromatograms taken during the photolysis of $[Ru(bpy)_2(PT)]^{2+}$ in $CH_3CN$ Irradiation times A, 900 sec , B, 4,740 sec , C, 9,480 Flow rate 2 0 ml/min detection wavelength 280 nm

After 900 s both peaks 1 and 4 increase, that is, there was more free ligand in solution, and more of the bis-acetonitrile complex formed As the shape of peak 3 is broad and has a certain amount of tailing, it suggests that this peak is that of a $2^+$ species, the low absorption maximum at 445nm possibly suggests the presence of the species $[Ru(bpy)_2(PT)(CH_3CN)]^{2+}$ A second possibility of the nature of this peak is that of the trans-$[Ru(bpy)_2(CH_3CN)_2]^{2+}$ which absorbs at 445 nm in aceto-nitrile However, this possibility has been ruled out as the HPLC chromatograms show that at one stage during the photolysis the decrease of this peak corresponds with the increase of the ligand This would suggest a reaction scheme for the photolysis in acetonitrile as shown below

Reaction Scheme

$$[Ru(bpy)_2(PT)]^{2+} \xrightarrow[hv]{CH_3CN} [Ru(bpy)_2(PT)(CH_3CN)]^{2+} \dashrightarrow$$

$$[Ru(bpy)_2(CH_3CN)_2]^{2+} + PT \quad (10)$$

3 3 2 2 Photolysis of $[Ru(bpy)_2(PT)]^{2+}$ in Acetonitrile - LiCl

The complex $[Ru(bpy)_2(PT)]^{2+}$ was also photolysed in $CH_3CN$/ 0 01M LiCl The chloride anions were added in order to shift the reaction equilibrium towards conditions more favourable for the formation of the complex $[Ru(bpy)_2(PT)-Cl]^+$ Observation of the uv/vis spectra (Figure 3 26) during photolysis immediately shows that a different reaction occurs in this solvent system As with the system above, an isosbestic point is clearly defined at 455 nm in the initial stage of the photolysis which subsequently shifts as species are formed which absorb at 475 and 550 nm

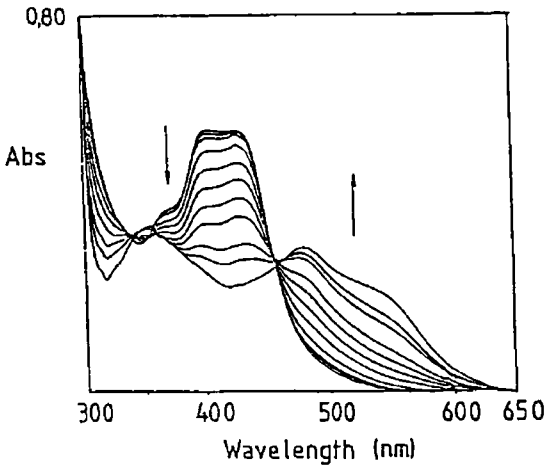


Figure 3 26 Uv/vis spectra of $[Ru(bpy)_2(PT)]^{2+}$ taken during a photolysis reaction in $CH_3CN$/0 01 M LiCl with respect to time, T = 0 to T = 10,000 sec

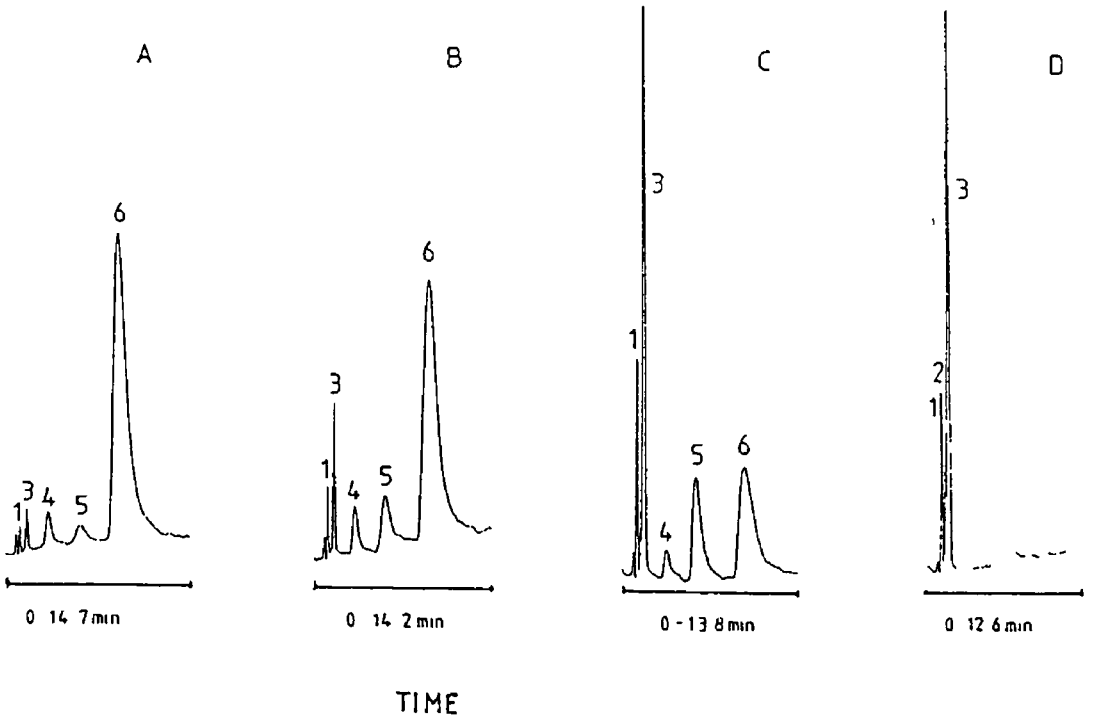


Figure 3 27 Chromatograms taken during the photolysis of $[Ru(bpy)_2(PT)]^{2+}$ in $CH_3CN$/0 01 M LiCl Irradiation times a 200 sec , B, 780 sec , C, 2,700 sec , D, 10,000 sec Flow rate 3 0 ml/min Detection wavelength 280 nm

The chromatograms in Figure 3 27, which were taken during the photolysis along with a diagrammatic representation of product formation in Figure 3 28 give a more complete picture of what is actually happening The sample photolyses quickly in this solvent system as seen at T = 0 about 4% of the $[Ru(bpy)_2(CH_3CN)Cl]^+$ has formed (retention time 2 12 min , peak 3) The intensity of this peak increases as the reaction proceeds However, the rate of increase slows down after 1200 s as the $CH_3CN$ is lost from the bis-(bipyridyl) acetonitrile chloride complex to form $[Ru(bpy)_2Cl_2]$ (peak-2 retention time 1 66 min) At the end of the photolysis, when all the starting material has been photolysed, $[Ru(bpy)_2(CH_3CN)Cl]^+$ is the main product comprising of 73% of the total chromatogram area, $[Ru(bpy)_2Cl_2]$ is present at 11% The remaining 16 is due to free ligand The bis-acetonitrile complex (peak 5, retention time 7 00 min, absorption maximum 425 nm ) was also formed and it reached its maximum intensity after 1200 s, and then subsequently decayed as peaks 2 and 3 formed

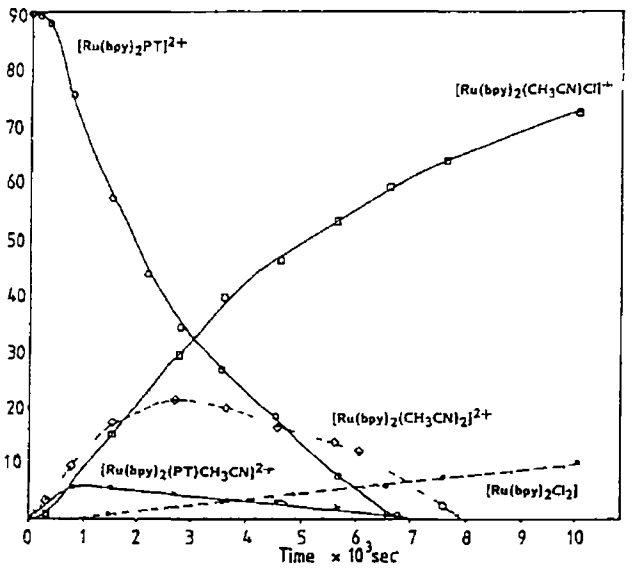


Figure 3 28 Diagrammatic representation of product formation during the photolysis of $[Ru(bpy)_2(PT)]^{2+}$ in $CH_3CN$/0 01 M LiCl as measured from peak area from the chromatograms

A minor product is observed at 1200 s but subsequently disappears (4 37 min , peak 4, absorption maximum 440 nm) This peak has a similar absorption maximum and retention time as peak 3 in Figure 3 25 This suggests that peak 4 in this photolysis is due to the complex $[Ru(bpy)_2(PT)(CH_3CN)]^{2+}$

3 3 2 3 Photolysis of $[Ru(bpy)_2(PT)]^{2+}$ in Methanol - LiCl

Interestingly, the monovalent complex $[Ru(bpy)_2(PT)Cl]^{+}$ was not formed under the reaction conditions described above In order to make conditions more favourable for the production of this species, the photolysis was carried, out in methanol/0 01M LiCl As methanol is not as good a co-ordinating solvent as acetonitrile, this system may favour the formation of $[Ru(bpy)_2(PT)Cl]^{+}$ Problems were incurred using this system as injection of methanol into an acetonitrile/water mobile phase produced a large negative peak, due to refractive index changes when the methanol passes through the detector This negative peak masked the peaks in the region between 1 0 to 2 5 min , no advantage was gained by slowing the flow rate down to 1 0 ml/min By way of blanking this negative peak, the solvent composition of the mobile phase was varied, without changing the overall solvent polarity, to $CH_3CN$ $H_2O$ MeOH in the ratios 70 20 10 containing 0 08 M $LiClO_4$ This proved to be more successful, as some information concerning the species which elute in that area was obtained The photolysis of $[Ru(bpy)_2(PT)]^{2+}$ in MeOH/LiCl was monitored using this mobile phase The uv/vis spectra obtained during the photolysis is shown in Figure 3 29 The decrease in absorbance of the starting material is observed, with a corresponding increase in the absorbance of a species at 500 nm

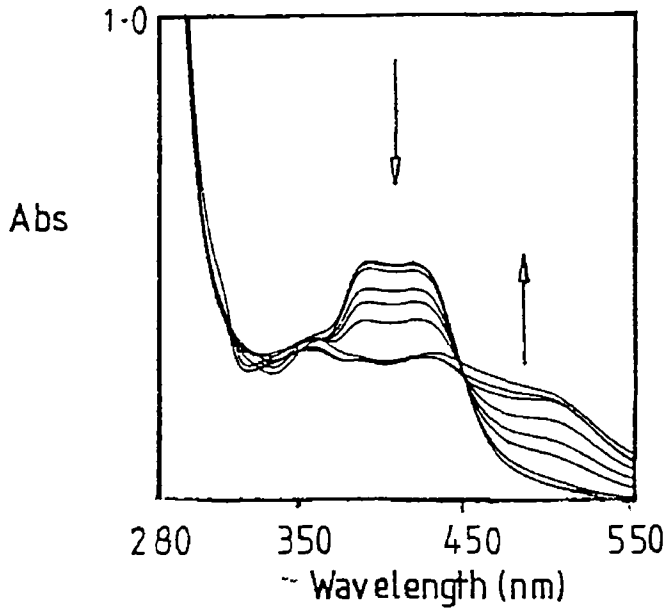


Figure 3 29 Uv/vis spectra of $[Ru(bpy)_2(PT)]^{2+}$ taken during a photolysis reaction in methanol/0 01 M LiCl with respect to time, T = 0 to T = 4,080

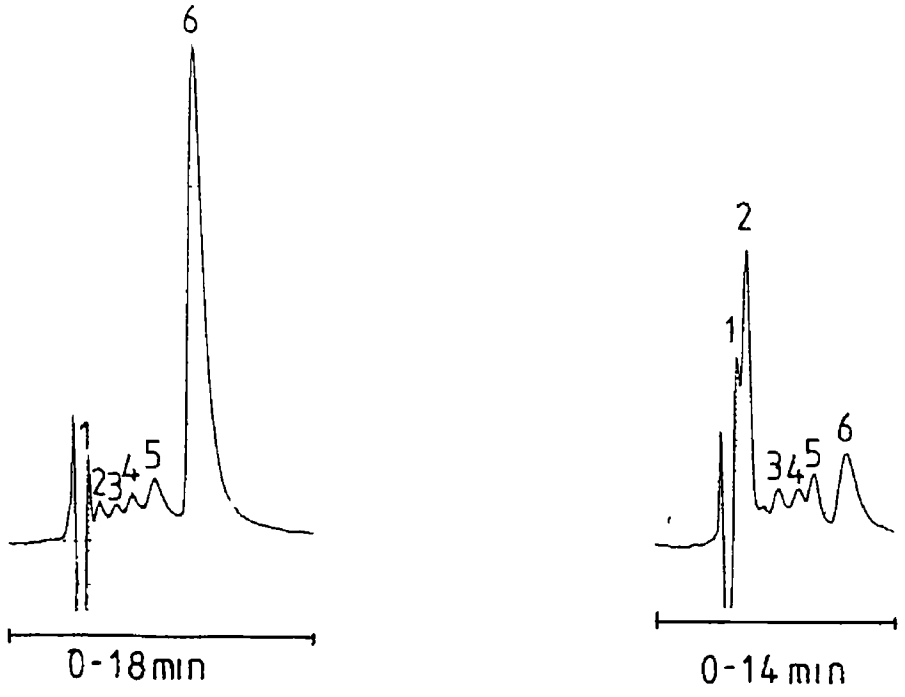


Figure 3 30 Chromatograms taken during the photolysis of $[Ru(bpy)_2(PT)]^{2+}$ in methanol/0 01 M LiCl Irradiation time 4,080 sec Flow rate 1 0 ml/min Detection wavelength 280 nm

This suggests that the species $[Ru(bpy)_2(PT)Cl]^+$ may be produced It must also be remembered, however, that there is a strong possibility of $[Ru(bpy)_2(MeOH)Cl]^+$ forming in solution, this species absorbs in the region of 500 nm This value was obtained by stirring $[Ru(bpy)_2Cl_2]$ in methanol and following the reaction by uv/vis spectroscopy Injection of the sample onto the HPLC yielded a peak for the $[Ru(bpy)_2(CH_3CN)Cl]^+$ species indicating that ligand exchange with the mobile phase occurs So, $[Ru(bpy)_2(MeOH)Cl]^+$ will be observed as $[Ru(bpy)_2(CH_3CN)Cl]^+$ under the HPLC conditions As this ligand exchange process occurs, $[Ru(bpy)_2(MeOH)Cl]^+$ and $[Ru(bpy)_2(PT)Cl]^+$ complexes can be eluted separately

Sample chromatograms from this reaction are presented in Figure 3 30 Photolysis proceeds at a slower rate in this solvent system, due to a combination of polarity and the different coordinating abilities of methanol compared with acetonitrile As is observed a negative peak produced by the different solvent fronts still masks some information in the 4 25 to 4 75 min region The flow rate has also been reduced to 1 0 ml/min However, the main feature is that in Figure 3 30, at T = 6120 s the monovalent complex $[Ru(bpy)_2(PT)Cl]^+$ has been produced (absorption maximum 500 nm, retention time 4 94 min, peak 1) From the HPLC chromatograms, a peak corresponding to the $[Ru(bpy)_2(CH_3CN)Cl]^+$ is observed (absorption maximum 475 and 340 nm, retention time 5 59 min, peak 2) This indicates that the $[Ru(bpy)_2(MeOH)Cl]^+$ species has been produced on photolysis and that ligand exchange occurs with the acetonitrile in the mobile phase The product $[Ru(bpy)_2(CH_3CN)Cl]^+$ is detected as the major product of the reaction along with peak 1, the $[Ru(bpy)_2(PT)Cl]^+$ complex Both peaks increase steadily throughout the reaction The bis-methanol complex is also formed which is detected as the bis-acetonitrile complex due to ligand

exchange (retention time 8 69 min, peak 5), and its maximum intensity is at the initial stage of the photolysis, and then it slowly decreases in intensity The $[Ru(bpy)_2(PT)(MeOH)]^{2+}$ complex, detected as $[Ru(bpy)_2(PT)(CH_3CN)]^{2+}$, is observed as a minor product (retention time 9 4 min, peak 6) Two other minor products are formed during the reaction (retention times 6 54 and 7 46 min, peaks 3 and 4 respectively), the identity of which is unknown No $[Ru(bpy)_2Cl_2]$ was observed in the chromatograms, unless it was masked by the negative peak

It must be noted that the chromatography of the MeOH/LiCl system needs to be improved on as separation of the monovalent species is not complete, and also for quantitative analysis the negative peak must be eliminated For our purposes, this system suffices in the respect that the formation of $[Ru(bpy)_2(PT)Cl]^+$ is observed qualitatively though not quantitatively As many other products are formed during the photolysis, isolation of the $[Ru(bpy)_2(PT)Cl]^+$ monovalent species would be difficult if the photolysis were carried out on a quantitative scale It is anticipated that if Sephadex LH-20 or Sephadex C-25 were used, separation of species of different charge would be possible but separation between species of the same charge would be difficult, i e separation between $[Ru(bpy)_2(PT)Cl]^+$ and $[Ru(bpy)_2(CH_3CN)Cl]^+$ would be difficult Another point to note is that Sephadex LH-20 and C-25 both require aqueous or polar organic mobile phases This would more than likely cause stability problems for the separation of the $[Ru(bpy)_2(PT)Cl]^+$ monovalent complex produced by photolysis, the $[Ru(bpy)_2(PT)Cl]^+$ monovalent complex produced thermally, decomposes in aqueous or polar organic solvents to yield the bivalent complex $[Ru(bpy)_2(PT)]^{2+}$ It is expected that the species produced photochemically would exhibit similar behaviour

(1) Acetonitrile

$$[Ru(bpy)_2(L\text{-}L')]^{2+} \longrightarrow [Ru(bpy)_2(L\text{-}L')(CH_3CN)]^{2+}$$
minor product

$$[Ru(bpy)_2(CH_3CN)_2]^{2+} + L\text{-}L'$$
major product

(2) Acetonitrile/LiCl

$$[Ru(bpy)_2(L\text{-}L')]^{2+} \longrightarrow [Ru(bpy)_2(CH_3CN)Cl]^{+} + L\text{-}L'$$
major product

$$[Ru(bpy)_2Cl_2]$$
minor product

$$[Ru(bpy)_2(L\text{-}L')(CH_3CN)]^{2+} \longrightarrow [Ru(bpy)_2(CH_3CN)_2]^{2+} + L\text{-}L'$$
minor product — minor product

(3) Methanol/LiCl

$$[Ru(bpy)_2(L\text{-}L')]^{2+} \longrightarrow [Ru(bpy)_2(MeOH)Cl]^{+} + L\text{-}L'$$

$$+ [Ru(bpy)_2(L\text{-}L')Cl]^{+}$$
major products

$$[Ru(bpy)_2(L\text{-}L')(MeOH)]^{2+} + [Ru(bpy)_2(MeOH)]^{2+} + L\text{-}L'$$
minor products

Figure 3 31 Schematic reaction scheme for compounds containing chelating PT type ligands in $CH_3CN$, $CH_3CN$/0 01 M LiCl and MeOH/0 01 M LiCl

The schematic diagram presented in Figure 3 31 is a summary of the reaction products for the photolysis of samples where (L-L') = PT, 3BrPT and 3MePT As can be seen from this reaction scheme, the same type of photoproducts are formed in the same solvent from different starting materials The exact percentage yields are not identical for each sample, but the same overall major and minor products are formed in each reaction However, the rates at which these photoproducts are formed vary according to the starting material and on the solvent This is in agreement with the results obtained for the photolysis of $[Ru(bpz)_3]^{2+}$ [40] where decomposition of the starting material occurs more readily when chloride anions are added to the acetonitrile rather than in pure acetonitrile As expected, the decomposition of all starting materials occurs at a slower rate when the solvent employed is methanol

As the reaction schemes for the photolysis of $[Ru(bpy)_2(3BrPT)]^{2+}$ and $[Ru(bpy)_2(3MePT)]^{2+}$ in acetonitrile and acetonitrile/LiCl are very similar, a detailed analysis will not be given For the photolysis of $[Ru(bpy)_2(3BrPT)]^{2+}$ in acetonitrile, the uv/vis spectra show that the absorbance of the lowest energy MLCT band (420 nm broad) of the starting material decreases as the absorption maximum shifts to 425 nm This is in agreement with the HPLC results obtained showing that $[Ru(bpy)_2(CH_3CN)_2]^{2+}$ is formed as the main product A similar shift from 435 nm to 425 nm is observed in the uv/vis spectra of the photolysis of $[Ru(bpy)_2(3MePT)]^{2+}$ in acetonitrile Again, the HPLC results confirm that $[Ru(bpy)_2(CH_3CN)_2]^{2+}$ is formed as the major product

Photolysis in acetonitrile/LiCl results in a shift in absorption maxima from 420 to 475 nm for $[Ru(bpy)_2(3BrPT)]^{2+}$ and 435 to 475 nm for $[Ru(bpy)_2(3MePT)]^{2+}$ The

HPLC results obtained show that $[Ru(bpy)_2(CH_3CN)Cl]^+$ is the major photoproduct formed for both complexes, see Figure 3 31 As with the photolysis reactions of $[Ru(bpy)_2(PT)]^{2+}$ in acetonitrile and acetonitrile/LiCl, evidence suggesting the presence of a bivalent species containing a monodentate pyridyltriazole ligand and an acetonitrile molecule was obtained However, no evidence for the formation of the monodentate-chloro complex was obtained in these reactions

Indeed, as for $[Ru(bpy)_2(PT)]^{2+}$, the monovalent complexes $[Ru(bpy)_2(3BrPT)Cl]^+$ and $[Ru(bpy)_2(3MePT)Cl]^+$ were formed upon photolysis of $[Ru(bpy)_2(3BrPT)]^{2+}$ and $[Ru(bpy)_2$-$(3MePT)]^{2+}$ in methanol/LiCl The uv/vis spectra of the photolysis of $[Ru(bpy)_2(3BrPT)]^{2+}$ shows a decrease in absorbance at 420 nm with a corresponding increase in absorbance at 500 nm As the photolysis proceeds a slight shoulder at 530 nm, corresponding to $[Ru(bpy)_2Cl_2]$ is formed

The absorbance shifts for $[Ru(bpy)_2(3MePT)]^{2+}$ are very similar, from 435 nm to 500 nm with a shoulder at 530 nm As with $[Ru(bpy)_2(PT)]^{2+}$, the HPLC of these compounds needs improvement, but the desired monodentate products are observed, each with an absorption maximum at 500 nm

### 3 3 2 4 Photolysis of $[Ru(bpy)_2(4MePyrtr)]^{2+}$ in Acetonitrile.

The photolysis of the title complex in acetonitrile produced some interesting results The uv/vis spectra as a function of photolysis time is shown in Figure 3 32 and the chromatograms as a function of photolysis time are shown in Figure 3 33 When all the starting material was decomposed, two products were formed

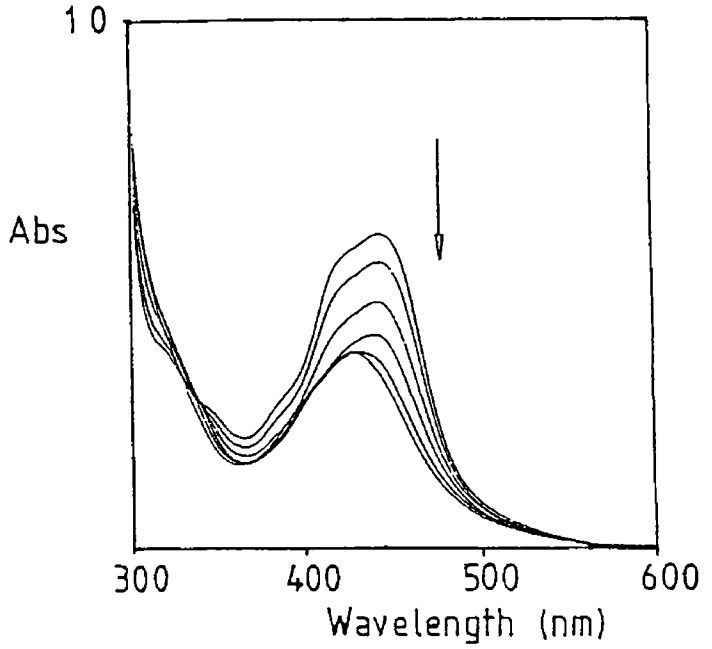


Figure 3 32 Uv/vis spectra of $[Ru(bpy)_2(4MePyrtr)](PF_6)_2$ taken during a photolysis reaction in $CH_3CN$ with respect to time, T = 0 to T = 5,820 sec

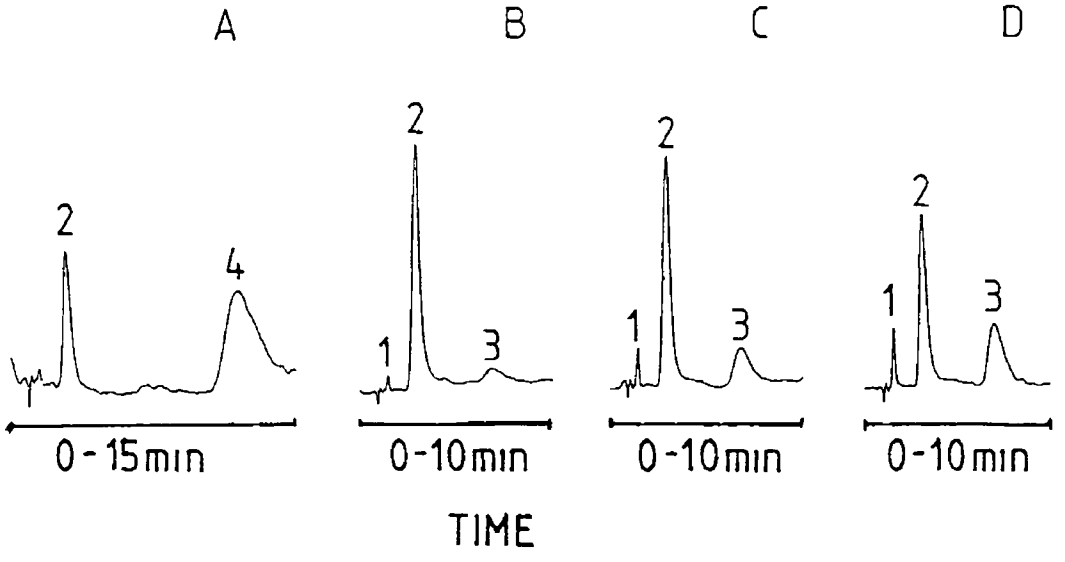


Figure 3 33 Chromatograms taken during the photolysis of $[Ru(bpy)_2(4MePyrtr)](PF_6)_2$ in $CH_3CN$ Irradiation times, A, 180 sec , B, 1,080 sec , C, 3,600 sec , D, 5,820 sec Flow rate 3 5 ml/min Detection wavelength 280 nm

The first, the major product, peak 2, has a retention time of 3 05 min and its maximum absorbance at 445 nm The second product, peak 3, the $[Ru(bpy)_2(CH_3CN)_2]^{2+}$ complex, has a retention time of 6 82 min and its maximum absorbance at 425 nm Peak 2 was assigned as the $[Ru(bpy)_2(4MePyrtr)(CH_3CN)]^{2+}$ complex on the following basis In the initial stages of the reaction, the intensity of peak 2 increases sharply At this stage the intensity of peaks 1 and 3 (peak 1 = ligand, retention time = 1 65 min) remain relatively constant However if the reaction is allowed to proceed when all the starting material has been photolysed then the intensity of peak 2 decreases and simultaneously both peak 1 and 3 increase It was therefore concluded that ligand was released while the bis-acetonitrile complex was formed This suggests that peak 2 is the $[Ru(bpy)_2(4MePyrtr)(CH_3CN)]^{2+}$ complex In addition, the broad shape of peak 2 indicates that it is a doubly charged species

From these results it is observed that the $[Ru(bpy)_2(4MePyrtr)(CH_3CN)]^{2+}$ complex is formed more readily than in the photolysis of the complexes $[Ru(bpy)_2(PT)]^{2+}$, $[Ru(bpy)_2(3BrPT)]^{2+}$ and $[Ru(bpy)_2(3MePT)]^{2+}$ As the 4MePyrtr ligand is able to coordinate in a monodentate fashion to the central metal atom to form the ligand - acetonitrile complex as a major product, it might be possible to form the monodentate chloride $[Ru(bpy)_2(4MePyrtr)Cl]^{+}$ species if the photolysis solvent was acetonitrile/LiCl

### 3 3 2 5 Photolysis of $[Ru(bpy)_2(4MePyrtr)]^{2+}$ in Acetonitrile-LiCl.

Figure 3 34 shows the uv/vis spectra of the photolysis of $[Ru(bpy)_2(4MePyrtr)]^{2+}$ as a function of time

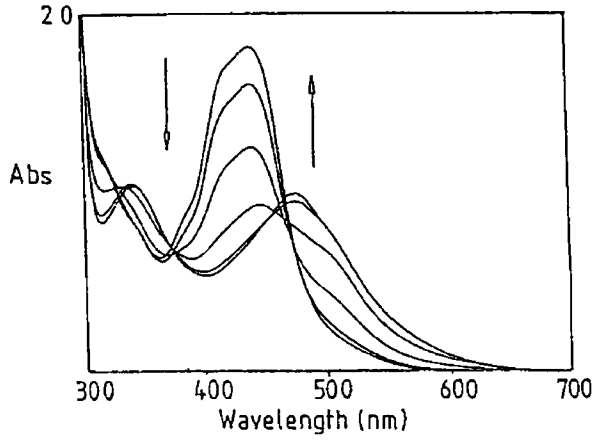


Figure 3 34 Uv/vis spectra of $[Ru(bpy)_2(4MePyrtr)](PF_6)_2$ undergoing a photolysis reaction in $CH_3CN$/0 01 M LiCl with respect to time, T = 0 sec to T = 3,300 sec

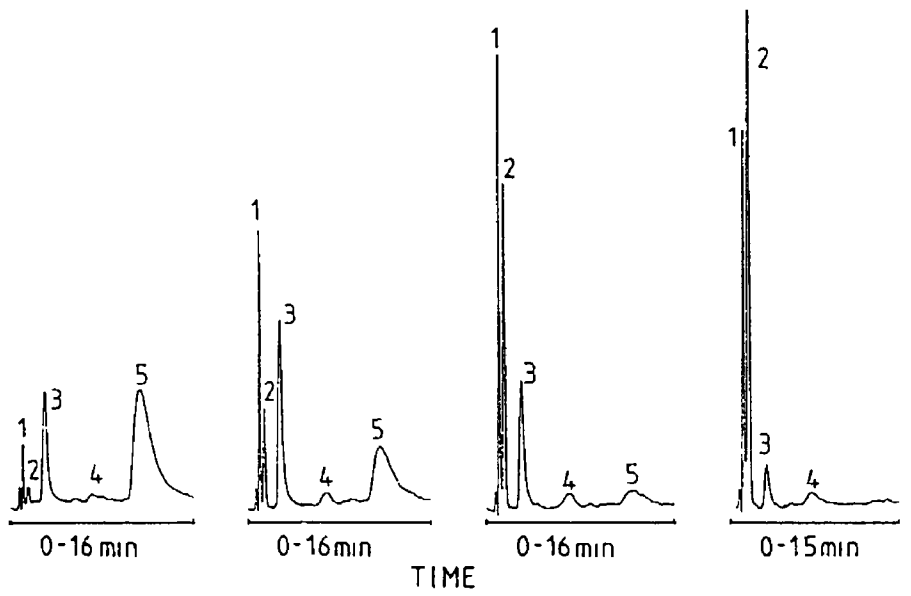


Figure 3 35 Chromatograms taken during the photolysis of $[Ru(bpy)_2(4MePyrtr)](PF_6)_2$ in $CH_3CN$/0 01M LiCl Irradiation times, A, 170 sec , B, 540 sec , C, 1,200 , D, 2,310 sec Flow rate 3 5 ml/min Detection wavelength 280 nm

Figure 3 35 shows a sample of the chromatograms taken during the photolysis The uv/vis spectra do not show a clear isosbestic point suggesting a complex reaction As the time increases, the shoulder at 497 nm increases in absorbance This suggests that the monovalent species $[Ru(bpy)_2(4MePyrtr)Cl]^+$ may be formed The chromatograms show that the photolysis is complex, as five reaction products are formed As the reaction is complex, a graph of relative percentage areas of the chromatograms vs photolysis time is plotted to give a clearer view of what is happening (Figure 3 36) At the initial stages of the reaction (up to T = 170s), the first product is peak 3 which has a retention time at 3 12 min and a maximum absorbance at 445 nm This is the same species as was produced as the major product for the photolysis of $[Ru(bpy)_2(4MePyrtr)]^{2+}$ in acetonitrile and is assumed to be $[Ru(bpy)_2(4MePyrtr)(CH_3CN)]^{2+}$ This complex reaches its maximum intensity at 540 s, after which it subsequently decreases in intensity As this peak decreases the formation of other complexes is observed

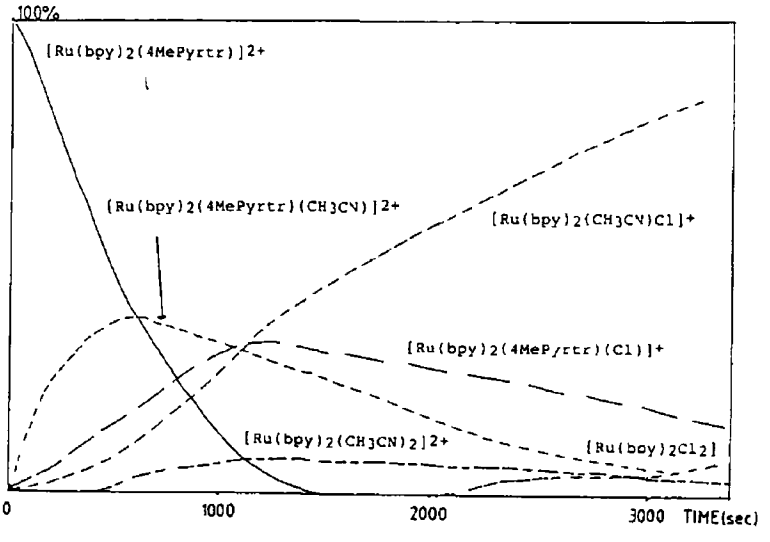


Figure 3 36 Diagrammatic representation of product formation during the photolysis of $[Ru(bpy)_2(4MePyrtr)]^{2+}$ in $CH_3CN$- 0 01 M LiCl as measured from peak area of chromatograms

The desired monovalent complex, $[Ru(bpy)_2(4MePyrtr)Cl]^+$ is formed (peak 1, retention time 1 30 min, absorption maxima 500 nm and 340 nm) The absorption spectrum of this peak obtained from the diode array detection system is shown in Figure 3 37 Peak 1 reaches its maximum intensity at 1200 s comprising of 30% of the total integration area at the end of the reaction, 30% of the area is due to the $[Ru(bpy)_2(CH_3CN)Cl]^+$ (peak 2) complex and the remainder is due to peaks 3 and 4 Peak 4 is due to the complex $[Ru(bpy)_2(CH_3CN)_2]^{2+}$, with a retention time of 7 01 min and absorbance at 425 nm If the reaction is allowed to proceed, then, as peaks 1 and 3 decompose, the major product formed is $[Ru(bpy)_2(CH_3CN)Cl]^+$ (peak 2, retention time 1 95 min, absorption maximum 475 nm) Also, towards the end of the reaction, a small amount of the $[Ru(bpy)_2Cl_2]$ complex (retention time 1 65 min, absorption maximum 530 nm) starts to form Separation of the photolysis products on a preparative scale was not attempted due to the reasons discussed earlier

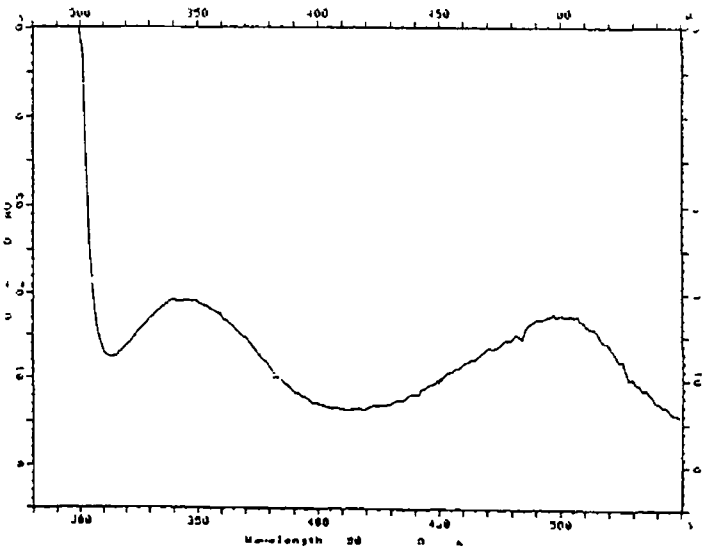

Figure 3 37 Absorption spectrum (from HPLC photo diode array detector) of $[Ru(bpy)_2(4MePyrtr)Cl]^+$ formed photochemically from the photolysis of $[Ru(bpy)_2(4MePyrtr)]^{2+}$ in acetonitrile-LiCl

### 3 3 2 6 Photochemical Stability of Compounds Containing the Chelating Ligands PT, 3BrPT, 3MePT and 4MePyrtr.

It is anticipated that the rate of product decomposition will lead to a better understanding of the excited state properties of compounds containing pyridyltriazole ligands However, a more detailed investigation is necessary in order to accurately determine the stabilities of the compounds photolysed Factors such as quantum yield, irradiation wavelength and light intensity (related to the lifetime of the lamp and decreases with time), must also be considered

These is no marked difference in the photolysis rates of the compounds containing the PT type ligands, whereas it is obvious that the compound containing 4MePyrtr decomposes at a faster rate Observation of the uv/vis spectra of the photolysis of $[Ru(bpy)_2(PT)]^{2+}$ and $[Ru(bpy)_2(4MePyrtr)]^{2+}$ in acetonitrile/LiCl (Figures 3 27 and 3 34 respectively) and the diagrammatic representation of these photolysis (Figures 3 29 and 3 36 respectively) show that the compound containing the PT ligand is more stable than that containing the 4MePyrtr ligand These results show that even though the concentration of $[Ru(bpy)_2(4MePyrtr)]^{2+}$ is approximately three times higher than that of $[Ru(bpy)_2(PT)]^{2+}$, the starting material of the former compound has decomposed within 1500 sec, while that of the latter decomposed at approximately 7000 sec Our photolysis results obtained suggest that the complex $[Ru(bpy)_2(4MePyrtr)]^{2+}$ was found to be the most reactive of the four bivalent species in both acetonitrile and methanol

These results obtained are quite unexpected as they suggest that the compounds containing the PT type ligands, which are weaker emitters (see Section 1), are more stable than

$[Ru(bpy)_2(4MePyrtr)]^{2+}$ which is a stronger emitter One would expect that the energy of the ligand field level, the d-d level, would be lower when the compound is a poor emitter, and hence, this compound would be more susceptible towards photochemical reactions However, our results show that this is not the case

### 3 3 3 Photolysis of Complexes Containing Monodentate Coordinated Pyridyltriazole Ligands.

This section will be treated in a similar manner to the section on photolysis of the bivalent complexes A detailed discussion on the photolysis of $[Ru(bpy)_2(PT)Cl]^+$ in acetonitrile and acetonitrile/LiCl will be given, followed by a general reaction scheme for monovalent samples The comparison of the photolysis of monovalent samples with each other and with the photolysis of their bivalent analogues will conclude this section

#### 3 3 3 1 Photolysis of $[Ru(bpy)_2(PT)Cl]^{\pm}$ in Acetonitrile.

As observed from the uv/vis spectra in Figure 3 38, the photolysis of $[Ru(bpy)_2(PT)Cl]^+$ in acetonitrile yields an isosbestic point at 485 nm The absorption maximum at 497 nm decreases with increasing time with a corresponding increase in absorption at 477 nm This suggests that the ligand is completely lost from the monovalent complex and the major photoproduct formed is $[Ru(bpy)_2(CH_3CN)Cl]^+$ The presence of the isosbestic point indicates that the photolysis reaction is not complex This is confirmed by the HPLC results shown in Figure 3 39 where the rapid decrease of peak 1 (retention time 1 66 min, absorption maximum 497 nm) coincides with the increase of peak 4 (retention time 2 10 min, absorption maximum 475 nm)

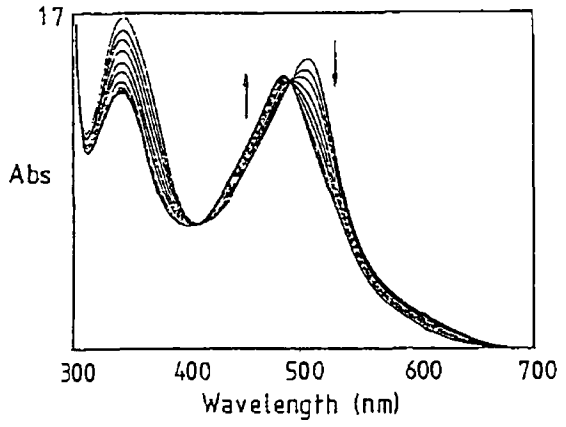


Figure 3 38 Uv/vis spectra of $[Ru(bpy)_2(PT)Cl](PF_6)$ undergoing a photolysis reaction in $CH_3CN$ with respect to time, T = 0 to T = 565 sec

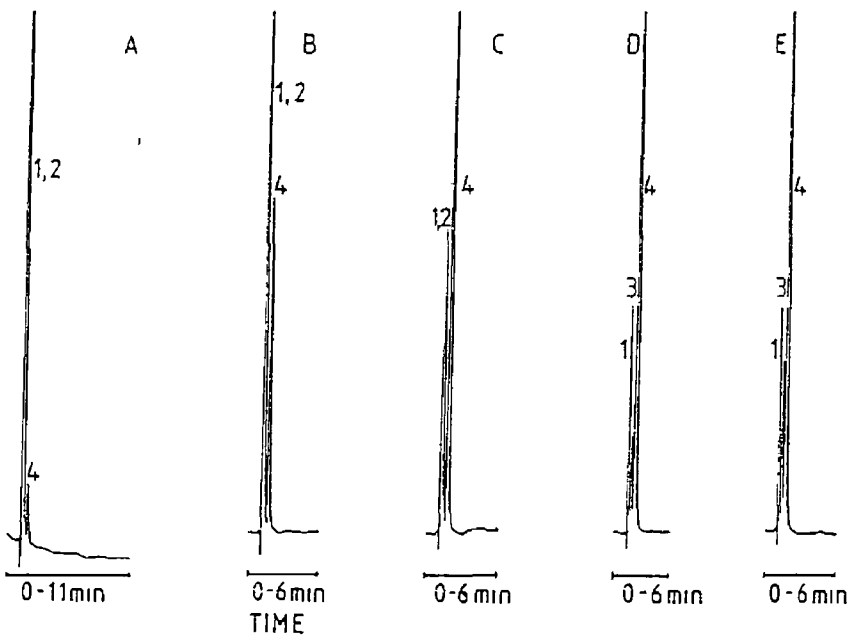


Figure 3 39 Chromatograms taken during the photolysis of $[Ru(bpy)_2(PT)Cl](PF_6)$ in $CH_3CN$ Irradiation times, A, 0 sec , B, 30 sec , C, 75 sec , D, 200 sec , E, 545 sec Flow rate 3 0 ml/min Detection wavelength 280 nm

However, the free ligand occurs at 1 66 min, the same time as that of the starting material The ligand peak (peak 2) is only observed when all the starting material has decomposed, and remains at a constant level as the photolysis proceeds indicating that all the free ligand has been released into the solution A small amount of the neutral species $[Ru(bpy)_2Cl_2]$ has been formed as some of the $[Ru(bpy)_2(CH_3CN)Cl]^+$ complex decomposes, the dichloride species is observed as peak 3, chromatogram E, (retention time 1 81 min, absorption maximum 530 nm) The monovalent species $[Ru(bpy)_2(PT)Cl]^+$ is not a very stable species in solution as it decomposes within minutes of irradiation

3 3 3 2 Photolysis of $[Ru(bpy)_2(PT)Cl]^+$ in Acetonitrile-LiCl.

Photolysis of this sample in acetonitrile/LiCl yields an isosbestic point in the uv/vis spectra (Figure 3 40) at the initial stage of the reaction However, due to the presence of the chlorine atoms supplied by the LiCl, the formation of the $[Ru(bpy)_2Cl_2]$ is more favoured than in the previous photolysis in acetonitrile The isosbestic point is lost as soon as $[Ru(bpy)_2Cl_2]$ (peak 3, retention time 1 81 min, absorption maximum 530 nm) starts to form (as only a small amount of $[Ru(bpy)_2Cl_2]$ formed in pure acetonitrile the isosbestic point was not affected) The HPLC results shown in Figure 3 41 are very similar to those obtained in the pure acetonitrile photolysis, except that a larger quantity of $[Ru(bpy)_2Cl_2]$ was formed The major product of the reaction is $[Ru(bpy)_2(CH_3CN)Cl]^+$ (peak 4, retention time 2 12 min, absorption maximum 475 nm) As with the previous photolysis, the retention time of the ligand was the same as that of the starting material, so the ligand (peak 2, retention time 1.66 min) was only observed when all the starting material has decomposed

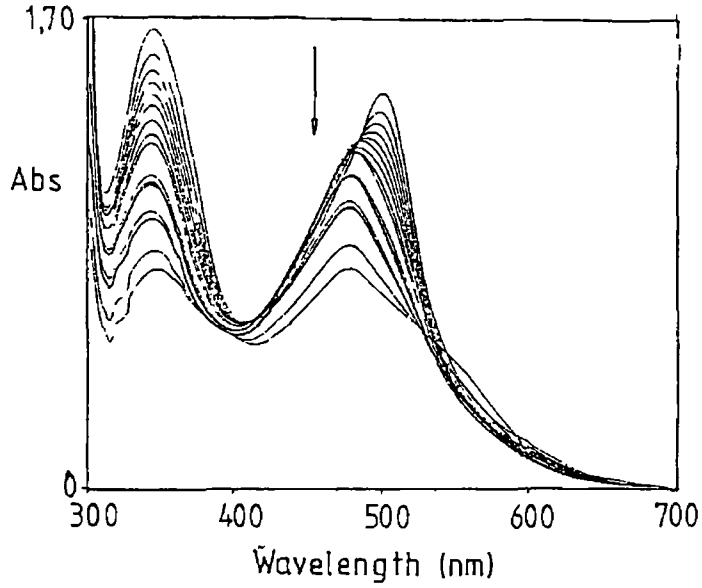


Figure 3 40 Uv/vis spectra of $[Ru(bpy)_2(PT)Cl](PF_6)$ undergoing a photolysis reaction in $CH_3CN$/0 01 M LiCl with respect to time, T = 0 to T = 900 sec

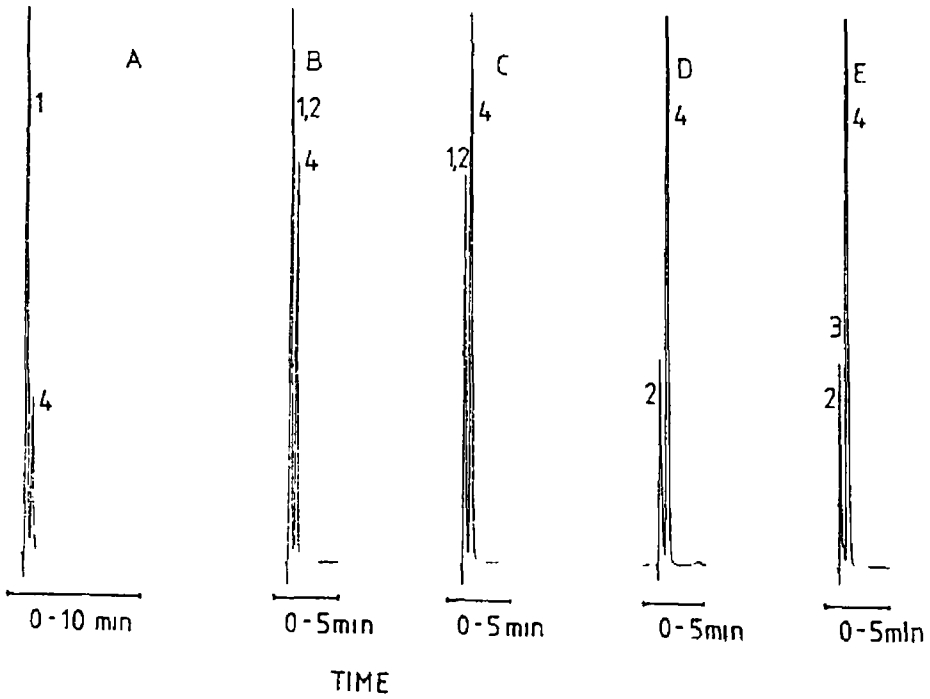


Figure 3 41 Chromatograms taken during the photolysis of $[Ru(bpy)_2(PT)Cl](PF_6)$ in $CH_3CN$/0 01 M LiCl Irradiation times, A, 0 sec , B, 20 sec , C, 90 sec , D, 420 sec , E, 900 sec Flow rate 3.0 ml/min Detection wavelength 280 nm

(1) Acetonitrile

$$[Ru(bpy)_2(L\text{-}L')Cl]^+ \longrightarrow [Ru(bpy)_2(CH_3CN)Cl]^+ + L\text{-}L'$$

(2) Acetonitrile/LiCl

$$[Ru(bpy)_2(L\text{-}L')Cl]^+ \longrightarrow \underset{\text{major product}}{[Ru(bpy)_2(CH_3CN)Cl]^+} + L\text{-}L'$$

$$+ \underset{\text{minor product}}{[Ru(bpy)_2Cl_2]}$$

Figure 3 42 Schematic reaction scheme for compounds containing monodentate PT type ligands in $CH_3CN$ and $CH_3CN$/0,01M LiCl

Figure 3 42 is a schematic diagram of the reactions of the photolysis of the monovalent compounds containing PT, 3BrPT and 3MePT Reactions are very similar for all compounds, resulting in rapid decomposition of starting material Photolysis of $[Ru(bpy)_2(3BrPT)Cl]^+$ and $[Ru(bpy)_2(3MePT)Cl]^+$ in acetonitrile results in the formation of $[Ru(bpy)_2(CH_3CN)Cl]^+$ as the main product This indicates that direct ligand substitution takes place

The photolysis of $[Ru(bpy)_2(3BrPT)Cl]^+$ in acetonitrile/LiCl results in a shift from 485 to 475 nm in the absorption spectra, while a shift from 497 to 475 nm is observed for $[Ru(bpy)_2(3MePT)Cl]^+$ These results indicate that $[Ru(bpy)_2(CH_3CN)Cl]^+$ was the main photoproduct formed The HPLC results show this to be true, but also show that some $[Ru(bpy)_2Cl_2]$ was also formed At no stage during the photolysis of monovalent species in these two solvents was the corresponding bivalent analogue observed as a

photoproduct No photolysis reactions were carried out on $[Ru(bpy)_2(4MePyrtr)Cl]^+$ due to sample shortage As the monovalent complexes are less stable than their corresponding bivalent analogues it is expected that the photolysis of this sample will proceed at a faster rate than its chelating analogue Indeed, complete photolysis of the monovalent complexes occurs within minutes while that of the bivalent complexes proceeds at a slower rate There is no marked difference between the photolysis rates of the compounds containing PT type ligands in a monodentate coordination mode From the results obtained above, however, the site of monodentate coordination for the species produced photochemically cannot be determined While the results obtained show that the ligands in the thermally produced monovalent complexes, $[Ru(bpy)_2(L\text{-}L')Cl]^+$, are coordinated via the $N^{4'}$ atom of the triazole ring, it cannot be concluded that the same monovalent species is produced photochemically as the absorption maxima for the thermally and photochemically produced species are all in the range 495 - 510 nm, see Table 3 15 There is however, a slightly larger difference between the absorption maximum of the thermally and photochemically produced $[Ru(bpy)_2(3BrPT)Cl]^+$ complex

This shift of 15 nm may signify a different coordination mode for the two species The slight differences in the absorption maxima of the other compounds are not sufficient to determine if structural differences exist between the thermally and photochemically produced compounds From HPLC it was not possible to distinguish if there is a difference, as both the thermally and photochemically produced monovalent complexes have the same retention time

Other samples of the type $[Ru(bpy)_2(L\text{-}L')]^{2+}$ where L-L' = HPyrtr, H3MePyrtr, 1MePyrtr and PNP, were photolysed in acetonitrile and acetonitrile/LiCl However, small

quantities of $[Ru(bpy)_2(L\text{-}L')CH_3CN]^{2+}$ were observed but no monodentate-chloride was observed For the photolysis where L-L' = HPyrtr, it is interesting to note that isomer 2 decomposed faster than isomer 1

During the photolysis reactions that were carried out all the products obtained were believed to be in their cis-geometry, from comparison with the literature [81] it is unlikely that trans-species were produced

Table 3 15 Absorption maximum of the monovalent complexes $[Ru(bpy)_2(L\text{-}L')Cl]^+$ produced thermally and photochemically as measured from the HPLC diode array system

| L-L' | Thermal $\lambda_{max}$ nm[a] | Photochemical $\lambda_{max}$ nm |
|---|---|---|
| 4MePyrtr | 500 | 500[a] |
| 3BrPT | 485 | 500[b] |
| 3MePT | 495 | 495[b] |
| PT | 495 | 500[b] |

[a] measured in the mobile phase acetonitrile water (80 20) with 0 08 M $LiClO_4$ [b] measured in the mobile phase acetonitrile water methanol (70 20 10) with 0 08 M $LiClO_4$

3 3 4 Conclusion.

The photolysis experiments were performed in order to investigate the possibilities of producing the monovalent complex $[Ru(bpy)_2(L\text{-}L')Cl]^+$ where L-L' = PT, 3BrPT, 3MePT or 4MePyrtr The monovalent complex $[Ru(bpy)_2(4MePyrtr)Cl]^+$ was observed during the photolysis of $[Ru(bpy)_2(4MePyrtr)]^{2+}$ in acetonitrile/LiCl, while monovalent complexes of the type $[Ru(bpy)_2(L\text{-}L')Cl]^+$ containing the

ligands PT, 3BrPT and 3MePT were observed while photolysing the bivalent analogues in methanol/LiCl

However, the site of monodentate coordination for the species produced photochemically cannot be determined from the results obtained above Knowing that the ligands in the thermally produced monovalent complexes, $[Ru(bpy)_2(L\text{-}L')Cl]^+$, are coordinated via the triazole ring, it cannot be concluded that the same monovalent species is produced photochemically From uv/vis and HPLC results it is not possible to distinguish if there is a difference between thermally and photochemically produced monovalent complexes

However, the two species are expected to have different coordination modes As the thermally produced species are coordinated via the triazole ring, $N^{4'}$ atom for PT type ligands and the $N^{1'}$ atom for 4MePyrtr, it is anticipated that for the photochemically produced species to be coordinated via this mode also, loss of the ligand would result followed by reorientation in solution and subsequent coordination via the triazole ring For this reason it seams likely that the coordination mode for the photochemically produced species is via the pyridine ring or $N^{2'}$ for PT type ligands and 4MePyrtr

The photolysis experiments also yielded information concerning the stability of the monovalent and bivalent complexes containing PT, 3BrPT, 3MePT and 4MePyrtr In acetonitrile or acetonitrile/LiCl the chelating 4MePyrtr complex was found to be less stable than the compounds containing PT, 3MePT and 3BrPT ligands This result suggests that the weaker emitting compounds are more photochemically stable than the stronger emitting 4MePyrtr compound

References.


1 A Juris, V Balzani, F Barigelletti, S Campagna, P Belser, and A von Zelewsky, Coord. Chem. Rev., 1988, 84, 85, and refs therein

2 K Kalyanasundaram, Coord. Chem. Rev., 1982, 46 159

3 E A Seddon and K R Seddon, "The Chemistry of Ruthenium", Monograph 19, Elsevier 1984, and refs therein

4 P S Braterman, A Harriman, G A Heath, and L J Yellowlees, J. Chem. Soc., Dalton Trans., 1983, 1801

5 Y Komada, S Yamauchi, and N Hirota, J. Phys. Chem., 1988, 92, 6511

6 L J Henderson Jr, F R Fronczek, and W J Cherry , J. Am. Chem. Soc., 1984 106, 5876

7 G A Crosby and W H Elfring, J. Phys. Chem., 1976, 80, 2206

8 S Anderson, K R Seddon, R D Wright, and A T Cocks, Chem. Phys. Lett , 1980, 71, 220

9 A T Cocks, R D Wright, and K R Seddon, Chem. Phys. Lett., 1982, 85, 369

10 P J Steel, F Lahousse, D Lerner, and C Marzin, Inorg Chem., 1983, 22, 1488

11 A M Bond and M Haga, Inorg Chem , 1986, 25, 4507

12 K R Barquai, T S Akasheh, P C Beaumount, B J Parsons, and G O Phillips, J. Phys. Chem., 1988, 92, 291

13 F Barigelletti, A Juris, V Balzani, P Belser, and A von Zelewsky, J. Phys. Chem., 1984, 23, 1440

14 A Juris, F Barigelletti, V Balzani, P Belser, and A von Zelewsky, Inorg. Chem., 1985, 24, 202

15 D M Klassen and G A Crosby, J. Chem. Phys., 1968, 48, 1853

16 F E Lytle and D M Hercules, J. Am. Chem. Soc., 1969, 91, 253

17 G H Allen, R P White, D P Rillema, and T J Meyer, J. Am. Chem. Soc., 1984, 106, 2613

18 R J Crutchley and A B P Lever, Inorg. Chem., 1982, 21, 2276

19 P A Mabrouk and M S Wrighton, Inorg. Chem., 1986, 25, 526

20 F Barigelletti, P Belser, A von Zelewsky, A Juris, and V Balzani, J. Phys. Chem., 1985, 23, 384

21 R Hage, R Prins, J G Haasnoot, J Reedijk, and J G Vos, J. Chem. Soc., Dalton Trans., 1987, 1389

22 L J Fitpatrick and H A Goodwin, Inorg. Chim. Acta, 1982, 61, 229

23 A von Zelewsky and G Gremaud, Helv. Chim. Acta, 1988, 71, 1108

24 D M Klassen, Chem. Phys. Lett., 1982, 93, 383

25 M Haga, Inorg. Chim Acta, 1983, 75, 29

26 W J Dressick, B L Hauenstein Jr , T B Gilbert, J N Demas, and B A DeGraff, J. Phys. Chem., 1984, 88, 3337

27 R Kroener, M J Heeg, and E Deutsch, Inorg. Chem., 1988, 27, 558

28 D Conrad, G H Allen, D P Rillema, and T J Meyer, Inorg. Chem., 1983 22, 1614

29 F Barigelletti, A Juris, V, Balzani, P Belser, and A von Zelewsky, Inorg. Chem., 1987, 26, 4115

30 D M Klassen, Inorg Chem., 1976, 15, 3166

31 P C Alford, M J Cook, A P Lewis, G S G McAuliffe, V Skarda, A J Thompson, J L Glasper, and D J Robins, J. Chem. Soc., Perkin Trans 2, 1984, 1293

32 L J Fitzpatrick, H A Goodwin, A Launikonis, A W H Mau, and W H F Sasse, Aust. J. Chem., 1983, 36, 2169

33 J M Kelly, C Long, C M O'Connell, J G Vos, and A H Tinnemans, Inorg. Chem , 1983, 22, 2818

34 D P Rillema, D G Taghdiri, D S Jones, C D Keller, L A Worl, T J Meyer, and H A Levy, Inorg.

Chem., 1987, 26, 578

35 M Haga, T Matsumura-Inoue, K Shimizu, and G P Sato, J. Chem. Soc., Dalton Trans., 1988, 1

36 J G Vos, J G Haasnoot, and G Vos, Inorg. Chim. Acta, 1983, 71, 155

37 B P Sullivan, D J Salmon, T J Meyer, and J Peedin, Inorg. Chem., 1978, 18, 3369

38 G A Crosby, W G Perkins, and D M Klassen, J. Chem. Phys., 1968, 48, 1853

39 J M Sprague and H A Land in "Heterocyclic Compounds", R C Elderfield, Ed., Vol 5, 484, Wiley, New York (1957)

40 K Kalyanasundaram, J. Phys. Chem., 1986, 90, 2285, and refs therein

41 J van Houten and R J Watts, Inorg. Chem., 1978, 17, 5381

42 R J Watts, J S Harrington, and J van Houten, "Inorganic and Organometallic Photochemistry", Amer. Chem Soc., 1978, Chapter 4, 57

43 H Gafney and A W Adamson, J. Amer. Chem. Soc., 1972, 94, 8238

44 S Tachiyashiki, N Nagao, and K Mizumachi, Chem. Lett., 1988, 1001

45 B Durham, J V Casper, J K Nagle, and T J Meyer, J. Am. Chem Soc., 1982, 104, 4803

46 R F Jones and R J Cole-Hamilton, Inorg. Chim. Acta, 1981, 53, L3

47 R G Pearson and O A Gansow, Inorg. Chem., 1968, 7, 1373

48 F Basolo, J C Heyes, and H A Newman, J. Am. Chem. Soc., 1953, 75, 1502

49 B Durham, J C Walsh, C L Carter, and T J Meyer, Inorg. Chem., 1980, 19, 860

50 (a) B Bosnich and F P Dwyer, Aust. J. Chem., 1966, 19, 2229 (b) F P Dwyer, H A Goodwin, and E C Gyarfas, Inorg. Chem., 1963, 16, 344 (c) F P Dwyer,

H A Goodwin, and E C Gyarfas, Inorg. Chem., 1963, 16, 540

51 C Marzin, F Budde, P J Steel, and D Lerner, Nouv. J. Chim., 1987, 11, 33

52 R Hage, J P Turkenbourg, R A G de Graaff, J G Haasnoot, J Reedijk, and J G Vos, Acta. Cryst., (C) in press

53 D S Eggleston, K A Goldsby, D J Hodgson, and T J Meyer, Inorg. Chem., 1985, 24, 4573

54 Hu Zhen-Shan, L Yong-Hua, J Song-Chun, and J G Vos, Acta Cryst., (C) in press

55 D P Rillema, D S Jones, and H Levy, J. Chem. Soc., Chem Commun., 1979, 849

56 R P Thummel, F Letoulon, and J D Korp, Inorg. Chem., 1987, 26, 2370

57 R Hage, R Prins, R de Graaff, J G Haasnoot, J Reedijk, and J G Vos, Acta Cryst, (C) 1988, 44, 56

58 R J Sundberg, R F Bryan, I F Taylor Jr , and H Taube, J Am Chem. Soc., 1974, 96, 381

59 B P Sullivan, D Conrad, and T J Meyer, Inorg. Chem., 1985, 24, 3640

60 J D Birchall, T D O'Donoghue, and J R Wood , Inorg. Chim. Acta, 1979, 37, L461

61 G M Byrant and J E Fergusson, Aust. J Chem., 1971, 24, 441

62 C M O'Connell, Thesis, 1983, Trinity College Dublin, Ireland

63 E C Constable and J Lewis, Inorg. Chim. Acta, 1983, 70, 251

64 D Barton and W D Ollis, "Comprehensive Organic Chemistry" Pergamon Press Ltd , 1979, 4, 361

65 J M Calvert, J V Casper, R A Binstead, T D Westmoreland, and T J Meyer, J. Am. Chem. Soc., 1982, 104, 6620

66 A Juris, V Balzani, P Belser, and A von Zelewsky, Helv Chim Acta, 1981, 64, 2175

67 J N Demas and G A Crosby, J. Mol. Spectrosc., 1976, 98, 286

68 B E Buchanan, unpublished results

69 S M Geraty and J G Vos, J. Chem. Soc., Dalton Trans., 1987, 3073

70 J C Curtis, J S Bernstein, and T J Meyer, Inorg. Chem., 1985, 24, 385

71 C D Tait, D M McQueen, R J Donohue, M K De Armond, K W Kanck, and D W Waltz, J. Phys. Chem., 1986, 90, 1766

72 J M Calvert and T J Meyer, Inorg. Chem., 1982, 21, 3978

73 S Geraty and J G Vos, J. Electroanal. Chem., 1984, 176, 389

74 E S Dodsworth and A B P Lever, Chem. Phys. Lett., 1986, 124 152

75 J V Casper and T J Meyer, Inorg. Chem., 1983 22 2444 (a) S J Valenti and P E Behken, Anal. Chem., 1978, 50, 834

76 J W O'Laughlin and R S Hanson, Anal. Chem., 1980, 52, 2263

77 J W O'Laughlin, Anal. Chem., 1982, 54, 178

78 P K Ghosh, B S Brunschwig, M Chou, C Creutz, and N Sutin, J. Am Chem. Soc., 1984, 106, 4472

79 L Roecker, W Kutner, J A Gilbert, M Simmons, R W Murray, and T J Meyer, Inorg Chem , 1985, 23, 3785

80 B E Buchanan, E Mc Govern, P Harkin, and J G Vos, Inorg. Chim. Acta, 1988, 154, 1

81 E Mc Govern, Thesis, 1988, National Institute for Higher Education, Dublin, Ireland

82 J C Walsh and B Durham, Inorg. Chem., 1982, 21, 329

83 B Durham, S R Wilson, D J Hodgson, and T J Meyer, J Am. Chem. Soc., 1980, 102, 600

# Chapter 4

## Acid-Base Chemistry of Ruthenium Compounds Containing Pyridyltriazole Ligands

## 4 0 Introduction.

During the past 15 years there has been great activity in the study of the ground state and excited state chemistry of the $[Ru(bpy)_3]^{2+}$ cation [1-4] Of particular importance to this chapter have been studies of the excited state photochemistry and photophysics of this species with a view to developing new photocatalysts [3] The considerable time and effort spent investigating this species has contributed greatly to our understanding of the chemistry of inorganic molecules in the excited state [5] It has been proposed that the study of acid-base chemistry in the excited state can provide information on the charge redistribution which occurs upon excitation Electronic spectra have been widely used in the study of organic bases, to evaluate $pK_a$ values [6, 7] The $pK_a$ is an indication of the strength or weakness of an acid, the smaller the $pK_a$, the stronger the acid In the literature, some studies of ruthenium compounds undergoing proton transfer reactions have been reported [7-19] Such studies are of interest as the acid-base properties of ground and excited state can often be related to electron density distributions in the compounds It is generally agreed that the excited state acidity can be related to the nature of the emitting states of the compounds investigated [20] If the acidity in the excited state has increased the ligand is not expected to be directly involved in the excited state process, but merely present as a spectator ligand If however, the acidity is decreased, the excited electron is thought to be localised on the ligand, and this ligand is therefore actively involved in the emission process of the ruthenium compounds [15-20]

For most compounds, the $pK_a$ of the coordinated ligand in the ground state is more acidic than the $pK_a$ of the un-coordinated ligand [7-18] One exception however is

$[(NH_3)_5Ru(pyrz)]^{2+}$, where pyrz = pyrazine, which exhibits reverse behaviour [19] In this case, the $pK_a$ of the doubly charged cation ($pK_a$ = 2 5± 0 1) is nearly two orders of magnitude more basic than the uncoordinated ligand ($pK_a$ = 0 6) [21] One would expect at first instance, that the electrostatic effect of coordination of pyrazine to the positively charged ruthenium (II) center would result in making the remaining nitrogen less basic than in the free ligand However, from the results obtained above, Taube et al [19] concluded that the ruthenium (II) center participates in some special interaction with the ligand that more than compensates for the expected electrostatic effect They therefore postulated that such an interaction could be attributed to back donation of electron density from the filled metal based $t_{2g}$ orbitals into the unoccupied $\pi$ antibonding orbitals of the ligand This increase in $pK_a$ is consistent with an increase in electron density on the pyrazine ring caused by overlap with the filled metal orbital The extent of this overlap will be determined by how close the pyrazine $\pi^*$ orbitals and the available metal orbital of proper symmetry are in energy and by the radial extension of this metal orbital In a general sense, the better the overlap between the metal and the pyrazine orbital the higher the $pK_a$ of the coordinated $Hpyrz^+$

Ligands similar in structure to pyrazine such as pyridazine and pyrimidine have conjugate acids with $pK_a$'s of 2 33 and 1 3 respectively [21] However, coordination of these ligands to the $(NH_3)_5Ru$ moiety results in $pK_a$'s of 0 03 and 0 00 respectively [19] That is, the ligands pyridazine and pyrimidine are more acidic when coordinated to the $(NH_3)_5Ru$ grouping This can be explained by assuming that the overlap of the ligand orbitals with the metal orbital is small and the dominating contribution from metal coordination at that site is electrostatic The excited

state $pK_a$'s of complexes of the type $[(NH_3)_5RuL]^{2+}$ where L = pyrazine, pyridazine and pyrimidine are 7 3, 6 5 and 1 9 respectively and were calculated using the Forster equation [6] This indicates that the ligands are more basic in the excited state than in the ground state, suggesting that the ligand electron density is significantly increased in the excited state [19]

The pyrazine ligand has been important in the development of the chemistry of the $[(NH_3)_5RuL]^{2+}$ series The $pK_a$ determination for $[(NH_3)_5Ru(PyrzH)]^{3+}$ by Taube et al [19] discussed above, and the subsequent synthesis of the Creutz and Taube dinuclear compound $[(NH_3)_5Ru(pyrz)Ru(NH_3)_5]^{4+,5+,6+}$ [22] illustrate this point Johnson and Shepherd [12] have reported the $pK_a$ for $[(CN)_5Ru(pyrzH)]^{2-}$ and have investigated the influence of $CN^-$ versus $NH_3$ in competition with pyrazine for back donation from Ru(II) In contrast to the $[(NH_3)_5Ru(pyrzH)]^{3+}$ system, coordination of pyrz to the $(CN)_5Ru$ group results in the increased acidity of the pyrazine ligand ($pK_a$ $[(CN)_5Ru(pyrz)]^{3-}$ = 0 4) This indicates that the replacement of the $NH_3$ with CN in the set of spectator ligand will cause the basicity of the coordinated $pzH^+$ to decrease as $CN^-$ competes effectively for $\pi$-electron density ($CN^-$ is a good $\pi$ acceptor) The excited state $pK_a$, $pK_a^*$ of $[(CN)_5Ru(Hpyrz)]^{2-}$ determined using the Forster equation [6], shows that the ligand is more basic in the excited state than in the ground state The $pK_a^*$ value for $[(CN)_5Ru(Hpyrz)]^{2-}$ is found at 14 7, considerably more basic than that of $[(NH_3)_5Ru(pyrzH)]^{3+}$ From these results, Johnson and Shepherd [12] have suggested that ammonia does not stabilize the $d\pi$ orbitals on the metal Thus the $d\pi$ orbitals remain high in energy and can interact strongly with the pyrz $\pi^*$ orbital Cyanide on the other hand lowers the $d\pi$ orbitals significantly through back-bonding This makes back bonding to pyrz less

favourable because the energy difference between the pyrz $\pi^*$ orbital and the metal orbital of proper symmetry is large So, these results suggest that metal-to-ligand back-donation onto pyrz in the cyano complex is small while in the pentamine de- localization is more extensive

Complexes of the type $[(NH_3)_5RuL]^{3+}$ have also been studied, where L = pyrazole (Hpz), imidazole (Him), 3,5-dimethyl-pyrazole ($HMe_2pz$) or 1,2,4 triazole (Htrz), and the $pK_a$ values are presented in Table 4 1 One of the effects of coordination of imidazole or pyrazole to a metal ion is that the pyrrole-like nitrogen becomes less basic compared to the free ligand [23, 24]

Table 4 1 Acid dissociation constants for $(NH_3)_5Ru$ containing compounds

| Compound | $pK_a$ |
|---|---|
| $[(NH_3)_5Ru(Hpz)]^{3+}$ | 5 98[a] |
| $[(NH_3)_5Ru(Him)]^{3+}$ | 8 90[b] |
| $[(NH_3)_5Ru(HMe_2pz)]^{3+}$ | 7 21[a] |
| $[(NH_3)_5Ru(Htrz)]^{3+}$ | 4 30[a] |

[a] reference 25, [b] reference 26

The $pK_a$ values for the free neutral ligands are 14 2 for both Hpz and Him [25], and 10 26 for Htrz [26] As can be seen for these values, $[(NH_3)_5Ru]^{3+}$ coordination lowers the $pK_a$ values considerably This is due to the positive charge of ruthenium, withdrawing electron density from the ligand, and thus lowering the $pK_a$ As expected, due to the electron donating properties of the methyl groups, the $pK_a$

of $[(NH_3)_5(HMe_2pz)]^{3+}$ is found at higher pH than $[(NH_3)_5Ru(Hpz)]^{3+}$

Other systems involving $CN^-$ ions were investigated by Peterson and Demas [11, 27] The complexes studied were $[Ru(bpy)_2(CN)_2]$ and $[Ru(phen)_2(CN)_2]$ In these compounds protonation can take place at the $CN^-$ sites For both complexes a strong blue shift in the absorption spectra is observed with increasing acidity but no isosbestic points are observed These results are consistent with the two step protonation of the CN groups to form species such as $[Ru(bpy)_2(HCN)(CN)_2]^+$ and $[Ru(bpy)_2(HCN)_2]^{2+}$ Acidified solutions of $[Ru(bpy)_2(CN)_2]$ and $[Ru(phen)_2(CN)_2]$ all emit with the characteristic orange spectrum of the parent unprotonated complexes in water, although with reduced intensity However, at 77 K in highly acidic 96% $H_2SO_4$ solution the emission of the protonated $[Ru(phen)_2(CN)_2]$ was found to be bright blue rather than the characteristic orange This emission spectrum and that of the protonated $[Ru(bpy)_2(CN)_2]$ complex bear a striking resemblance to that of the $^3(\pi - \pi^*)$ phosphorescence of $[Rh(phen)_3]^{3+}$ The authors have concluded that for both complexes, the lowest MLCT state of the doubly protonated species is raised above the lowest ligand localised $^3(\pi - \pi^*)$ and emission changes from MLCT in nature to $^3(\pi - \pi^*)$ phosphorescence These results are interesting as they present the first case of inversion of excited state type on undergoing a protonation reaction

Studies on complexes containing the $Ru(bpy)_2$ moiety include the $[Ru(bpy)_2(bpy(COOH)_2)]^{2+}$ system where investigations were initially carried out by Wrighton et al [8] The absorption spectra of $[Ru(bpy)_2(bpy(COOH)_2)]^{2+}$ as a function of pH exhibits only one isosbestic point, indicating that both -COOH groups have approximately the

same $pK_a$ value A $pK_a$ of 5 5 was observed for a two proton equilibrium However, a more recent investigation of the acid-base properties of this system using pH's < 1 0 show that a slight shift off the isosbestic point is observed [10] Two inflection points were observed at 2 65 and ~0 5 indicating that a two step acid-base equilibrium of the carboxyl moieties in the $bpy(COOH)_2$ ligand exists as shown below

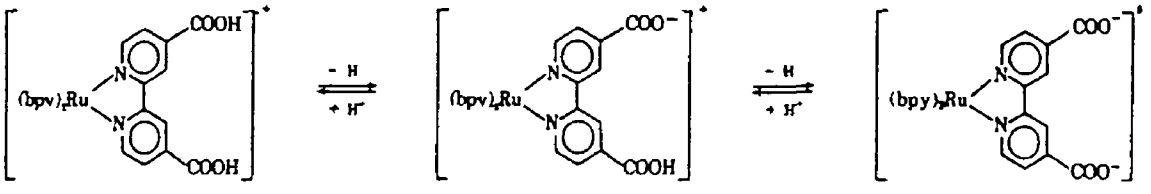


(1)

In contrast to the results obtained by Wrighton et al [8], these results suggest that the two carboxyl acid groups behave independently In agreement with this, the acid-base properties of the free ligand exhibits two $pK_a$ values ($pK_{a1}$ = 3 7 and $pK_{a2}$ < 2 0) Upon coordination of the $bpy(COOH)_2$ ligand to ruthenium the carboxyl moiety in the $bpy(COOH)_2$ ligand ($pK_{a2}$ = 2 65) is nearly one order of magnitude more acidic than that of the free ligand This suggests that the coordination of the ligand reduces the electron density of the carboxyl moiety, which results from $\pi$ back-donation from ruthenium to ligand, and from the electrostatic interaction effected by the coordination of the ligand to the ruthenium center responsible for the increase of the acidity This is again in contrast to the $[(NH_3)_5Ru(pyrz)]^{2+}$ complex where the $pK_a$ has been shown to be increased by the $\pi$ back-donation which more than

compensates for the electrostatic effect [19] Therefore, the increase of acidity of $[Ru(bpy)_2(bpy(COOH)_2)]^{2+}$ implies that the interaction with the unoccupied $\pi$ orbitals of the parent bipyridine is smaller than that with the electrostatic effect

The excited state protonation equilibrium of $[Ru(bpy)_2(bpy(COOH)_2)]^{2+}$ has been measured by luminescence titration, by exciting at one of the isosbestic points [3, 5] Shimidzu et al [10] observed one inflection point at pH = 3 9 which is different to that obtained from the absorbance titration curve of by about 1 5 pH units The authors suggest that, since the two acid groups are expected to have two distinct $pK_a$'s in the excited state, the inflection point represents the equilibrium between the deprotonated and the monoprotonated form and indicates that the other equilibrium (between monoprotonated and diprotonated forms) is lower than pH 0 2 The results illustrate that the excited state complex can be protonated without electronic deactivation, i e when at pH 3 5 one excites in the deprotonated form, emission which is predominantly from the monoprotonated form is observed

An excited state $pK_a$, $pK_a^*$ of 4 3 was determined by Shimidzu et al [10], the lifetimes of the mono and deprotonated forms are 0 21 and 0 46 $\mu$s respectively A $pK_a^*$ value of 3 9 was calculated using the Forster equation [6] These two values of $pK_a^*$ are quite similar, in contrast to the large difference in $pK_a^*$ values of 8 5 and 5 9 obtained by Wrighton et al [8] which resulted from failure of assuming the one step acid -base equilibrium in the ground state The result obtained by Shimidzu et al [10] relied upon observations of a two step equilibrium The difference observed between $pK_a$ and $pK_a^*$ indicates that the deprotonated complex is a stronger base in the excited state than in the ground state This suggests that the

ligand electron density is significantly higher in the excited state than in the ground state This suggests that the excited electron may be located on the bpy(COOH)$_2$ ligand

Wrighton et al [9] have reported on the ground and excited state acid-base chemistry of the four complexes [(4,7-dihydroxy-1,10-phenanthroline)RuL$_2$]$^{2+}$ [L = bpy, Me$_2$bpy, phen and Me$_4$phen) The deprotonation equilibria are shown below

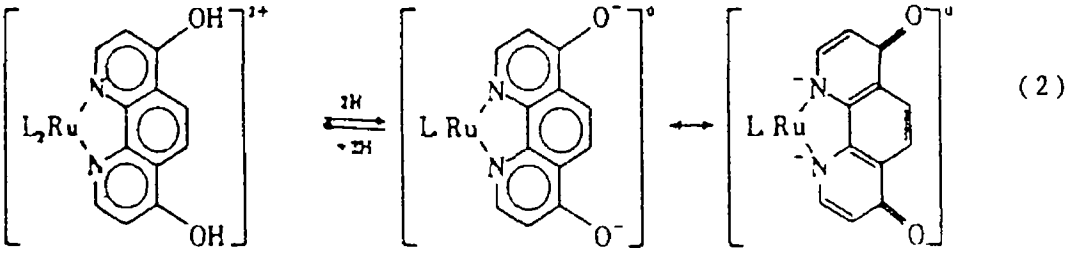


(2)

The titration of [(phen(OH)$_2$)RuL$_2$]$^{2+}$ shows only one end-point consistent with the plots of change in optical density versus pH which shows only one inflection point The pK$_a$ values obtained for the dihydroxy phenthroline compounds are all approximately 10 The excited state pK$_a$ values for the [(4,7-dihydroxy-1,10-phenanthroline)RuL$_2$]$^{2+}$ compounds were calculated using the Forster equation [6], and also by using the lifetimes of the protonated and deprotonated complex The results, in Table 4 2 clearly show that the excited species are stronger acids than their ground state counterparts The change in the value of the overall dissociation constant is very substantial and much larger than the change previously reported for

$[Ru(bpy)_2(bpy(COOH)_2)]^{2+}$ [8, 10] There is a net drain of electron density from the deprotonated 4,7-dihydroxy-phenanthroline ligand in the excited state via electron donation to the ruthenium metal

Table 4.2 Acid dissociation constants for the $[(phen(OH)_2)RuL_2]^{2+}$ series of compounds, where L = bpy, $Me_2bpy$, phen and $Me_4phen$

| L | $pK_a$ | $pK_a$*[a] | $pK_a$*[b] |
|---|---|---|---|
| bpy | 10 1 | 5 1 | 6 7 |
| $Me_2bpy$ | 10 0 | 5 4 | 6 5 |
| phen | 10 0 | 4 7 | 6 1 |
| $Me_4phen$ | 9 8 | 5 6 | 6 1 |

[a] calculated using the Forster equation, [b] calculated using lifetime measurements

The acid-base chemistry of $[Ru(bpz)_3]^{2+}$ where bpz = bipyrazine, has been investigated by Crutchley et al [5] This cation has six uncoordinated nitrogen atoms potentially available for protonation A combined absorption and emission study was able to delineate all six protonation steps The first three protonation steps involve nitrogen atoms, one to each ligand, which in the excited state are more basic than the ground state, the difference decreasing with each protonation step Thus, in general, excitation results in an excited state which is quenched by reaction with a proton during its lifetime, i e , the excited state under the given acid conditions, contains at equilibrium one more proton than the ground state The first three $pK_a$ values for $[Ru(bpz)_3]^{2+}$ are

more negative than the value obtained for the free ligand indicating that the coordinated $bpzH^+$ is a stronger acid than the free protonated ligand

The subsequent three protonation steps take place at a ligand which already possesses a proton and at a nitrogen atom which is less basic than the ground state The subsequent three protonation steps take place at a ligand which already posses a proton and at a nitrogen atom that is less basic than the ground state Other systems of interest include the acid-base spectroscopic studies on complexes of the type $[Ru(bpy)_2(L\text{-}L)]^{2+}$, where L-L = 2-(2-pyridyl)benzimidazole (PbzimH), 2-(2-pyridylimidazole) (PimH), 2,2'-bibenzimidazole ($bibzimH_2$) and 2,2'-biimidazole ($biimH_2$) (see Figure 3 3, Chapter 3 for structures) [28, 29] Deprotonation of $[Ru(bpy)_2(bibzimH_2)]^{2+}$ results in a shift to lower energy of the absorption maximum A similar effect is observed for the deprotonation of complexes containing PbzimH, pimH and $biimH_2$ The acid ionization constants $pK_{a1}$ and pKa2 for these compounds are listed in Table 4 3

Table 4.3 Acid ionization constants of $[Ru(bpy)_2(L\text{-}L)]^{2+}$, where L-L = PbzimH, PimH, $bibzimH_2$ and $biimH_2$ at 25°C [29]

| Compound | $pK_{a1}$ | $Pk_{a2}$ | $pK_a{}^{*a}$ |
|---|---|---|---|
| $[Ru(bpy)_2(PbzimH)]^{2+}$ | 6 8 | | 4 1 |
| $[Ru(bpy)_2(PimH)]^{2+}$ | 7 9 | | 5 2 |
| $[Ru(bpy)_2(bibzimH_2)]^{2+}$ | 5 7 | 10 1 | 2 6[a] |
| $[Ru(bpy)_2(biimH_2)]^{2+}$ | 7 3 | 12 0 | 5 0[a] |

a $pk_{a1}{}^*$ value

Comparison of the $pK_a$ values of the PimH and PbzimH complexes with those of free PimH and PbzimH (13 4 and >12 respectively [29]) indicates that the acidity of the conjugate acids of these ligands increases upon their coordination to the ruthenium ion The $pK_a$ values of complexes of the benzimidazole derivatives are smaller than those of the imidazole derivatives This is due to the electron withdrawing effect of the benzimidazole benzene

The excited state $pK_a^*$ values for the compounds are evaluated from the absorption band maxima of the protonated and deprotonated forms in these complexes using the Forster cycle [6] (the emission bands could not be used as the emission of the protonated species is very weak) The values obtained for the $pK_a^*$ suggest that the excited state species are stronger acids than the ground state complexes

In our investigations of the series of pyridyltriazole compounds in Chapter 3, it was observed that some of the ligands such as 3-(pyridin-2-yl)-1H-1,2,4-triazole and 3-methyl-5-(pyridin-2-yl)-1H-1,2,4-triazole easily deprotonate when bound to the $Ru(bpy)_2$ moiety In this chapter, the pH dependence of the ground state and of the excited state properties of these compounds (and of the free ligands) has been investigated using spectrophotometric and emission lifetime techniques The results obtained are discussed in relation to the nature of the emitting triplet metal-to-ligand charge-transfer state ($^3$MLCT) of the ruthenium compounds and the electronic properties of the ligands

## 4 1 Acid-base chemistry of the free ligands HPyrtr and H3MePyrtr

In order to be able to compare the acid-base chemistry of

the coordinated ligand with that observed for the free ligand, titration experiments were first carried out with uncoordinated HPyrtr and H3MePyrtr Investigations of the ground state properties were carried out using uv/vis spectroscopy, while the excited state behaviour was studied using luminescence spectroscopy All spectral changes observed were reversible UV/vis spectra obtained in typical experiments with the free ligands are shown in Figure 4 1 Both ligands were investigated in the pH range from 1 0 to 11 0 Between pH 1 0 and 6 0 isosbestic points were observed at 272 nm for HPyrtr and at 275 nm for H3MePyrtr In this pH range the lowest energy absorption shifts from about 272 nm at pH 2 0 to 286 at pH 6 0 In the pH range from 6 0 to 11 0 isosbestic points were observed at 239 nm for HPyrtr and at 243 nm for H3MePyrtr together with shifts to lower energy of both absorption bands with increasing pH (See Table 4 4) $PK_a$ values obtained from these experiments are listed in Table 4 5

Table 4.4 Acid-Base Properties of the Pyridyltriazole Ligands, Spectroscopic Data

| Species | abs max (nm) (log ∈) | em max (nm) |
|---|---|---|
| $H_2Pyrtr^+$ | 286(4 17),232(4 24) | 435 |
| $H_23MePyrtr^+$ | 290(4 14),230(3 97) | 475 |
| HPyrtr | 273(4 03),232(4 12) | 370 |
| H3MePyrtr | 272(4 06),235(4 02) | 375 |
| $[Pyrtr]^-$ | 279(4 04),243(4 11) | 435 |
| $[3MePyrtr]^-$ | 283(4 05),252(4 01) | 460 |

Measurements were carried out in Britton-Robinson buffers using $10^{-4}$ mol/dm$^3$ solutions of the ligands for the absorption experiments and $10^{-6}$ mol/dm$^3$ for the emission studies

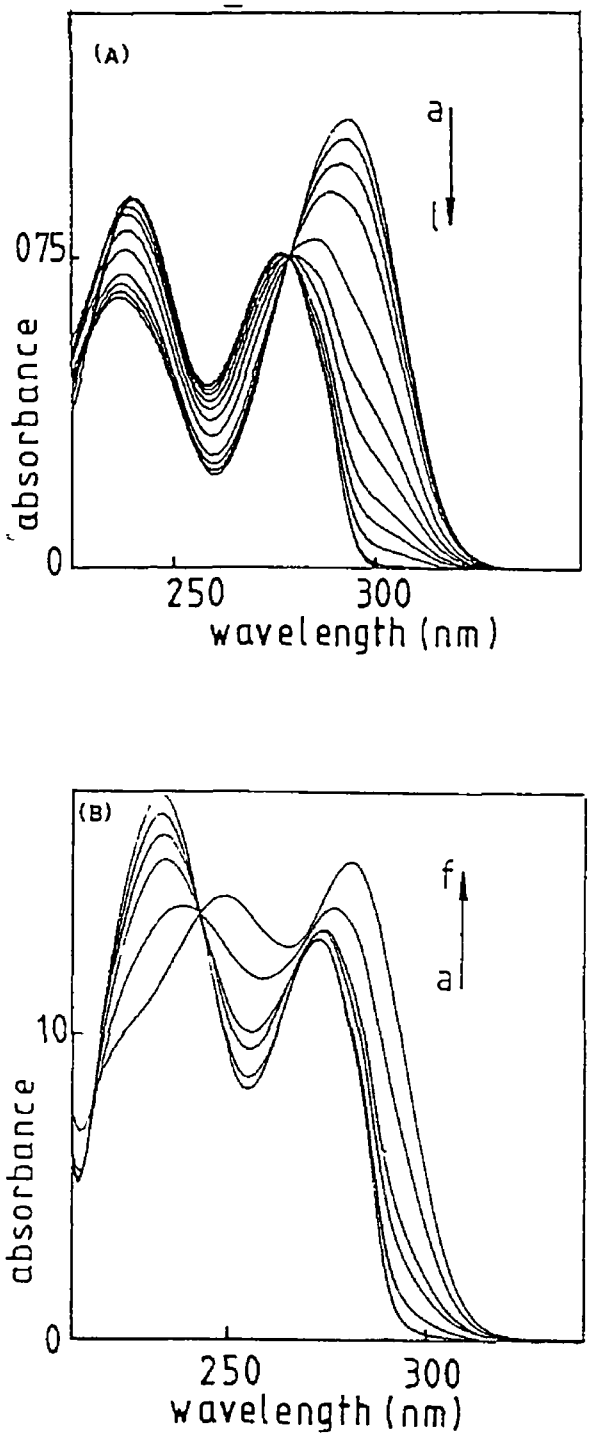


Figure 4 1 PH dependence of the absorption spectrum of HPyrtr in aqueous Britton robinson buffer (1 0 x $10^{-4}$ mol $dm^{-3}$) (a) for curves (a)-(1) pH 1 21, 2 36, 2 46, 2 89, 3 30, 3 63, 3 84, 4 13, 4 36, 4 69, 5 39, 6 20 (b) for curves (a)-(f) pH 7 97, 8 89, 9 37, 9 62, 10 16, 11 00

The pH dependence of the emission of the compounds was investigated over the same pH range Going from pH 6 0 to 1 0 a significant increase of the emission intensity was observed parallel with a shift of the emission maxima to lower energy When the data were analysed as emission titrations, inflection points at pH = 2 9 (± 0 3) and 3 1 (± 0 3) were found for HPyrtr and H3MePyrtr respectively Going from pH 6 0 to pH 11 0 again an increase of the emission intensity is observed, combined with an increase in the emission wavelength In this pH range inflection points were obtained at pH values of 8 9 (± 0 3) and 9 8 (± 0 2) for HPyrtr and H3MePyrtr respectively The emission maxima of the different species involved have been listed in Table 4 4

The spectroscopic changes observed with changing pH can be rationalised by assuming protonation of the ligands at low pH and deprotonation at higher pH as described in reaction 3

$$(H_2Pyrtr)^+ \overset{pK_a(base)}{\underset{H^+}{\rightleftharpoons}} HPyrtr \overset{pK_a(acid)}{\underset{H^+}{\rightleftharpoons}} (Pyrtr)^- \qquad (3)$$

This interpretation is consistent with experiments carried out with N-substituted ligands, such as 4-methyl-3-(pyridin-2-yl)-4H-1,2,4-triazole (4MePyrtr) For this ligand a variation of the absorption spectrum was only observed in the pH range from 1-6, yielding a $pK_a$(base) of 4 2 ± 0 2 [30] The $pK_a$(acid) values observed for the neutral ligands of about 9 50 are somewhat smaller than obtained for 1,2,4-triazole (10 26) [31], while the $pK_a$(base) values obtained are similar to those reported for pyridine (5 25) [32], 2,2-bipyridyl (4 45) [33], and 1,2,4-triazole (2 27) [31] From the $pK_a$(base) values one would expect protonation of the neutral ligand to occur first at the pyridine ring, however hydrogen bridge

formation to the adjacent triazole N-atom is likely

It is important to note that the lowest energy absorption maxima observed for the pyridyltriazole ligands are very close to the $\pi$ ----> $\pi^*$ transitions (280 nm) in 2,2'-bipyridyl, this could result in an electronic interaction between these orbitals in the ruthenium compounds However, the reduction potentials of HPyrtr and H3MePyrtr are found at more negative values than that of bpy, indicating that the $\pi^*$ orbitals of bpy lie at lower energy than the $\pi^*$ orbitals of the pyridyltriazole ligands The first reduction potentials of HPyrtr, H3MePyrtr and 4MePyrtr are found at a more negative potential than bpy (see Chapter 3) Also the changes in the emission spectra can be rationalised by the occurrence of protonation and deprotonation reactions as described for the ground state The excited state properties of the free ligands will be discussed below, together with those observed for the ruthenium compounds

## 4 2 Acid-base Chemistry of Ruthenium Compounds in the Ground State

Figures 4 2 (a) and (b) show the effect of the change of pH on the uv/vis spectrum of isomer 1 and isomer 2 of $[Ru(bpy)_2(HPyrtr)]^{2+}$ respectively For isomer 1, isosbestic points are observed at 322, 390 and 458 nm and the $\lambda_{max}$ of the lowest absorption maximum shifts from 450 nm to 470 nm For isomer 2, isosbestic points are observed at 322, 386 and 457 nm and the $\lambda_{max}$ of the lowest energy absorption maximum shifts from 437 to 465 nm For $[Ru(bpy)_2(H3MePyrtr)]^{2+}$ similar behaviour is observed with isosbestic points at 321, 387 and 456 nm and a shift in the position of the lowest absorption band from 438 to 467 nm going from low to high pH

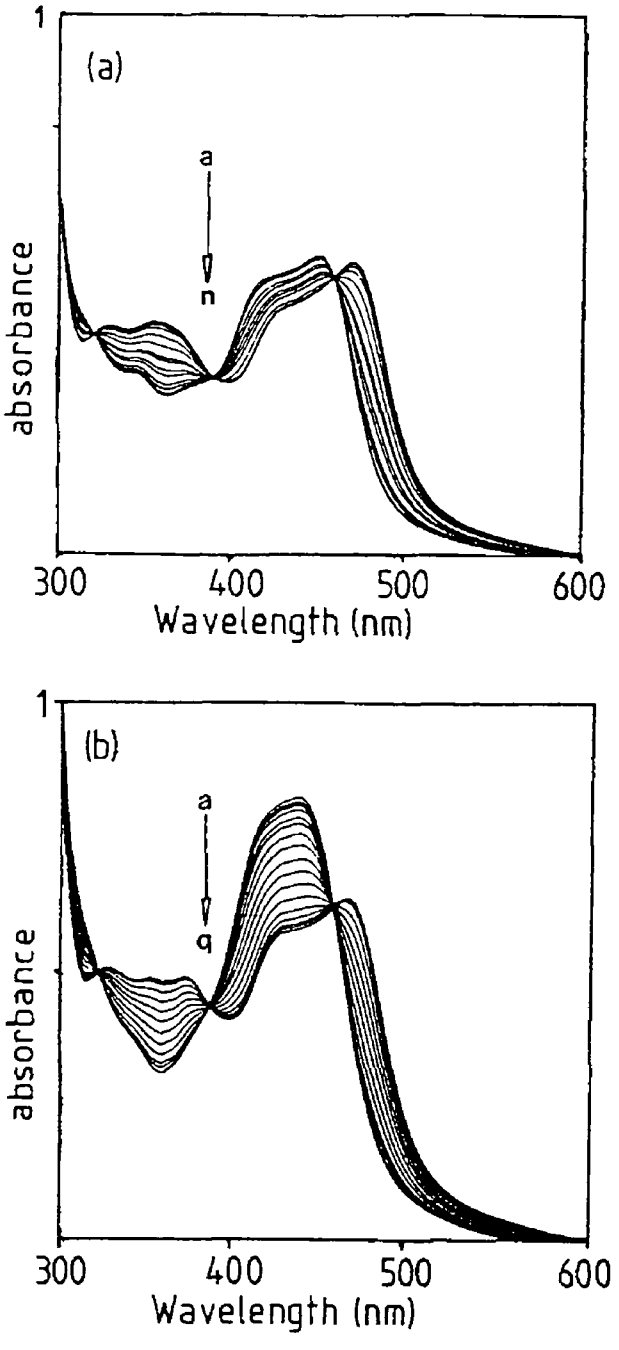


Figure 4 2 PH dependence of the absorption spectrum of (a) isomer 1 of $[Ru(bpy)_2(HPyrtr)]^{2+}$ in an aqueous Britton Robinson buffer (6 3 x $10^{-5}$ mol $dm^{-3}$), for curves (a)-(n) pH 2 42, 3 52, 4 25, 4 93, 5 16, 5 53, 5 70, 5 95, 6 07, 6 33, 7 07, 7 47, 7 99, 8 53 and (b) isomer 2 of $[Ru(bpy)_2(HPyrtr)]^{2+}$ in an aqueous Britton Robinson buffer (6 3 x $10^{-5}$ mol $dm^{-3}$) for curves (a)-(q) pH 1 58, 1 93, 2 18, 2 51, 2 97, 3 18, 3 48, 3 70, 3 93, 4 14, 4 35, 4 60, 4 92, 5 33, 5 75, 6 17, 6 73

All changes are fully reversible and independent of the direction of the pH change The changes in spectroscopic features for all compounds are summarised in Table 4 6 The $pK_a$(acid) values of the ruthenium compounds obtained are listed in Table 4 5

Table 4.5 Dissociation constants of Free and Complexed Pyridyltriazoles

| Compound | $pK_a$ (acid) | $pK_a$ (base) | $pK_a$*a (acid) | $pK_a$*b (acid) | $pK_a$*b (base) |
|---|---|---|---|---|---|
| HPyrtr | 9 20 | 3 32 | - (8 9) | 7 5 | 6 9 (2 9) |
| H3MePyrtr | 9 80 | 3 40 | - (9 8) | 6 8 | 8 3 (3 1) |
| Isomer 1 | 5 95 | - | 4 22(5 1) | 4 9 | |
| Isomer 2 | 4 07 | - | 2 12(2 7) | 2 1 | |
| 3 | 4 87 | - | 4 44(4 2) | 3 5 | |

Isomers 1 and 2 are the two isomers of $[Ru(bpy)_2(HPyrtr)]^{2+}$, 3 = $[Ru(bpy)_2(H3MePyrtr)]^{2+}$ All ground state $pK_a$ values and inflection points are ± 0 05, excited state $pK_a$ ± 0 2, values in parentheses are the inflection points of the emission titration curves, [a] $pK_a$*(acid) calculated using equation 6, [b] $pK_a$* values obtained using Equation 5, for details see text

It is generally agreed that the lowest energy absorptions, found around 450 nm in the absorption spectrum of ruthenium bis(bpy) compounds, can be described as singlet metal-to-ligand charge-transfer ($^1$MLCT) transitions, in which the electron is excited from a metal based d-orbital to a ligand based $\pi^*$ orbital The emission occurs in most of these compounds from a bpy-based $^3$MLCT state, which is populated from the singlet state with an efficiency of

close to 1 [1, 14, 34] The changes in the absorption and emission spectra with pH of isomers 1 and 2 and $[Ru(bpy)_2(H3MePyrtr)]^{2+}$ can be explained by deprotonation of the pyridyltriazole ligands at higher pH, yielding respectively $[Ru(bpy)_2(Pyrtr)]^{+}$ (isomers 1 and 2), and $[Ru(bpy)_2(3MePyrtr)]^{+}$ (see Equation 4)

$$[Ru(bpy)_2(HPyrtr)]^{2+} \underset{H^+}{\overset{pK_a(acid)}{<\!\!-\!\!-\!\!-\!\!-\!\!-\!\!-\!\!-\!\!-\!\!>}} [Ru(bpy)_2(Pyrtr)]^{+} \quad (4)$$

Results obtained [30] in similar experiments with the compound $[Ru(bpy)_2(4MePyrtr)]^{2+}$, where 4MePyrtr is the neutral ligand 4-methyl-3(pyridin-2-yl)-1,2,4-triazole, confirm this interpretation For this last compound no variation of the absorption spectrum with pH was observed The changes observed in the absorption spectra of isomers 1 and 2, and $[Ru(bpy)_2(H3MePyrtr)]^{2+}$ can be explained by an increased ease of electron donation from the deprotonated ligand to the ruthenium center This results in a destabilisation of the metal based ground state and a decrease in the energy of both absorption and emission maxima [6]

The $pK_a$ values given in Table 4 5 show that the ligands act as much stronger acids after coordination to the $Ru(bpy)_2$-moiety, with the $pK_a$(acid) being changed by between three and five orders of magnitude Similar behaviour has been observed for a number of related ruthenium compounds, such as the $Ru(bpy)_2$ complexes of 4,7-dihydroxy-1,10-phenanthroline [9], 4,4'-dicarboxy -2,2'-bipyridine [8, 10], 2,2'-benzimidazole [28, 35] and others The only exception is the compound $[(NH_3)_5Ru(pyrz)]^{2+}$ (pyrz = pyrazine) reported by Taube et al [19] The increased acidity in the compounds reported here can be attributed to electron donation from the pyridyltriazole ligand to the

central metal ion On the other hand the increase in the basicity of the pyrazine ligand on coordination has been attributed to strong metal-to-ligand backdonation [19] The increased acidity observed for the pyridyltriazoles upon coordination suggests therefore that in the ruthenium reported here, electron donation from the pyridyltriazole ligands to the central metal atom is more important than metal-to-pyridyltriazole back-donation

Table 4 6 Excited State Properties of Compounds of the Type $[Ru(bpy)_2(L\text{-}L')]^{2+}$ where L-L' = Hpyrtr and $Pyrtr^-$ (isomers 1 and 2) and H3MePyrtr and $3MePyrtr^-$

| L-L' | Abs max [a] (nm) | Em max [a] (nm) | Em max [b] (nm) 77K | Lifetime (ns) [a,c] | Quantum Yield emission [a,d] |
|---|---|---|---|---|---|
| HPyrtr 1 | 450 | 615 | 590 | 18(99)67(1) | $2\ 0\times10^{-3}(\pm\ 0\ 2)$ |
| HPyrtr 2 | 437 | 620 | 575 | 30(90)15(10) | $1\ 4\times10^{-3}(\pm\ 0\ 2)$ |
| $Pyrtr^-$ 1 | 470 | 650 | 609 | 143 | $6\ 0\times10^{-3}(\pm\ 0\ 2)$ |
| $Pyrtr^-$ 2 | 465 | 650 | 608 | 110 | $3\ 8\times10^{-3}(\pm\ 0\ 2)$ |
| H3MePyrtr | 440 | 612 | 587 | 29(50)150(50) | $4\ 0\times10^{-3}(\pm\ 0\ 2)$ |
| $3MePyrtr^-$ | 466 | 645 | 610 | 85 | $2\ 7\times10^{-3}(\pm\ 0\ 2)$ |

[a] data obtained in Britton-Robinson buffers for 1 and 3 pH = 1 94 for the protonated compounds and pH = 8 00 for the deprotonated compounds, [b] measured in methanol glass at 77 K [c] lifetime values obtained from Japan, values in brackets are the values obtained for the quantum yields, [d] quantum yields of emission obtained by comparison with $[Ru(bpy)_3]^{2+}$

Interestingly, in comparison with the $pK_a$ value of 4 48 obtained for the mixture of isomers of $[Ru(bpy)_2(HPyrtr)]^{2+}$, isomer 1 and isomer 2 yield very different $pK_a$ values of 5 95 and 4 07 respectively For isomer 2 the difference in optical density (OD) in acid and base is much larger than the difference in optical density for the protonated and deprotonated forms of isomer 1 Due to this small difference in optical density observed over the pH range for isomer 1, the absorption (and emission) titrations of the mixture of isomers results in a $pK_a$ similar to that of isomer 2 being determined For the %OD versus pH plots for the mixture of isomers of $[Ru(bpy)_2(HPyrtr)]^{2+}$, no clear evidence was observed for the presence of two $pK_a$ values The $pK_a$ results obtained for the isomers indicate that the $pK_a$ depends on the mode of coordination of the pyridyltriazole ligand The position of the proton on the coordinated HPyrtr ligand, which will be affected by the coordination mode of the ligand, will also affect the $pK_a$ determination

As suggested in Chapter 3, the coordination mode for the ligand in isomer 1 is via the $N^{4'}$ position on the triazole ring and the coordination mode for isomer 2 is via $N^{1'}$ of the triazole ring The $pK_a$ value for isomer 2 is found at 4 07 which is in agreement with the $pK_a$ value of 4 87 obtained for $[Ru(bpy)_2(H3MePyrtr)]^{2+}$ which is also coordinated via the $N^{1'}$ of the triazole ring The presence of the extra methyl group in H3MePyrtr does not greatly effect the ground-state acid-base properties of the compounds But as expected from the electron donor properties of the methyl group H3MePyrtr and its ruthenium compound are slightly weaker acids

No evidence was found for protonation of the neutral coordinated ligand at low pH This suggests that the basicity of the coordinated ligand is highly reduced At

the same time it should be realised that protonation is hindered by coordination of the ligand to the ruthenium ion Given the fact that pyridine is more basic than 1,2,4-triazole it is worthwhile to remember that protonation of the free ligand occurs most likely at the pyridine nitrogen

## 4 3 Excited State Properties Including Lifetime and Quantum Yield Measurements

The pH dependence of the emission properties of the compounds was also investigated Figure 4 3 (a) and (b) shows the emission spectra of isomers 1 and 2 of $[Ru(bpy)_2(HPyrtr)]^{2+}$ as a function of pH The initial studies on the acid-base behaviour of these ruthenium compounds were carried out on $[Ru(bpy)_2(HPyrtr)]^{2+}$ that is, the mixture of isomers 1 and 2 and $[Ru(bpy)_2(H3MePyrtr)]^{2+}$ Lifetime studies of these compounds were carried out in Trinity College Dublin using the Time Correlated Single Photon Counting (TCSPC) apparatus described in Chapter 2 The results obtained are presented in Figure 4 4 (a) and (b), and Table 4 7 along with the results obtained for the absorption, emission and quantum yields of these two compounds Separation of the two isomers of $[Ru(bpy)_2(HPyrtr)]^{2+}$ (see Chapter 3) enabled the excited state properties of each isomer to be investigated Lifetime measurements of the two isomers and $[Ru(bpy)_2(H3MePyrtr)]^{2+}$ were carried out in the Riken Institute, Tokyo [36], and are listed in Table 4 6 along with the absorption, emission and quantum yield data The decay curves are presented in Figures 4 5 and 4 6 The changes observed in the emission spectra as a function of pH are consistent with those observed for the absorption spectra and agree with deprotonation of the pyridyltriazole ligands in $[Ru(bpy)_2(HPyrtr)]^{2+}$ and $[Ru(bpy)_2(H3MePyrtr)]^{2+}$

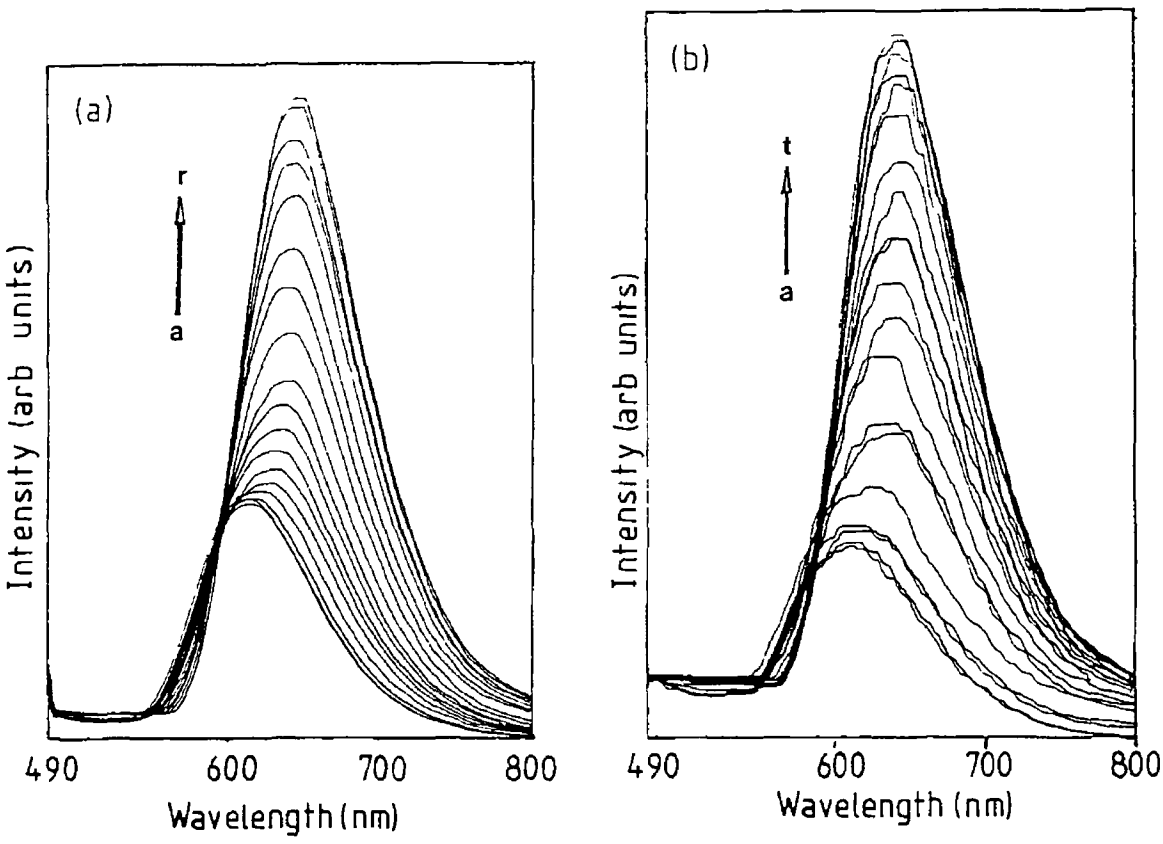


Figure 4 3 PH dependence of the emission spectrum of (a) isomer 1 of $[Ru(bpy)_2(HPyrtr)]^{2+}$ in aqueous Britton Robinson buffer (1 x $10^{-5}$ mol $dm^{-3}$), for curves (a)-(r) pH 1 64, 2 02, 2 98, 3 66, 4 13, 4 21, 4 31, 4 58, 4 78, 4 92, 5 23, 5 48, 5 72, 5 99, 6 19, 6 46, 6 87, 7 21 and (b) isomer 2 of $[Ru(bpy)_2(HPyrtr)]^{2+}$ in aqueous Britton Robinson buffer (1 x $10^{-5}$ mol $dm^{-3}$), for curves (a)-(t) pH 0 97, 1 13, 1 35, 1 47, 1 68, 1 96, 2 01, 2 27, 2 53, 2 73, 2 92, 3 23, 3 56, 3 93, 4 45, 4 74, 5 09, 5 71, 6 68, 7 09

Interestingly, the emission intensities of $[Ru(bpy)_2(HPyrtr)]^{2+}$ and $[Ru(bpy)_2(H3MePyrtr)]^{2+}$ are different For $[Ru(bpy)_2(HPyrtr)]^{2+}$ the emission intensity increases with increasing pH, however, for $[Ru(bpy)_2(H3MePyrtr)]^{2+}$ a decrease of the emission intensity with increasing pH is observed As $[Ru(bpy)_2(H3MePyrtr)]^{2+}$ is coordinated via the $N^{1'}$ of the triazole ring (see Chapter 3), it is anticipated that the emission intensity of the acid-base equilibria is dependent on the coordination mode of the triazole ring The emission properties of the separated isomers were expected to confirm this However, this is not the case as the emission intensities for both isomers increase with increasing pH This is an unexpected result as it indicates that the presence of a methyl group on the 3' position of the triazole ring is responsible for this "inversion" of emission properties In comparison with the emission properties of the two isomers, where deprotonation is reflected by an increase in emission intensity, that is, the negative charge on the ligand causes an increase in energy of the d-d ligand field level (see Figure 1 1, Chapter 1), deprotonation of $[Ru(bpy)_2(H3MePyrtr)]^{2+}$ results in a decrease of emission intensity This suggests that the electron donating properties of the methyl group may decrease the energy of the d-d level, allowing thermal population of this ligand field level to be possible and thus reducing the emission intensity

The variations in the emission intensities of the two isomers and $[Ru(bpy)_2(H3MePyrtr)]^{2+}$ are reflected in the quantum yield measurements in Table 4 6 The emission quantum yields in acid and base of isomer 1 being higher than that of isomer 2 The quantum yields of the mixture of isomers of $[Ru(bpy)_2(HPyrtr)]^{2+}$ (Table 4 7) in acid and base represent the average values obtained for the two isomers

Table 4.7 Lifetime and Quantum Yield Data of the Ruthenium Compounds $[Ru(bpy)_2(L\text{-}L')]^{n+}$ where L-L' = HPyrtr and H3MePyrtr for n = 2, and $Pyrtr^-$ and $3MePyrtr^-$ for n = 1

| L-L' | lifetime[a] (ns)[b] | Quantum yield[a,c] emission |
|---|---|---|
| HPyrtr | 10(0 6) 60(0 4) | $1\ 5x10^{-3}(\pm\ 0\ 2)$ |
| $Pyrtr^-$ | 125 | $5\ 0x10^{-3}(\pm\ 0\ 2)$ |
| H3MePyrtr | 20(0 7)120(0 3) | $4\ 0x10^{-3}(\pm\ 0\ 2)$ |
| $3MePyrtr^-$ | 85 | $2\ 7x10^{-3}(\pm\ 0\ 2)$ |

[a] data obtained in Britton-Robinson buffers for L-L' = HPyrtr and H3MePyrtr pH = 1 94 for L-L' = $Pyrtr^-$ and $3MePyrtr^-$ pH = 8 00, [b] lifetime values obtained from Trinity College Dublin, values in brackets are the values obtained for the pre-exponential factors, [c] quantum yields of emission obtained by comparison with $[Ru(bpy)_3]^{2+}$

The data in Table 4 6 show that the emission quantum yields for the compounds reported here are between ten and thirty times lower than observed for $[Ru(bpy)_3]^{2+}$ [34]

The emission spectra, as a function of pH, of the two isomers of $[Ru(bpy)_2(HPyrtr)]^{2+}$ are presented in Figure 4 3 (a) and (b) The data obtained were analysed as emission titration curves and the inflection points of these curves have been given in Table 4 5 As with the absorption spectra of the isomers, the difference in intensity for the protonated and deprotonated complex of isomer 2 is much larger than that for isomer 1 Hence, the value of the inflection point obtained for the mixtures of isomers is closer to that of isomer 2 than isomer 1

The inflection point in a luminescence intensity versus pH

plot gives an excited state $pK_a$ value, $pK_a^*$, which is called an "apparent" $pK_a^*$ value, because it is not known a priori whether it corresponds to a true thermodynamic acid-base equilibrium in the excited state [13] The values obtained for the apparent $pK_a^*$ for $[Ru(bpy)_2(H3MePyrtr)]^{2+}$ and the two isomers of $[Ru(bpy)_2(HPyrtr)]^{2+}$ are given in Table 4 7 These values indicate that the pyridyltriazole ligands are better acids in the excited state than in the ground state Using the emission wavelength observed for the protonated and deprotonated compounds an estimate can be obtained for the excited state $pK_a$, $pK_a^*$, using the Forster cycle as in Equation 5 [6],

$$pK_a^* = pK_a + \frac{0\ 625}{T}(\upsilon_b - \upsilon_a) \qquad (5)$$

where T is the absolute temperature, $\upsilon_a$ and $\upsilon_b$ are the energies of the (0-0) transition from the ground state to the excited state involved in the deprotonation equilibrium, for the acid and base forms respectively

The results obtained for the free ligands from Equation 5, using the lowest energy absorption wavelengths, have been given in Table 4 5 If the emission frequencies or the average between emission and absorption maxima are used even more unrealistic results are obtained The values obtained suggest that, in the excited state, both the neutral pyridyltriazole ligands become stronger bases (have a higher $pK_a$(base)) and stronger acids (have a lower $pK_a$(acid)) Similar results were obtained by Aaron et al in their study of a series of purine derivatives [37]

An estimate of the $pK_a^*$(acid) values of the ruthenium compounds can be made using the same approach It seems reasonable to assume that the excited state acid-base equilibrium will be established in the long-lived triplet

state and not in the singlet state that has a much shorter lifetime So when Equation 5 is applied to estimate of the $pK_a^*$ of such ruthenium compounds, the emission energies should be used, rather than the absorption energies For our calculations the emission frequencies obtained at 77 K were used as they are the best means to obtain an estimate for the energy difference involved in the (0-0) transition The results obtained have been given in Table 4 5 These results indicate that the pyridyltriazole ligand becomes a stronger acid in the excited state when bound to the $Ru(bpy)_2$- moiety

Other methods have been reported to calculate $pK_a^*$ values [6] Good results are in general obtained using the emission lifetimes of the acid and base forms as in Equation 6,

$$pK_a^* = pH_1 + \log(\tau_a/\tau_b) \qquad (6)$$

where $pH_1$ is the inflection point in the luminescence titration curve and $\tau_a$ and $\tau_b$ the excited state lifetimes of the acid and base forms respectively

For the emission lifetime results obtained in Trinity College Dublin and Japan, the decay curves were analysed for both single- and double-exponential decays The lifetime measurements carried out at pH 8 0 could consistently be analysed as single exponential decays Experiments carried out at pH 13 gave essentially the same results However, for the experiments carried out at pH 1 94 the data obtained were best fit as double exponential decays Variation of the buffer concentration did not have any effect on the emission intensity

From the results obtained in TCD, Table 4 6, (Figure 4 4) at high pH a single exponential decay of the emission is

observed for both $[Ru(bpy)_2(Pyrtr)]^+$ and $[Ru(bpy)_2(3MePyrtr)]^+$ yielding $\tau_b$ values of respectively 125 and 85 ns This suggests, as expected, the presence of only one, most likely bpy based, emitting state The lifetimes of the acid forms of the compounds ($\tau_a$) were obtained at pH 1 94 The double exponential decay of the emission at pH 1 94 is unexpected and makes the application of Equation 6 less straightforward From the ground state $pK_a$ value it can be calculate that at this pH, less than 1 % of $[Ru(bpy)_2(HPyrtr)]^{2+}$ and $[Ru(bpy)_2(H3MePyrtr)]^{2+}$ is deprotonated in the ground state So at this pH only the acid form is excited and the double exponential decay cannot be caused by a dual excitation The emission intensities were not effected by the buffer concentration, so quenching by the buffer can be ruled out The double exponential decay observed cannot be explained by the presence of two coordination isomers in 1, as for $[Ru(bpy)_2(3MePyrtr)]^+$ only one isomer has been observed

Lifetime measurements of the two isomers of $[Ru(bpy)_2(HPyrtr)]^{2+}$, and $[Ru(bpy)_2(H3MePyrtr)]^{2+}$ which were carried out with a different instrument [36] at another excitation wavelength (438 nm) yielded the results listed in Table 4 6

Again, the results obtained at pH 8 for $[Ru(bpy)_2(H3MePyrtr)]^{2+}$ and the two isomers of $[Ru(bpy)_2(HPyrtr)]^{2+}$ can be consistently analysed as a single exponential decays The lifetime of $[Ru(bpy)_2(H3MePyrtr)]^{2+}$ at pH 8 agrees well with the results measured in TCD The lifetime measurement of $[Ru(bpy)_2(HPyrtr)]^{2+}$ (both isomers) at pH = 8 (Table 4 7) is approximately the average value of the independent results obtained for each isomer (Table 4 6)

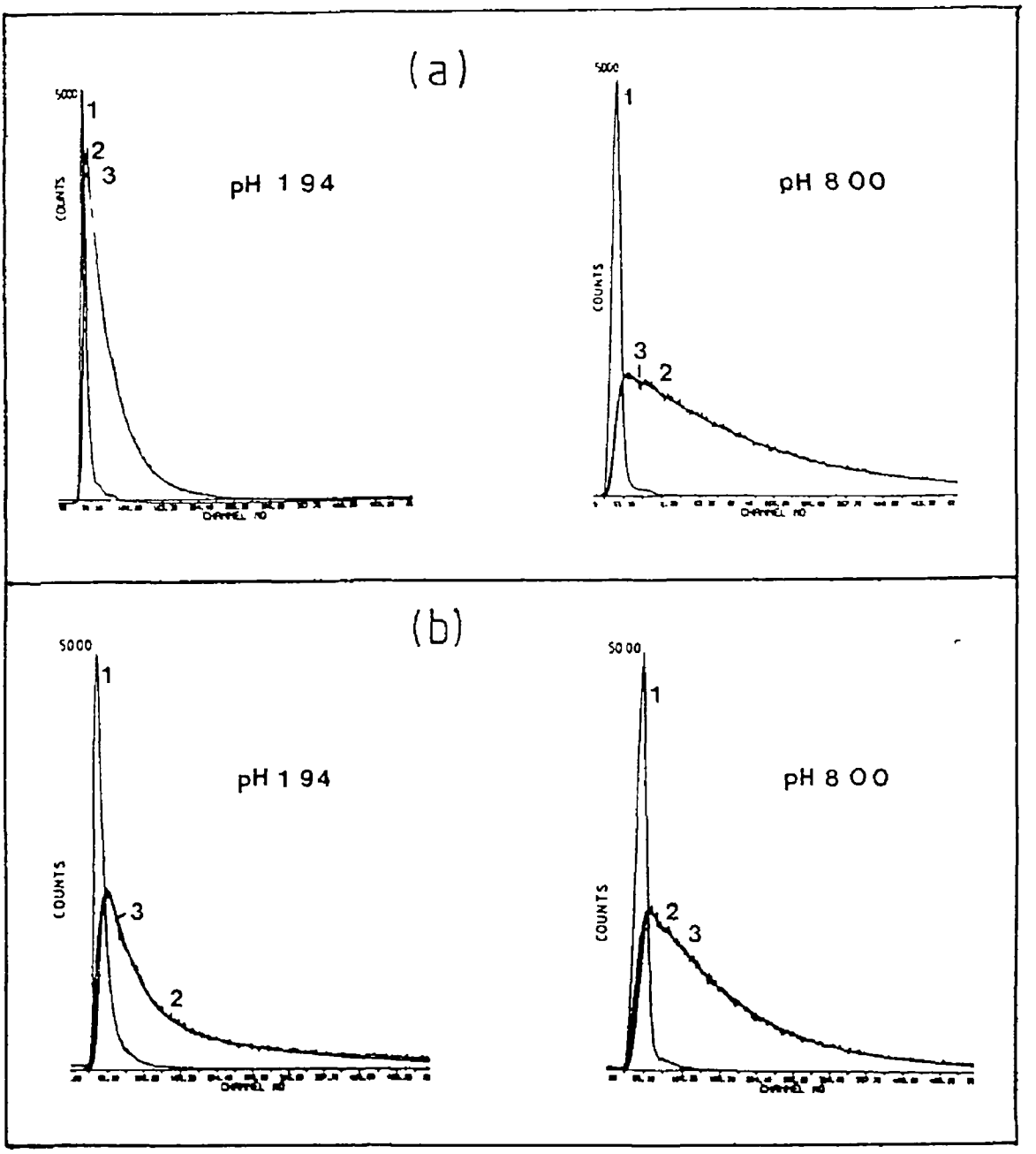


Figure 4 4 Luminescent decay curves for the protonated and deprotonated forms of (a) $[Ru(bpy)_2(HPyrtr)]^{2+}$ and (b) $[Ru(bpy)_2(H3MePyrtr)]^{2+}$ ($1x10^{-5}$ M) in Britton Robinson buffer at pH 1 94 and 8 00 1-lamp profile, 2-sample decay curve, 3-best fit exponential decay Results obtained from TCD (see Chapter 2)

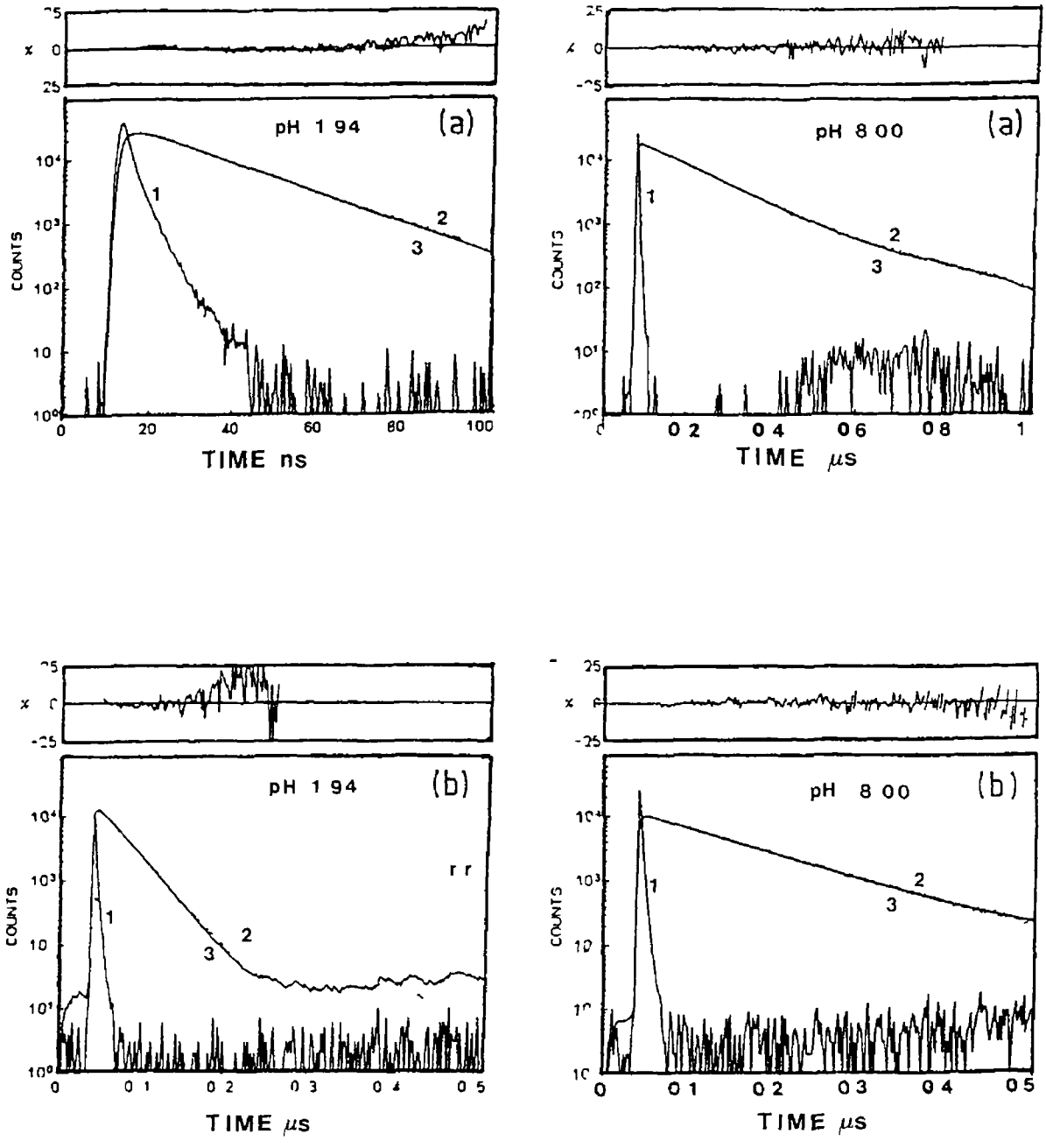


Figure 4 5 Luminescent decay curves for the protonated and deprotonated forms of $[Ru(bpy)_2(HPyrtr)]^{2+}$ isomer 1 (a) and isomer 2 (b) ($1x10^{-5}$ M) in Britton Robinson buffer at pH 1 94 and 8 00 1-lamp profile, 2-sample decay curve, 3-best fit exponential decay Results obtained in Riken Institute, Tokyo [36]

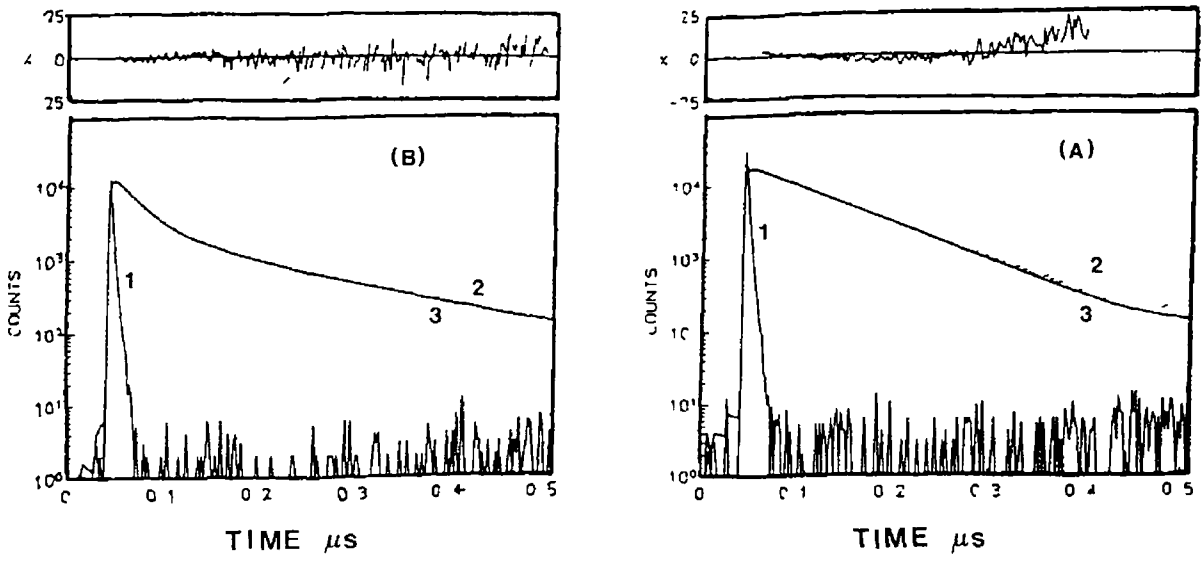


Figure 4 6 Luminescent decay curves for (a) protonated and (b) deprotonated forms of $[Ru(bpy)_2(H3MePyrtr)]^{2+}$ ($1x10^{-5}$ M) in Britton Robinson buffer at pH 1 94 and 8 00 1-lamp profile, 2-sample decay curve, 3-best fit exponential decay Results obtained in Riken Institute, Tokyo [36]

The results obtained for the two isomers at pH 1 94 again were analysed best as double exponential decays Nonetheless, consistent results were obtained As can be seen from Table 4 6 the lifetime results for the two isomers at pH 1 94 contain a short lifetime and a longer one For isomer 1, the longer lifetime of 67 ns constitutes only 1% of the integrated area while the shorter lifetime of 18 ns constitutes 99% of the integrated area Similarly, for isomer 2, the ratio of the two lifetimes of 30 and 15 nm obtained is 90 10 The lifetime results for both isomers which were analysed using a single exponential decay fit yield similar results of 18 and 30 ns respectively for isomer 1 and isomer 2

The results obtained for $[Ru(bpy)_2(H3MePyrtr)]^{2+}$ in pH 1 94

also require a double exponential decay to obtain the best fit analysis The results are similar to those obtained in TCD where a short lifetime of 20 ns and a much longer one of 120 ns are obtained in the ratio of 70 30 (see Table 4 7) The results obtained in Japan are 29 and 150 ns in the ratio of 1 1

The lifetime results strongly suggest the presence at low pH of either two emitting states, or two different species It is however possible that the position of the N-H proton, in H3MePyrtr either at $N^{2'}$ or at $N^{4'}$, has an effect on the excited state process On the other hand the similarity of the $\pi^*$ orbital energies of the bpy and pyridyltriazole ligands, makes it possible for the pyridyltriazole ligands to be involved in the emission process and this might result in emission occurring from both bpy and pyridyl-triazole based triplet states The quantum yields of isomer 1 and 2, and $[Ru(bpy)_2(H3MePyrtr)]^{2+}$ were also measured at pH 1 and are $1\ 79x10^{-3}$, $0\ 71x10^{-3}$ and $7\ 9x10^{-3}$ respectively As the quantum yields for both isomers decrease with increasing pH may suggest that quenching may be a factor contributing to the double exponential decay This however is contradicted by the fact that the quantum yield of $[Ru(bpy)_2(H3MePyrtr)]^{2+}$ increases with increasing pH Quenching therefore cannot be the reason for the presence of the double exponential decay at pH 1 94 From these results, it seams likely that the anomalies in the decay curves at pH 1 94 are due to (a) the position of the N-H proton or (b) chemical interaction between constituents of the buffer or (c) hydrogen bridging between triazole rings of different molecules forming a dimeric species However, as the nature of the double exponential decay at low pH is at present not clear, and further investigations, involving temperature dependent measurements, are needed to clarify the situation

As the single and double exponential analysis for the lifetimes of the two isomers agree well, the lifetimes of isomers 1 and 2 are taken to be 18 and 30 ns respectively As the quantum yield of this compound in acid is higher than that in base, a longer lifetime in acid for this compound is expected For this reason, the longer lifetime of 150 ns is used for $\tau_a$ in Equation 6 Unfortunately the emission lifetimes of the free ligands could not be obtained because of instrumental limitations We can therefore only estimate the excited state $pK_a$ of the free ligands using Equation 5 The $pK_a^*$(acid) values obtained for the ruthenium compounds using Equation 6 have been listed in Table 4 5

The agreement between the two methods of calculating the excited state $pK_a$(acid) values is in general not very good, one of the reasons being the difficulty in obtaining the energy for the (0-0) transitions These $pK_a^*$(acid) values suggest that the ruthenium compounds are stronger acids in the excited state than in the ground state This suggests that upon excitation the electron populates a bpy based $\pi^*$ orbital This will create an effective Ru(III) atom and result in an increased electron donation from the pyridyltriazole ligand to the central metal atom A similar increased acidity in the excited state has been observed before for ruthenium compounds such as $[Ru(bpy)_2(1,2,4\text{-triazole})_2]^{2+}$ [38], and $[Ru(bpy)_2(4,7\text{-dihydroxy-1,10-phenanthroline})]^{2+}$ [9] The $pK_a^*$(acid) values obtained using the longer lifetimes are higher As for the compounds $[Ru(bpy)_2(4,4'\text{-dicarboxy-2,2'-bipyridine})]$ dichloride [8, 10] and for $[Ru(bipyrazine)_3]^{2+}$ [5] in increased basicity suggests that the ligands involved in the protonation process are also involved in the emission process

## 4 5 Conclusion.

The ground state $pK_a$'s of the complexes $[Ru(bpy)_2(HPyrtr)]^{2+}$ and $[Ru(bpy)_2(H3MePyrtr)]^{2+}$ show that the ligands HPyrtr and H3MePyrtr act as much stronger acids when bound to a $Ru(bpy)_2$- moiety This increased acidity of the coordinated pyridyltriazole ligands, of about 5 orders of magnitude, points to electron donation from the ligand to the metal center This behaviour is similar to that obtained for other $Ru(bpy)_2$ type complexes However, the excited state properties of our compounds are quite unexpected On the basis of the results reported by Haga, emission of the deprotonated species was not expected [28] The acid-base properties of the excited state appear rather complicated Using the Forster cycle an increase of the acidity of the pyridyltriazole ligands in the excited state is observed, suggesting that emission occurs from a bpy based triplet state The lifetime experiments did yield less clear results Results obtained at pH 8 on the TCSPC instruments in TCD and also in Japan could consistently analysed as a single exponential decay Consistent results were also obtained on both instruments at pH 1 94 but these were best analysed as double exponential decays The double exponential decay observed at low pH is at present not fully understood Three possible explanations are,

1) The presence of two emitting states in $[Ru(bpy)_2(HPyrtr)]^{2+}$ (isomers 1 and 2) and $[Ru(bpy)_2(H3MePyrtr)]^{2+}$

2) The position of the protonation in the triazole ring has an effect on the excited state properties

3) Chemical interaction between molecules and solvent and/or between different molecules

With these possibilities in mind, further work is required such as low temperature studies to determine the anomalies at pH 1 94

References.


1 E A Seddon and K R Seddon, "The Chemistry of Ruthenium", Elsevier, Amsterdam, 1984

2 A Juris, V Balzani, F Barigelletti, S Campagna, P Belser, and A von Zelewsky, Coord. Chem. Rev., 1988, 84, 85

3 K Kalyanasundaram, Coord. Chem. Rev., 1979, 46, 159

4 K Seddon, Coord. Chem. Rev., 1982, 41, 79

5 R J Crutchley, N Kress, and A B P Lever, J. Am. Chem. Soc., 1983, 105, 1170

6 J F Ireland and P A H Wyatt, Adv. Phys. Org. Chem., 1976, 12, 131

7 N Lasser and J Feitelson, J. Phys. Chem., 1873, 77, 1011

8 P J Giordano, C R Bock, M S Wrighton, L V Interrante, and R F X Williams, J. Am. Chem. Soc., 1977, 99, 3187

9 P J Giordano, C R Bock, and M S Wrighton, J. Am. Chem. Soc , 1978, 100, 6960

10 T Shimidzu, T Iyoda, and K Izaki, J. Phys Chem., 1985, 89, 642

11 S H Peterson and J N Demas, J. Am. Chem. Soc., 1979, 101, 6521

12 C R Johnson and R E Shepherd, Inorg. Chem., 1983, 22, 1117

13 A Kirsh de Mesmaeker, L Jacquet and J Nasielski

14 P Sullivan, D J Salmon, and T J Meyer, Inorg. Chem., 1979, 18, 3369

15 M Venturi, Q G Mulazzani, M Ciano, and M Z Hoffman, Inorg. Cham., 1986, 25, 4493

16 D E Morris, Y Ohsawa, D P Segers, M K De Armond, and K W Kanck, Inorg. Chem., 1984, 23, 3010

17 S H Peterson and J N Demas, J. Am. Chem. Soc., 1979, 101, 6571

18 A Juris, F Barigelletti, V Balzani, P Belser, and A von Zelewsky, J. Chem. Soc., Faraday Trans. 1987, 83, 2295

19 P Ford, D F P Rudd, R Gaunder, and H Taube, J. Am. Chem. Soc , 1968, 90, 1187

20 T J Meyer, Pure and App. Chem., 1986, 57, 1193

21 R M Acheson "An Introduction to the Chemistry of Heterocyclic Compounds", Interscience Publishers, Inc , New York, N Y , 1960

22 C Creutz and H Taube, J. Am. Chem. Soc., 1969, 91, 3988

23 R J Sundberg and R B Martin, Chem. Rev., 1974, 471 C R Johnson, R E Shepherd, B Marr, S O'Donnell, and W Dressick, J. Am. Chem. Soc., 1980, 102, 6227

24 C R Johnson, W W Henderson, and R E Shepherd, Inorg. Chem., 1984, 23, 2754

25 G Yagil, Tetrahedron Lett., 1967, 23, 2855

26 C F Kroger and W Freilberg, Chimica, 1967, 21, 161

27 S H Peterson and J N Demas, J. Am. Chem. Soc., 1976, 51, 7880

28 M Haga, Inorg. Chim Acta, 1983, 75, 29

29 R K Boggess and R B Martin, Inorg. Chem., 1974, 13, 1525

30 B E Buchanan, unpublished results

31 K T Potts, in "Comprehensive Heterocyclic Chemistry" Vol 5, A R Katrinsky, C W Rees, Eds, Pergamon Press, Oxford, 1984

32 A J Boulton, A McKillop, in "Comprehensive Heterocyclic Chemistry" Vol 5, A R Katrinsky, C W Rees, Eds, Pergamon Press, Oxford, ,1984

33 K Nakamoto, J. Phys. Chem., 1960, 64, 1420

34 J van Houten and R J Watts, J. Am. Chem. Soc., 1976, 98, 4853

35 A M Bond, M Haga, Inorg. Chem. 1986, 25, 4507

36 Experiments were carried out by J G Vos in the Riken

Institute, Tokyo, using a Hitachi-Horiba NAES-1100 instrument Apart from the excitation wavelength the experimental conditions were the same

37 J J Aaron and J D Wineforder, Photochem. Photobiol , 1973, 18, 97

38 C Long and J G Vos, Inorg. Chim. Acta, 1984, 89, 125

# Chapter 5

## Synthesis and Characterisation of Mononuclear and Dinuclear Compounds Containing Asymmetric Potentially Bridging Ligands

## 5 0 Introduction.

In the past 15 years the Ru(II)-polypyridine family of coordination compounds has been the object of extensive investigation related to the photochemical, photophysical and electrochemical properties of most of its members [1-9] Also, there has been a growing interest towards supramolecular species (dinuclear and polynuclear complexes, host-guest systems, etc ) with the aim to arrive at the design of photochemical molecular devices (proper assemblies of molecular components capable of performing useful light induced functions) [10] Ru(II) polypyridine complexes are excellent building blocks for the construction of such devices, especially for light induced migration and/or collection of electronic energy or electronic charge In addition, dinuclear compounds have attracted much attention because in principle, they may act as a two electron transfer agent when excited by two photons Hence they have potential application as catalysts for the photochemical cleavage of water, providing other criteria such as lifetimes and redox potentials are satisfied

A key component in dinuclear and polynuclear systems is the bridging ligand since the interaction between the bridging units, and thereby the properties of the supramolecular species, is critically dependent on the size, shape and electronic nature of the bridge [11] In a photomolecular device there must be an appropriate energy ordering of the lowest (longest-lived, redox active and/or luminescent) excited state and of the first oxidation and reduction potentials of the various components So, in choosing a suitable bridging ligand much caution must be used since it is well known that subtle changes in coordination about Ru(II) can lead to the loss of valuable properties (e g luminescence) of the original component [1] Many

complexes of the type $[Ru(bpy)_2(L\text{-}L)]^{n+}$ and $[Ru(bpy)_2(L\text{-}L')]^{n+}$ have been synthesised over the past few decades [1-9], where (L-L) is a symmetric and (L-L') is an asymmetric bidentate coordinating ligand such as 2,2'-bipyrimidine (bpym)[5, 12, 13], 2,2'-biimidazole ($biimH_2$) [5, 12] and 2,5-bis(2-pyridyl)pyrazine (bppz) [13] to name but a few However, the possibility also exists for some of these type of ligands to act as bridging ligands between two metal centers

Studies on dinuclear compounds have also concentrated on the area of mixed-valence compounds and their physical properties have been discussed in the light of models published by Hush [14, 15] Mixed-valence studies are a means of probing in depth the energetics of solution electron transfer processes and the mechanisms and magnitudes of electronic interactions between metal centers In particular the intervalence (IT) transition of mixed-valence compounds has been studied extensively, as its position, shape and intensity yield information about the interaction between metal centers The extent of electron delocalisation between the metal centers can be established by the use of the following formulae given by Hush [14, 15]

$$\upsilon_{1/2} = (2310E_{op})^{1/2} \text{ cm}^{-1} \qquad (1)$$

$$\alpha^2 = \frac{(4\ 2\text{x}10^{-4})\epsilon(\Delta\upsilon_{1/2})}{d^2E_{op}} \qquad (2)$$

where $\Delta\upsilon_{1/2}$ is the bandwidth at half intensity, $E_{op}$ is the band maximum ($\upsilon$ in $cm^{-1}$), $\alpha^2$ is the extent of delocalisation, $\epsilon$ is the extinction coefficient of the IT band ($\epsilon$ in $dm^3\ mol^{-1}\ cm^{-1}$) and d is the distance between the ruthenium centers (estimated to be 6 1 Å) The larger the value of $\alpha^2$ the higher the extent of electron

delocalisation The magnitude of this electron delocalisation can be calculated using the following equation

$$H_{ab} = 2.05\times10^{-2}\ \frac{\epsilon_{max}(\Delta\upsilon_{1/2})^{1/2}}{E_{op}}\ \frac{E_{op}}{d}\ cm^{-1} \qquad (3)$$

Robin and Day [16] have distinguished three broad classes of mixed valence materials These classes depend on the value of $H_{ab}$ obtained for the complex and are as follows,

Class 1 the interaction between the M and $M^+$ centers is so weak that the mixed valence material exhibits only the properties observed for the isolated mononuclear M and $M^+$ complexes

Class 2 the mixed valence dimers exhibit slightly perturbed M and $M^+$ characteristics and may also manifest properties not associated with isolated units

Class 3 the interaction between the two centers is so great that the properties of the isolated M and $M^+$ are absent and only new properties characteristic of the $(M\text{-}M^+)$ unit are discerned

Although a number of dimeric Ru(II) complexes have previously been prepared for the purpose of studying the IT transition in the mixed - valence ($5^+$) system [17-20], none satisfy the criteria of field strength and/or coordination about each Ru(II) ion necessary for luminescence Luminescence is not a necessary criteria for photoredox behaviour, but its presence is a desired property as a convenient probe of the excited state and redox potentials

Studies with previously synthesized Ru(II) dimers suggest

that, in general, deviations from a bipyridine-like structure in the bridging ligand causes a loss of the d - $\pi^*$ luminescence characteristic of $[Ru(bpy)_3]^{2+}$ and its homologues For example, Dose et al [5] and Hunziker et al [12] report that although the monomer $[Ru(bpy)_2(bpym)]^{2+}$ is luminescent in acetonitrile at room temperature the corresponding bridged dimer $[(bpy)_2Ru(bpym)Ru(bpy)_2]^{4+}$ is not The same situation applies where the bridging ligand is 2,2'-bibenzimidazole or 2,3-bis(2-pyridyl)-quinoxaline These results suggest that slight differences in structure are sufficient to prevent luminescence Consequently, preparation of luminescent binuclear ruthenium complexes demands a bridging ligand that resembles as close as possible 2,2'-bipyridine

For this reason, the ligand 2,3-bis(2-pyridyl)pyrazine (dpp), was used by Braunstein et al [6] to synthesise mononuclear and dinuclear (see Figure 5 1), compounds containing $Ru(bpy)_2$ moieties Each bidentate coordination site on this ligand resembles the coordination site of bpy to ruthenium, with the obvious difference that the two ruthenium centers share the same pyrazine ring for coordination It was expected that the properties of these two complexes will resemble more closely the properties of $[Ru(bpy)_3]^{2+}$

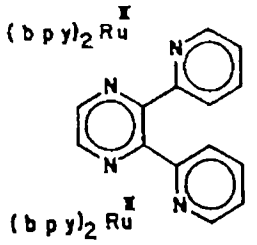


Figure 5 1 Structure of $[(bpy)_2Ru(dpp)Ru(bpy)_2]^{4+}$ containing the bridging ligand 2,3-bis(2-pyridyl)pyrazine

The absorption spectra of the monomeric and dimeric compounds are similar to those of other Ru(II) polypyridine complexes [1] in which the absorption bands are assigned to $d\pi$ ---> $\pi^*$ MLCT transitions The absorption maximum for the monomer is found at 430 nm with a shoulder at 470 nm while that of the dimer consists of two well resolved absorption bands at 425 nm and 525 nm Unlike other dinuclear compounds synthesised, $[(bpy)_2Ru(dpp)Ru(bpy)_2]^{4+}$, emits in solution at room temperature at 755 nm, which then shifts to 675 nm for $[Ru(bpy)_2(dpp)]^{2+}$ An IT band has not been detected for this complex, results of experiments suggest that either the mixed-valence complex is cleaved or that the IT band of the $5^+$ ion must have $\epsilon < 10$ $dm^3$ $mol^{-1}$ $cm^{-1}$ in the near infrared absorption and hence has escaped detection limits

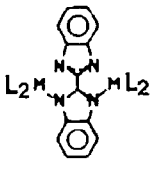


(a)

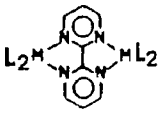


(b)

Figure 5 2 Structures of dinuclear compounds containing (a) 2,2'-bibenimadazolate ($bibzim^{2-}$) and (b) 2,2'-bipyrimidine (bpym) and M = Ru

Other examples of potentially bridging bidentate symmetrical ligand include 2,2'-bipyrimidine (bpym), 2,2'-bibenzimidazolate ($bibzim^{2-}$) and 2,2'-biimidizole ($biimH_2$) [5, 12, 21, 22] The selection of the bridging ligands used for the preparation of dinuclear complexes can change the nature of the metal-metal interactions [14, 15] Figure 5 2 shows the structures of the dinuclear compounds containing the ligands bpym and $bibzim^{2-}$ These two

ligands give rise to almost the same metal-metal separation distance, however, the charge on the ligands is different as bibzim is a dinegative ligand and bpym is neutral Thus, these two ligands would give rise to different metal-metal interactions

For both the monomeric complexes $[Ru(bpy)_2(bibzimH_2)]^{2+}$ and $[Ru(bpy)_2(bpym)]^{2+}$ the coordination of a second $Ru(bpy)_2$ unit results in a decrease in absorption energy of the dimeric compound If the oxidation potentials of the dinuclear complex $[(bpy)_2Ru(bibzim)Ru(bpy)_2]^{2+}$ are compared with those of the mononuclear complex, it is found that the first oxidation potential of the dinuclear complex is 0 3 V lower than that of the mononuclear one [22] This indicates that the bibzim bridging ligand in the dinuclear complex has electron donor properties In contrast, the first oxidation potential of $[(bpy)_2Ru(bpym)Ru(bpy)_2]^{4+}$ is 0 2 V higher than the mononuclear analogue, there bpym has been shown to act as an electron acceptor [21] This dimer is not stable on a preparative time scale while that containing the bridging ligand $bibzim^{2-}$ is stable This high stability is attributed to the superior donor property of the anionic $bibzim^{2-}$ as the dianionic bibzim ligand reduces the cationic charge of ruthenium and decreases the electrostatic repulsion between the two positively charged metal centers [21]

$\Delta E_{1/2}$, the difference between the oxidation potentials of the two ruthenium centers, for the two dimers are quite different, that of the bibzim dimer is 0 29 V and that of the bpym dimer is 0 16 V [13] The oxidation potentials thus depend on the nature of the bridging ligand The effects which are operative and contribute to the non zero values obtained for $\Delta E_{1/2}$ are as follows

(1) ELectrostatics or ionization energies - since the

second oxidation occurs adjacent to a greater positive charge than the first oxidation, it will occur at a higher potential

(2) Solvation energies - the solvation energies will be different for the $Ru^{II}$-$Ru^{II}$, $Ru^{II}$-$Ru^{III}$, and $Ru^{III}$-$Ru^{III}$ dimers

(3) Delocalization or resonance - the unpaired electron is partially delocalised onto the $Ru^{III}$ site, shifting the second oxidation to potentials higher than one would expect with a totally localised electron

(4) Statistical contributions - the Ru(II)-Ru(II) dimer can be oxidised to give either Ru(II)-Ru(III) or Ru(III)-Ru(II) and the Ru(III)-Ru(III) dimer reduced to give Ru(II)-Ru(III) or Ru(III)-Ru(II) [23]

Whether interaction exists between two redox sites in one molecule is commonly traced by considering $K_{com}$, the comproportion equilibrium, calculated using Equation 5 The most relevant equilibrium for mixed valence complexes is that for comproportionation since the mixed valence state is only present when this equilibrium is favourable [24]

$$M(III)\text{-}M(III) + M(II)\text{-}M(II) \quad 2M(II)\text{-}M(III) \qquad (4)$$

The comproportion equilibrium is calculated from the following equation,

$$RT\ln K_{com} = F(\Delta E_{1/2}) \qquad (5)$$

where $\Delta E_{1/2}$ is the observed difference in redox potentials of the dinuclear complex The $K_{com}$ value for the dinuclear complex containing $bibzim^{2-}$ is $9.8 \times 10^4$ and that for the

dinuclear complex containing bpym is 1 1x10$^3$ This suggests that the metal-metal interaction is stronger in the bibzim$^{2-}$ dimer due to the strong $\sigma$ donor properties of the bridging ligand

For both dimers near-infrared spectra may be expected to give an insight into the extent of electron delocalization between the two ruthenium sites [14, 15] The [(bpy)$_2$Ru-(bpym)Ru(bpy)$_2$]$^{4+}$ dimer was not stable enough on the time scale required to measure the IT band Attempts by Haga et al [22] to study the IT band of [(bpy)$_2$Ru(bibzim)-Ru(bpy)$_2$]$^{2+}$ were carried out by oxidising the first Ru site at 0 9 V, this yielded a band at 712 nm Further oxidation at 1 30 V to form the 4$^+$ complex resulted a the decrease in intensity of the band at 712 nm and a corresponding increase of a band at 754 nm For this complex, both the bands at 712 and 754 nm have been assigned to ligand $\pi$-to-ruthenium(III) charge transfer transitions [25] Further experiments are required to investigate this phenomenon No evidence was found for the presence of an IT band

The discussion so far has centered on the formation of dinuclear complexes where the bridging ligand is a doubly chelating symmetrical ligand Potentially bridging ligands such as pyrazine, triazoles, pyrazole and 4,4'-bipyridine may also be used as bridging ligands for the formation of dinuclear complexes Mononuclear complexes such as [Ru(bpy)$_2$(Htrz)$_2$]$^{2+}$ where Htrz = 1,2,4-triazole coordinated in a monodentate form have been prepared [26] but the formation of dinuclear complexes is in principle also possible with this ligand A similar situation holds for the pyrazolato anion Upon deprotonation of the pyrazole ligand (Hpz) the doubly bridged dimer is formed [(bpy)$_2$Ru(pz)$_2$Ru(bpy)$_2$]$^{2+}$ [8] see Figure 5 3 below

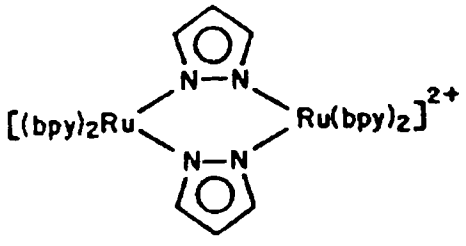


Figure 5 3 Dinuclear complex containing the doubly bridged pyrazolato anion

This dimer is unstable in acidic solution resulting in unsymmetrical bridge cleavage reaction as shown in equation below

$$[(bpy)_2Ru(pz)_2Ru(bpy)_2]^{2+} + 2H^+ + 2S \text{ -----} \rightarrow [Ru(bpy)_2(pzH)_2]^{2+} + [Ru(bpy)_2S_2]^{2+} \quad (6)$$

where S is a solvent molecule The mixed valence dimer $[(bpy)_2Ru^{III}(pz)_2Ru^{II}(bpy)_2]^{3+}$ is also a very unstable species upon further oxidation of this compound in acetonitrile the formation of $[Ru(bpy)_2(Hpz)_2]^{2+}$ and $[Ru(bpy)_2(CH_3CN)_2]^{2+}$ is observed [8] This prohibits the investigation of the inter-valence transfer band The situation is entirely analogous to the di-$\mu$-chloro-bridged dimer $[(bpy)_2RuCl_2Ru(bpy)_2]^{2+}$ [27] where, upon oxidation in acetonitrile, the products formed are the monomeric complexes $[Ru(bpy)_2Cl_2]$ and $[Ru(bpy)_2(CH_3CN)_2]^{2+}$

This halide bridged dimer, $[(bpy)_2RuCl_2Ru(bpy)_2]^{2+}$ synthesised by Meyer et al [27] has the advantage that it can be used successfully as a synthetic intermediate based on facile bridge cleavage reactions

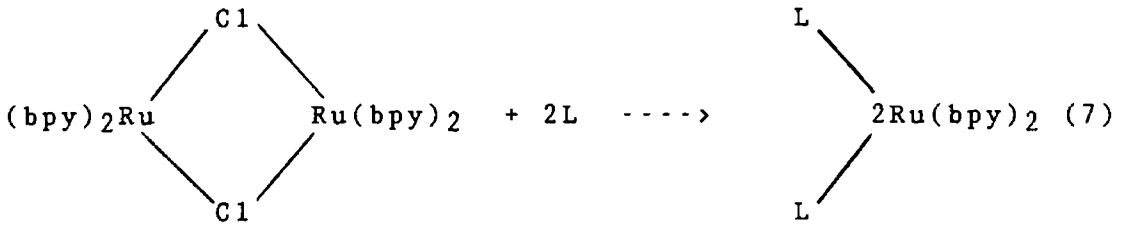

(7)

This reaction is the result of a symmetrical bridge cleavage with the insertion of L which may be a solvent molecule or a monodentate ligand such as pyrazine, pyridine etc

Other ligands that have been used in the preparation of dinuclear complexes include pyrazine (pyrz) and 4,4'-bipyridine (4,4'-bpy) Goldsby and Meyer [28] have prepared dinuclear complexes of the type $[Ru(bpy)_2Cl(L)Cl(bpy)_2Ru]^{2+}$ where L = pyrz or 4,4'-bpy Coordination of a second $Ru(bpy)_2Cl$ moiety to the mononuclear complex $[Ru(bpy)_2(pyrz)Cl]^+$ results in the decrease of energy in the absorption maximum This has been explained by the strong $\pi$ acceptor properties of the pyrazine ligand As the ligand bridges the two ruthenium centers the $d\pi$ orbitals of ruthenium are stabilized and hence absorption occurs at lower energy

Meyer et al successively oxidised the dinuclear complex $[(bpy)_2ClRu(pyrz)ClRu(bpy)_2]^{2+}$ to a 4+ species and showed that the absorption energy maximum increases in energy correspondingly [23] The absorption band for the monomeric Ru(II) or Ru(III) complexes are found in the uv/vis spectra of the oxidised mixed-valence dimeric complexes The spectral similarities indicate that discrete $Ru^{II}$ and $Ru^{III}$ sites are present in the dimer and that the electron environment at the two sites is little changed from the monomeric complexes

The difference between the oxidation potentials of the two ruthenium centers for the dimers where L = pyrz and 4,4'-bpy is quite different Where L = pyrz the difference is 130 mV and where L = 4,4'-bpy the difference is 50 mV [28] The ionization energy term leads to an increase in $\Delta E_{1/2}$ as the distance between the metal sites is decreased while the solvation energy term varies in the opposite sense The magnitude of the resonance energy depends on the electronic properties of the metal and of the bridging ligand, however, from the intensities of the IT band this contribution appears to be very small As there is a large difference between the metal centers when the bridging ligand is 4,4'-bpy and a much smaller distance when pyrz is the bridging ligand then the origin of the increase in $\Delta E_{1/2}$ as distance decreases must be in the ionisation energy [28]

For mixed metal dimers of the type $[(bpy)_2ClRu(L)\text{-}OsCl(bpy)_2]^{2+}$, where L = pyrz or 4,4'-bpy then the effects of ionization energy, solvation energies and delocalization will also determine the magnitude of $\Delta E_{1/2}$ [28] The differences in the oxidation potentials in the mixed metal complexes is much larger than when two ruthenium metals are present The first oxidation potential for the Ru-Os dimer is at much lower potential than for the Ru-Ru dimer, this is because the oxidation is at osmium The second oxidation potential for both Ru-Ru and Ru-Os dimers are similar This indicates that the contribution to $\Delta E_{1/2}$ from the increased charge following the initial oxidation and from the delocalization of the unpaired electron must be comparable for the analogous Ru-Ru and Ru-Os dimers

If the chlorine atoms present in the dimer $[(bpy)_2ClRu\text{-}(4,4'\text{-bpy})RuCl(bpy)_2]^{2+}$ were substituted by pyridine to form the dinuclear complex $[(bpy)_2(py)Ru(4,4'\text{-bpy})\text{-}Ru(py)(bpy)_2]^{4+}$ then the absorption maximum shifts to

higher energy as pyridine is a weaker $\sigma$ donor than chlorine The spectrum of this dimer resembles that of $[Ru(bpy)_3]^{2+}$ except for the appearance of a shoulder on the high energy side of 450 nm [29] Luminescence from the dimer also occurred at the same wavelength of 610 nm as that of $[Ru(bpy)_3]^{2+}$, however, this luminescence is very weak In contrast with other dimers previously reported [5, 7, 22, 23, 28, 29], a cyclic voltammogram of this dimer results in a broad wave for the metal based oxidations and for the ligand based reductions This behaviour is typical for dimers where the bridging ligand is 4,4'-bpy, trans-1,2-bis-(4-pyridyl)ethylene, or 1,2-bis-(4-pyridyl)ethane [27] For such complexes only a single broad wave was observed in the same potential region observed for the Ru(III)/Ru(II) couples for the related monomer The CV of the dinuclear complexes have been shown to consist of two closely spaced one-electron waves corresponding to the successive oxidations of the 4+ ion to the 5+ ion and of the 5+ ion to the 6+ ion [23] As the $\Delta E_{1/2}$ value for this complex is very small this suggests that the interactions between the Ru(II) and Ru(III) sites are very weak

The mixed valence ions $[(NH_3)_5Ru(4,4'\text{-bpy})Ru(NH_3)_5]^{5+}$ [30, 31], $[(bpy)_2ClRu(pyrz)RuCl(bpy)_2]^{3+}$ and $[(NH_3)_5Ru(L)RuCl(bpy)_2]^{4+}$ [19, 32, 33] where L = pyrz or 4,4'-bpy have localised valences [34], and only slight Ru(II) to Ru(III) delocalization, and exhibit class II behaviour in the Robin and Day sense [16] The extent of delocalization in the unsymmetrical ions is somewhat limited by the redox inequivalency of the different ruthenium sites [34] The most interesting comparison with these mixed-valence ions is the comparison with the Creutz and Taube ion $[(NH_3)_5Ru(pyrz)Ru(NH_3)_5]^{5+}$ [17, 18] Previous results obtained on the IT band of this ion have been interpreted in terms of different, chemically discrete Ru(II) and Ru(III) sites [17, 18] However, suggestions have also

been made that the Creutz and Taube ion may represent an intermediate case lying between the limiting localized and delocalized description [35, 36]

A recent publication by Best et al [37] shows that by using spectroelectrochemical techniques, the near- and mid-infrared spectral changes which accompany oxidation or reduction of the ion can be identified The changes in the vibrational spectra clearly reveal the delocalised character of the Creutz and Taube ion, at least on a vibrational time scale So, each ruthenium center contains a charge of 2 5 when the complex is in the mixed valence state, i e $[(NH_3)_5Ru^{2\ 5}(pyrz)Ru^{2\ 5}(NH_3)_5]^{5+}$

The discussion above has shown that some interesting results may be obtained for the dinuclear studies The electrochemical measurements in particular yield much information concerning the metal-metal interaction of these complexes Variations in the dinuclear complexes include changing one or two of the metals, changing the bridging ligand and/or varying the Ru(L-L)- moiety where L-L represents a symmetrical bidentate ligand

As most of the research has been concentrated on the symmetric bridging ligands, very little work has involved the use of asymmetric bridging ligands The aim of this chapter is the preparation and characterisation of mono-nuclear and dinuclear complexes containing asymmetric bidentate bridging ligands The two ligands chosen are similar to the pyridyltriazole ligands HPyrtr and PT used in Chapter 1, but contain an additional pyridine ring bound via the 3' carbon to form 3,5-bis-(pyridin-2-yl)-1,2,4-triazole (Hbpt), or bound via the 1'nitrogen to form 1,3-bis-(pyridin-2-yl)-1,2,4 -triazole (bptn) It is anticipated that the use of these ligands in monomer and dimer studies will yield some interesting results

## 5 1 Preparation of Mononuclear and Dinuclear Ruthenium Compounds Containing Asymmetric Bridging Ligands.

### 5 1 1 Preparation of Mononuclear Compounds.

A series of mononuclear complexes of the type $[Ru(L\text{-}L)_2(L'\text{-}L'')]^{n+}$ have been prepared where L-L = bpy, 4,4'-dimethyl-2,2'-bipyridine ($Me_2bpy$) or 1,10-phenanthroline (phen), and L'-L'' are the ligands 1,3-bis-(pyridin-2-yl)-1,2,4-triazole (bptn) and 3,5-bis-(pyridin-2-yl)-1,2,4-triazole (Hbpt), see Figure 5 4

The preparation of the mononuclear complexes is similar to that for the pyridyltriazole compounds prepared in Chapter 3, where a 1 1 2 molar ratio of $[Ru(L\ L)_2Cl_2]$ and ligand is refluxed in ethanol/water (2 1) for 6 hours, according to the following reaction

$$[Ru(L\text{-}L)_2Cl_2] \xrightarrow{L'\text{-}L''} [Ru(L\text{-}L)_2(L'\text{-}L'')]^{n+} \qquad (8)$$

The complexes were isolated as the $PF_6^-$ salt in yields of between 70 to 90%

Both the ligands bptn and Hbpt are composed of a triazole ring containing two pyridine ring substituents The ligand bptn (Figure 5 4 (a)) is similar to HPyrtr but contains an additional pyridine ring at the $N^{1'}$ position of the triazole ring In effect, this ligand is a combination of the ligands HPyrtr and PT Coordination via the $N^1$ (ring A) and the $N^{4'}$ or $N^{2'}$ is expected to yield a complex with similar properties as complexes containing HPyrtr type ligands Similarly, coordination via $N^1$ (ring B) and $N^{2'}$ is expected to yield a complex with properties similar to complexes containing PT type ligands

(a)

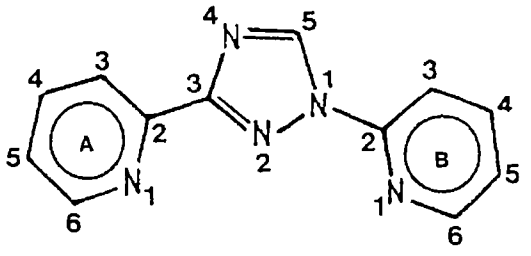


(b)

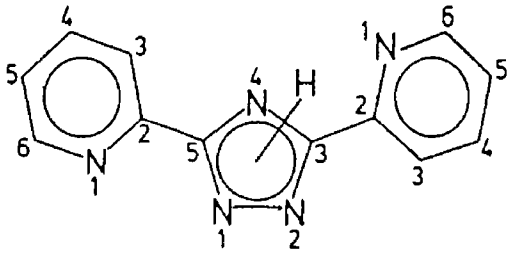


Figure 5 4 (a) 1,3-bis-(pyridin-2-yl)-1,2,4-triazole (bptn) and (b) 3,5-bis-(pyridin-2-yl)-1,2,4-triazole (Hbpt)

For the complex $[Ru(bpy)_2(bptn)]^{2+}$, the formation of three possible isomers is possible Figure 5 5 depicts the three coordination modes possible for this ligand Coordination may take place either (1), $N^1$ (A) and $N^{2'}$ triazole, (2), $N^1$ (A) and $N^4$ triazole or (3), $N^1$ (B) and $N^{2'}$ triazole From the structure of the ligand it would appear that the most feasible coordination mode from steric reasons would be via $N^1$ (A) and $N^{4'}$ triazole It is anticipated that due to steric hindrance between pyridine ring (B) and the bi-pyridine ligands coordination between $N^1$ (A) and $N^{2'}$ triazole and also between $N^1$ (B) and $N^{2'}$ triazole would not be favoured This therefore suggests that the formation of dinuclear compounds containing this bridging ligand may prove difficult

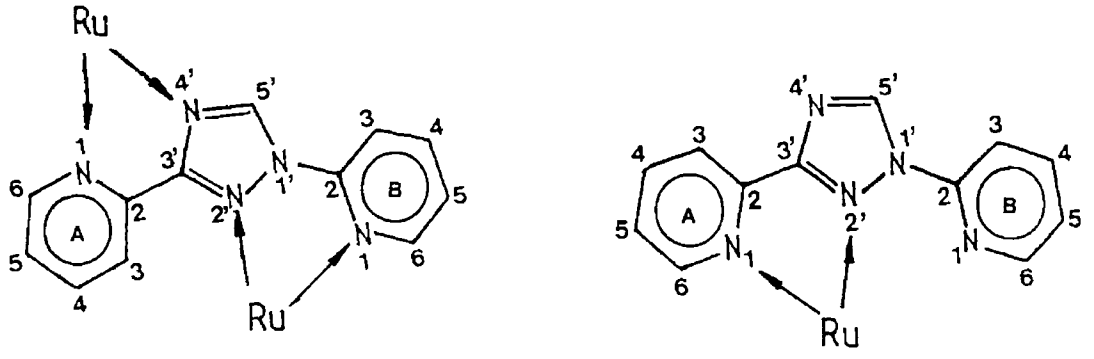


Figure 5 5 Possible coordination modes for bptn

The elemental analysis of the mononuclear compounds containing bptn are all good (see Chapter 2 Experimental), though the $^{1}H$ n m r of $[Ru(phen)_2(bptn)]^{2+}$ shows the presence of a second species (<5%) From the $^{1}H$ n m r spectrum it is not possible determine the nature of the impurity due to the small quantity present As suggested earlier, the formation of the dinuclear compound containing this bridging ligand or the formation of the isomers coordinated via $N^{1}$ (A) and $N^{2'}$, and $N^{1}$ (B) and $N^{2'}$ seems unlikely due to steric reasons, but these possibilities cannot be eliminated

The ligand Hbpt (Figure 5 4 (a)) is similar to the ligand HPyrtr except that the second pyridine ring is bound to the triazole ring via the 5' carbon atom and so the ligand contains two possible sites for bidentate coordination So, the formation of two mononuclear isomers is possible with this ligand, the first via a pyridine ring and the $N^{1'}$ atom of the triazole ring and the second via a pyridine ring and the $N^{4'}$ atom of the triazole ring Previous studies on this complex show that only one isomer is formed and coordination takes place via the $N^{1'}$ atom and a

pyridine ring [38] The steric interaction is less when $Ru(bpy)_2$ is bound via $N^{1'}$ triazole and $N^1$ pyridine than when bound via $N^{4'}$ triazole and $N^1$ pyridine It is therefore anticipated that reactions of $[Ru(Me_2bpy)_2Cl_2]$ and $[Ru(phen)_2Cl_2]$ with Hbpt should also yield one isomer

However, unexpectedly, both $^1H$ n m r and electrochemical studies of $[Ru(Me_2bpy)_2(bpt)]^+$ and $[Ru(phen)_2(bpt)]^+$ indicate the presence of a second species Purity of samples was also determined using the HPLC system described earlier (Chapter 3 Section 3) For both compounds one peak eluted and using the diode array detection system the uv/vis spectra of different sections of the chromatogram could be obtained The results in Figure 5 6 show that for both compounds different sections of the chromatograms yield similar, but not identical uv/vis absorption spectra This indicates that both samples contain a second species and that separation on the HPLC column has not occurred

Electrochemical results yield two oxidation potentials for the mononuclear complexes $[Ru(Me_2bpy)_2(bpt)]^+$ and $[Ru(phen)_2(bpt)]^+$, and in agreement with the $^1H$ n m r spectra, the ratio's of the main component to the second species are 80 20 for $[Ru(Me_2bpy)_2(bpt)]^+$ and 70 30 for $[Ru(phen)_2(bpt)]^+$ From $^1H$ n m r spectroscopy the resonances of the major component in each sample are very similar to the resonances obtained for $[Ru(bpy)_2(bpt)]^+$, suggesting that the main isomer formed for $[Ru(Me_2bpy)_2(bpt)]^{2+}$ and $[Ru(phen)_2(bpt)]^+$ is coordinated via $N^1$ pyridine and $N^{1'}$ triazole It must also be noted that elemental analysis for $[Ru(Me_2bpy)_2(bpt)]^{2+}$ is reasonable and for $[Ru(phen)_2(bpt)]^+$ the elemental analysis is good (see Chapter 2 Experimental)

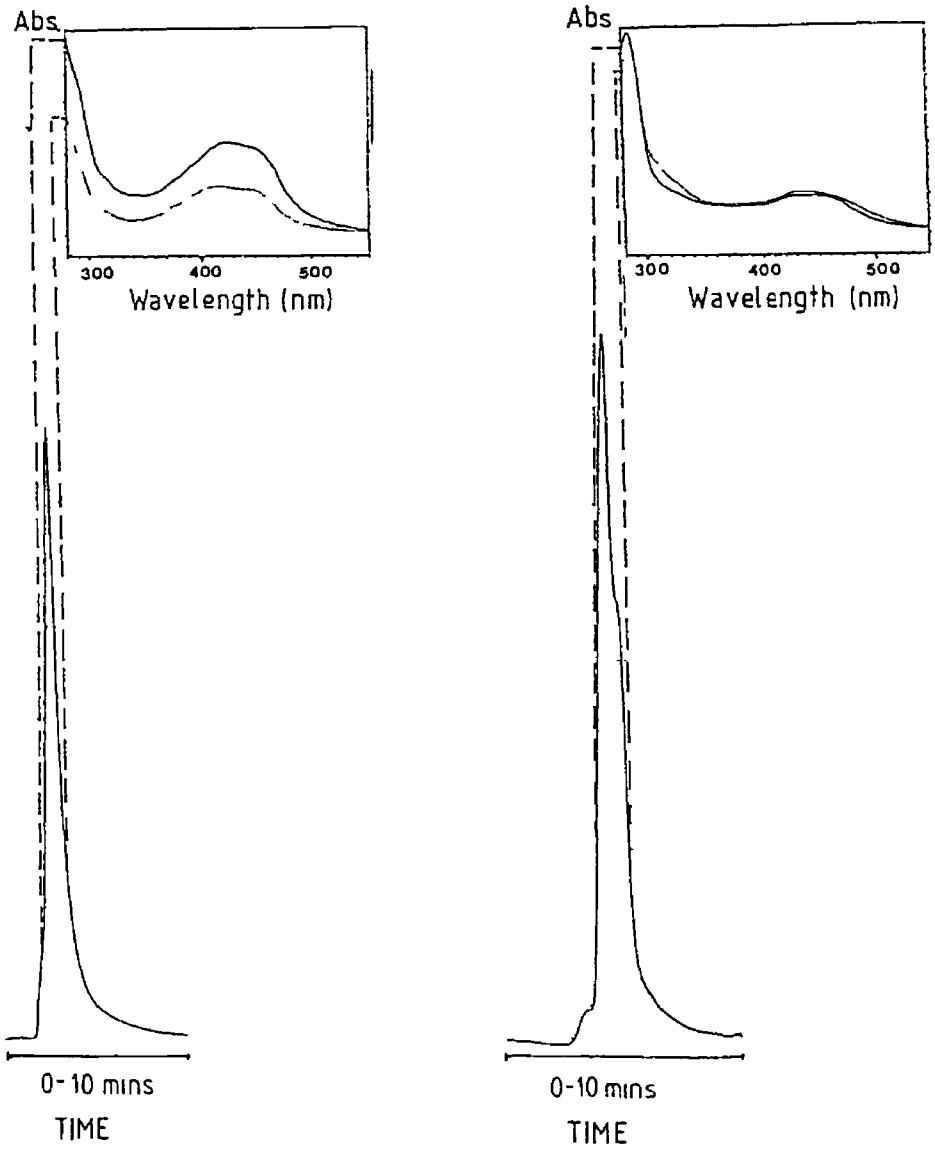


Figure 5 6 Chromatgrams of (a) $[Ru(Me_2bpy)(Hbpt)]^{2+}$ and (b) $[Ru(phen)_2(Hbpt)]^{2+}$ with corresponding uv/vis spectra taken at different retention times on the chromatogram Mobile phase acetonitrile water (80 20) with 0 08 M $LiClO_4$ Flow rate 3 0 ml/min

The elemental analysis results may suggest that the "impurity" is the isomer that is coordinated via $N^1$ pyridine and $N^{4'}$ triazole The exact nature of the impurities/isomers is at present not known Further experiments are required to determine the nature of these "second products" Semi - preparative HPLC using a suitable mobile phase is necessary for isolation of pure samples followed by $^1H$ n m r spectroscopy for identification The compounds $[Ru(Me_2bpy)_2(bpt)]^{2+}$ and $[Ru(phen)_2(bpt)]^{+}$ have been characterised by uv/vis and emission spectroscopy and electrochemistry and their $pK_a$ values have also been determined However, these results must be treated with caution as the exact composition of the samples is not known Deprotonation of the triazole ring may also occur leaving a negative charge on the ligand Hence the protonated and deprotonated form of the mononuclear compounds may be isolated

5 1 2 Preparation of Dinuclear Compounds.

During the attempt to prepare the dimeric species containing the ligand bptn no evidence for the formation of dinuclear compounds was observed from the reaction of $[Ru(L\text{-}L)_2Cl_2]$ where L-L = bpy, phen or $Me_2bpy$ with bptn Also, reaction of the monomeric species $[Ru(L\text{-}L)_2(bptn)]^{2+}$ with excess $[Ru(L\text{-}L)_2Cl_2]$ yielded no dimer

The dinuclear complexes of the type $[(Ru(L\text{-}L)_2)_2(bpt)]^{3+}$ were prepared by heating $[Ru(L\text{-}L)Cl_2]$ and ligand under reflux in a molar ratio in ethanol/water (2 1) for 12 hours according to the equation below

$$[Ru(L\text{-}L)_2Cl_2] \xrightarrow{Hbpt} [(L\text{-}L)_2Ru(bpt)Ru(L\text{-}L)_2]^{3+} \quad (9)$$

The complexes were precipitated as the $PF_6^-$ salt For these complexes, it is interesting to note that deprotonation of the neutral ligand, Hbpt, occurs upon formation of the dimeric species This suggests that protonation of the triazole ring is not favoured under these circumstances, perhaps due to steric hindrance of the bipyridyl ligands or alternatively deprotonation of this ligand may provide additional stabilization due to the stronger σ donor properties of the $bpt^-$ ligand The dinuclear complexes may also be obtained by refluxing the monomer $[Ru(L\text{-}L)_2(bpt)]^+$ in ethanol/water (2 1) with an excess of $[Ru(L\text{-}L)_2Cl_2]$ where L-L = bpy, $Me_2bpy$ of phen, according to the equation

$$[Ru(L\text{-}L)_2(bpt)]^+ + [Ru(L\text{-}L)_2Cl_2] \dashrightarrow [(L\text{-}L)_2Ru(bpt)Ru(L\text{-}L)_2]^{3+} \quad (10)$$

The elemental analysis for the compound $[(Me_2bpy)_2Ru(bpt)\text{-}Ru(Me_2bpy)_2](PF_6)_3$ gave a low percentage carbon, hydrogen and nitrogen (see Chapter 2 Experimental), suggesting that something inorganic may be present The presence of ammonium hexafluorophosphate and water decreases the percentages of carbon, hydrogen and nitrogen but leave nitrogen a little high Electrochemical measurement yields two peaks of equal intensity characteristic of dinuclear compounds Due to the small quantity of sample obtained $^1H$ n m r analysis could not be obtained

Each dinuclear complex of the type $[(bpy)_2Ru(bpt)\text{-}Ru(bpy)_2]^{3+}$ may exist in two geometrical isomers depending on the relative orientation of the bipyridine ligands (see Figure 5 10 Section 5 2 1)

The dinuclear complexes $[(bpy)_2Ru(bpt)Ru(phen)_2]^{3+}$, $[(bpy)_2Ru(bpt)Ru(Me_2bpy)_2]^{3+}$ and $[(phen)_2Ru(bpt)\text{-}$

$Ru(Me_2bpy)_2]^{3+}$ have also been prepared by reacting the monomeric species $[Ru(L\text{-}L)_2(Hbpt)]^{2+}$ with an excess of the dichloride $[Ru(L'\text{-}L')_2Cl_2]$ according to equation (II)

$$[Ru(L\text{-}L)_2(bpt)]^{+} + [Ru(L'\text{-}L')_2Cl_2] \dashrightarrow [(L\text{-}L)_2Ru(bpt)Ru(L'\text{-}L')_2]^{3+} \quad (II)$$

when L-L = bpy, L'-L' = $Me_2$bpy or phen, and when L-L = phen, L'-L' = $Me_2$bpy

It must be noted at this stage that the elemental analysis obtained for $[(bpy)_2Ru(bpt)Ru(phen)_2]^{3+}$ was not good (see Chapter 2 Experimental) The $^1H$ n m r obtained for this compound indicates the presence of an impurity or isomer though differential pulse voltammetry shows the presence of two peaks characteristic of dinuclear compounds

Studies on the mononuclear and dinuclear compounds prepared include $^1H$ n m r spectroscopy, electronic spectroscopy and electrochemical measurements and will be discussed in the following sections

## 5 2 $^1H$ N.m.r. Spectra.

### 5 2 1 Proton Resonance Spectra of the Free Ligands.

The assignment of the bptn protons has been made by comparison with the $^1H$ n m r data of the free ligands HPyrtr and PT [38] (see Chapter 3 Section 1) and also by comparison with the $^1H$ n m r data obtained for Hbpt [39] The proton resonances obtained for the ligands bptn and bpt are presented in Table 5 1 For bptn, the resonance of the highest $H^6$ doublet at 8 70 p p m has been assigned to the $H^6$ proton of ring A by comparison with the $H^6$ resonance for

the free ligand HPyrtr, which is also observed at 8 70 p p m A second doublet is found at 8 57 p p m , in the spectrum of bptn, this has been assigned to the $H^6$ proton of pyridine ring B, bound to the triazole ring via the 1' nitrogen atom This value is in good agreement with the value for the $H^6$ doublet of the ligand PT (8 53 p p m ), which also contains a C-N pyridyltriazole bond The 5' proton of the triazole ring is found as a singlet downfield at 9 48 p p m , which is in reasonable agreement with the value of the $H^5$ singlet for PT, found at 9 99 p p m With the results obtained, the resonances of the two different pyridine rings can be easily distinguished For Hbpt, the protons for each pyridine ring are in the same environment and hence exhibit the same resonance frequencies

Table 5 1 Proton N m r Resonances for Free Ligands (Solvent dimethyl sulfoxide 200 MHz)

| Ligand | Proton Resonances (p p m ) | | | | | |
|---|---|---|---|---|---|---|
| | $H^3$ | $H^5$ | $H^3$ | $H^4$ | $H^5$ | $H^6$ |
| bptn | | 9 48 | 8 09 | 7 92-8 02 | 7 47-7 51 | 8 70(a) |
| | | | 7 92-8 02 | 8 15 | 7 47-7 51 | 8 57(b) |
| Hbpt | - | | 8 15 | 8 00 | 7 52 | 8 67 |
| PT | 8 30 | 9 37 | 7 86 | 8 06 | 7 47 | 8 53 |
| HPyrtr | - | 8 27 | 8 09 | 7 98 | 7 51 | 8 70 |

5 2 2 $^{1}$H N.m.r. Spectra for Mononuclear Complexes Containing 1,3-Bis(pyridin-2-yl)1,2,4-triazole.

The $^{1}$H n m r spectral data obtained for the mononuclear compounds containing bptn are presented in Table 5 2 A schematic diagram of the mononuclear complexes containing bptn is presented in Figure 5 7

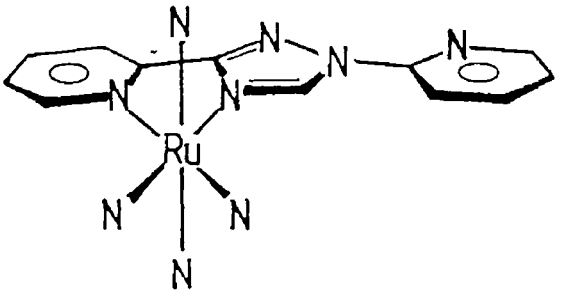


Figure 5 7 Proposed structure of $[Ru(L\text{-}L)_2(bptn)]^{2+}$ complexes where N-N = bpy, $Me_2bpy$ or phen

A complete assignment of the spectra of $[Ru(bpy)_2(bptn)]^{2+}$ and $[Ru(Me_2bpy)_2(bptn)]^{2+}$ could be made using COSY techniques and by comparison with literature data [25, 39-42]

No complete assignment could be made for $[Ru(phen)_2(bptn)]^{2+}$, but by comparison with the literature [39-46] parts of the spectrum could be assigned The structure and numbering scheme for bptn is shown in Figure 5 4 (a) and the proposed structure is illustrated in Figure 5 7

As can be seen from Figure 5 5 the formation of three isomers is possible for the preparation of mononuclear compounds containing bptn The COSY n m r spectra of $[Ru(bpy)_2(bptn)]^{2+}$ presented in Figure 5 8, reveals the presence of only one isomer

Table 5 2 Correlation Spectroscopy Data for Mononuclear Compounds

Containing bptn (Solvent acetone-$d_6$, 300 MHz) (ppm)

| Compound | | Pyridyl-Triazole ligand (bptn) | | | | |
|---|---|---|---|---|---|---|
| | | $H^{5'}$ | $H^3$ | $H^4$ | $H^5$ | $H^6$ |
| $[Ru(bpy)_2(bptn)]^{2+}$ | | 9 59 | (a) 8 61 | 8 24 | 7 60 | 7 95 |
| | | | (b) 8 09 | 8 17 | 7 56 | 8 47 |
| $[Ru(Me_2bpy)_2(bptn)]^{2+}$ | | 9 56 | (a) 8 65 | 8 43 | 7 38 | 7 85 |
| | | | (b) 8 09 | 8 18 | 7 55 | 8 45 |
| $[Ru(phen)_2(bptn)]^{2+}$ | | 9 53 | (a) 8 65 | 8 22 | 7 58 | 7 92 |

(a) Ruthenium-bound pyridine ring of bptn (b) Free ring of bptn

Table 5 3 Correlation Spectroscopy Data for Mononuclear Compounds

containing $bpt^-$ (Solvent acetone - $d_6$, 300 MHz) (ppm)

| Compound | | Pyridyl-Triazole Ligand ($bpt^-$) | | | |
|---|---|---|---|---|---|
| | | $H^3$ | $H^4$ | $H^5$ | $H^6$ |
| $[Ru(bpy)_2(bpt)]^+$ | (a) | 8 25 | 8 00 | 7 27 | 7 70 |
| | (b) | 8 10 | 7 75 | 7 20 | 8 45 |
| $[Ru(Me_2bpy)_2(bpt)]^+$ | (a) | 8 61 | 7 95 | 7 38 | 7 82 |
| $[Ru(phen)_2(bpt)]^+$ | (a) | 8 41 | 8 09 | 7 31 | 7 86 |
| | (b) | 7 04 | 8 15 | 7 53 | 8 52 |

(a) Ruthenium-bound ring of $bpt^-$ (b) Free ring of $bpt^-$

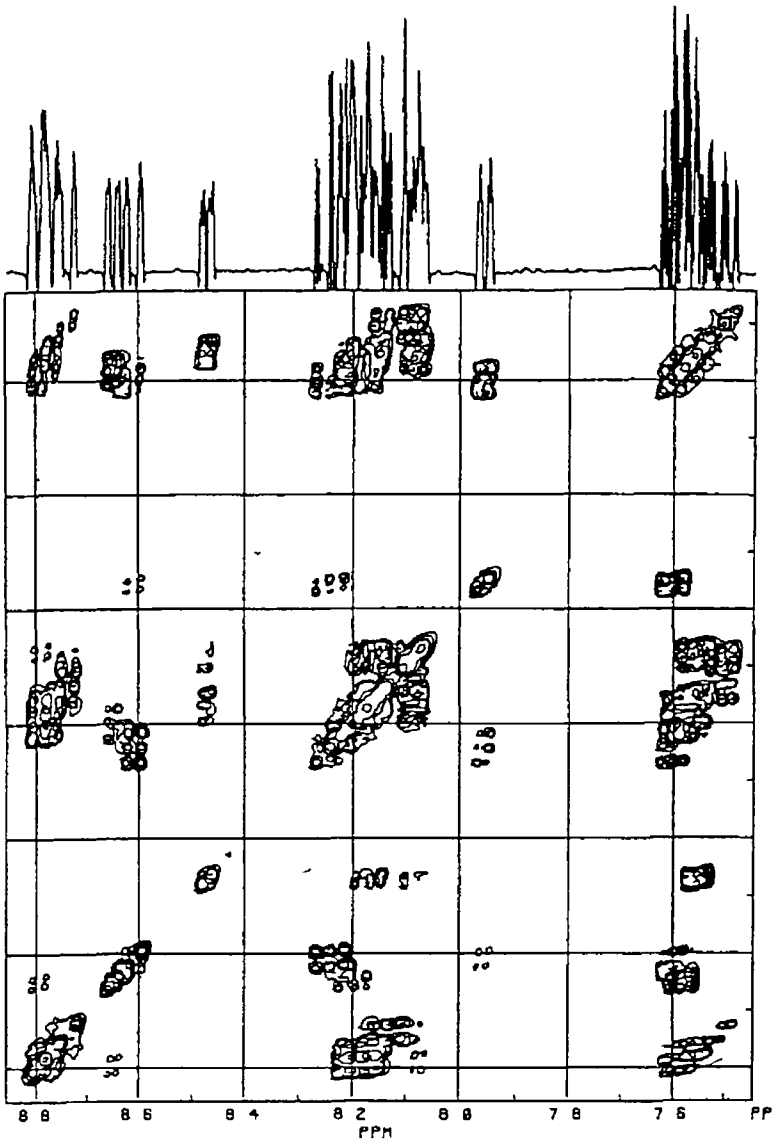


Figure 5.8 COSY spectrum of $[Ru(bpy)_2(bptn)]^{2+}$ in acetone-$d_6$.

From the proton resonance data listed in Table 5 2, it is not possible to unambiguously assign the mode of coordination of $Ru(bpy)_2$ to bptn However, evidence suggests, according to comparisons made with the free and bound ligands Hpyrtr and PT that coordination takes place via $N^1$ pyridine ring A and the triazole ring Unfortunately, a direct comparison with the monomer $[Ru(bpy)_2(bpt)]^+$ cannot be made as the Hbpt ligand is in the deprotonated form

The proton resonances containing the $H^6$ doublet at highest field, (a) in Table 5 2 are those of the bound pyridine ring while the (b) resonances are those of the unbound pyridine ring The $H^6$ protons are especially diagnostic for the assignment of bound and unbound pyridine rings, as the $H^6$ protons of the bound ring are shifted upfield with respect to those of the free ligand For the unbound ring the shift for the $H^6$ proton is relatively small in comparison with those of the free ligand, this is because the unbound ring is free to rotate and hence the $H^6$ protons of this ring will not be in the shielding cone of a bipyridine ligand

The proton resonance data of $[Ru(bpy)_2(bptn)]^{2+}$ suggests that the bound pyridine can be assigned to pyridine ring A on the following basis The resonances obtained for the pyridine ring in the coordinated Hpyrtr (two isomers) and PT are similar to the results obtained for the bound pyridine ring of bptn On this basis the mode of coordination cannot be ascertained The resonances of the unbound pyridine ring are more diagnostic The $H^6$ resonance of the unbound ring (b) at 8 57 p p m is more similar to the resonance at 8 53 p p m for the free PT ligand than that of 8 70 p p m for free HPyrtr The $H^3$, $H^4$ and $H^5$ resonances of ring B (see Table 5 2) are very similar to the resonances of the free PT ligand This

suggests that the free pyridine ring is ring B in Figure 5 5

The resonance of the $H^{5'}$ proton of bptn might also be considered diagnostic when compared with the resonances of the $H^{5'}$ protons of PT, 3BrPT and 3MePT (see Table 3 7 Section 2 of Chapter 3) The resonances of the $H^{5'}$ singlets in the last three ligands are at 9 37, 9 21 and 8 89 p p m respectively The $H^{5'}$ resonances for pyridyltriazole compounds containing a C-C bond are found at higher field The $H^{5'}$ values for HPyrtr, 4MePyrtr and 1MePyrtr are 8 27, 8 62 and 8 61 p p m respectively (see Table 5 1, 3 7 and Chapter 2 respectively) The $H^{5'}$ singlet for bptn is found at 9 37 p p m , a value more similar to the values obtained for the singlets in PT type ligands, it is again suggested that the bound pyridine ring is ring A in Figure 5 5

From Figure 5 5 it is observed that pyridine ring B is a substituent on the 1' nitrogen of the triazole ring For the ligand 1MePyrtr in $[Ru(bpy)_2(1MePyrtr)]^{2+}$, the methyl group on the 1' nitrogen provides enough steric hindrance for coordination not to occur at the $N^{2'}$ position [39] Coordination of the 1MePyrtr ligand in this compound is via the pyridine ring and the $N^{4'}$ nitrogen of the triazole ring This would suggest that coordination to bptn takes place via $N^1$ and $N^{4'}$ as the pyridine ring substituent on the 1' position of the triazole ring would provide more steric hindrance than the methyl group of 1MePyrtr In this coordination mode the steric effects of ring B on the bipyridine ligands would be minimal, see Figure 5 5

The resonances for the bipyridine ligands of $[Ru(bpy)_2(bptn)]^{2+}$ are similar to those for other bis-bipyridine Ru(II) complexes containing pyridyltriazole ligands [39, 40]

The complex $[Ru(Me_2bpy)_2(bptn)]^{2+}$ exhibits very similar shifts to $[Ru(bpy)_2(bptn)]^{2+}$, suggesting that coordination to ruthenium is also via pyridine ring A and $N^{4'}$ of the triazole ring The $H^3$, $H^5$ and $H^6$ resonances of the protons of the 4,4'-dimethyl-2,2'-bipyridine) ligands are similar to those obtained for $[Ru(Me_2bpy)_3]^{2+}$ [43] As the four methyl groups on the $Me_2bpy$ ligands are in different environments four singlets are expected Four methyl group singlets are present in the region 2 56 - 2 58 p p m This also indicates the presence of one isomer only

The $^1H$ n m r data for the complex $[Ru(phen)_2(bptn)]^{2+}$ did not yield as much information as for the other two bptn monomeric complexes The $^1H$ n m r spectra for complexes containing $Ru(phen)_2$ moieties is much more complex than that containing $Ru(bpy)_2$ moieties, due to the non-equivalence of the two halves of each phenanthroline ligand [44] This makes the $^1H$ n m r analysis very complex as in the higher-field region of the spectrum of $[Ru(phen)_2(bpy)]^{2+}$ the $H^5$ and $H^6$ signals appear as an AB quartet and not as a singlet as found for $[Ru(bpy)_2(phen)]^{2+}$ [43] and $[Ru(phen)_3]^{2+}$ [46] The coupling from only one of the pyridine rings of the bptn ligand was obtained from the COSY spectrum From Table 5 2 the proton resonances for this pyridine ring are very similar to those of the bound pyridine ring of $[Ru(bpy)_2(bptn)]^{2+}$ and $[Ru(Me_2bpy)(bptn)]^{2+}$, more similar to the former complex than the latter For this reason, the coordination mode of bptn to cis-$(phen)_2Ru(II)$ is suggested to be the same as that of the bipyridine and methyl-bipyridine bptn monomeric complexes, that is, via pyridine ring A and the $N^{4'}$ atom of the triazole ring

From the $^1H$ n m r of $[Ru(phen)_2(bptn)]^{2+}$ it is observed that the sample contains a 5% impurity Analysis of this impurity by COSY is not possible due to the small amount

present Some highfield resonances are present but cannot conclusively be assigned to the dimeric species Using differential pulse voltametry only one oxidation potential for this compound was observed This result, along with the structural constraints of the ligand indicate that the formation of the dimeric species is unlikely The elemental analysis of $[Ru(phen)_2(bptn)]^{2+}$ is good (see Chapter 3, Experimental) suggesting that a second isomer of $[Ru(phen)_2(bptn)]^{2+}$ may have been formed

In conclusion, the $^1H$ n m r data of the monomeric complexes containing bptn suggests that the $Ru(bpy)_2$ moiety preferentially coordinates to the bptn ligand via the $N^1$ of pyridine ring A and $N^{4'}$ of the triazole ring This is an indication that steric hindrance with bptn occurs and coordination to ring A and $N^{4'}$ of the triazole ring is favoured These results may also suggest that reaction with a pyridyltriazole ligand containing a C-C bond is more favourable than that containing a C-N connecting bond

### 5 2 3 $^1$H N m r Spectra of Mononuclear Compounds Containing 3,5-Bis(pyridin-2-yl)-1,2,4-triazole,

The proton n m r resonances obtained for the Hbpt ligand in the mononuclear complexes containing the deprotonated form of this ligand are listed in Table 5 3 The structure of $[Ru(bpy)_2(bpt)]^+$ as determined from X-ray crystallography is presented in Figure 5 9 [38] The crystal structure of the deprotonated $[Ru(bpy)_2(bpt)]^+$ complex confirms that the coordination mode of $bpt^-$ to $Ru(bpy)_2$ is via $N^1$ pyridine ring and $N^{2'}$ triazole ring As can be seen from Figure 5 9, the formation of two isomers is possible, the first via $N^1$ pyridine and $N^{2'}$ triazole and the second via $N^1$ pyridine and $N^{4'}$ triazole The $^1H$ n m r data [40] suggests the presence of only one isomer No

complete assignment of the COSY spectrum could be made, but by comparison with literature data the major part of the spectrum could be understood [39-45] The chemical shifts of the protons of the ruthenium coordinated pyridine ring of the bpt⁻ ligand are noticeably different from those observed for the non-coordinating ring

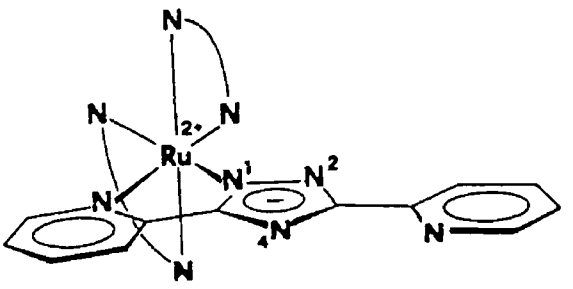


Figure 5 9 Structure of $[Ru(bpy)_2(bpt)]^+$ as determined by X-ray crystallography

This is especially clear for the $H^6$ doublets For the coordinated pyridine ring, the $H^6$ doublet shifts upfield by 0 97 p p m in comparison with that of the free ligand This is explained by the magnetic anisotropic effect from a pyridine ring of one of the bipyridine ligands The $H^6$ doublet of the non-coordinated pyridine ring shifts very slightly upfield by 0 20 p p m compared with the free ligand This indicates that it is not influenced by other parts of the molecule The resonances for the bipyridine rings (not included) are similar to those obtained for other pyridyltriazole ligands coordinated to $Ru(bpy)_2$ - moieties [39]

$^1H$ n m r and electrochemical analysis of $[Ru(Me_2bpy)_2(bpt)]^+$ and $[Ru(phen)_2(bpt)]^+$ reveal the presence of a second product in each complex This is an

unusual result as no impurities were observed in the $^1H$ n m r spectra of $[Ru(bpy)_2(bpt)]^+$ [40] The proton n m r spectra of these complexes do not contain any characteristic doublets at high field which are present in the n m r spectra of the dinuclear compounds This indicates that the impurity is not a dinuclear species The proton n m r resonances for the $bpt^-$ ligands of $[Ru(Me_2bpy)_2(bpt)]^+$ and $[Ru(phen)_2(bpt)]^+$ are presented in Table 5 3 Eight singlets that can be attributed to methyl groups are observed in the region 2 38-2 58 p p m for $[Ru(Me_2bpy)_2(bpt)]^+$ This may suggest that the second species present is the second possible isomer The ratio of which is approximately 80 20 (by peak height analysis) From the resonances of the $bpt^-$ ligand the predominate isomer seems to be the same as that for $[Ru(bpy)_2(bpt)]^+$, that is, coordinated via $N^1$ and $N^{2'}$ As two isomers are present this complicates the interpretation of the COSY spectra A detailed analysis has not been given as it is the $bpt^-$ protons that are of interest here Only one of the pyridine rings of $bpt^-$ could be fully assigned A remarkable doublet belonging to one of the $Me_2bpy$ rings is found at 7 16 p p m The reason for the presence of this doublet at highfield is at present not known

$^1H$ n m r data for complex $[Ru(phen)_2bpt]^+$ in Table 5 3 also reveals the presence of 30% of a second species The proton shifts of the main species are similar to those of the other $bpt^-$ monomers suggesting that coordination in the main species is via $N^1$ and $N^{2'}$ Now, a doublet at low field is present in the n m r spectra of $[(phen)_2Ru(bpt)\text{-}Ru(phen)_2]^{3+}$ A doublet is also present at low field (9 10 p p m ) in the n m r spectra of $[Ru(phen)_2(bpt)]^+$ which is not coupled to any of the $bpt^-$ protons and is absent in any of the other $bpt^-$ monomer spectra This suggests that the doublet belongs to a phenanthroline proton and is only observed when the $Ru(phen)_2$ moiety is coordinated via $N^1$

and $N^{4'}$ of the triazole ring This suggests that the second species may be the isomer that is coordinated via $N^{1}$ pyridine and $N^{4'}$ triazole

To conclude, the formation of the $[Ru(bpy)_2(bpt)]^+$ monomer results in the formation of only one isomer bound via $N^{1}$ of a pyridine ring and $N^{2'}$ of the triazole ring On the other hand, it is suggested that the formation of both $[Ru(Me_2bpy)_2(bpt)]^+$ and $[Ru(phen)_2(bpt)]^+$ result in the formation of two isomers in the approximate ratio 75 25 The major isomer is coordination via $N^{1}$ of a pyridine ring and $N^{2'}$ of the triazole ring For the minor isomer coordination takes place via $N^{1}$ of a pyridine ring and $N^{4'}$ of the triazole ring For the latter more steric interaction is expected, so this type of coordination mode would not be as favourable

### 5 2 4 $^{1}$H N.m.r. Spectra of Dinuclear Complexes Containing 3,5-Bis(pyridin-2-yl)1,2,4-triazole)

The $^{1}$H n m r spectral data for the dinuclear compounds is presented in Table 5 4 The $^{1}$H n m r spectra of all dinuclear complexes contain a characteristic highfield doublet This doublet of the $[(bpy)_2Ru(bpt)Ru(bpy)_2]^{3+}$ dimer has been assigned to the $H^{3}$ proton of ring A of the $bpt^-$ ligand [40] Because of the short distance between the $H^{3}$ of the $bpt^-$ ligand and one of the bipyridine rings (ring C Figure 5 10) a large diamagnetic anisotropic interaction should occur, resulting in a shift of the resonance of $H^{3}$ to higher field [47] As this doublet is present in the n m r spectra of all the dinuclear compounds, it indicates that this doublet occurs irrespective of the nature of the $Ru(L\text{-}L)_2$ moiety coordinated to $bpt^-$ where L-L = bpy, $Me_2bpy$ of phen

Table 5 4 Correlation Spectroscopy Data of the Bridging Ligand in the Dinuclear Compounds (Solvent Acetone - $d_6$ 300 MHz) (ppm)

| Compound | | Pyridyl-Triazole Ligand (bpt) | | | |
|---|---|---|---|---|---|
| | | $H^3$ | $H^4$ | $H^5$ | $H^6$ |
| $[(bpy)_2Ru(bpt)Ru(bpy)_2]^{3+}$ | Isomer 1 | 6 69 | 7 33 | 7 21 | 7 82 |
| | | 7 11 | 7 29 | 8 08 | 8 73 |
| | Isomer 2 | 6 83 | 7 35 | 7 15 | 7 73 |
| | | 7 27 | 7 71 | 8 18 | 8 67 |
| $[(phen)_2Ru(bpt)Ru(phen)_2]^{3}$ | Isomer 1 | 6 52 | 7 12 | 6 98 | 7 75 |
| | | 7 48 | 7 70 | 8 23 | 8 69 |
| | Isomer 2 | 6 60 | 7 18 | 6 88 | 7 58 |
| | | 7 44 | 7 14 | 7 98 | 8 02 |
| $[(bpy)_2Ru(bpt)Ru(Me_2bpy)_2]^{3+}$ | | 6 69 | 7 39 | 7 15 | 7 96 |
| | | 6 82 | 7 38 | 7 56 | 8 40 |
| $[(bpy)_2Ru(bpt)Ru(phen)_2]^{3+}$ | | 6 48 | | | |
| | | 6 66 | 7 18 | 7 50 | 7 99 |
| $[(phen)_2Ru(bpt)Ru(Me_2bpy)_2]^{3}$ | | 6 76 | 7 13 | 7 34 | 7 87 |
| | | 6 79 | 7 31 | 7 01 | 7 69 |

The presence of two of these doublets at high field indicates the presence of two isomers

The two isomers of the dinuclear complex $[(bpy)_2Ru(bpt)Ru(bpy)_2]^{3+}$ have been isolated in a ratio of 1 1 by careful recrystallisation [40] The n m r data of the bpt ligand of these two isomers are presented in Table 5 4 The dinuclear compound may exist in two geometrical isomers as shown in Figure 5 10 Major steric interactions between the $Ru(bpy)_2$ moieties prevents a configuration in which the two $Ru(bpy)_2$ moieties are coordinated via $N^{1'}$ and $N^{2'}$ respectively, of the triazole ring, assuming a bpt⁻ conformation with pyridine rings A & B in a cis orientation Therefore, only the two geometrical isomers each with an optical pendant are assumed to be formed (Figure 5 10 (a) and (b))

The proton assigned to the doublet with the lowest p p m value (6 69 p p m of isomer 1 and 6 83 p p m of isomer 2) is the $H^3$ proton of a pyridine ring in the bpt⁻ ligand

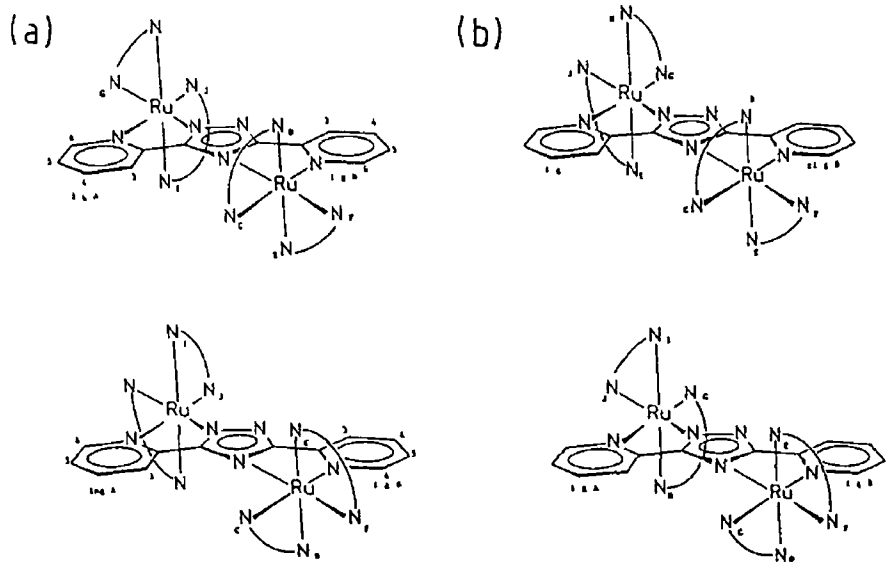


Figure 5 10 Proposed molecular structures of the two geometrical isomers (a) and (b) each with an optical pendant of the dinuclear complexes.

This is because of the short distance between $H^3$ of the bpt$^-$ ligand and one of the pyridine rings (ring C Figure 5 10), revealed by space filling models, a large diamagnetic anisotropic interaction should occur shifting the resonance of the $H^3$ doublet to higher field [40] This effect is even more pronounced than the diamagnetic anisotropic interaction between $H^6$ and pyridine rings found in $[Ru(bpy)_3]_2$ [47] The $H^3$ proton of ring B, on the other hand, is quite a large distance away from any other pyridine ring, therefore this proton will have a different chemical shift compared to those of the $H^3$ protons of ring A of bpt$^-$

The COSY experiment for isomer 1 yielded eight different sets of pyridine protons A less detailed analysis was made for isomer 2 due to the complexity of the spectrum However, from the results obtained (not included) it was shown that isomer 1 and isomer 2 have a different orientation of bipyridine ligands [39] The $^1H$ n m r data of isomer 2 contain a doublet at 8 4 p p m which is absent in the n m r spectrum of isomer 1 This doublet has been assigned to a $H^6$ proton of ring 1 or ring E (Figure 5 10 (b)) It has been shown that the bpy ligands IJ and EF of isomer 2 are more or less coplanar whereas in isomer 1 this coplanarity does not exist Because of the moderate steric interactions between the $H^6$ protons of the coplanar bipyridine ligands in the plane, a shift of higher p p m value is expected Normally a chemical shift to 7 8 p p m is observed for the $H^6$ protons in Ru(II) polypyridine systems [39, 44, 47]

As has been mentioned previously, two isomers of the dinuclear complex $[(phen)_2Ru(bpt)Ru(phen)_2]^{3+}$ were isolated The COSY n m r spectrum of isomer 1 is presented in Figure 5 11 (a) and the n m r of isomer 2 is presented in Figure 5 11 (b)

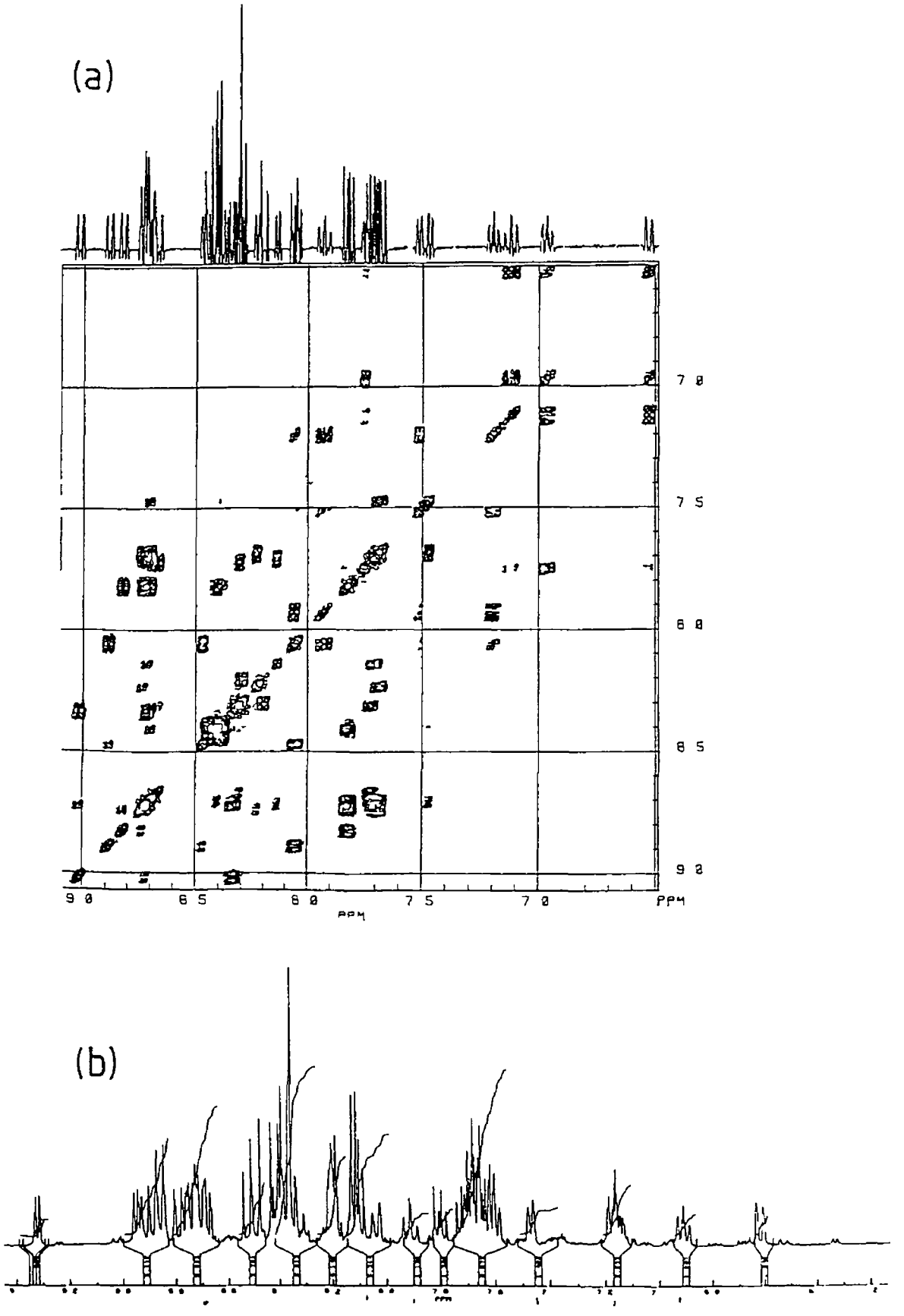


Figure 5 11 (a) COSY spectrum of isomer 1 and (b) $^{1}H$ n m r spectrum of isomer 2 of $[(phen)_2Ru(bpt)Ru(phen)_2]^{3+}$ in acetone-$d^6$

However, only a small quantity of the second isomer was obtained, enough just for $^1H$ n m r analysis This second fraction was removed from the alumina column with water during purification The first isomer was obtained upon recrystallisation of the column purified mixture The $^1H$ n m r spectral data for the two isomers are presented in Table 5 4 For both isomers a doublet is found at high field (6 52 for isomer 1 and 6 60 for isomer 2) and in comparison with the $^1H$ n m r of the bpy dimer, these have been assigned to the $H^3$ doublet of the bpt$^-$ ligand

The doublet at high field for isomer 1 has been assigned to the $H^3$ proton in pyridine ring A of bpt$^-$, which, because of the short distance from $H^3$ to phenanthroline ligand ($N_c$-$N_d$ Figure 5 10 (a)), should produce a large diamagnetic anisotropic interaction and hence shift the proton resonance to higher field A similar effect occurs for isomer 2 For both isomers the second set of $H^3$ protons of pyridine ring B are found at lower field (7 48 p p m for isomer 1 and 7 44 p p m for isomer 2), than those of pyridine ring A Both sets of $H^3$ protons are diagnostic for the bpt$^-$ ligand and very useful for the interpretation of the complicated COSY spectra

The $^1H$ n m r spectra of both isomers contain a doublet at low field (9 26 for isomer 1 and 9 02 for isomer 2) This resonance present in n m r spectra is suggested to belong to a proton on a phenanthroline ligand and is only present in the n m r spectrum when bpt$^-$ is bound to a $Ru(phen)_2$ moiety via ring B and the $N^{4'}$ of the triazole ring This doublet is also present as an impurity in the n m r spectra of $[Ru(phen)_2(bpt)]^+$, and it is therefore suggested that the mixture of $[Ru(phen)_2(bpt)]^+$ contains 30% of the isomer that is bound via $N^1$ pyridine and $N^{4'}$ triazole, as it is in this configuration that the doublet at low field is obtained The COSY spectra reveals that this doublet is

coupled to two other resonances, so the doublet belongs to either the $H^2$, $H^9$, $H^4$ or $H^7$ proton, each of these protons is split as a doublet However, due to the complex nature of the phenanthroline spectra a complete assignment cannot be given A more detailed comparison with complexes containing the $Ru(phen)_2$ moiety is required [44] The assignment of each isomer, for the dimeric complex $[(phen)_2Ru(bpt)Ru(phen)_2]^{3+}$ to a particular structure, that is, a particular orientation of phenanthroline ligands cannot be made due to the complex nature of the spectrum

The $^1H$ n m r spectra of the dimeric complex $[(bpy)_2Ru(bpt)Ru(phen)_2]^{3+}$ is also very complex especially in the region 6 98 to 8 92 p p m Nonetheless certain information has been obtained from the spectra Two high field doublets, at 6 48 and 6 86 p p m in the ratio 1 1, diagnostic of the $H^3$ protons of the pyridine rings of $bpt^-$ are observed This indicates that two isomers are present in the sample The $[Ru(bpy)_2(bpt)]^+$ monomer along with $[Ru(phen)_2Cl_2]$ were the starting materials for the reaction As the $[Ru(bpy)_2(bpt)]^+$ monomer is coordinated via $N^1$ pyridine ring A and $N^{2'}$ triazole of $bpt^-$ then the coordination site for the $Ru(phen)_2$ moiety must be at $N^1$ pyridine ring B and $N^{4'}$ triazole ring This coordination arrangement is confirmed by the presence of a doublet at 9 30 p p m indicative of coordination of a $Ru(phen)_2$ moiety via $N^1$ pyridine ring and $N^{4'}$ triazole ring As only one set of pyridine ring protons of $bpt^-$ have been resolved from the spectra, it is not possible to determine from which pyridine ring the protons are situated

The $^1H$ n m r spectrum of $[(bpy)_2Ru(bpt)Ru(Me_2bpy)_2]^{2+}$ is presented in Figure 5 12 Eight methyl groups are present in the region 2 46 - 2 57 p p m indicating the presence of two isomers The geometrical isomers are present in the ratio 70 30 (by peak height analysis)

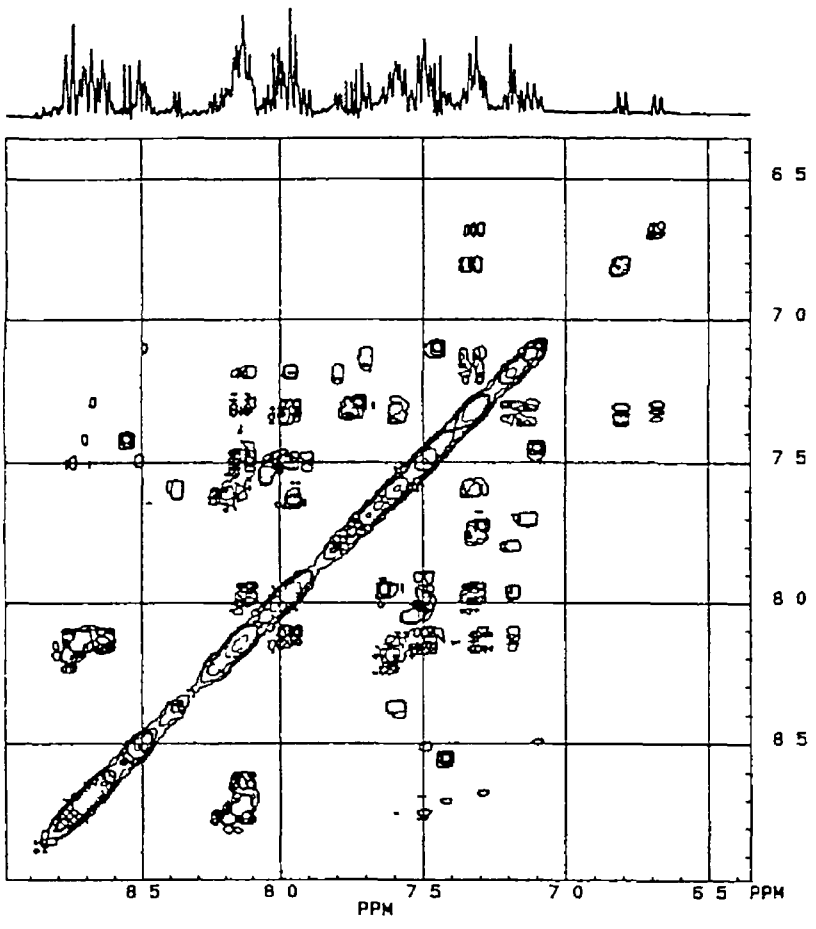


Figure 5 12 COSY spectrum of $[(bpy)_2Ru(bpt)Ru(Me_2bpy)_2]^{3+}$

The starting materials for the reaction were $[Ru(bpy)_2(bpt)]^+$ and $[Ru(Me_2bpy)_2Cl_2]$ Similarly, as for the $[(bpy)_2Ru(bpt)Ru(phen)_2]^{3+}$ dinuclear complex, the $Ru(bpy)_2$ moiety is coordinated via $N^1$ pyridine and $N_2$, triazole and consequently the $Ru(Me_2bpy)_2$ moiety is bound via $N^1$ pyridine and $N^{4'}$ triazole The spectrum contains two doublets at high field which are characteristic of the $H^3$ protons of the pyridine rings of $bpt^-$ when bound in the dinuclear form, again indicating the presence of two isomers On the basis of the assignment of 6 82 and 6 69 p p m to the $H^3$ protons of the pyridine rings of $bpt^-$, the COSY spectrum easily permitted the assignment of the remaining protons of the rings (Table 5 4) As the resonances of the $bpt^-$ protons are the most important feature of the n m r and due to the complexity of the spectra the resonances of the bpy and $Me_2bpy$ ligands were not assigned

The $bpt^-$ proton resonances $[(phen)_2Ru(bpt)Ru(Me_2bpy)_2]^{3+}$ are presented in Table 5 4 The starting material for the formation of this dinuclear complex are $[Ru(phen)_2(bpt)]^+$ and $[Ru(Me_2bpy)_2Cl_2]$ The n m r data, previously discussed, suggests two isomers in the mononuclear complex $[Ru(phen)_2(bpt)]^+$, in the ratio 70 30, where the major isomer binds to $bpt^-$ via $N^1$ pyridine and $N^{2'}$ triazole, while the latter binds via $N^1$ and $N^{4'}$ triazole A complicated reaction product containing many isomers is expected

The $^1H$ n m r data contains eight methyl groups in the region 2 53 to 2 69 p p m indicating the presence of two isomers The intensity of the peaks reveal that the isomers are present in a 1 1 ratio There is no doublet present at low field, i e at about 9 20 p p m , in the n m r spectrum This means that there is no dinuclear complex containing the $Ru(phen)_2$ moiety bound via $N^1$

pyridine and $N^{4'}$ triazole present in the sample Either this isomer, the presence of which had been proposed in the monomer on the basis of n m r data, has been lost during purification and/or recrystallisation procedure or else it remained unreacted This suggests that the two isomers in the n m r are geometrical isomers of $[(phen)_2Ru(bpt)\text{-}Ru(Me_2bpy)_2]^+$ where the $Ru(phen)_2$ moiety is coordinated via $N^1$ pyridine and $N^{1'}$ triazole and the $Ru(Me_2bpy)_2$ moiety is coordinated via $N^1$ pyridine and $N^{4'}$ triazole

In conclusion, the $^1H$ n m r data reported here show clearly the importance of this technique in determining the structures of the mononuclear complexes and the dinuclear complex $[(bpy)_2Ru(bpt)Ru(bpy)_2]^{3+}$ As the n m r 's of the dinuclear complexes are complicated, complete assignments were not made and for the $[(phen)_2Ru(bpt)Ru(phen)_2]^{3+}$ isomers the difference in structure could not be determined More important, the necessary information concerning the protons of the $bpt^-$ ligand could be obtained from most of the spectra

## 5 3 Electronic and Electrochemical Measurements.

### 5 3 1 Mononuclear Complexes Containing 1,3-Bis(pyridin-2-yl)-1,2,4-triazole.

Comparison of the electronic and electrochemical properties of $[Ru(bpy)_2(PT)]^{2+}$ and $[Ru(bpy)_2(HPyrtr)]^{2+}$, with the electronic and electrochemical properties of the mononuclear compounds containing bptn can be diagnostic in ascertaining the coordination mode of $Ru(L\text{-}L)_2$ to bptn, where L-L = bpy, $Me_2bpy$ or phen The absorption and emission data for all mononuclear and dinuclear compounds are presented in Table 5 5 while the electrochemical data are listed in Table 5 6

Table 5 5 Absorption and Emission data for Mononuclear and Dinuclear compounds

| Compounds | Absorption [A] | | Emission [B] | |
|---|---|---|---|---|
| | λMax | (log ε) | λMax 300K | λMax 77K |
| $[Ru(bpy)_2(bptn)]^{2+}$ | 448 | (3 91) | 610 | 573 |
| $[Ru(Me_2bpy)_2(bptn)]^{2}$ | 446 | (4 01) | 622 | 576 |
| $[Ru(phen)_2(bptn)]^{2}$ | 410 | (4 13) | 594 | 565 |
| $[Ru(bpy)_2(bpt)]$ | 475 | (4 05) | 650 | 624 |
| $[Ru(bpy)_2(Hbpt)]^{2}$ | 429 | (4 19) | 636 | 612 |
| $[Ru(Me_2bpy)_2(bpt)]$ | 460 | (3 96) | 652 | 601 |
| $[Ru(Me_2bpy)_2(Hbpt)]^{2}$ | 432 | (4 15) | 637 | 589 |
| $[Ru(phen)_2(bpt)]$ | 458 | (4 11) | 655 | 595 |
| $[Ru(phen)_2(Hbpt)]^{2}$ | 420 | (4 17) | 635 | 585 |
| $[(bpy)_2Ru(bpt)Ru(bpy)_2]^{3}$ | 452 | (4 35) | 625 | 600 |
| $[(bpy)_2Ru(Hbpt)Ru(bpy)_2]^{4}$ | 434 | (4 37) | c | c |
| $[(Me_2bpy)_2Ru(bpt)Ru(Me_2bpy)_2]^{3}$ | 450 | (4 35) | 635 | 608 |
| $[(phen)_2Ru(bpt)Ru(phen)_2]^{3}$ | 436 | (4 41) | 625 | 590 |
| $[(bpy)_2Ru(bpt)Ru(Me_2bpy)_2]^{3}$ | 456 | (4 32) | 640 | 600 |
| $[(bpy)_2Ru(bpt)Ru(phen)_2]^{3}$ | 452 | (4 31) | 632 | 597 |
| $[(phen)_2Ru(bpt)Ru(Me_2bpy)_2]^{3}$ | 430 | (4 39) | 635 | 597 |
| $[Ru(bpy)_3]^{2}$ [d] | 452 | (4 11) | 608 | 582 |
| $[Ru(Me_2bpy)_3]^{2}$ | 450 | (4 23) [e] | 618 [e] | 593 [f] |
| $[Ru(phen)_3]^{2}$ [e] | 447 | (4 26) | 604 | 565 |
| $[Ru(bpy)_2(PT)]^{2}$ | 420 | (4 03) | – | 560 |
| $[Ru(bpy)_2(HPyrtr)]^{2}$ Isomer 1 | 452 | (4 05) | 630 | 585 |
| Isomer 2 | 444 | (4 11) | 650 | 599 |

[A] Measured in $CH_3CN$ , λmax in nm, ε in $dm^3\ mol^{-1}\ cm^{-1}$ [B] Spectra at room temperature in $CH_3CN$ at 77K in Ethanol , λmax in nm [C] Emission not observed for protonated dimer [D] reference 62
[E] Reference 50 [F] Reference 63

Table 5.6 Electrochemical Data for Mononuclear and Dinuclear Compounds

| Compound | Redox Properties [A] Oxidation Pot (V) | Reduction Pot (V) | $K_{com}$ |
|---|---|---|---|
| $[Ru(bpy)_2(bptn)]^{2+}$ | 1.22 | −1.44 −1.68 | – |
| $[Ru(Me_2bpy)_2(bptn)]^{2+}$ | 1.12 | −1.51 −1.70 | – |
| $[Ru(phen)_2(bptn)]^{2}$ | 1.24 | −1.34 −1.54 | – |
| $[Ru(bpy)_2(bpt)]^{2}$ | 0.87 | −1.42 | – |
| $[Ru(bpy)_2(Hbpt)]^{2}$ | 1.00 | −1.42 | – |
| $[Ru(Me_2bpy)_2(bpt)]$ | 0.78 0.88 | −1.60 −1.84 | – |
| $[Ru(Me_2bpy)_2(Hbpt)]^{2}$ | 0.88 0.96 | −1.50 −1.60 | – |
| $[Ru(phen)_2(bpt)]$ | 0.72 0.96 | −1.48 −1.62 | – |
| $[Ru(phen)_2(Hbpt)]^{2}$ | 1.14 | −1.52 −1.78 | – |
| $[(bpy)_2Ru(bpt)Ru(bpy)_2]^{3}$ | 1.04 1.34 | −1.42 | $9.45 \times 10^4$ |
| $[(bpy)_2Ru(Hbpt)Ru(bpy)_2]^{4}$ | 0.89 1.10 | −1.42 | $0.3 \times 10^4$ |
| $[(Me_2bpy)_2Ru(bpt)Ru(Me_2bpy)_2]^{3+}$ | 0.98 1.25 | −1.54 −1.83 | $2.98 \times 10^4$ |
| $[(phen)_2Ru(bpt)Ru(phen)_2]^{3}$ | 1.00 1.31 | −1.41 −1.63 | $13.72 \times 10^4$ |
| $[(bpy)_2Ru(bpt)Ru(Me_2bpy)_2]^{3}$ | 1.01 1.24 | −1.44 −1.68 | $0.68 \times 10^4$ |
| $[(bpy)_2Ru(bpt)Ru(phen)_2]^{3}$ | 1.02 1.32 | −1.45 −1.66 | $9.37 \times 10^4$ |
| $[(phen)_2Ru(bpt)Ru(Me_2bpy)_2]^{3+}$ | 1.01 1.24 | −1.38 −1.62 | $0.64 \times 10^4$ |
| $[Ru(bpy)_3]^{2+}$ [B] | 1.22 | −1.36 −1.53 | – |
| $[Ru(Me_2bpy)_3]^{2+}$ [C] | 1.10 | −1.45 | – |
| $[Ru(phen)_3]^{2+}$ | 1.40 [D] | −1.35 [C] | – |
| $[Ru(bpy)_2(PT)]_y^{2+}$ | 1.35 | −1.42 −1.63 | – |
| $[Ru(bpy)_2(HPyrtr)]^{2+}$ Isomer 1 | 1.20 | −1.47 −1.72 | – |
| Isomer 2 | 1.10 | – | |

[A] measured in $CH_3CN$ with 0.1M $NEt_4ClO_4$, volts vs S.C.E., nhe = S.C.E. + 0.2415V

[B] reference 48 [C] reference 64 [D] reference 61

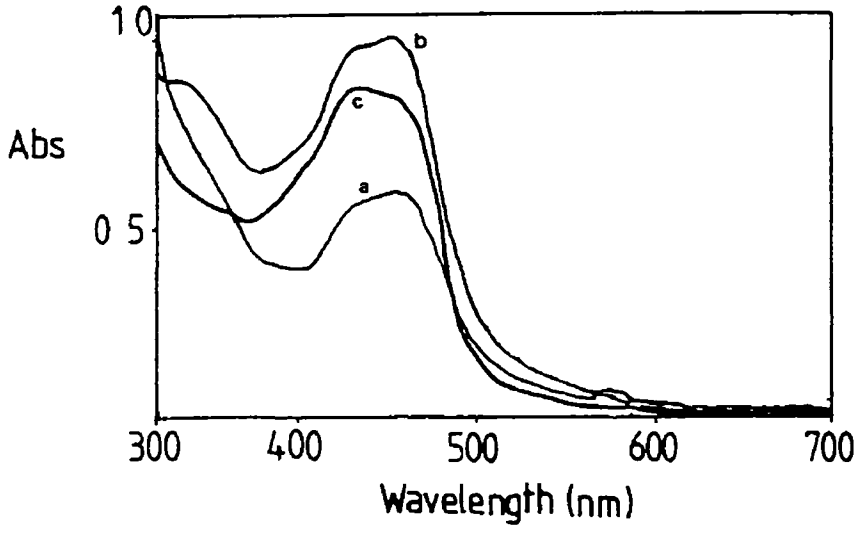


Figure 5 13 Absorption spectra in acetonitrile of (a) $[Ru(bpy)_2(bptn]^{2+}$ (b) $[Ru(Me_2bpy)_2(bptn)]^{2+}$ and (c) $[Ru(phen)_2(bptn)]^{2+}$

The absorption spectra for the mononuclear compounds containing bptn are presented in Figure 5 13 The absorption maxima for the mononuclear complexes $[Ru(bpy)_2$-$(bptn)]^{2+}$ (448 nm) and $[Ru(Me_2bpy)_2(bptn)]^{2+}$ (446 nm) are quite similar to that of $[Ru(bpy)_3]^{2+}$ (452 nm) However, the mononuclear complex $[Ru(phen)_2(bptn)]^{2+}$ absorbs at considerably higher energy (410 nm) than the other two monomeric complexes containing bptn Even though the $[Ru(phen)_3]^{2+}$ complex absorbs at slightly higher energy than $[Ru(Me_2bpy)_3]^{2+}$ and $[Ru(bpy)_3]^{2+}$ [48-51] this large shift in the absorption maximum for the mononuclear complex $[Ru(phen)_2(bptn)]^{2+}$ would not be expected The absorption maximum of $[Ru(bpy)_2(PT)]^{2+}$ is found at 420 nm, that is, higher energy than that of complexes where the pyridyl-triazole ligands contains a C-C bond (see Table 3 6 Chapter 3) This suggests that the coordination mode of the PT and bptn ligands containing $Ru(bpy)_2$ and $Ru(Me_2bpy)_2$ moieties are not the same, indicating that coordination to bptn may

take place via the pyridine and triazole ring which are bound by a C-C bond and not a C-N bond as in the PT ligand These results also suggest that the coordination mode for $[Ru(phen)_2(bptn)]^{2+}$ may be different to that of $[Ru(bpy)_2(bptn)]^{2+}$ and $[Ru(Me_2bpy)_2(bptn)]^{2+}$ From these results, coordination via pyridine ring A and the triazole ring is suggested as the coordination mode for bptn in the mononuclear compounds $[Ru(bpy)_2(bptn)]^{2+}$ and $[Ru(Me_2bpy)_2(bptn)]^{2+}$ However, as the results obtained for the $[Ru(phen)_2(bptn)]^{2+}$ complex are slightly different to the other two mononuclear compounds, it is not possible to unambiguously assign the coordination mode for the phen monomer

The absorption spectra results obtained also suggest that coordination to the triazole ring of bptn is via $N^{4'}$ This has been postulated on the following observations In comparison with the two compounds $[Ru(bpy)_2(1MePyrtr)]^{2+}$ and $[Ru(bpy)_2(4MePyrtr)]^{2+}$ whose electronic properties can be found in Table 3 6 (Chapter 3 Section 1) it is observed that the former compound absorbs at a lower energy (452 nm) than the latter (440 nm) As the 1MePyrtr ligand in $[Ru(bpy)_2(1MePyrtr)]^{2+}$ is bound to ruthenium via the $N^{4'}$ atom, results suggest that this ligand is a better $\pi$ acceptor than 4MePyrtr which is bound via the $N^{2'}$ atom of the triazole ligand A similar result is also obtained for the isomers, of $[Ru(bpy)_2(HPyrtr)]^{2+}$ whereby the first isomer believed to be coordinated via $N^{4'}$ of the triazole ring, absorbs at lower energy and has a higher oxidation potential than the second which is coordinated via $N^{2'}$ of the triazole ring This suggests that when the triazole ring is coordinated to ruthenium via $N^{4'}$ the pyridyltriazole ligand becomes a better $\pi$ acceptor As the absorption energy of $[Ru(bpy)_2(bptn)]^{2+}$ is at 448 nm, at similar energy to the absorbances of $[Ru(bpy)_2(1MePyrtr)]^{2+}$ and $[Ru(bpy)_2(HPyrtr)]^{2+}$ (isomer 2), both bound via the $N^{4'}$

atom Therefore, it may be suggested that the triazole ring is coordinated to ruthenium via the $N^{4'}$ atom A similar argument holds for the $[Ru(Me_2bpy)_2(bptn)]^{2+}$ complex

Of particular interest are the emission results of these compounds All mononuclear compounds containing bptn emit at room temperature and at low temperature, with $[Ru(phen)_2(bptn)]^{2+}$ having a particularly intense emission The emission of all monomers is more intense at 77 K and the wavelength of maximum emission has shifted to higher energy in comparison with the emission at room temperature This is in agreement with the emission behaviour observed for complexes containing pyridyltriazole ligands [38] Comparison with $[Ru(bpy)_2(PT)]^{2+}$ which has no emission at room temperature but does emit at 77 K, suggests again that coordination to bptn takes place via $N^1$ pyridine ring A and the triazole ring It is anticipated that coordination via ring B and the triazole ring would at least at room temperature result in a poorly emitting species

The oxidation potentials of the mononuclear complexes containing bptn in Table 5 6 also give a good indication that coordination to bptn is via $N^1$ pyridine ring A and the triazole ring This is because of the rather high oxidation potential exhibited by $[Ru(bpy)_2(PT)]^{2+}$ that is absent in the redox properties of these mononuclear compounds If coordination to bptn is via pyridine ring B and the triazole ring then the oxidation potentials of the monomers would be anticipated to be at a higher potential The oxidation potentials of $[Ru(bpy)_2(bptn)]^{2+}$ and $[Ru(phen)_2(bptn)]^{2+}$ are similar to those obtained for $Ru(bpy)_2$ complexes containing other pyridyltriazole ligands [38], suggesting that the coordination mode for these two monomers is the same The oxidation potential for $[Ru(Me_2bpy)_2(bptn)]^{2+}$ is found at is also slightly lower

energy than the other two mononuclear compounds This result is consistent with the oxidation potentials obtained for the tris compounds $[Ru(bpy)_3]^{2+}$, $[Ru(Me_2bpy)_3]^{2+}$ and $[Ru(phen)_3]^{2+}$ where $[Ru(Me_2bpy)_3]^{2+}$ has the lowest oxidation potential and $[Ru(phen)_3]^{2+}$ has the highest [50-53]

The emission results obtained for the three monomers are very similar to those of the analogous tris compounds suggesting that emission occurs via the triplet states of bpy, $Me_2bpy$ and phen The first reduction potential of $[Ru(bpy)_2(bptn)]^{2+}$, $[Ru(phen)_2(bptn)]^{2+}$ and $[Ru(Me_2bpy)_2(bptn)]^{2+}$ corresponds to that of the first reduction potential of the tris compounds $[Ru(bpy)_3]^{2+}$, $[Ru(Me_2bpy)_3]^{2+}$ and $[Ru(phen)_3]^{2+}$, suggesting that the bptn $\pi^*$ orbitals are not involved in the reduction process Both the emission results and reduction potentials indicate that bptn acts as a spectator ligand while the bpy, $Me_2bpy$ and phen ligands are the luminactive ligands No evidence of multiple emission was observed for these monomers

### 5 3 2 Mononuclear Compounds Containing 3,5-Bis)pyridin-2-yl)-1,2,4-triazole,

The absorption and emission data of $[Ru(bpy)_2(bpt)]^+$, and $[Ru(Me_2bpy)_2(bpt)]^+$ and $[Ru(phen)_2(bpt)]^+$ are presented in Table 5 5 In comparison with $[Ru(bpy)_3]^{2+}$, the replacement of a bpy ligand by $bpt^-$ to give $[Ru(bpy)_2(bpt)]^+$ causes an increase in the electron density on the metal, with a consequent red shift of the MLCT (Ru ---> bpy) band In comparison with the tris complexes $[Ru(Me_2bpy)_3]^{2+}$ and $[Ru(phen)_3]^{2+}$ the MLCT band of $[Ru(Me_2bpy)_2(bpt)]^+$ and $[Ru(phen)_2(bpt)]^+$ both red shift with the replacement of $bpt^-$ with a $Me_2bpy$ and phen ligand respectively Both the deprotonated $[Ru(Me_2bpy)_2(bpt)]^+$ and $[Ru(phen)_2(bpt)]^+$

complexes absorb at slightly higher energy than $[Ru(bpy)_2(bpt)]^+$

As expected, protonation of $[Ru(bpy)_2(bpt)]^+$ $[Ru(Me_2bpy)_2(bpt)]^+$ and $[Ru(phen)_2(bpt)]^+$ to yield $[Ru(bpy)_2(bptH)]^{2+}$, $[Ru(Me_2bpy)_2(bptH)]^{2+}$ and $[Ru(phen)_2(bptH)]^{2+}$ results in a shift to higher energy of the lowest MLCT band Similar behaviour has been observed for the pyridyltriazoles studied in Chapter 3 Section 1, and for a series of compounds containing imidazole, pyrazole and triazole moieties and is explained by the increased $\pi$ donor capacity of the deprotonated ligand [39, 40, 52-54]

The ground state and excited state $pK_a$'s for the mononuclear complexes containing bpt are listed in Table 5 7 It must be noted that the $pK_a$ values obtained for $[Ru(Me_2bpy)_2(bpt)]^+$ and $[Ru(phen)_2(bpt)]^+$ must be treated with caution due to the presence of a second species in the sample It is suggested from the $pK_a$ values obtained for the two isomers of $[Ru(bpy)_2(HPyrtr)]^{2+}$, that the $pK_a$ value largely depends on the coordination mode of the pyridyltriazole ligand Now, if there are two isomers present in the samples, that is, one coordinated via the pyridine ring of $bpt^-$ and $N^{1'}$ triazole and the second coordinated via a pyridine ring and $N^{4'}$ triazole then quite a variation of $pK_a$ for each isomer would be expected If, on the other hand the "impurity" (which may possibly be $[Ru(Me_2bpy)_3]^{2+}$ or $[Ru(phen)_3]^{2+}$) has no pH dependence then the $pK_a$ values obtained for these monomers are acceptable The $pK_a$'s for the mononuclear complexes are represented by the following equation,

$$[Ru(L\text{-}L)_2(Hbpt)]^{2+} \underset{+H^+}{\overset{-H^+}{<\!\!-\!\!-\!\!-\!\!-\!\!-\!\!-\!\!-\!\!-\!\!>}} [Ru(L\text{-}L)_2(bpt)]^+ \qquad (12)$$

The $pK_a$'s of the mononuclear complexes are considerably

lower than the value of 8 4 ± 0 1 obtained for the free ligand Hbpt [40] So, when bound to the $Ru(bpy)_2$, $Ru(Me_2bpy)_2$ and $Ru(phen)_2$ moieties, the Hbpt ligand is stronger acid than the free ligand by approximately 4 orders of magnitude This suggests substantial electron donation from the ligand to the ruthenium

Table 5.6 Ground State and Excited State $PK_a$'s For Mononuclear Complexes Containing Hbpt

| Complex | $pK_a$ | $pH_1$ | $pK_a^*$ |
|---|---|---|---|
| $[Ru(bpy)_2(bptH)]^{2+}$ | 4 00 | | 3 35 |
| $[Ru(Me_2bpy)_2(bptH)]^{2+}$ | 4 40 | 4 10 | 3 70 |
| $[Ru(phen)_2(bptH)]^{2+}$ | 4 25 | 3 70 | 3 64 |
| $[Ru(bpy)_2(HPyrtr)]^{2+}$ (1) | 5 95 | 5 13 | 4 90 |
| $[Ru(bpy)_2(HPyrtr)]^{2+}$ (2) | 4 00 | 2 68 | 2 10 |
| $[Ru(bpy)_2(H3MePyrtr)]^{2+}$ | 4 87 | 4 20 | 3 50 |

$pH_1$ values are the inflection points on the luminescent titration curves, $pK_a^*$ is calculated using Equation 5, Chapter 4

Protonation of the dinuclear compounds proved very difficult Experiments carried out in aqueous solution suggest a $pK_a$ as low as -0 6 ± 0 3 for $[(bpy)_2Ru(bpt)Ru(bpy)_2]^{3+}$ [40] As a result of the difficulty of protonation of dinuclear species no $pK_a$ experiments were carried out on the other dimers

The $pK_a$ for $[Ru(bpy)_2(bpt)]^+$ is found at lower pH than those of the $[Ru(Me_2bpy)_2(bpt)]^+$ and $[Ru(phen)_2(bpt)]^+$ However, as isomers may be present their pH dependency may

interfere with the results obtained In comparison with the series of 3MePyrtr bivalent complexes a similar trend is observed in the $pK_a$'s of $[Ru(bpy)_2(3Mepyrtr)]^+$, $[Ru(phen)_2(3MePyrtr)]^+$ [55] and $[Ru(Me_2bpy)_2(3MePyrtr)]^+$ [55] whose pKa's are respectively 4 87, 5 2 and 5 5 For these compounds only one isomer is possible and coordination is via the $N^{4'}$ atom on the triazole ring The mononuclear complexes containing the bridging ligand bptn have no acid-base dependency as the second pyridine ring is bound via the $N^1$ atom

Protonation of the mononuclear complexes containing $bpt^-$ also has the expected effect on the emission spectra with a shift to higher energy for the emission maximum upon protonation (see Table 5 5) These changes are also reflected in the low temperature emission maxima

Differential pulse voltametry (DPV) of the mononuclear complex $[Ru(bpy)_2(bpt)]^+$ and its protonated analogue $[Ru(bpy)_2(bptH)]^{2+}$ yield values of 0 87 and 1 00 V respectively that are similar to those obtained for the protonated and deprotonated forms of $Ru(bpy)_2$ complexes containing HPyrtr and H3MePyrtr (see Table 5 6) DPV of the $[Ru(phen)_2(bpt)]^+$ complex yields two oxidation potentials suggesting the presence of a second species in the ratio of 75 25 DPV of the protonated form of $[Ru(Me_2bpy)_2(bpt)]^+$ also yields two oxidation potentials in the ratio 75 25, each of which is about 100 mV higher than the oxidation potentials observed for the deprotonated form This indicates that the protonated forms of the isomers are better $\pi$-acceptors than the deprotonated forms Protonation of the $[Ru(phen)_2(bpt)]^+$ monomer results in the observation of one peak at 1 14 V

Both the emission results and reduction potentials indicate that $bpt^-$ is the spectator ligand in the mononuclear

complexes and the bpy, $Me_2bpy$ and phen are the luminactive ligands No evidence for multiple emission was observed at room temperature or at 77 K

### 5 3 3 Dinuclear Complexes Containing 3,5-Bis(pyridin-2-yl)-1,2,4-triazole.

Coordination of a second $Ru(bpy)_2^{2+}$ unit to the bpt-bridging ligand to form the dinuclear complex $[(bpy)_2Ru(bpt)Ru(bpy)_2]^{3+}$ results in an increase in the energy of the MLCT band This blue shift of the Ru ---> bpy CT levels suggests the sharing of the $\sigma$ donor power of the anionic ligand between the two $Ru(bpy)_2^{2+}$ units causing a decrease of electron density on the Ru(II) ions A similar behaviour has been observed for complexes containing imidazole type bridging ligands [53, 56-59] This result is quite in contrast with results obtained for related dinuclear systems where the MLCT band is shifted to lower energy when compared with that of the mononuclear analogues [6, 28, 58, 59]

The absorption spectra of the mixed ligand dimers are presented in Figure 5 14 Both the $[(phen)_2Ru(bpt)Ru(phen)_2]^{3+}$ and $[(Me_2bpy)_2Ru(bpt)Ru(Me_2bpy)_2]^{3+}$ dinuclear complexes absorb at higher energy than the analogous mononuclear complexes This is in agreement with the blue shift obtained upon coordination of a second $Ru(bpy)_2$ unit to $[Ru(bpy)_2(bpt)]^+$ As anticipated, the phenanthroline dimer absorbs at higher energy than the bpy or $Me_2bpy$ dinuclear complexes [49-51] The $[(bpy)_2Ru(bpt)Ru(bpy)_2]^{3+}$, $[(Me_2bpy)_2Ru(bpt)Ru(Me_2bpy)_2]^{3+}$, $[(bpy)_2Ru(bpt)Ru(Me_2bpy)_2]^{3+}$, and the $[(bpy)_2Ru(bpt)Ru(phen)_2]^{3+}$ dimers absorb at similar energies The mixed ligand dinuclear complex $[(phen)_2Ru(bpt)Ru(Me_2bpy)_2]^{3+}$ absorption occurs at similar energy to that of the phenanthroline

dinuclear complex This may suggest that the lowest energy MLCT band of $[(bpy)_2Ru(bpt)Ru(phen)_2]^{3+}$ is $d\pi(Ru) \dashrightarrow \pi^*(bpy)$ in nature but that in $[(phen)_2Ru(bpt)Ru(Me_2bpy)_2]^{3+}$ it is a $d\pi(Ru) \dashrightarrow \pi^*(phen)$ transition It is not possible to assign MLCT transitions to the other mixed ligand dimers due to the similarity on the absorption spectra

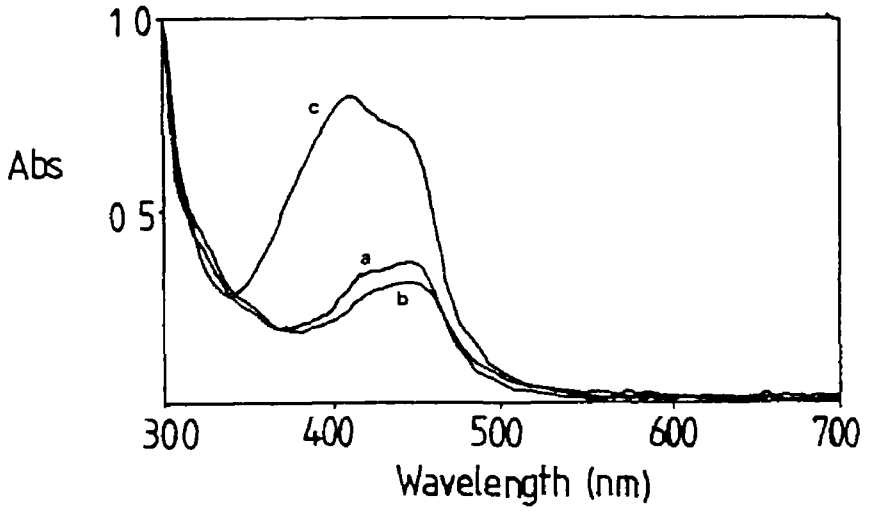


Figure 5 14 Absorption spectra in acetonitrile of (a) $[(bpy)_2Ru(bpt)Ru(Me_2bpy)_2]^{3+}$, (b) $[(bpy)_2Ru(bpt)(phen)_2]^{3+}$ and (c) $[(phen)_2Ru(bpt)Ru(Me_2bpy)_2]^{3+}$

As the emission spectra and first reduction of the dinuclear complexes are quite similar little information has been obtained regarding the lowest $\pi^*$ level However, it is anticipated that, based on the reduction potentials of the free ligands [51], in the coordinated dimeric complexes the $\pi^*$ level of phenanthroline ligand lies at lowest energy

Protonation of $[(bpy)_2Ru(bpt)Ru(bpy)_2]^{3+}$ results in an increase in absorption energy which is consistent with the result obtained for protonation of the mononuclear compound No emission of the protonated dimer was observed

probably due to quenching by acid

Interestingly, all dinuclear compounds synthesised emit in acetonitrile at room temperature (with the exception of $[(bpy)_2Ru(Hbpt)Ru(bpy)_2]^{4+}$) This is in contrast to previously reported data for bridged dimers [5, 12] where the mononuclear complexes emit and the dinuclear complexes do not For all dinuclear complexes emission intensity is stronger at low temperature than at room temperature as expected As expected, the emission maximum for these complexes at 77 K is observed at higher energy than that observed at room temperature

Resonance Raman spectroscopy carried out by Hage et al [59] shows that the lowest MLCT band of the mononuclear and dinuclear $bpt^-$ complexes can be explained by $d\pi(Ru) \dashrightarrow \pi^*(bpy)$ MLCT transitions No transitions to $\pi^*$ ($bpt^-$) orbitals are observed in this part of the absorption spectra As similar shifts in absorption and emission spectra are observed for all mononuclear and dinuclear complexes, it is therefore likely that no $bpt^-$ levels are involved in the absorption, emission and electrochemical processes of any mononuclear and dinuclear complexes

The Differential Pulse Voltamograms of the dinuclear compounds are presented in Figure 5 15 and the oxidation potentials for the dinuclear compounds are listed in Table 5 6 Knowing the sites of coordination on $bpt^-$ for the mixed ligand dimers discussed, it is possible to say which oxidation potential belongs to which ruthenium center for some of the dimers As there is little difference between the oxidation potentials of $[(bpy)_2Ru(bpt)Ru(bpy)_2]^{3+}$, $[(phen)_2Ru(bpt)Ru(phen)_2]^{3+}$ and $[(bpy)_2Ru(bpt)Ru(phen)_2]^{3+}$, the 1 01 and 1 30 V oxidation cannot be assigned to specific groups

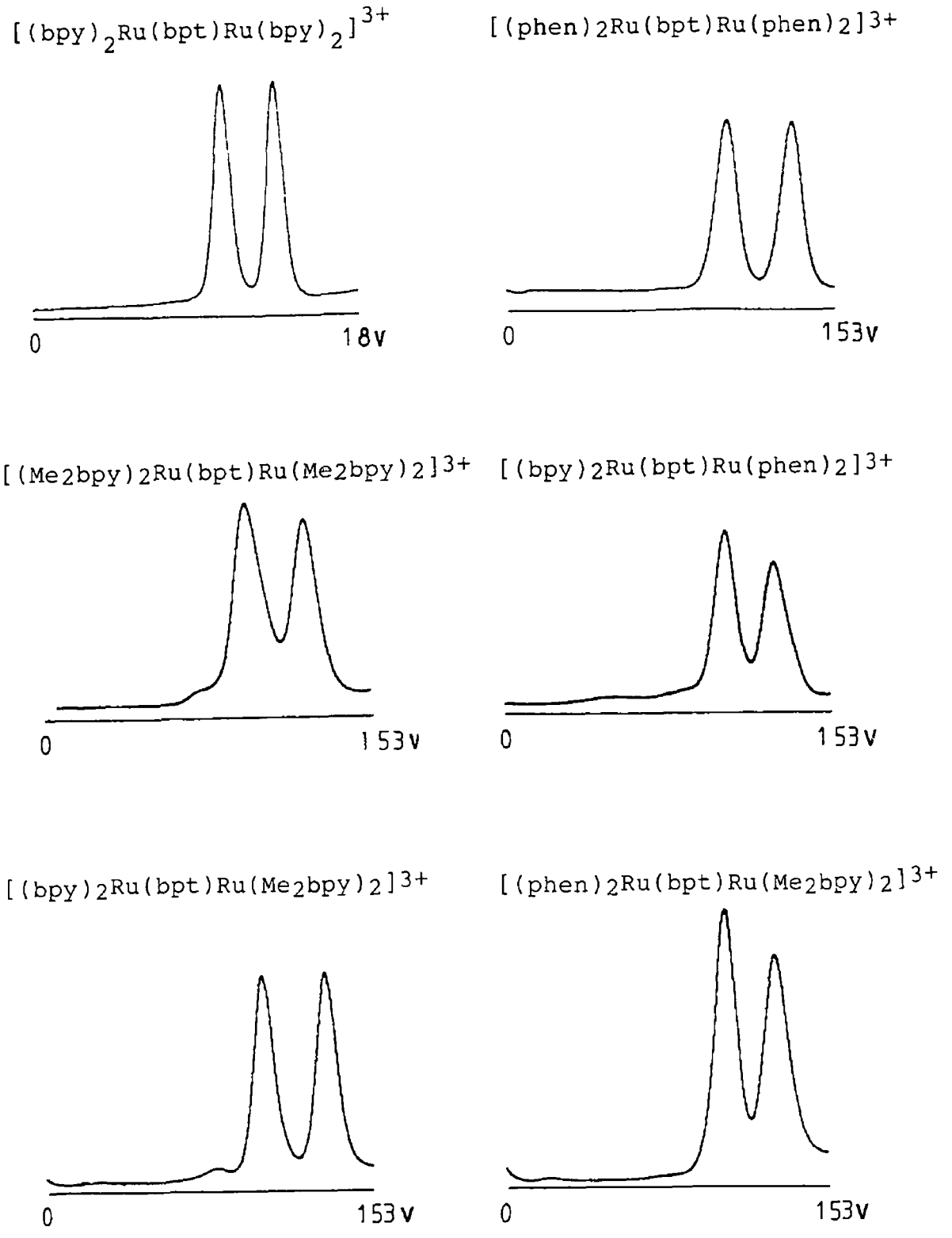


Figure 5 15 Differential pulse voltammograms in acetonitrile/0 1 M $NEt_4ClO_4$ of the dinuclear compounds prepared

The second oxidation potential for $[(Me_2bpy)_2Ru(bpt)$-$Ru(Me_2bpy)_2]^{3+}$ is found at 1 24 V, somewhat lower than that found for the other dimers For the mixed ligand complexes $[(bpy)_2Ru(bpt)Ru(Me_2bpy)_2]^{3+}$ and $[(phen)_2Ru(bpt)Ru$-$(Me_2bpy)_2]^{3+}$ a second oxidation potential is found at 1 25 V suggesting that this oxidation occurs at the $Ru(Me_2bpy)_2$ moiety, while the first occurs at the $Ru(bpy)_2$ and $Ru(phen)_2$ moieties respectively As the starting material for the preparation of $[(bpy)_2Ru(bpt)Ru(Me_2bpy)_2]^{3+}$ was $[Ru(bpy)_2(bpt)]^+$ which is coordinated to $bpt^-$ via $N^{1'}$ and a pyridine ring this indicates that $Ru(Me_2bpy)_2$ moiety is coordinated to $bpt^-$ via a pyridine ring and the $N^{4'}$ atom of the triazole ligand The oxidation potential at 1 24 V for this dimer can be assigned to the oxidation of ruthenium at the $Ru(Me_2bpy)_2$ moiety which is coordinated through $N^1$ pyridine and $N^{4'}$ triazole

Likewise from comparison with the oxidation potentials of the $[(Me_2bpy)_2Ru(bpt)Ru(Me_2bpy)_2]^{3+}$ and $[(bpy)_2Ru(bpt)$-$Ru(Me_2bpy)_2]^{3+}$ dimers it is concluded that the oxidation potential of the $(Me_2bpy)Ru$ moiety coordinated to $bpt^-$ via the $N^1$ and $N^{4'}$ positions is at 1 24 V This is also in agreement with the value obtained for the $Ru(Me_2bpy)_2$ portion of $[(phen)_2Ru(bpt)Ru(Me_2bpy)_2]^{3+}$ which was synthesised from the $[Ru(phen)_2(bpt)]^+$ monomer This indicates that the $Ru(Me_2bpy)_2$ moiety of this dimer is coordinated to $bpt^-$ via $N^1$ pyridine and $N^{4'}$ triazole ring The potential at 1 01 V may then be assigned to the $N^1$ and $N^{1'}$ coordination mode As this $N^{1'}$ of the triazole ring is adjacent to another nitrogen, this side of the triazole ring will be a stronger $\sigma$ donor and oxidation at the $N^1$ and $N^{1'}$ site should be easier than at the $N^1$ and $N^{4'}$ site

The oxidation potentials obtained for the isomers of $[Ru(bpy)_2(HPyrtr)]^{2+}$ (Chapter 3) indicate that coordination via $N^1$ pyridine and $N^{1'}$ yields a lower oxidation potential

then the isomer coordinated via $N^1$ pyridine and $N^{4'}$ triazole This indicates at that upon coordination via $N^1$ pyridine and $N^{4'}$ the pyridyltriazole ligand is a better $\pi$ acceptor and hence the oxidation potential will be higher than the $N^{1'}$ and pyridine coordination mode. The results obtained for the oxidation potentials for our dinuclear compounds (where specific coordination sites are known) suggest that the oxidation at $N^{1'}$ is found at lower potential than that at $N^{4'}$ This suggests that the redox potential depends on the site of coordination and also on the nature of the of the $(L\text{-}L)_2Ru$ moieties

The difference in oxidation potentials between the two oxidation waves of the deprotonated $[(bpy)_2Ru(bpt)\text{-}Ru(bpy)_2]^{3+}$ is 0 32 V The reason for this large difference may be due to one or more of the reasons discussed in the introduction to this chapter To investigate the reason for this large difference in oxidation potential the mixed metal complexes $[(bpy)_2Ru\text{-}(bpt)Os(bpy)_2]^{3+}$ (RuOs) and $[(bpy)_2Os(bpt)\text{-}Ru(bpy)_2]^{3+}$ (OsRu) were prepared by Hage [60] The results showed that for the RuOs complex where Ru is coordinated via $N^1$ and $N^{1'}$ and Os is coordinated via $N^1$ and $N^{4'}$ the oxidation potentials are 0 73 and 1 20 V and for the OsRu complex the coordination modes are reversed and the potentials are 0 65 and 1 30 V The low oxidation potential corresponds to osmium while the higher corresponds to ruthenium The results obtained suggest that when the metal is coordinated to the $N^{1'}$ position of the triazole ring it has a lower oxidation potential In the RuOs complex the oxidation potential of ruthenium is at 1 20 V while in the OsRu complex it is at 1 30 V Likewise for osmium the potential in the OsRu complex is 0 65 V and 0 73 V in the RuOS complex Therefore, in agreement with our results Hage [60] suggests that the redox potential for each metal is dependent on the site of coordination

In general, in dinuclear compounds, with small electron delocalisation and resonance stabilisation effect, the first oxidation potential is expected to be similar to that observed for the mononuclear complexes [21] The first oxidation potentials for the mixed ligand dimers containing bpy and phen and bpy and $Me_2bpy$ are higher than the oxidation potential for the monomer $[Ru(bpy)_2(bpt)]^+$ Likewise the first oxidation potential for $[(Me_2bpy)_2Ru(bpt)Ru(Me_2bpy)_2]^{3+}$ is higher than that of the mononuclear $[(Me_2bpy)_2Ru(bpt)]^+$ and the first oxidation potentials for $[(phen)_2Ru(bpt)Ru(phen)_2]^{3+}$ and $[(phen)_2Ru(bpt)Ru(Me_2bpy)_2]^{3+}$ are higher than that of either isomer of $[Ru(phen)_2(bpt)]^+$

There is quite a large difference between the first and second oxidation potential for the dinuclear complexes Whether interaction exists between two redox sites in one molecule is determined by the value of $K_{com}$ [24], Equation 5 The $\Delta E$ values are represented schematically by horizontal lines in Figure 5 16 allowing a direct comparison to be made of the $Ru(L\text{-}L)_2$ moieties where L-L = bpy, $Me_2bpy$ or phen while the bridging ligand remains unchanged The $K_{com}$ values obtained for the dinuclear complexes are also listed in Table 5 6 The larger the $K_{com}$ value means the stronger the interaction between the metal centers Of all the dinuclear complexes synthesised the $[(phen)_2Ru(bpt)Ru(phen)_2]^{3+}$ complex has the highest $K_{com}$ value of $13\ 72 \times 10^4$ In comparison with other dinuclear complexes the dinuclear complexes presented in Table 5 6 have rather large $K_{com}$ values Complexes with a larger $K_{com}$ value than $24 \times 10^4$ included the Creutz and Taube ion $[(NH_3)_5Ru(pyz)Ru(NH_3)_5]^{5+}$ and $[(NH_3)_5Ru(pyz)RuCl(bpy)_2]^{4+}$ which have $K_{com}$ values of $4 \times 10^6$ and $1 \times 10^7$ respectively (where pyz - pyrazine) indicating that strong interaction between the metal centers exists in these systems [61]

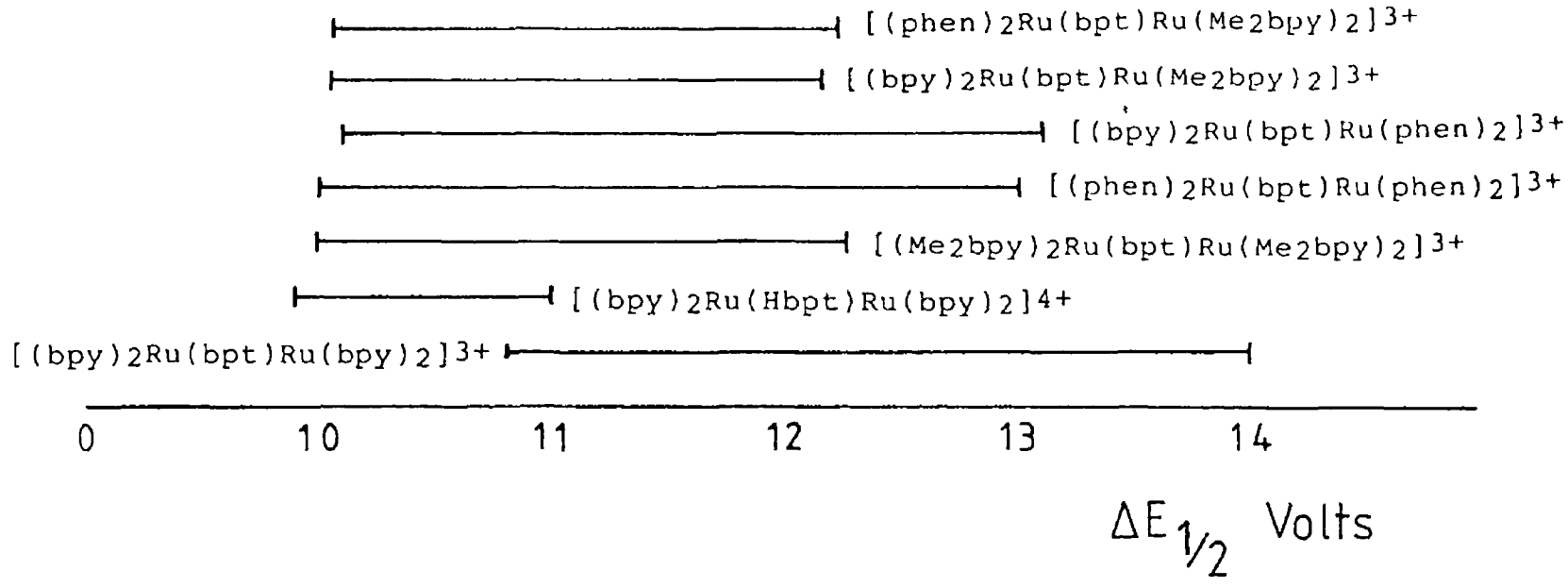


Figure 5 16 Schematic diagram of $\Delta E_{1/2}$ for the dinuclear compounds prepared

From Table 5 6 the lowest $K_{com}$ value is of 0 3x10$^4$ found for the protonated $[(bpy)_2Ru(Hbpt)Ru(bpy)_2]^{4+}$ Low values are also obtained for the mixed ligand dimer containing bpy and $Me_2bpy$, and phen and $Me_2bpy$ This suggests that the interaction between metal centers is also dependent, apart from the bridging ligand, on the nature of the other ligands present in the complex

The $K_{com}$ values for $[(bpy)_2Ru(bpt)Ru(bpy)_2]^{3+}$ and the mixed ligand dimer $[(bpy)_2Ru(bpt)Ru(phen)_2]^{3+}$ are very similar at 9 45x10$^4$ and 9 37x10$^4$ respectively This result is consistent with the results obtained by Haga for $[(bpy)_2Ru(bibzim)Ru(bpy)_2]^{2+}$ and the mixed ligand dimer $[(bpy)_2Ru(bibzim)Ru(phen)_2]^{2+}$ [22] The $K_{com}$ values for both these dimers is 9 8x10$^4$, similar to our results These $K_{com}$ values are slightly larger than the value of 1 1x10$^3$ reported for $[(bpy)_2Ru(bpym)Ru(bpy)_2]^{5+}$ [5] and 1x10$^2$ for $[(bpy)_2ClRu(pyr)RuCl(bpy)_2]^{3+}$ [8] where the interaction between the metal centers is relatively weak This suggests that the interaction between the two ruthenium centers for all our dimers is stronger due to the negative charge on the bridging triazole ring, and that they belong to class II in the Robin and Day sense [16]

To obtain more information about the extent of electron delocalisation, the dinuclear complex may be partially oxidised to form the mixed-valence complex so that the metal centers are in different oxidation states Previous experiments show that partial oxidation with $(NH_4)_2Ce(NO_3)_6$ gives rise to a band at 750 nm which was originally thought to be the inter-valence transfer band However, this band is also produced on addition of $(NH_3)_2Ce(NO_3)_6$ to a solution of monomer This band is now thought to be due to LMCT band Similar behaviour was observed for the $[(bpy)_2Ru(bibzim)Ru(bpy)_2]^{2+}$ complex where two bands appear at 712 and 754 nm upon partial oxidation to form the

mixed-valence complex $[(bpy)_2Ru(bibzim)Ru(bpy)_2]^{2+}$ [22] These bands have been assigned to ligand $\pi$-to-ruthenium (III) charge transfer transitions [25] In order to study mixed valence systems with these dinuclear complexes spectroelectrochemistry would be an ideal technique This would involve oxidising one Ru center in solution while observing the change in the uv/vis spectra

The charge on the bridging ligand is expected to strongly effect the properties of the mononuclear and dinuclear compounds The effect of this charge on variables such as $\Delta E_{1/2}$, absorption and emission spectra is not fully understood Conclusions about electronic interaction based on these data therefore must be treated with caution

## 5 5 Conclusion.

For the mononuclear compounds containing bptn, the electronic and electrochemical and n m r properties suggest that coordination to bptn occurs via $N^1$ of pyridine ring A and the triazole ring All data suggest, but, there is no conclusive evidence that coordination to the triazole ring takes place via the $N^{4'}$ atom However, due to steric limitations of this ligand this mode of coordination is most favourable, so it is anticipated that the site of coordination at the triazole ring is at the $N^{4'}$ position This is confirmed by the fact that no dimer formation has been observed for this ligand, suggesting that due to steric reasons coordination via the $N^{2'}$ atom does not occur under any circumstances

The preparation of the mononuclear compound $[Ru(bpy)_2(bpt)]^+$ results in the formation of only one isomer, the crystal structure of which shows that coordination occurs via the $N^1$ of a pyridine ring and $N^{1'}$

of the triazole ring However, the preparation of the compounds $[Ru(Me_2bpy)_2(bpt)]^+$ and $[Ru(phen)_2(bpt)]^+$ results in the formation of either two isomers or one isomer and an impurity These "impurities" present in about 20%, are observed in the n m r spectra, oxidation potentials and HPLC analysis The identity of the "impurities" is not known at the present, but the n m r spectra indicate that the main component of these monomers is coordinated in the same coordination mode as that of $[Ru(bpy)_2(bpt)]^+$ That is via $N^1$ of a pyridine ring and $N^{1'}$ of the triazole ring All mononuclear compounds containing bptn and Hbpt exhibit similar electronic and electrochemical behaviour as those of other pyridyltriazole compounds reported [39] All mononuclear compounds containing Hbpt absorb at higher energy and have lower oxidation potentials than the mononuclear compounds containing bptn This indicates that Hbpt is a weaker $\pi$ acceptor ligand than bptn and the deprotonated form of Hbpt is a weaker $\pi$ acceptor than Hbpt and bptn

The results obtained in this chapter for the dinuclear compounds show that $bpt^-$ is an interesting bridging ligand The ligand bptn on the other hand, does not act as a bridging ligand as no dinuclear compounds were obtained Apart from steric limitations of this ligand, a second reason for lack of formation of the dinuclear compounds may be due to the fact that the double bonds in the triazole ring of bptn are localised and would not have the same stabilizing delocalisation effect as $bpt^-$

The decrease in $pK_a$ for the mononuclear compounds containing $bpt^-$ and the dinuclear compound $[(bpy)_2Ru(bpt)Ru(bpy)_2]^{3+}$ suggest a strong electron donation from the $bpt^-$ ligand to the ruthenium center The increased delocalization of the charge in the dinuclear compound is most likely responsible for the difference in acidity of

about 10 orders of magnitude between the dinuclear ruthenium compound and the free ligand

Purity of the samples $[(Me_2bpy)_2Ru(bpt)Ru(Me_2bpy)_2]^{3+}$ and $[(bpy)_2Ru(bpt)Ru(phen)_2]^{3+}$ posed a problem as the oxidation potentials and n m r spectrum of $[(bpy)_2Ru(bpt)$-$Ru(phen)_2]^{3+}$ yielded reasonable results yet the CHN analysis were not good Dinuclear compounds containing the protonated $bpt^-$ are much more difficult to investigate as protonation occurs only at very low pH As expected, two oxidation potentials are obtained for each compound The resulting comproportion constant calculated from these potentials suggest that this series of oxidised dinuclear complexes may be an example of a class II system In its de- protonated form the bridging ligand mediates a strong interaction between the ruthenium centers This strong electron delocalization is most likely facilitated by the low $\pi^*$ orbital in the bridging ligand and also by the presence of a negative charge on the bridging triazole ring From our results it is clear that further work is necessary, in particular, the formation of mixed valence dimers to have a better understanding of the dinuclear compounds containing the charged bridging ligand $bpt^-$

References.


1 A Juris, V Balzani, F Barigelletti, S Campagna, P Belser, and A von Zelewsky, Coord. Chem. Rev., 1988 84, 85

2 K Kalyanasundaram, Coord Chem. Rev., 1982, 46, 159

3 E A Seddon and K R Seddon, "The Chemistry of Ruthenium", Elsevier, Amsterdam, 1984, Ch 15

4 T J Meyer, Pure and App. Chem., 1986 58, 1193

5 E V Dose and L J Wilson, Inorg. Chem., 1978, 17, 2660

6 C H Braunstein, A D Baker, T C Strekas, and H D Gafney, Inorg. Chem., 1984 23, 857

7 J A Gilbert, D S Eggleston, W R Murphy Jr , D A Geselowitz, S W Gersten, D J Hodgson, and T J Meyer, J. Am Chem. Soc., 1985, 107, 3855?

8 B P Sullivan, P J Salmon, T J Meyer, and J Peedin, Inorg. Chem , 1979, 18, 3369

9 D P Rillema, G Allen, T J Meyer, and D Conrad, Inorg Chem., 1983, 22, 1617

10 V Balzani, "Supramolecular Photochemistry", Reidel Dortrect, 1987

11 D E Richardson and H J Taube, J. Am. Chem. Soc., 1983, 105, 40

12 M Hunziker and A Ludi, J. Am. Chem. Soc., 1977, 99, 7370

13 W Kaim and S Kohlmann, Inorg. Chem., 1987, 26, 66

14 N S Hush, Prog Inorg. Chem., 1967, 8, 391

15 N S Hush, Electrochem. Acta, 1968, 13, 1005

16 M B Robin and P Day, Adv. Inorg. Chem., Radiochem., 1967, 10, 247

17 C Creutz and H Taube, J. Am. Chem Soc., 1969, 91, 3986

18 C Creutz and H Taube, J. Am. Chem. Soc., 1973, 95, 1086

19 R W Callahan, G M Brown, and T J Meyer, J Am Chem Soc , 1974, 96, 7829

20 R W Callahan, G M Brown, and T J Meyer, Inorg. Chem., 1975, 14, 1443

21 M Haga, T Matsumura-Inoue, and S Yamabe, Inorg. Chem., 1987, 26, 4148

22 M A Haga, Inorg. Chim. Acta, 1980, 45, 1183

24 C Creutz, Prog. Inorg. Chem., 1983, 30, 1

25 G M Bryant and J E Fergusson, Aust. J. Chem., 1971, 24, 441 2726

27 E C Johnson, B P Sullivan, D J Salmon, S A Adeyemi, and T J Meyer, Inorg. Chem., 1978, 17, 2211

28 K A Goldbsy and T J Meyer, Inorg. Chem., 1984, 23, 3002

29 M J Powers and T J Meyer, Inorg Chem., 1978 17, 1785

30 G M Tom, C Creutz, and H Taube, J. Am. Chem. Soc., 1974, 96, 7827

31 J T Hupp, G A Neyhart, and T J Meyer, J. Am. Chem. Soc., 1986, 108, 5349

32 R W Callahan, F R Keen, T J Meyer, and D J Salmon, J. Am. Chem. Soc., 1977, 99, 1064

33 M J Powers, R W Callahan, D J Salmon, and T J Meyer, Inorg. Chem., 1976, 15, 894

34 J C Curtis, J S Bernstein, and T J Meyer, Inorg. Chem., 1985, 24, 385

35 G M Tom, and H Taube, J. Am. Chem. Soc., 1975, 97, 5310

36 T J Meyer, Adv. Chem. Serv., 1976, No. 150, Chapter 7

37 S P Best, R J H Clark, R C S McQueen, and S Joss, J. Am. Chem. Soc., 1989 111, 548

38 R Hage, R Prins J G Haasnoot, J Reedijk, and J G Vos, J. Chem. Soc., Dalton trans, 1987, 1389

39 R Hage, A H J Dijkhuis, T G Haasnoot, R Prins, J Reedijk, B E Buchanan, and J G Vos, Inorg. Chem., 1988, 27, 2185

40 J D Birchall, T D O'Donoghue,and J R wood, Inorg. Chim. Acta, 1979, 37, L461

41 J L Walsh and B Durham, Inorg. Chem., 1982, 21, 329

42 S F Mc Clanahan, R F Dallinger, F J Holler, and J R Kincaid, J. Am. Chem. Soc., 1985, 107, 4853

43 E C Constable and J Lewis, Inorg. Chim. Acta, 1983, 70, 251

44 J E Baggot, G K Gregory, M J Pilling, S Anderson, K R Seddon, and J E Turp, J. Chem. Soc., Faraday Trans. 2, 1983, 79, 195

45 P J Steel, F Lahousse, D Lerner, and C Marzin, Inorg Chem., 1983, 22, 1488

46 G A Crosby and W H Elfring, J. Phys. Chem., 1976, 80, 2206

47 F E Lytle, L M Petrosky, and L R Carlson, Anal. Chim Acta, 1971, 57, 239

48 J V Casper and T J Meyer, Inorg. Chem , 1983, 22, 2444

49 R C Young, T J Meyer, and D G Whitten, J. Am. Chem Soc , 1976, 98, 286

50 P A Mabrouk and M S Wrighton, Inorg. Chem., 1986, 25, 526

51 F Barigelletti, A Juris, V, Balzani, P Belser, and A von Zelewsky, Inorg Chem , 1987, 26, 4115

52 B P Sullivan, D J Salmon, and T J Meyer, Inorg. Chem , 1978, 17, 85

53 A M Bond and M Haga, Inorg Chem., 1986, 25, 4507

54 J G Vos, J G Haasnoot, and G Vos, Inorg. Chim. Acta, 1983, 71, 155

55 E Ryan and J G Vos To be published

56 M Haga, M I Takeko, and S Yamabe, Inorg. Chem., 1987, 26, 4148

57 M Haga, Inorg. Chim. Acta, 1983, 75, 29

58 (a) D P Rillema, R W Callahan, and K B Mack, Inorg. Chem., 1982, 21, 2589 (b) D P Rillema and K B. Mack, Inorg. Chem., 1982, 21, 3849

59 R Hage, J G Haasnoot, D J Stufkens, T L Snoeck, J G Vos, and J Reedijk To be submitted to Inorg Chem

60 R Hage To be published

61 A Kirsh-De Mesmaeker, R Naisielsky-Hinkens, D Maetens, D Pauwels, and J Nasielsky, Inorg. Chem., 1984, 23, 377

62 K Nakamuru, Bull. Chem. Soc. Jpn., 1982, 55 2697

63 W H Elfring and G A Crosby, J. Am. Chem. Soc., 1981, 103, 2683

64 Y Kawanishi, N Kitamura, Y Kim, and S Tazuke, Riken Q., 1984, 78, 212

# Chapter 6

## Conclusion

## 6 0 Conclusion.

From this work it is clear that the asymmetric pyridyltriazole ligands are interesting For some of these ligands such as HPyrtr, H3MePyrtr and 1MePyrtr, the formation of two isomers is possible upon coordination to a $Ru(bpy)_2$ moiety However, due to steric hindrance of the methyl groups in H3MePytr and 1MePyrtr only one coordination mode is favoured The x-ray crystal structure of $[Ru(bpy)_2(3MePyrtr)]^+$ confirms that coordination to ruthenium takes place via the 1' nitrogen on the triazole ring For HPyrtr, two isomers are formed upon coordination to a $Ru(bpy)_2$ group in a 1 1 ratio as observed by $^1H$ n m r and HPLC Using semi preparative HPLC techniques, the isomers were separated in milligram quantities Each isomer was characterised using spectrophotometry, electrochemistry and correlation spectroscopy The isomers show slightly different uv/vis and emission spectra, and oxidation potentials to each other The $pK_a$ values of the isomers also differ, the $pK_a$ of isomer 1 = 5 95 while the $pK_a$ of isomer 2 is 4 07 The results obtained on the isomers suggests that the pyridyltriazole ligand in isomer 1 is bound to ruthenium via the pyridine ring and the $N^{4'}$ nitrogen of the triazole ring, while that of isomer 2 is bound via the pyridine ring and $N^{2'}$ nitrogen of the triazole ring However, x-ray cryatallography is necessary to confirm the coordination modes of the isomers These results suggest that the properties of each isomer depend on the mode of coordination of the pyridyltriazole ligand

Photochemical reactions of complexes of the type $[Ru(bpy)_2(L\text{-}L')]^{2+}$ where L-L' = PT, 3BrPT, 3MePT or 4MePyrtr result in the formation of a monovalent complex, among other products, containing the pytridlytriazole ligand coordinated in a monodentate mode For complexes containing PT, 3BrPT and 3MePT photolysis in acetonitrile

or acetonitrile-LiCl results in the formation of $[Ru(bpy)_2(L\text{-}L')(CH_3CN)]^{2+}$ type complexes Photolysis of $[Ru(bpy)_2(4MePyrtr)]^{2+}$ in acetonitrile results in the formation of $[Ru(bpy)_2(4MePyrtr)(CH_3CN)]^{2+}$ while photolysis in acetonitrile-LiCl also results in the formation of $[Ru(bpy)_2(4MePyrtr)Cl]^{+}$ For complexes containing PT type ligands this monodentate-chloro complex was only formed upon photolysis in methanol-LiCl Complexes of the type $[Ru(bpy)_2(L\text{-}L')Cl]^{+}$ were prepared thermally and COSY n m r indicate that the these complexes are coordinated to ruthenium via the $N^{4'}$ atom of the triazole ring for PT, 3BrPT and 3MePT, and via $N^{1'}$ for 4MePyrtr The x-ray crystal structure of $[Ru(bpy)_2(3MePT)Cl](PF_6)$ confirms that the coordination site for 3MePT is via the 4' nitrogen on the triazole ring The uv/vis spectra, obtained form the diode array HPLC detection system, of the monodentate-chloro complexes produced photochemically and thermally are quite similar However, from the photochemical experiments it seams unlikely that the coordination mode for the monodentate species produced is via the same coordination site on the triazole ring as for the species produced thermally For coordination to occur at the same site as the thermally produced species, this would mean that the pyridyltriazole ligand would be lost completely from the complex and react again via the $N^{4'}$ of the triazole ring for PT, 3BrPT and 3MePT and the $N^{1'}$ for 4MePyrtr

Investigations into the formation of mononuclear and dinuclear complexes containing asymmetric di-pyridyl-triazole bridging ligands were carried out using the ligands 1,3-bis(pyridin-2-yl)-1,2,4-triazole (bptn) and 3,5-bis(pyridin -2-yl)-1,2,4-triazole (Hbpt) For bptn only the formation of the mononuclear complex was possible, suggesting that steric limitations of the ligand prevent the coordination of a second $Ru(bpy)_2$ moiety Both mono-

and di- nuclear complexes were formed containing $bpt^-$ However, in the formation of the complexes $[Ru(Me_2bpy)_2(bpt)]^+$ and $[Ru(phen)_2(bpt)]^+$ a second species is produced, the identity of which at present is not known Further analytical chromatography work is required in order to gain separation of the products Semi-preparative HPLC would then be necessary to obtain milligram quantities of the products The complexes were characterised using correlation spectroscopy, spectrophotometry and electrochemistry COSY n m r spectroscopy was found to be a useful technique for determining the proton resonances for the $bpt^-$ ligand in the dinuclear complexes The n m r spectra of the dinuclear compounds are complex as geometrical isomers have been formed Differential pulse voltammetry was also a useful technique in detecting the presence of dimeric species The results suggest that for the dimeric complexes the ruthenium which has the lowest oxidation potential is that which is coordinated to a pyridine ring and the $N^{2'}$ nitrogen of $bpt^-$ These results are consistent with the results obtained for the isomers of $[Ru(bpy)_2(Pyrtr)]^+$ where isomer 2 having the coordination mode at the pyridine ring and the $N^{2'}$ atom of the triazole ring has the lowest oxidation potential

# Appendix

Table I Oxygen-oxygen, oxygen-nitrogen and oxygen fluorine distances (Å) and angles (°) in bis(2,2-bipyridine) ruthenium-(3-methyl-5 pyridin-2-yl)-1,2,4-triazole) Hexafluorophosphate tetrahydrate

| | | | |
|---|---|---|---|
| N(4) - O(1) | 2 790 (5) | N(4) - O(1) - O(3) | 107 |
| O(1) - O(3) | 2.74 | O(1) - O(3) - O(4) | 132 6 |
| O(3) - O(4) | 2 81 (1) | O(3) - O(4) - O(2) | 117 |
| O(4) - F(3) | 2 970 (9) | O(3) - O(4) - F(3) | 100 0 (3) |
| O(4) - O(2) | 2 83 | O(4) - O(2) - N(2) | 119 |
| O(2) - N(2) | 2 865 (5) | | |
| O(1) - O(2) | 2 742 | | |

Table II Fractional atomic coordinates ($x10^5$ for Ru, $x10^4$ for C, N, F, and O) and isotropic thermal parameters ($x10^3$ for Ru and $x10^2$ for C, N, F, and O) for atoms in the structure of bis(2,2'-bipyridine)ruthenium-(3-methyl-5-pyridin-2-yl)-1,2,4-triazole Hexafluorophosphate tetrahydrate

$$B_{iso} = \frac{8\pi^2}{3} \text{ trace } U$$

| ATOM | X/A | Y/B | Z/C | B(ISO) |
|---|---|---|---|---|
| RU | 19465(3) | -14734(3) | -3603(1) | 293(1) |
| P(1) | 42355(20) | 42355(20) | 0(0) | 580(12) |
| F(1) | 3101(4) | 3775(4) | 256(2) | 1004(21) |
| F(2) | 4727(5) | 5372(4) | 259(2) | 986(21) |
| F(3) | 4693(4) | 3759(4) | 369(2) | 973(20) |
| P(2) | 0(0) | 80590(17) | 16667(0) | 548(10) |
| F(4) | 668(5) | 8396(5) | 1226(1) | 979(21) |
| F(5) | -805(4) | 8471(3) | 1483(1) | 748(16) |
| F(6) | -819(4) | 6853(3) | 1490(2) | 881(19) |
| N(1) | 1093(3) | -2614(3) | -847(1) | 364(12) |
| N(2) | 1333(4) | -2897(4) | -1248(1) | 370(12) |
| C(3) | 344(5) | -3647(5) | -1403(2) | 402(16) |
| C(31) | 179(6) | -4186(5) | -1842(2) | 614(23) |
| N(4) | -535(4) | -3874(4) | -1142(2) | 444(14) |
| C(5) | -31(4) | -3223(4) | -796(2) | 353(15) |
| N(51) | 298(3) | -2246(4) | -131(1) | 326(10) |
| C(52) | -493(4) | -3044(4) | -394(2) | 351(14) |
| C(53) | -1599(5) | -3600(5) | -287(2) | 510(19) |
| C(54) | -1963(5) | -3386(5) | 98(2) | 539(19) |
| C(55) | -1193(5) | -2584(6) | 369(2) | 488(19) |
| C(56) | -49(5) | -2028(5) | 242(2) | 440(17) |
| N(11) | 3478(3) | -715(4) | -670(1) | 346(11) |
| C(12) | 3654(4) | 128(4) | -949(2) | 375(15) |
| C(13) | 4667(5) | 721(5) | -1179(2) | 555(20) |
| C(14) | 5488(5) | 422(6) | -1114(2) | 637(22) |
| C(15) | 5279(5) | -436(6) | -840(2) | 579(23) |
| C(16) | 4293(5) | -966(6) | -620(2) | 497(19) |
| N(11') | 1815(4) | -313(4) | -734(1) | 369(13) |
| C(12') | 2729(5) | 339(4) | -993(1) | 384(14) |
| C(13') | 2733(6) | 1138(5) | -1282(2) | 561(20) |
| C(14') | 1805(6) | 1271(6) | -1290(2) | 604(24) |
| C(15') | 903(6) | 621(5) | -1025(2) | 579(23) |
| C(16') | 940(5) | -142(5) | -759(2) | 484(19) |
| N(21) | 2659(3) | -492(3) | 187(1) | 340(11) |
| C(22) | 3031(4) | -954(5) | 503(2) | 431(16) |
| C(23) | 3535(6) | -340(6) | 884(2) | 638(24) |
| C(24) | 3665(7) | 686(6) | 944(2) | 740(27) |
| C(25) | 3283(5) | 1150(5) | 636(2) | 604(21) |
| C(26) | 2791(5) | 540(4) | 256(2) | 465(17) |
| N(21') | 2270(3) | -2516(3) | 18(1) | 356(12) |
| C(22') | 2849(4) | -2041(5) | 394(2) | 387(16) |
| C(23') | 3226(6) | -2613(6) | 651(2) | 560(23) |
| C(24') | 3015(6) | -3685(6) | 522(2) | 684(25) |
| C(25') | 2414(6) | -4158(6) | 156(2) | 589(23) |
| C(26') | 2050(5) | -3544(5) | -95(2) | 486(19) |
| O(1) | 5210(4) | 7227(4) | 1394(2) | 743(19) |
| O(2) | 6851(4) | 3171(4) | 1544(1) | 740(19) |
| O(3) | 6873(6) | 6611(6) | 1235(2) | 1129(30) |
| O(4) | 6746(6) | 4635(6) | 920(2) | 1018(27) |

Table III Fractional atomic coordinates for Ru, C, N, F, and O in the structure of bis(2,2'-bipyridine)chloro ruthenium-(3-methyl-1-pyridin-2-yl)-1,2,4-triazole Hexafluorophosphate

| | | FRACTIONAL COORDINATES | | |
|---|---|---|---|---|
| ATOM | | X | Y | Z |
| RU | 1 | 0.96000 | 0.23060 | 0.29250 |
| CL | 1 | 1.23890 | 0.30190 | 0.27340 |
| N | 1 | 1.09540 | 0.36730 | 0.39380 |
| C | 1 | 1.07540 | 0.46190 | 0.37990 |
| C | 2 | 1.18670 | 0.55300 | 0.45140 |
| C | 3 | 1.31980 | 0.54740 | 0.53840 |
| C | 4 | 1.33680 | 0.44970 | 0.55120 |
| C | 5 | 1.22380 | 0.36010 | 0.47830 |
| N | 2 | 1.11020 | 0.17890 | 0.40640 |
| C | 6 | 1.23290 | 0.25460 | 0.48560 |
| C | 7 | 1.35320 | 0.25170 | 0.56760 |
| C | 8 | 1.34470 | 0.12830 | 0.56600 |
| C | 9 | 1.21810 | 0.04610 | 0.48560 |
| C | 10 | 1.10090 | 0.07610 | 0.40590 |
| N | 3 | 0.72520 | 0.15490 | 0.30420 |
| C | 11 | 0.69150 | 0.18860 | 0.37010 |
| C | 12 | 0.52220 | 0.13380 | 0.37210 |
| C | 13 | 0.38430 | 0.04310 | 0.30490 |
| C | 14 | 0.41290 | 0.00360 | 0.23790 |
| C | 15 | 0.59070 | 0.06150 | 0.23970 |
| N | 4 | 0.82900 | 0.09040 | 0.19600 |
| C | 16 | 0.84920 | 0.02530 | 0.17980 |
| C | 17 | 0.93790 | -0.07080 | 0.13280 |
| C | 18 | 0.91710 | -0.09630 | 0.06420 |
| C | 19 | 0.80100 | -0.03090 | 0.07860 |
| C | 20 | 0.90190 | 0.06790 | 0.14720 |
| N | 3 | 0.82000 | 0.29780 | 0.17770 |
| C | 21 | 0.67950 | 0.33490 | 0.15100 |
| C | 22 | 0.57400 | 0.33610 | 0.21290 |
| C | 23 | 0.86730 | 0.30900 | 0.11010 |
| N | 6 | 0.75810 | 0.25270 | 0.04760 |
| N | 7 | 0.63900 | 0.36990 | 0.07280 |
| N | 8 | 0.67020 | 0.44430 | -0.08140 |
| C | 24 | 0.76530 | 0.37890 | -0.03590 |
| C | 25 | 0.85960 | 0.34120 | -0.09710 |
| C | 26 | 0.86930 | 0.36500 | -0.13440 |
| C | 27 | 0.78340 | 0.46910 | -0.16250 |
| C | 28 | 0.78510 | 0.43170 | -0.18660 |
| F | - | 0.08140 | 0.16130 | 0.71640 |
| F | 1 | 0.18070 | 0.28590 | 0.82510 |
| F | 2 | 0.36270 | 0.26470 | 0.72880 |
| F | 4 | -0.00700 | 0.24190 | 0.61030 |
| F | 6 | 0.11540 | 0.37180 | 0.73340 |
| F | 5 | -0.10390 | 0.25590 | 0.70290 |
| F | 7 | 0.03110 | 0.31970 | 0.71500 |

LIST OF PUBLICATIONS.

"The Application of High-Performance Liquid Chromatography in the Investigation of Reactions Involving Ruthenium (II)bis(bipyridyl) Compounds"
B E Buchanan, E McGovern, P Harkin, and J G Vos, Inorg. Chim Acta, 1988, 154, 1

"Synthesis and Spectroscopic and Electrochemical Properties of Mononuclear and Dinuclear Bis(2,2'-bipyridyl)ruthenium Complexes Containing 3,5-Bis(pyridin-2-yl)-1,2,4-triazole"
R Hage, A H J Dijkhuis, J G Haasnoot, R Prins, J Reedjik, B E Buchanan, and J G Vos, Inorg. Chem., 1988, 27, 2185-2189

Acid-Base Chemistry of Bis(2,2'-bipyridyl)ruthenium(II) Complexes Containing Pyridly-1,2,4-triazole Ligands"
B E Buchanan, J G Vos, W J M van der Putten, J M Kelly, R Hage, R A G de Graffe, R Prins, J G Haasnoot, and J Reedijk To be submitted

"X-Ray Crystal Structure of bis(2,2 bipyridyl)-chloro-ruthenium-(3-Methyl-1-(pyridin-2-yl)-1,2,4-(triazole) Hexafluorophosphate"
B E Buchanan, B Creaven, A Howie, C Long, and J G Vos To be submitted to Acta Crystallography, Section C

"Synthesis of Complexes Containing Monodenmtate Pyridyl -1,2,4-triazoles in an Attempt to Prepare Intermediates Normally Formed in Photochemical Reactions of the Corresponding Chelating Ligands"
B E Buchanan and J G Vos, To be submitted

POSTERS.

R Hage, J G Haasnoot, B E Buchanan, and J G Vos Book of Abstracts XXVI International Conference on Coordination Chemistry, August 28-September 2 1988, Porto, Portugal

B E Buchanan, J M Kelly, W J M van der Putten, and J G Vos Royal Society of Chemistry Annual Meeting, April 1987, Swansea, Wales

A H J Dijkhuis, R Prins, J G Haasnoot, B E Buchanan, and J G Vos Book of Abstracts XXV ICCC Meeting, July 1987, Nanjing, China

B E Buchanan, J G Vos, R Hage, J G Haasnoot, and J Reedijk, Book of Abstracts XXIV International Conference on Coordination Chemistry, August 1986, Athens, Greece